Origin of the Immiscibility of Alkanes and Perfluoroalkanes

Originally published in:
Journal of the American Chemical Society 141(8), https://doi.org/10.1021/jacs.8b10745

Origin of the Immiscibility of Alkanes and Perfluoroalkanes

Robert Pollice, Peter Chen*

Abstract

Perfluoroalkanes are considered generally to have weak inter- and intramolecular forces compared to alkanes explaining their relatively low boiling points, low surface tensions and poor solvent properties. However, currently accepted models do not satisfactorily explain several trends in their properties, for instance boiling point trends as size increases. Herein, we report a comprehensive computational study of the intermolecular interaction of alkanes and perfluoroalkanes demonstrating that perfluoroalkanes have a higher intrinsic ability for dispersive interactions than their alkane counterparts and that dispersion in perfluoroalkane dimers mainly stems from fluorine—fluorine interactions. In addition, the reasons for relatively weak intermolecular forces in perfluoroalkanes compared to alkanes are their ground-state geometries, which are increasingly unsuitable for intermolecular interactions as the carbon chain length increases, and their rigidity, which makes deformation from the ground-state geometries unfavorable. Overall, these trends are reflected in a dependence of the bulk properties of perfluoroalkanes on the carbon chain length as the fluorine content decreases and the interaction geometries become increasingly unsuitable.

Introduction

Perfluoroalkanes differ from alkanes on many accounts:[1–5] One of the most fundamental difference is the larger size of perfluoroalkanes compared to their counterparts.[1,6] For comparison, looking at various steric parameters, it was shown that a trifluoromethyl group is at least as large as an isopropyl group.[4] In addition, the electronegative fluorine atom depletes the carbon chain of electrons and results in a negatively polarized shell in perfluoroalkanes, whereas in alkanes the hydrogen atoms are slightly positively polarized. Furthermore, perfluoroalkanes are significantly more rigid than alkanes[7] and the low miscibility of perfluoroalkanes with alkanes is generally known as *fluorophobic effect*,[8–11] sometimes referred to as *fluorous effect*. Perfluoroalkanes are generally assumed to have weak intermolecular interaction energies compared to alkanes, both in bulk media and in molecular complexes, explaining their relatively low boiling points, small cohesive energies as well as the *fluorophobic effect*.[2–4,8,12,13] It has been argued that, due to the low atomic polarizability of the fluorine atom, perfluoroalkanes have a low propensity to interact with any other molecule (by London dispersion[14]) and therefore segregate to minimize intermolecular contacts with non-fluorous matter thereby maximizing the contact of non-fluorous matter with itself.[3,8] However, several trends in their properties are not readily explained by that model, for instance the boiling point inversion of linear alkanes and perfluoroalkanes as a function of chain length.[4,12] Additionally, high-level ab initio calculations of molecular dimers of methane and perfluoromethane found CF_4-dimer to be significantly stronger bound than the CH_4-dimer suggesting that the ubiquitous and general assumption that perfluoroalkanes show weaker intermolecular forces needs to be reassessed.[15–17]

We herein report on a computational study of the interaction energies of homo- and heterodimers of alkanes and perfluoroalkanes of increasing carbon chain length in which:

i. We observe that several state-of-the-art computational methods have problems to estimate accurately the interaction energies of alkane-perfluoroalkane and perfluoroalkane-perfluoroalkane complexes compared to benchmark results;

ii. We find that dispersion in interacting perfluoroalkanes originates mainly from contacting fluorine atoms;
iii. We show that perfluoroalkanes have a higher intrinsic ability for intermolecular dispersion than alkanes with the same carbon chain length;
iv. We establish that the preferred geometries of perfluoroalkanes get increasingly unsuitable for interactions with either alkanes or perfluoroalkanes as the carbon chain length increases, which is the principal reason for the interaction energies being weaker than expected from shorter analogues.
v. We demonstrate that trends in interaction energies and various experimental properties are determined by the concomitant decreasing fluorine content and the increasingly unsuitable interaction geometries.

Test Systems

In this work, we study the interactions of alkane-alkane (**HH**), alkane-perfluoroalkane (**HF**) and perfluoroalkane-perfluoroalkane (**FF**) complexes wherein the interacting molecules have the same number of carbons. The number of carbons is varied systematically from one to six. The abbreviations used to refer to particular molecules and molecular complexes are explained in Table 1.

Table 1. Explanation of abbreviations used in this work with two examples.

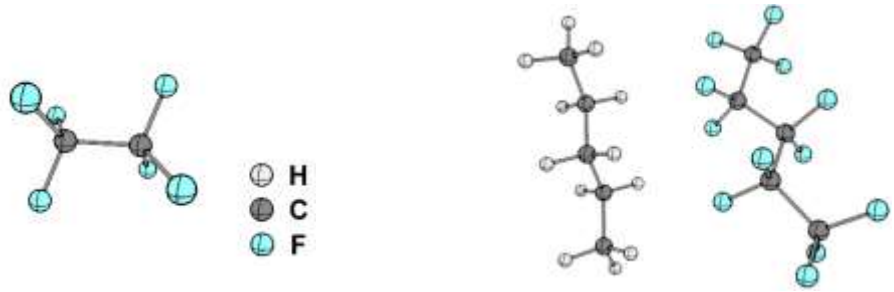

2-**F**		**5**-**HF3**
Number of carbon atoms in the molecule(s)	One or two-letter code describing the molecule(s) (H=alkane, F=perfluoroalkane)	Optional number to distinguish between several conformers

Additionally, a consistent color-coding will be used in Figures and Tables when a particular subclass of the molecular complexes is investigated. Magenta will be used for **HH**, cyan for **HF** and yellow for **FF**.

Computational Details and Definitions

Computed energies discussed in this work are either bond association energies (BAEs), i.e. the relaxation of the interacting fragments to their respective ground-state geometries is included, or bond interaction energies (BIEs), i.e. the corresponding relaxation is not included. Various programs were employed in this study including (but not limited to) Orca (versions 3.0.3 and 4.0.1),[18,19] PSI4 (versions 1.1 and 1.2),[20,21] Molpro (version 2015.1.18),[22] Gaussian (version 09, revision D.01),[23] ADF (version 2016)[24] and Q-Chem (version 4.3).[25] A more detailed description of all the programs and methods used is included in the Supporting Information.

For benchmarking of computational methods, we look at the following statistical measures describing the deviation of a dataset with values x_i from a reference dataset with values x_i^{ref} (Equations 1 – 4). It should be noted that the relative mean absolute deviation (MAD_{rel}) is sometimes also referred to as mean absolute relative deviation (MARE) in the literature. Notably, the MAD from the mean is always smaller than the corresponding standard deviation, i.e. the MAD gives a lower estimate of the deviation in the data.

$$\text{Mean Absolute Deviation: } MAD = \sum_i | x_i - x_i^{ref} | \quad (1)$$

$$\text{Relative Mean Absolute Deviation: } MAD_{rel} = \sum_i \left| \frac{x_i - x_i^{ref}}{x_i^{ref}} \right| \quad (2)$$

$$\text{Mean Signed Deviation: } MSD = \sum_i \left(x_i - x_i^{ref} \right) \quad (3)$$

$$\text{Relative Mean Signed Deviation: } MSD_{rel} = \sum_i \frac{x_i - x_i^{ref}}{x_i^{ref}} \quad (4)$$

One central measure of interest is the relative molar content of a certain atom type X in a molecule (Equation 5) describing the atomic composition.

$$\text{Relative Molar Content of X: } n_{rel}(X) = \frac{Number\ of\ X\ Atoms}{Total\ Number\ of\ Atoms} \quad (5)$$

Results

Benchmarking. We set out this study by looking for literature of computational benchmark data of complexes of alkanes (**H**) and perfluoroalkanes (**F**) in order to select suitable computational methods for geometry optimizations and subsequent single point calculations. We realized that the available benchmark data for perfluoroalkanes are extremely sparse[15–17,26,27] and therefore decided to begin by benchmarking computational methods against interaction energies from high-level ab initio methods. We chose DSD-PBEP86/def2-TZVP(spd) as density functional theory (DFT) method for geometry optimizations because of its good performance over a wide range of benchmarks, which indicates its robustness.[28] To assess the performance of DSD-PBEP86 in geometry optimizations for our test systems we performed rigid geometry scans of the intermolecular separation of interacting molecules using MP2/CBS and DLPNO-CCSD(T)/QZ.[29–31] These results suggest that DSD-PBEP86 geometries are appropriate for all the molecular complexes under study (Details in the Supporting Information).

On the basis of general literature benchmarks for noncovalent interactions and dispersion[32,33] we selected CCSD(T)/CBS and CCSD(T)-F12/VTZ as reference methods for single point energies; we looked for a cheaper method that reproduces these interaction energies best. CCSD(T)-F12/VDZ, which has a significantly lower computational cost, shows only minor deviations (Details in the Supporting Information). Using CCSD(T)-F12/VDZ, we were able to perform benchmark calculations for most of our complexes under study. To do that, we determined DSD-PBEP86 geometries and single point energies to find the lowest energy conformers for each complex. These conformers were then used to benchmark interaction energies using various methods (Details in the Supporting Information). The performance of all the DFT and wavefunction theory (WFT) approaches tested against the CCSD(T)-F12/VDZ reference values is illustrated in Table 2.

Table 2. Benchmark of various WFT and DFT methods against CCSD(T)-F12/VDZ energies of most of the molecular complexes studied. Numbers in parentheses indicate the corresponding standard

deviations. B97M-V[34]/def2-QZVP, ωB97M-V[35]/def2-QZVP, DLPNO-CCSD(T)/CBS beyond TightPNO and B3LYP-XDM[36–39]/aTZ perform best across the three subclasses.

Method	HH		HF		FF		Overall	
	MAD_{rel} [%]	MSD_{rel} [%]	MAD_{rel} [%]	MSD_{rel} [%]	MAD_{rel} [%]	MSD_{rel} [%]	MAD_{rel} [%]	MSD_{rel} [%]
B97M-V	7(5)	5(7)	3(2)	3(3)	3(1)	0(3)	4(3)	3(5)
ExtremePNO	2(1)	-1(2)	3(4)	3(4)	9(4)	9(4)	4(4)	3(4)
ωB97M-V	5(3)	5(3)	4(2)	-4(2)	7(4)	-7(4)	5(3)	-2(6)
B3LYP-XDM	3(1)	1(4)	2(2)	2(2)	14(3)	14(3)	5(5)	4(6)
VeryTightPNO	2(1)	0(2)	5(2)	5(2)	13(4)	13(4)	6(5)	5(5)
TightPNO	1(1)	1(1)	6(2)	6(2)	17(5)	17(5)	7(6)	7(6)
CCSD(T)/CBS(LPNO-CEPA/1)	3(3)	1(5)	11(2)	-11(2)	7(3)	-7(3)	8(4)	-7(6)
RI-MP2	4(3)	-3(4)	5(5)	5(5)	17(7)	17(7)	8(7)	5(9)
PBE-XDM	10(13)	-8(15)	7(8)	-6(9)	16(8)	12(14)	10(10)	-3(13)
SAPT2+	4(2)	4(3)	9(3)	9(3)	20(5)	20(5)	10(7)	10(7)
DSD-PBEP86	5(5)	-5(5)	12(2)	12(2)	28(1)	28(1)	13(9)	10(12)
BLYP-XDM	9(7)	5(10)	10(4)	10(4)	26(3)	26(3)	13(8)	12(10)
M06L	9(12)	8(13)	13(13)	13(13)	19(15)	19(15)	13(13)	13(13)
B3LYP-NL	22(10)	22(10)	7(4)	-5(6)	20(4)	-20(4)	14(9)	-1(17)
CCSD(T)/CBS(MP2)	3(2)	-2(3)	19(5)	-19(5)	19(3)	-19(3)	14(9)	-14(9)
PBE-D3	22(16)	-22(16)	8(8)	1(11)	23(14)	22(15)	15(14)	-1(21)
GFN2-xTB	24(13)	23(14)	9(8)	-6(10)	19(12)	2(24)	15(12)	4(19)
M06-2X-D3	6(4)	-4(6)	15(5)	15(6)	27(5)	27(5)	15(9)	12(13)
BLYP-NL	28(18)	28(18)	9(6)	-5(10)	20(6)	-20(6)	17(13)	1(22)
B3LYP-dDsC	22(15)	-20(18)	8(7)	7(8)	29(8)	29(8)	17(13)	4(21)
NormalPNO	4(4)	4(4)	18(4)	18(4)	33(5)	33(5)	17(11)	17(11)
M06L-D3	18(9)	-15(14)	19(6)	-17(11)	14(4)	-3(15)	18(7)	-14(14)
B2PLYP-D3	11(4)	11(4)	18(3)	18(3)	30(2)	30(2)	18(7)	18(7)
TPSS-D3	10(10)	-3(14)	20(8)	19(9)	39(18)	39(18)	21(15)	17(19)
B3LYP-D3	3(1)	1(3)	23(3)	23(3)	40(3)	40(3)	21(14)	20(15)
GFN1-xTB	27(18)	27(18)	14(5)	14(5)	37(5)	37(5)	23(14)	23(14)
ωB97X-D3	13(7)	-13(7)	20(5)	20(5)	65(13)	65(13)	28(21)	20(29)
vdW-DF10	14(9)	-14(9)	36(7)	-36(7)	32(12)	-32(12)	29(13)	-29(13)
PBE-dDsC	37(6)	-37(6)	34(6)	-34(6)	22(6)	-22(6)	32(8)	-32(8)
BLYP-D3	12(9)	12(9)	36(6)	36(6)	58(5)	58(5)	34(18)	34(18)
M06-2X	16(6)	16(6)	42(10)	42(10)	46(9)	46(9)	35(15)	35(15)
B97-D3	18(9)	-18(9)	33(8)	33(8)	67(22)	67(22)	36(21)	26(33)
SCS-MP2	38(3)	38(3)	41(6)	41(6)	50(6)	50(6)	42(7)	42(7)
sSAPT0	53(13)	53(13)	64(11)	64(11)	79(14)	79(14)	64(15)	64(15)

Table 2 shows that B97M-V performs best across all methods together with DLPNO-CCSD(T)/CBS in conjunction with ExtremePNO parameters (Supporting Information). In general, DLPNO-CCSD(T)/CBS methods with TightPNO parameters and beyond provide good results. However, MP2[40]/CBS energies are not considerably worse than DLPNO-CCSD(T)/CBS numbers using TightPNO parameters, at a significantly smaller computational cost (especially when RI-MP2[41,42] is used). Additionally, B97M-V and ωB97M-V are very considerably computationally less expensive compared to the DLPNO-CCSD(T) methods but perform equally well. It is also worth to mention the relatively good performance of all

the XDM-corrected[36–39] methods using various functionals (i.e. B3LYP, PBE and BLYP, cf. Table 2). B3LYP-XDM is only outperformed by DLPNO-CCSD(T)/CBS in conjunction with ExtremePNO parameters, which is very considerably more expensive, as well as B97M-V and ωB97M-V. Overall, B97M-V is the most efficient approach to compute accurate interaction energies across all the classes of complexes, especially for **HF** and **FF**, with B3LYP-XDM being slightly better for **HF** and B3LYP-D3 being most efficient for **HH**.

Energy Decomposition Analysis. After benchmarking, we moved on to carry out energy decomposition analysis (EDA) using symmetry adapted perturbation theory (SAPT).[43–46] The corresponding results are illustrated in Figure 1.

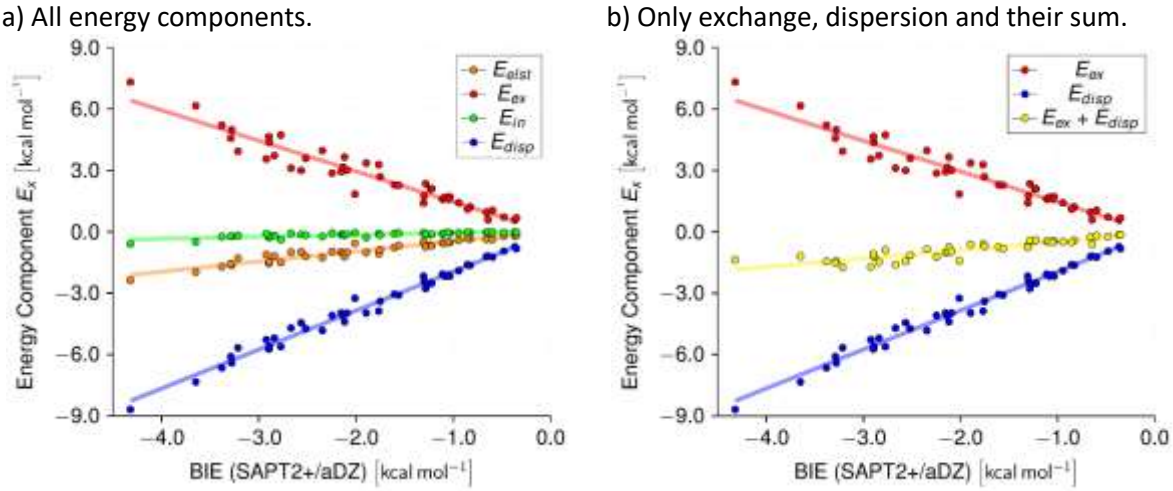

Figure 1. Interaction energy decomposition of the molecular complexes using SAPT2+ illustrated by plotting the energy components against the corresponding overall BIEs. a) Pauli repulsion and dispersion show the biggest change with interaction energy. b) The sum of Pauli repulsion and dispersion is overall still attractive.

When plotting the SAPT2+ energy components against the corresponding BIEs for all the test systems (Figure 1a) the relative importance of the energy components is essentially invariant, irrespective of whether the system belongs to **HH**, **HF** or **FF**. Figure 1a also shows that induction is almost zero across all the complexes whereas the electrostatic component does show a small but significant contribution. Exchange and dispersion are much larger in magnitude and steeper in slope but are of opposite sign in both energy and slope. Additionally, the sum of exchange and dispersion is overall attractive for all complexes showing that dispersion outweighs repulsive exchange (Figure 1b). Looking into the sum of exchange and dispersion in the three subsystems **HH**, **HF** and **FF** separately, it can be seen that **FF** provide overall more stabilization due to dispersion than the corresponding **HF** or **HH** (Details in the Supporting Information), at least in the SAPT partitioning.

Next, we compared dispersion from SAPT and LED[47,48] and found an excellent correlation (Supporting Information). Additionally, we used LED-DLPNO-CCSD(T)/QZ to gain insight into the contributions of specific groups and atoms towards dispersion by dissecting the dimers into fragments containing only one atom type (Scheme 1, Details in the Supporting Information).

Scheme 1. Decomposition of dispersion energy of complex A-B into contributions of atoms and bonds.

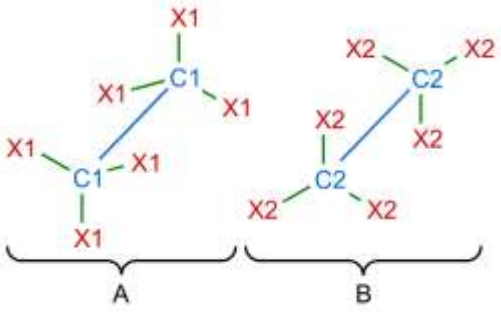

$$E_{disp}(A-B) = E(C1-C2) + E(C1-X2) + E(X1-C2) + E(X1-X2) + E(C1-CX2) + E(CX1-C2) + E(X1-CX2) + E(CX1-X2) + E(CX1-CX2)$$

The overall intermolecular dispersion is dissected into the interactions of the carbon chains, the C-X bonds and the X atoms with each other (where X = H,F) resulting in nine terms overall (Scheme 1). Looking into the relative importance of these terms for each of the three complex subclasses revealed differing main contributors (Figure 2).

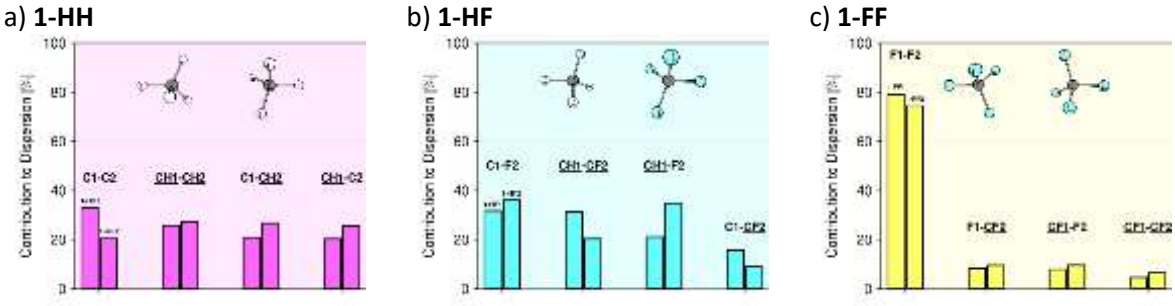

Figure 2. Decomposition of dispersion using LED into contributions from atoms and bonds for methane complexes divided into the subclasses a) **HH**, b) **HF** and c) **FF**. Only non-zero contributions are depicted.

Figure 2 shows that while in **1-H** fragments the dispersion originates from the carbon atoms and the C—H bonds, the dispersion in **1-F** fragments originates from the fluorine atoms and the C—F bonds. Consequently, almost all of the intermolecular dispersion in **1-FF** originates from interactions between fluorine atoms, while in **1-HH** and **1-HF** it is distributed more equally between different interactions. When looking at model systems with longer carbon chains, for **HH** and **HF** the relative contributions of the different interactions do not change significantly (Supporting Information). However, for **FF** the relative contribution of the F1—F2 interactions decreases as the chain length is increased and correlates linearly with the relative molar fluorine content (Supporting Information).

An alternative approach to interrogate the origin of dispersion is provided by the dispersion interaction density (DID) developed recently by Wuttke and Mata.[49] DIDs are determined on the basis of local orbital spaces using wavefunction methods and extract the origin of dispersion as a 3D scalar field in molecules.[49] This scalar field can be visualized using voxel plots showing the extent of dispersion provided by a specific region in a molecule. The DID plots of **1-HH1**, **1-HF1** and **1-FF1** are depicted in Figure 3 (DID plots of additional complexes are provided in the Supporting Information). They show again that dispersion in **1-H** originates mainly from the electron density of the C-H bonds and the carbon atom and in **1-F** mainly from the contacting fluorine atoms. This is fully consistent with the results from LED (*vide supra*).

a) **1-HH1**. b) **1-HF1**. c) **1-FF2**.

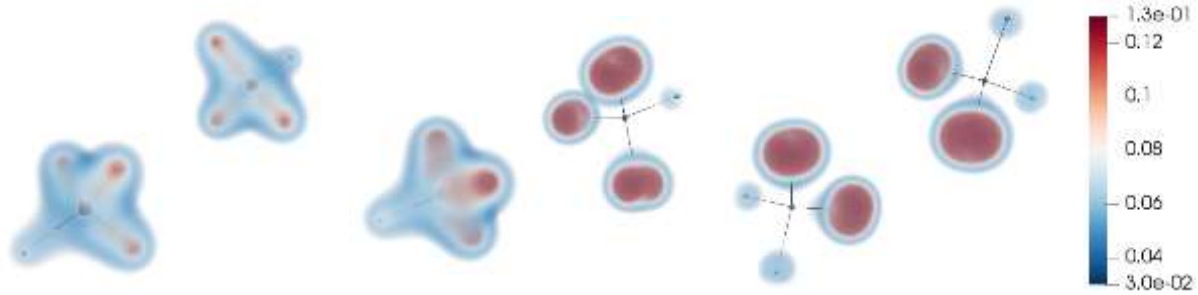

Figure 3. DID plots of complexes of **1-H** and **1-F**. a) **1-HH1**. b) **1-HF1**. c) **1-FF2**. Red depicts strong contributions towards dispersion, blue depicts weak contributions.

Yet another approach to gauge the origin of dispersion is to estimate atomic polarizabilities using a quantum theory of atoms in molecules (QTAIM) approach.[50] We employed the software PolaBer[51] which uses the partitioning of molecular (hyper)polarizabilities proposed by Keith and implemented in *AIMAll*.[52] The atomic polarizabilities were determined from MP2/def2-TZVPPD relaxed electron densities and visualized by tri-axial ellipsoids. The three axes of the ellipsoids represent the anisotropic polarizabilities with their volumes proportional to the corresponding isotropic values (Figure 4). The atomic polarizabilities in **1-H** and **1-F** are compared to the isolated ground-state values in Table 3.

a) **1-H** b) **1-F**

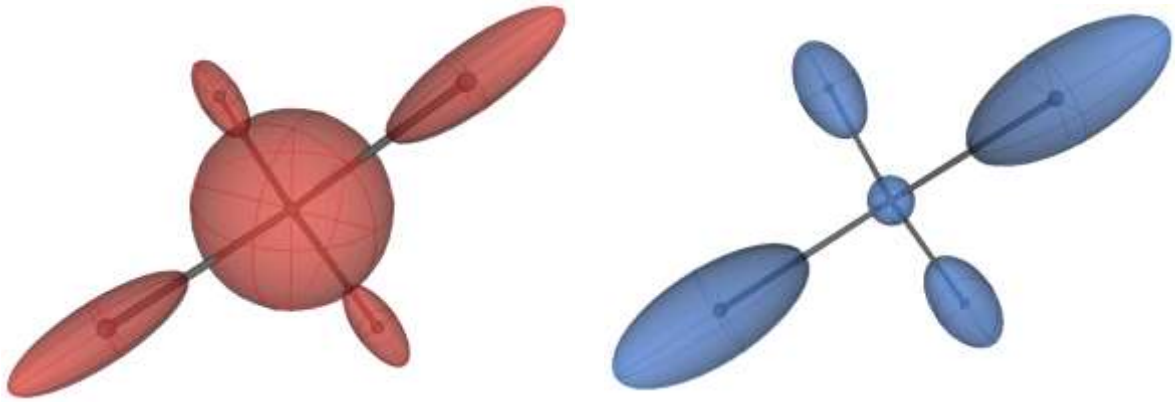

Figure 4. PolaBer plots visualizing the atomic polarizabilities of a) **1-H** and b) **1-F** using tri-axial ellipsoids representing the anisotropy with volumes depicting the isotropic values.

Table 3. Polarizabilities of carbon, hydrogen and fluorine as free atoms and in CH_4 or CF_4 molecules, respectively, as obtained from PolaBer.

Atom Type	**Polarizabilities [Å³]**		
	Free Atom	**CH_4**	**CF_4**
C	1.76[53]	0.867	0.283
H	0.667[54]	0.376	-
F	0.557[53]	-	0.618

The results show that in **1-H** the atomic polarizability of the carbon atom is the biggest while in **1-F** the atomic polarizabilities of the fluorine atoms are larger (cf. Figure 4). This is in contrast to the relative magnitude of the polarizabilities of atomic carbon and fluorine (atomic carbon is more polarizable than atomic fluorine, cf. Table 3).[55] This suggests that London dispersion in **FF** systems originates mainly from fluorine atoms because not only are they most polarizable, they are also on the outside of the molecules.

Simple Interaction Models. After EDA, we were interested in using simple interaction models to describe trends in dispersion. The idea was to use the London dispersion formula[56] (Equation 6) to approximate the interaction between the interacting molecules, which would effectively be treated as interacting spheres having the properties of the whole molecules:

$$E_{disp} = -\frac{3}{2}\,\frac{I_1 I_2}{I_1 + I_2}\,\frac{\alpha_1 \alpha_2}{R^6} \qquad (6)$$

For this admittedly crude model, we used MP2/CBS(34) ionization potentials and MP2/def2-TZVPD molecular polarizabilities. When using the average distance of the two carbon chains the resulting energies correlated poorly to benchmark BIEs (Supporting Information). Using the R^{-6}-weighted distance between the atoms mainly responsible for dispersion, i.e. using carbon atoms in **H** and fluorine atoms in **F**, a linear correlation was obtained (cf. Figure 5a).

a) Molecular London Dispersion Model. b) Atom-pairwise London Dispersion Model.

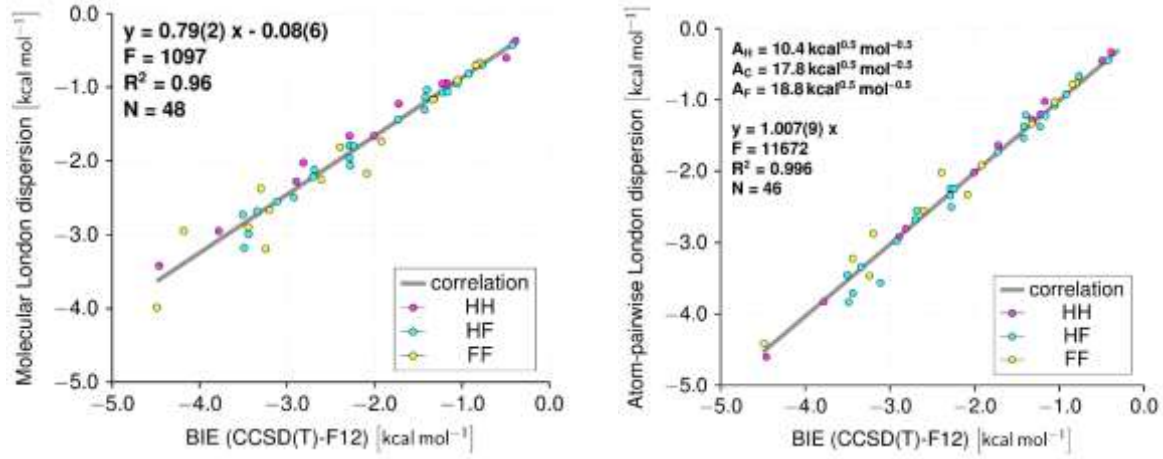

Figure 5. a) Intermolecular dispersion was estimated with the London dispersion formula (Equation 6) using molecular ionization potentials and molecular polarizabilities and compared to CCSD(T)-F12 BIEs. b) Intermolecular dispersion was estimated using atom-pairwise London dispersion by optimizing atom-type-dependent pre-factors A (cf. Equation 8) to reproduce the benchmark BIEs. The corresponding best set of A parameters is provided in the top-left of the diagram.

As an alternative, we also applied an atomistic interaction model using the London dispersion formula (Equation 6), very much akin to the approach of atom-pairwise dispersion corrections.[57] We determined all atom-pairwise contributions to the overall BIEs using the atomic polarizabilities of the isolated non-interacting molecules as obtained from PolaBer. Then, we optimized the atom-type dependent parameters for the ionization potential contributions to best reproduce the benchmark energies. To do that, we used an approximation of the London dispersion formula explained in the following section simplifying the ionization potential pre-factor (which we term A_{12}) as product of atom-type dependent pre-factors A_1 and A_2 (cf. right-hand side of Equation 8). The motivation for using this approximation is explained in the following section. The corresponding results are depicted in Figure 5b. It shows that with the optimized set of A pre-factors the overall BIEs are reproduced well across all the complexes. Additionally, based on this model, we decomposed the overall dispersion into contributions of atom type pairs. The corresponding results provide even quantitatively comparable results to LED (Details in the Supporting Information).

Interaction Descriptors. After having looked into interaction models, we were interested in simple interaction descriptors that would characterize the dispersive interaction capabilities of **H** and **F**. Dunitz proposed the ratio Q of polarizability α and volume V, a dimensionless quantity, as a simple measure to quantify dispersion of atoms and molecules:[3]

$$Q = \frac{\alpha}{V} \tag{7}$$

However, as he also acknowledged,[3] he ignored the linear dimensions of the molecules and did not account for the actual polarizabilities of the atoms in the molecules and their spatial distribution. When comparing the definition of Q (Equation 7) and the London dispersion formula (Equation 6) one can see that the dimensionless fraction of the product of polarizabilities α_1 and α_2 divided by the sixth power of the distance R is effectively the product of two Q values (Q_1 and Q_2):

$$E_{disp} = -\frac{3}{2}\,\frac{I_1 I_2}{I_1 + I_2}\,\frac{\alpha_1 \alpha_2}{R^6} = -\frac{3}{2}\,\frac{I_1 I_2}{I_1 + I_2}\,\frac{\alpha_1 \alpha_2}{R^3 R^3} = A_{12}\, Q_1 Q_2 \approx A_1 A_2\, Q_1 Q_2 \tag{8}$$

From this comparison, it is clear that the volume in Equation 7 should not be an atomic or a molecular volume but rather the "interaction volume" R^3, i.e. a volume derived from the interaction distance of the atoms. Using "interaction volumes" one explicitly accounts for the linear dimensions of molecules and the spatial distribution of polarizability therein. Therefore, we defined an alternative atomic Q metric called Q_{atom} as the fraction of the atomic polarizability of an atom in a molecule and the interaction volume R^3 of the atom with respect to a specific point in space. Hence, Q_{atom} is a function of the reference point used for its computation. It quantifies the dispersive interaction capability of specific atoms in a molecule with respect to that point in space and explicitly accounts for the position of an atom in a molecule. Using this definition, we computed the maximum Q_{atom} of hydrogen, carbon and fluorine in **H** and **F** of different carbon chain lengths with respect to points on their van der Waals surface (Details in the Supporting Information). The corresponding results are depicted in Figure 6a showing that the maximum Q_{atom} of fluorine in **F** is larger than the value of either hydrogen or carbon in **H**. However, in **F** the value of carbon is reduced significantly compared to **H**.

a) Q_{atom} against carbon chain length.

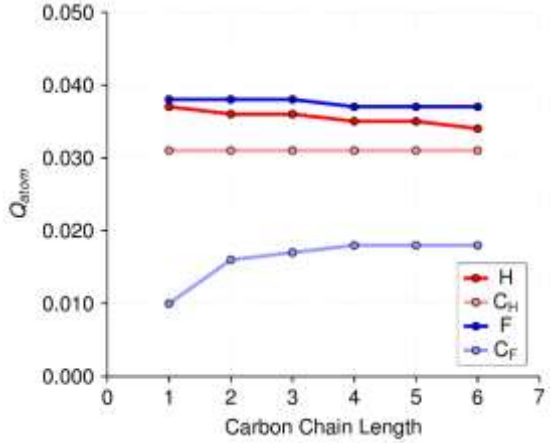

b) P_{atom} against carbon chain length.

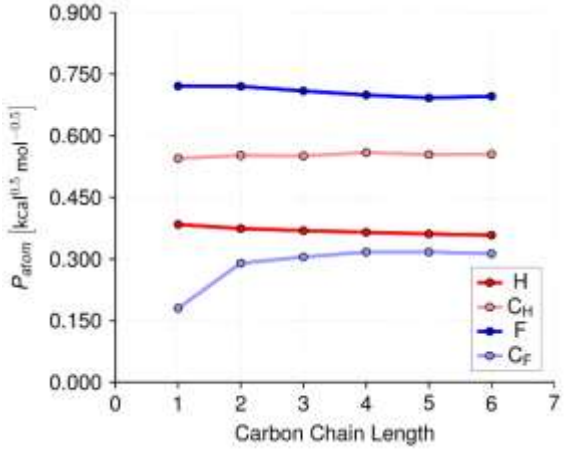

Figure 6. a) Maximum Q_{atom} values on the van der Waals surface for all atom types in **H** and **F** (cf. Equation 7). b) Maximum P_{atom} values on the van der Waals surface for all atom types in **H** and **F** (cf. Equation 9). C_H refers to carbon atoms in **H**, C_F to carbon atoms in **F**.

To judge also the total dispersive interaction capability of a molecule we defined a second type of Q metric termed Q_{tot} as the sum of all Q_{atom} of a molecule and hence it quantifies the dispersive interaction capability of a molecule with respect to a specific point in space. This metric explicitly accounts for the linear dimensions and the spatial distribution of polarizability of a molecule. Using this definition, we computed the average Q_{tot} of **H** and **F** with respect to points on their van der Waals surface (Details in the Supporting Information). We find that Q_{tot} of **F** having one to six carbon atoms is about 83% of Q_{tot} of the corresponding **H**. The main reasons for the lower Q_{tot} in **F** are the significantly reduced Q_{atom} of carbon in **F** compared to **H** and the larger size of fluorine compared to hydrogen. Using Dunitz' Q metric (i.e. using molecular polarizability and molecular volume) one would estimate the corresponding ratio to be only 64%. These results show that Dunitz' Q metric significantly underestimates the interaction capabilities of **F** and, hence, stress the importance of accounting for linear dimensions and spatial polarizability distributions.

These results also show that, from Q_{tot}, one would estimate the dispersive interaction capabilities of **F** to be generally weaker than **H**. However, when looking again at the London dispersion formula (Equation 8, *vide supra*) we can see that in order to determine the dispersion energy we need the product of Q_1 and Q_2 as well as the pre-factor A_{12}. In the London dispersion formula, the pre-factor is estimated from the ionization potentials I_1 and I_2 of the interacting atoms. When comparing the dispersive interaction capability of different classes of compounds, which likely have distinct atomic ionization potentials, the pre-factor needs to be taken into account. We assumed that A_{12} can be separated into the product of atom-type-dependent factors A_1 and A_2 (cf. Equation 8, right-hand side). We determined these factors for carbon, hydrogen and fluorine by reproducing the benchmark BIEs of all our model systems using the atom-pairwise London dispersion model (*vide supra*). With the optimized parameters, the benchmark energies could be reproduced with an overall MAD_{rel} of 5% and all subsystems were reproduced equally well. Using these atom-type-dependent factors, we defined a new measure to quantify dispersive interaction capabilities termed P. It is the product of the atom-type-dependent factor A and Q and has the dimension of the square root of energy. It is defined such that the dispersion energy could be estimated as the product of two P measures, P_1 and P_2 (cf. right-hand side of Equation 8):

$$P = AQ = A\frac{\alpha}{V} \tag{9}$$

Analogously to Q_{atom} and Q_{tot}, we defined P_{atom} and P_{tot} and determined P_{atom} values of hydrogen, carbon and fluorine atoms in **H** and **F**. The results are depicted in Figure 6b. Compared to the relative magnitudes of the corresponding Q_{atom} values, the P_{atom} values of carbon and fluorine are elevated, the values of hydrogen reduced (the ratio of the pre-factors is $A_H : A_C : A_F = 0.55 : 0.94 : 1.0$). In addition, we also determined the corresponding P_{tot} values and found that the average value of **F** is about 116% of the corresponding value of **H**. Furthermore, the ratios of P_{tot} of **F** and **H** decrease linearly with the relative molar carbon content (Details in the Supporting Information). However, since the relative molar carbon content in **H** and **F** is always between a fifth and a third, based on this linear correlation, the lowest possible ratio of the P_{tot} of **F** and **H** is 108%. This suggests that, at least in the respective extended conformer, no fully saturated **F** with a weaker intrinsic dispersion interaction capability than the analogous **H** can exist.

It should be noted that the difference in P_{tot} of **H** and **F** is only properly reflected in the interaction energies of **1-FF** and **1-HF** compared to **1-HH** but not in the complexes with longer carbon chains. This suggests that the main reason for **FF** and **HH** having about equal interaction energies in longer systems

(and **HF** having weaker interaction energies) is not the respective intrinsic capability for dispersive interactions but rather the interaction geometries. Therefore, we will investigate them in more detail in the following section.

Interaction Geometries. We already used DID plots to visualize the origin of disperion in the intermolecular complexes (*vide supra*). An alternative way to visualize non-covalent interactions (NCIs) is provided by the NCI plots.[58] They are based on the analysis of electron densities and their derivatives and provide a visualization of interaction surfaces together with information about which portions of the surface are attractive or repulsive.[58] Notably, they are based solely on electron density and cannot distinguish between different types of van der Waals interactions.[58] They provide orthogonal information compared to DID plots as they allow assessing how well molecular complexes are aligned. Figure 7 shows 3D NCI plots of complexes of **5-H** and **5-F**. The striking difference between the interaction surfaces in **5-HH1**, **5-HF4** and **5-FF1** is the very regular shape in **5-HH1** compared to the increasingly irregular shapes observed in **5-HF4** and **5-FF1**. Only certain portions of the interaction surfaces of **5-HF4** and **5-FF1** show strong interactions (attractive or repulsive) while in **5-HH1** strong interactions are distributed uniformly over the whole intermolecular interface. These observations suggest that the preferred intramolecular geometries of **F** are unsuitable for intermolecular interactions with either **H** or **F** which results in lower interaction energies for these complexes than would otherwise be attainable.

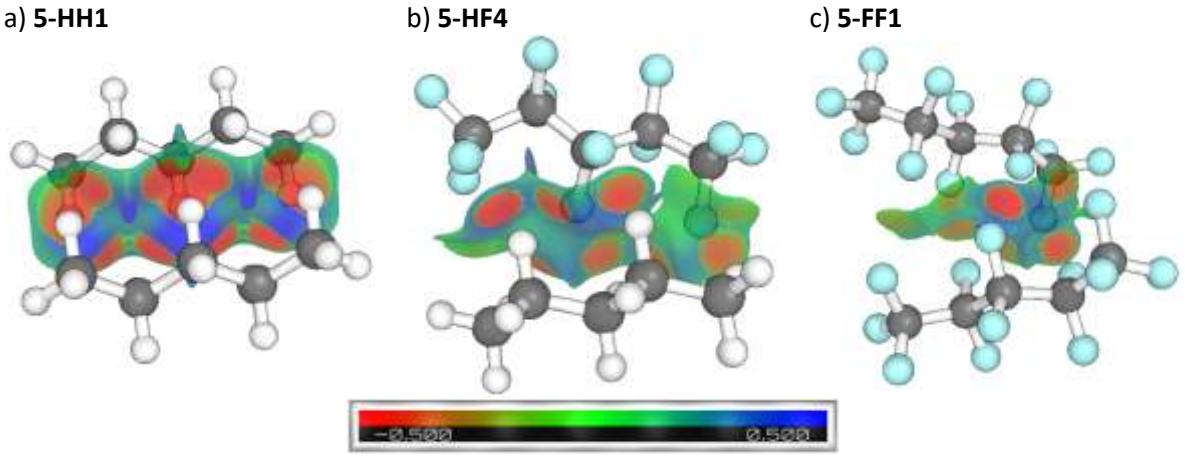

Figure 7. 3D NCI plots of complexes of pentanes: a) **5-HH1**. b) **5-HF4**. c) **5-FF1**. Red depicts repulsive interactions, green depicts neither attractive nor repulsive interactions, and blue depicts attractive interactions. The selected conformers have the strongest BIEs of the corresponding type of complex.

Consequently, we sought to collect further evidence about the interaction geometries. Therefore, we looked into the scaling of the total surface area and the interaction surface area of the different complex classes. The total surfaces of **H** and **F** and the interaction surfaces of **HH**, **HF** and **FF** increase linearly with the carbon chain length (Details in the Supporting Information). Using simple geometric models of cuboids to represent the interacting molecules we deduced that in **FF** only about 81% and in **HF** only about 85% of the additional interaction surface is used for interactions when the chains are elongated (Details in the Supporting Information). These results corroborate the visual impression of Figure 7 and confirm that in both **HF** and **FF** not all the potential surface is used for intermolecular interactions.

To obtain more direct evidence for the differences in interaction geometries of **HH**, **HF** and **FF** we introduced a new geometric measure to characterize the alignment between two interacting fragments, which we term the number of van der Waals contacts ($n_{contact}$). We defined one contact as

two atoms at a distance equal to the sum of their van der Waals radii (R_{vdW}). To have a continuous scale for atoms that are closer or farther apart than R_{vdW} and to account for the distance dependence of van der Waals interactions we defined the number of contacts between two atoms as follows:

$$n_{contacts} = \frac{{R_{vdW}}^6}{R^6} \tag{10}$$

The number of contacts between two interacting molecules then is the sum of all atom-pairwise contacts. We computed this new geometric measure for all complexes under study and investigated it as a function of carbon chain length (Figure 8a). There are several things to be noted. First, all the complexes with one carbon atom in the monomers have about the same number of contacts. Secondly, all classes of intermolecular complexes show a linear correlation of $n_{contacts}$ with the number of carbon atoms. Additionally, **HH** have a significantly larger increase of the number of contacts with the carbon chain length than either **HF** or **FF**. Furthermore, **HF** shows a marginally larger increase of the number of contacts with the carbon chain length than **FF**. These results provide additional evidence for the poor interaction geometries in **HF** and **FF**. Moreover, to test our newly introduced parameters, we correlated the BIEs of all the complexes against the product of $n_{contacts}$ and the P_{tot} values of the respective interacting molecules and observed a reasonable correlation (cf. Figure 8b).

a) Number of contacts.

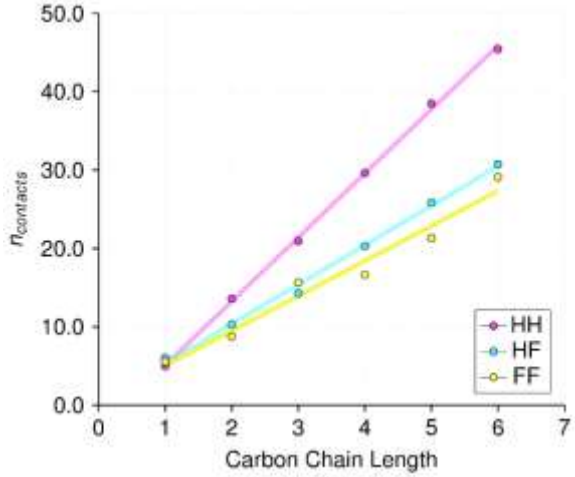

b) Correlation of BIE against $n_{contacts}$ $P_{tot,1}$ $P_{tot,2}$.

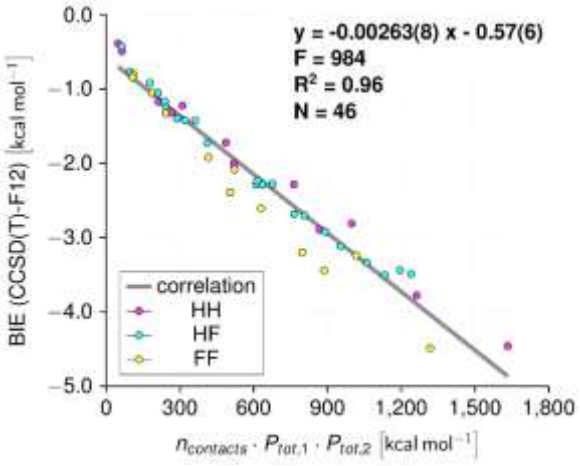

Figure 8. a) Number of van der Waals contacts ($n_{contacts}$) in **HH**, **HF** and **FF** as a function of carbon chain length. b) BIE of the intermolecular complexes correlated against the product of $n_{contacts}$ and the P_{tot} values of the respective interacting molecules.

Computed Microscopic and Macroscopic Mixing Behavior. Having established reliable methods to compute the interaction energies of **H** and **F** we compared the relative BAEs of **HH**, **HF** and **FF** as a function of carbon chain length (Figure 9a). As the carbon chain length is increased, the relative BAEs of both **HF** and **FF** get weaker compared to **HH**. The effect is most pronounced in **HF** and somewhat less so in **FF**. Furthermore, assuming that **HH**, **HF** and **FF** have comparable interaction geometries both in the molecular complexes and in the bulk phase (i.e. including packing effects), we estimated the bulk BAEs in pure **H**, pure **F**, as well as in mixed bulk phases of **H** and **F**. To do that, we multiplied the association energies by the average coordination numbers derived from the molecular and the interaction surfaces, which is a treatment of the bulk phase at the level of Flory-Huggins solution theory (Details in the Supporting Information).[59,60] The corresponding results are illustrated in Figure 9b.

a) Relative Microscopic BAEs. b) Relative Macroscopic BAEs.

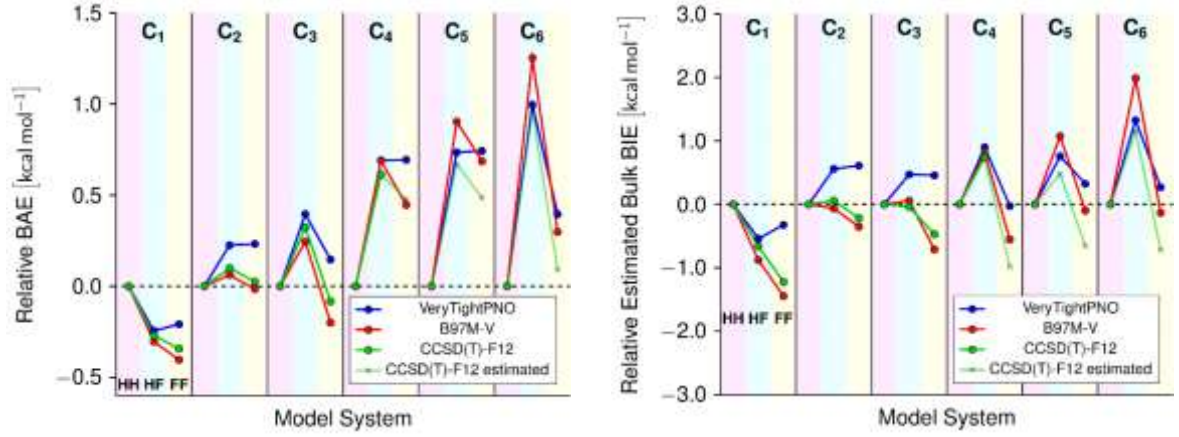

Figure 9. Relative BAEs of strongest binding isomers of **HF** and **FF** compared to the respective **HH** from one to six carbon atoms (labelled C_1 to C_6). a) Microscopic BAEs, b) bulk BAEs.

Additionally, we also looked into the relative energies of mixing of **HH** and **FF** to form two complexes of **HF** (Table 4, "CCSD(T)"). The relative energies of microscopic and macroscopic mixing on the basis of CCSD(T)-F12 change from favorable (C_1) to increasingly unfavorable (C_2 to C_6). As the carbon chain length is increased, two **HF** complexes are increasingly unfavorable compared to one **HH** and one **FF** complex. The mixing properties are almost equally determined when using the interaction energies of the crude molecular London dispersion model (Table 4, "London"). The trends of these energies are governed by the distances. When the ionization potential pre-factor and the polarizabilities are assumed to be one (with the appropriate unit), i.e. only the distances are taken into account, the computed mixing remains unaffected (Table 4, "Distance").

Table 4. Relative energies of mixing as a function of carbon chain length: HH + FF ⇌ 2 HF.

Chain Length	Accounted Isomers	Relative Energies of Mixing [kcal mol^{-1}]					
		CCSD(T) Microscopic	CCSD(T) Macroscopic	London Microscopic	London Macroscopic	Distance Microscopic	Distance Macroscopic
1	Strongest	-0.20	-0.19	-0.06	1.29	$-4.0 \cdot 10^{-5}$	$33 \cdot 10^{-5}$
	Average	0.07	0.32	0.04	0.14	$1.9 \cdot 10^{-5}$	$11 \cdot 10^{-5}$
2	Strongest	0.18	0.67	0.17	0.24	$4.9 \cdot 10^{-5}$	$9.5 \cdot 10^{-5}$
	Average	0.24	0.93	0.12	0.15	$3.7 \cdot 10^{-5}$	$3.8 \cdot 10^{-5}$
3	Strongest	0.73	0.79	0.81	1.85	$10 \cdot 10^{-5}$	$16 \cdot 10^{-5}$
	Average	0.62	0.95	0.68	1.53	$8.2 \cdot 10^{-5}$	$13 \cdot 10^{-5}$
4	Strongest	0.75	6.31	0.37	0.21	$3.2 \cdot 10^{-5}$	$0.02 \cdot 10^{-5}$
	Average	0.25	2.91	-0.02	0.25	$-0.2 \cdot 10^{-5}$	$1.2 \cdot 10^{-5}$
5	Strongest	0.85	3.23	0.67	1.98	$3.7 \cdot 10^{-5}$	$6.8 \cdot 10^{-5}$
	Average	0.72	3.01	0.36	0.75	$1.8 \cdot 10^{-5}$	$2.0 \cdot 10^{-5}$
6	Strongest	1.84	6.01	0.93	0.93	$3.5 \cdot 10^{-5}$	$3.4 \cdot 10^{-5}$
	Average	0.99	6.08	0.46	1.66	$1.5 \cdot 10^{-5}$	$4.4 \cdot 10^{-5}$

"Strongest" denotes that only the strongest isomer was considered. "Average" denotes that the energies of all isomers were averaged. "CCSD(T)" values are based on CCSD(T)-F12/VDZ energies (Details in the Supporting Information). "London" values are based on the molecular London dispersion model (cf. Figure 5a). "Distance" values are based on the R^{-6}-weighted average distances assuming the other factors to have numerical values of 1 with the appropriate units.

Trends in Experimental Properties. The last step was to look into trends of experimental properties of **H** and **F** and compare them to our computational results. The properties considered and the corresponding information they provide are summarized in Table 5.

Table 5. Experimental bulk properties of **H** and **F** selected and the information they provide.

Symbol	Bulk Property	Unit	Information

$\Delta_{vap}H°$	Enthalpy of Vaporization	kcal mol^{-1}	Strength of intermolecular interactions and packing in the liquid.
T_{boil}	Boiling Point	K	Strength of intermolecular interactions, packing in the liquid and conformational flexibility.
a/b	Critical Parameters Ratio	kcal mol^{-1}	Strength of intermolecular interactions and dependence on intermolecular orientation in the fluid.
γ	Surface Tension	mN m^{-1}	Strength of intermolecular interactions and packing in the liquid.
π_T	Internal Pressure	MPa	Dependence of strength of intermolecular interactions on incremental volume changes and packing in the liquid.
K	Bulk Modulus	MPa	Dependence of strength of intermolecular interactions on incremental volume changes and packing in the liquid.
β_T	Isothermal Compressibility	GPa^{-1}	Dependence of strength of intermolecular interactions on incremental volume changes and packing in the liquid.
η	Dynamic Viscosity	mPa s	Strength of intermolecular interactions and shape of molecules.
c_p	Molar Heat Capacity	cal mol^{-1} K^{-1}	Number of internal degrees of freedom and barrier height between them.
B_{ij}	Second Virial Coefficients	dm^3 mol^{-1}	Strength of homomolecular and heteromolecular interactions and orientational dependence of energies in the gas.

Most of the bulk properties investigated provide direct or indirect information about the strength of intermolecular interactions, about the packing in the liquid or a combination thereof. However, since they are based on distinct experimental measurements they provide mutually supporting evidence about the corresponding molecular origins. The comparison of the trends of all these experimental measures for **H** and **F** with respect to the carbon chain length is illustrated in Table 6. Individual values with the corresponding references are provided in the Supporting Information. All properties considered except for the dynamic viscosity and the molar heat capacity show an inversion when **F** and **H** with increasing carbon chain length are compared. The enthalpies of vaporization show an inversion between seven and eight carbon atoms, the boiling points show an inversion between three and four carbon atoms and all the other properties show an inversion between one and two carbon atoms. Notably, the boiling point differences and the differences in the critical parameters ratio correlate reasonably with the relative molar carbon content in the molecules (Details in the Supporting Information). The ratio of surface tensions also correlates somewhat with the relative molar carbon content and the differences in the enthalpies of evaporation correlate with the number of carbon atoms.

Table 6. Comparison of trends of experimental bulk properties in **F** and **H**. The second column specifies whether the difference between **F** and **H** or the ratio of **F** to **H** was used to compare the properties.

Legend: **F > H** **F = H** **F < H**

Property	Comparison	Carbon Chain Length								
		1	2	3	4	5	6	7	8	9
$\Delta_{vap}H°$	Difference	0.88	0.35	0.50	0.46	0.31	0.29	0.17	-0.17	-0.33
T_{boil}	Difference	34.1	10.4	2.9	-2.0	-6.6	-11.6	-16.5	-19.7	n.a.[a]
a/b	Difference	0.25	-0.08	-0.17	-0.26	-0.32	-0.39	-0.44	-0.45	n.a.[a]
γ	Ratio – 1	0.28	-0.22	-0.23	-0.30	-0.37	-0.38	-0.34	-0.34	n.a.[a]
π_T	Difference	21	-26	-41	-67	-67	-59	-46	-26	n.a.[a]
K	Ratio – 1	0.48	-0.33	-0.54	-0.57	-0.52	-0.42	-0.40	-0.38	n.a.[a]
β_T	Ratio – 1	-0.32	0.21	0.94	0.76	1.35	0.92	0.58	0.39	n.a.[a]
η	Difference	0.05	0.11	0.19	0.38	0.62	0.97	1.31	2.02	n.a.[a]
c_p	Difference	5.8	13.6	19.9	30.0	35.4	37.7	45.1	n.a.[a]	n.a.[a]

[a]n.a. means data not available.

In addition to the properties compared in Table 6, we used experimental second interaction virial coefficients[61–63] to assess energies of mixing of **H** and **F** having equal carbon chain length (cf. Figure 10a). First, it should be noted that all the second interaction virial coefficients are negative indicating that they are measured below the respective Boyle temperature and, hence, in the attractive regime of intermolecular gas interactions. Secondly, the sum of the homomolecular second interaction virial coefficients is more attractive than the corresponding heteromolecular coefficients indicating that interactions between **H** and **F** are less favorable than interactions of **H** with **H** and **F** with **F**. Additionally, Knobler *et al.*[61–63] found the interactions in hydrocarbon-fluorocarbon mixtures to be about 10% weaker than estimated by the geometric mean. On average, we obtain comparable results when looking at CCSD(T)-F12 energies, the London dispersion interaction model and the R^{-6}-weighted distances (11%, 9% and 9% weaker interactions on average, respectively, Details in the Supporting Information).

a) Second Interaction Virial Coefficients. b) $\Delta_{vap}H°$ against bulk BAEs.

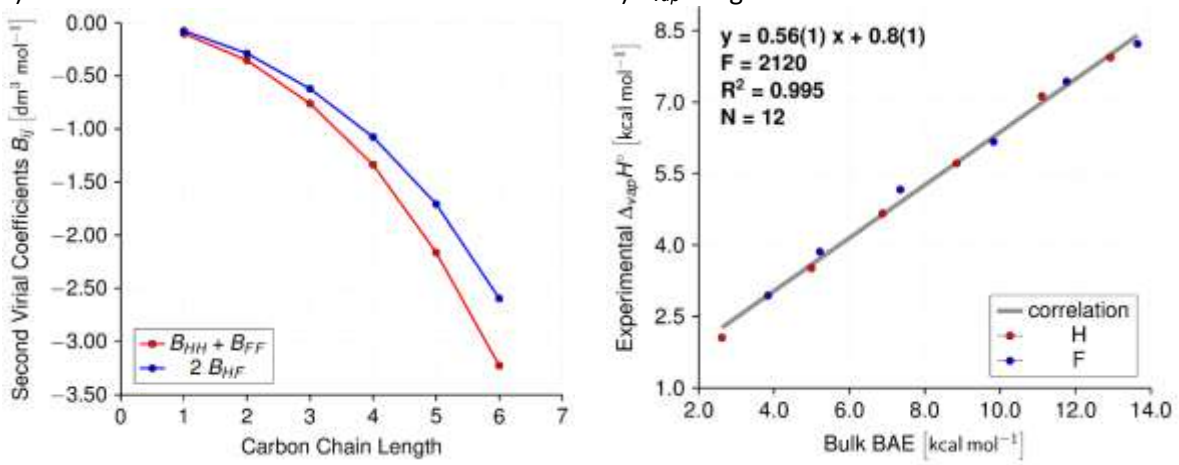

Figure 10. a) Comparison of experimental second virial coefficients of homomolecular (red) and heteromolecular (blue) interactions as a function of carbon chain length. Homomolecular interactions are more attractive. b) Experimental enthalpies of evaporation ($\Delta_{vap}H°$) of **H** and **F** of increasing carbon chain length correlated against computed bulk BAEs from CCSD(T)-F12/VDZ.

Lastly, we also compared the estimated bulk-phase interaction energies in **H** and **F** against experimental enthalpies of evaporation (Figure 10b). For these values to be as comparable as possible, we chose experimental values at rather low and comparable temperatures (Details in the Supporting Information). Figure 10b shows a good correlation suggesting the computational BAEs to be a good estimate of the strength of intermolecular interactions. However, it needs to be emphasized that we are only considering enthalpies here and, hence, neglect entropy.

Discussion

Summarizing our results leads to four main conclusions:

i. Most well-established computational methods for describing dispersion have difficulties to properly describe the interactions in alkane-perfluoroalkane and perfluoroalkane-perfluoroalkane complexes.
ii. The dispersive interactions in perfluoroalkane dimers come mainly from interactions between fluorine atoms.

iii. Perfluoroalkanes have a higher intrinsic ability for intermolecular dispersion than alkanes with equal carbon chain length but the unsuitable interaction geometries of perfluoroalkane dimers compared to alkane dimers result overall in roughly equal interaction energies.
iv. The differing trends of various experimental porperties of alkanes and perfluoroalkanes with increasing carbon chain length can be explained by the concomitant increasing relative molar carbon content and the increasingly unsuitable interaction geometries of perfluoroalkanes.

We will investigate these four claims in detail.

Benchmarking Interaction Energies. The accurate description of noncovalent intermolecular interactions, especially of London dispersion, has been one of the main themes of research in the field of computational chemistry in recent years.[57,64–68] In DFT, several dispersion correction schemes have been developed[57,64] in order to obtain accurate intermolecular interaction energies of (partially) dispersion-bound molecular complexes and many of them have been shown to be accurate in describing the interactions of "ordinary" organic molecules.[67,69,78–80,70–77] Within this work, we made use of the D3 correction,[81,82] the XDM correction,[36–39,83] the dDsC correction,[84–86] the VV10 correction,[87] Minnesota functionals[88,89] with implicit treatment of dispersion and the vdW-DF10 density functional[90] to test their performance in the computation of intermolecular complexes of **H** and **F**. In WFT, CCSD(T) energies at the CBS limit are considered the gold standard for computing interaction energies of dispersion-bound systems.[16,66,75,91–95] In addition, recently, the low scaling DLPNO-CCSD(T) approach has been developed which promises near CCSD(T) accuracy at significantly lower computational cost, especially for medium-sized molecules with 20 – 200 atoms, or even larger systems.[29–31,96–99] However, the systematic investigation of interaction energies of perfluoroalkanes has not received wide attention[15–17,26,27] and, to the best of our knowledge, there are currently no good benchmark data available for the interaction between linear perfluoroalkanes of increasing chain length. Our CCSD(T)-F12/VDZ interaction energies fill that gap. Surprisingly, we find that many computational methods designed to describe dispersion accurately fail in reproducing benchmark interaction energies of **HF** and, especially, **FF**. Even DLPNO-CCSD(T), the most systematic low-cost computational method we tested, requires tighter than usual cutoff parameters to obtain most accurate results and even then the errors still amount to 9% of the benchmark energies for **FF**.

We find that the most robust and efficient level of theory to determine the interaction energies of alkane and perfluoroalkane dimers is B97M-V.[34] Most notably, it performs as well as DLPNO-CCSD(T) with extremely tight parameters (ExtremePNO, Details in the Supporting Information) across all the systems, and performs by far the best for **FF** with an MAD_{rel} of only 3% (cf. Table 2). ωB97M-V performs only slightly worse but is also more expensive. Additionally, the XDM dispersion correction performs very well compared to most of the alternative corrections. B3LYP-XDM yields excellent results for both **HH** and **HF**, and is acceptable for **FF** despite significant underestimation of the corresponding BIEs. Overall, many DFT and WFT approaches show different problems in calculating the BIEs of our model systems and, therefore, there is likely not one universal explanation for their failure (Details in the Supporting Information). While most approaches perform well for estimating the interaction energies of **HH**, **HF** and **FF** seem to be problematic for most of the methods used. The ad-hoc explanation for that failure is the absence of good benchmark data for these types of interactions. Therefore, the benchmark data provided will contribute to the development of more accurate (cheap) electronic structure methods. Additionally, the benchmarking was the stepping-stone for all subsequent analyses to understand the quality and quantity of the intermolecular interactions in the investigated complexes.

Energy Decomposition Analysis and Interaction Models. The decomposition of interaction energies of molecular complexes is one of the main computational approaches to gain physical and chemical insight into structure and reactivity.[100] Symmetry-adapted perturbation theory (SAPT)[43–46] belongs to the more widely used methods of EDA. It decomposes the overall interaction energy into electrostatics, exchange, induction and dispersion in a well-defined way. Local energy decomposition (LED), which is based on DLPNO methods, is a very recent addition to the multitude of EDA methods.[47] However, only the dispersion energy components of LED and SAPT can be directly compared because the underlying theoretical framework for the other components is different. Therefore, we decided to use SAPT for interpretation of all the energy components provided therein and only looked into the dispersion energy components of LED. In addition to classical EDA methods, an increasing number of methods for the visualization of intermolecular interactions and their origin have been developed, of which DORI,[101] NCI,[102] DID[49] and PolaBer[103] are just a few more recent examples. Their appeal lies in the connection of computed numbers indicating interaction strengths and visual images illustrating the results, which makes them easier for the human brain to grasp.

As would be expected for complexes of nonpolar molecules,[3] SAPT determines repulsive exchange and dispersion to be the major energy components in our test systems. Based on Figure 1, no significant difference in the contributions of the energy components between **HH**, **HF** and **FF** can be seen, suggesting that the general type of interaction is of the same nature. However, when looking closer at the effective dispersion contributions in the three subclasses, the contribution of dispersion increases slightly when going from **HH** via **HF** to **FF** (Supporting Information). These results are in contrast to the results of previous EDA studies of **H** and **F** homo- and heterodimers which found effective dispersion to be weakest in **HF** and strongest in **HH**.[3] Notably, SAPT does not estimate the electrostatic component to be bigger in **HF** than in either **HH** or **FF**, which has also been found by previous EDA studies.[3] This might seem surprising as the hydrogen and fluorine atoms on the outside of the interacting molecules have opposite polarization. However, for every attractive electrostatic contribution stemming from interactions between hydrogen and fluorine atoms there are repulsive electrostatic contributions between hydrogen and carbon atoms and between carbon and fluorine atoms which compensate the attractive components.[3]

The major finding of LED, the DIDs and the PolaBer plots is the identification of fluorine atoms being the major dispersion energy donors in **F**. The strong electronegativity difference between carbon and fluorine results in an *Umpolarisierung* of the isolated atomic polarizabilities, a phenomenon well-known in the computational community but its implications are usually not clearly expressed.[36,39,57,64,82,104,105] This *Umpolarisierung* can be readily understood using Sanderson's electronegativity equalization principle.[106–110] Fluorine atoms are much more electronegative than carbon atoms. Hence, electronegativity equalization estimates transfer of electron density from carbon to fluorine until the corresponding local electronegativites are equal. The local electronegativity of fluorine bonded to carbon will be lower than its isolated atomic electronegativity. The corresponding local electronegativity of carbon will be higher. Polarizability was shown to be correlated reasonably well to electronegativity[111] resulting in the estimation that the polarizability of fluorine bonded to carbon will be higher than its isolated atomic polarizability and that the corresponding polarizability of carbon will be lower with the caveat that the presence of the bond between the two atoms reduces both polarizabilities. Alternatively, the change in local polarizabilities can also be explained using hardness and softness from conceptual density functional theory,[109,110,112,113] which are closely related to the concept of hard and soft acids and bases (HSAB).[114,115] Electronegativity equalization of fluorine and carbon will lead to a local positive charge

on carbon and a local negative charge on fluorine. The local positive charge on carbon will increase its local hardness and, hence, decrease its local softness. Softness has been shown to be correlated reasonably well to polarizability[109,110] inferring a concomitant decrease in polarizability. The local negative charge on fluorine will decrease its local hardness and increase its local softness leading to a concomitant increase in polarizability. Therefore, *Umpolarisierung*, i.e. effective transfer of polarizability from one bonding partner to another, is expected to occur whenever polar covalent bonds are formed and can therefore be understood using well-established chemical principles.

Further support is obtained from the simple interaction models used to estimate the BIEs in the complexes (cf. Figure 5). Using the molecular interaction model, only when dispersion was assumed to originate from carbons in **H** and fluorines in **F** were we able to reproduce the general BIE trends (Figure 5a). This simple interaction model using only molecular polarizabilities, molecular ionization potentials and the R^{-6}-weighted average interaction distance demonstrates that qualitative trends in dispersion can be estimated using very crude approaches. While many of the electronic structure methods show distinct deviations in the three subclasses of complexes (cf. Table 2), the molecular London dispersion model shows uniform systematic deviations from the benchmark BIEs indicating its robustness. Using the atom-pairwise dispersion interaction model, the benchmark BIE values were reproduced with an MAD_{rel} of 5% which is not much worse than the best ab initio methods employed (cf. Table 2). Together with the fact that also the decomposition into atomic contributions compares surprisingly well with the LED results, it suggests that the underlying model is physically meaningful and its parameters can be used and interpreted quantitatively. However, notably, the atom-pairwise interaction model estimates effective dispersion, which is a sum of the attractive and repulsive contributions to the overall interaction. This complicates the direct interpretation of the pre-factors obtained as differences in the repulsive part of the interaction potential will also impact their values.

Interaction Descriptors and Interaction Geometries. The recent paradigm shift in the recognition of the importance of dispersion in small molecules[116,117] has initiated a search for reliable dispersion energy donor descriptors that could quantitatively assess the ability of substituents in molecules for dispersion. Already several years ago, Dunitz proposed the ratio Q (Equation 7) as dimensionless quantity to gauge the potential of molecules for dispersive interactions.[117] He estimated atomic Q values for hydrogen, carbon and fluorine using polarizabilities and volumes of the free atoms and found that Q of fluorine is significantly smaller than Q of either carbon or hydrogen.[3] He also found the corresponding molecular Q values (using molecular polarizabilities and molecular volumes) of **F** to be significantly lower compared to Q values of **H**. Consequently, he assigned these low Q values as the origin of the distinct properties of **F** compared to **H**.[3]

Based on that work we defined an alternative Q measure using the "interaction volume" instead of the molecular volume. This is important because it explicitly accounts for the spatial distribution of polarizability within a molecule and the fact that close contacts result in higher dispersion. Using the molecular volume instead leads to a significant underestimation of the dispersive interaction abilities of **F** because the biggest portion of the polarizability is on the outside of these molecules (cf. Figure 4 and Table 3). To adequately quantify dispersive interaction capabilities across different classes of compounds, we introduced the P measure, which also accounts for the influence of the ionization potential of atoms on dispersion. The London dispersion formula estimates stronger dispersive interactions the larger the ionization potential of an atom. It is instructive in that regard to note that the trends of the ionization potentials in the periodic table are opposite to the trends of polarizabilities

which suggests that only looking at polarizabilities when estimating the strength of dispersion is insufficient.

The average P_{tot} on the van der Waals surface estimates **F** between one and six carbon atoms to have a stronger dispersive interaction ability compared to the corresponding **H**. In that regard it gives the opposite answer about **F** to the Q values proposed by Dunitz[3] and even the modified Q values proposed in this work. Additionally, it is counter to the general notion in literature that **F** have a low propensity to interact with other molecules,[3,8] despite the fact that both experimental[4,12] and computational[15–17] results show that, at least for **1-FF**, the interactions are significantly stronger compared to **1-HH** (*vide supra*). The average P_{tot} on the van der Waals surface does not quantify how strong molecules actually interact by dispersion but rather how strong molecules in principle could interact by dispersion if interaction geometries were ideal. However, they are not ideal in **HF** and **FF** with more than one carbon atom (cf. Figure 7) which is a consequence of the ground-state geometries of **F** being unsuitable for interaction and of the rigidity of **F**, a property well-established within the field of organofluorine chemistry.[7] Deformation of **F** from the ground-state geometries requires a significant portion of additional energy and is overall unfavorable. The ground-state geometries of short chain **H** are already ideal for intermolecular interaction and therefore no significant deformation is required for **HH**.

There is another notable aspect to the differences in the interaction geometries of **HH** and **FF**. While two molecules of **H** try to bring mainly the carbon atoms close together, two molecules of **F** try to bring as many fluorine atoms as possible close together to gain intermolecular interaction energy. Therefore, even if **F** was not too rigid the ideal interaction geometries of **FF** would still differ from **HH** because carbon atoms are in the center of the structures while fluorine atoms are on the outside of **F**. This is reflected in the interaction geometries of **2-FF** and **3-FF**. Figure 11 shows that while **3-HH** prefers the conformer which is based on inversion followed by translation normal to the plane of the carbon atoms, **3-FF** prefers the conformer that is based on inversion followed by translation in that plane (with some additional displacement normal to the plane). This observation supports our conclusions even further because this intrinsic difference in the interaction geometry preference also makes the ground-state geometries of dimers of increasingly long **F** less ideal for intermolecular interactions compared to **H.** It is easier for **H** to align many carbon atoms than it is for **F** to align many fluorine atoms.

a) **3-HH1** b) **3-FF2**

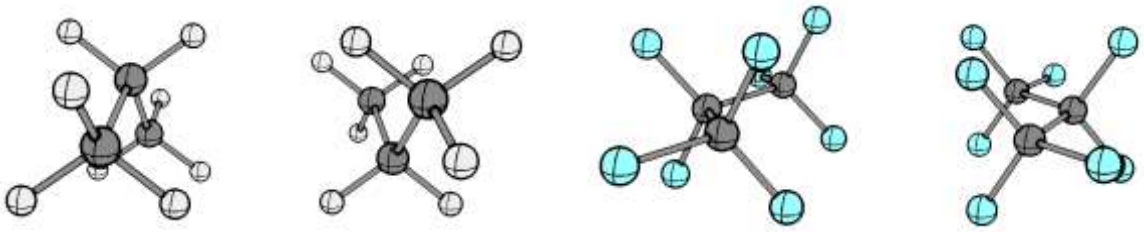

Figure 11. Comparison of most stable conformers of a) **3-HH** and b) **3-FF**.

The number of contacts ($n_{contacts}$, cf. Equation 10) is a quantitative measure to assess the interaction geometries and determines the number of van der Waals contacts between two interacting molecules. The idea is to define one van der Waals contact as two atoms at a distance corresponding to the sum of their van der Waals radii. This basic concept is closely related to the normalized contact distance which is commonly used in the analysis of intermolecular interactions in crystal structures.[118] The main difference is the use of the sixth power of the ratio of distances to account explicitly for the distance dependence of van der Waals interactions. The number of contacts does not suffer from significant systematic discrepancies for the different atom types as can be gleaned from the close values for **1-**

HH1, **1-HF1** and **1-FF2**, which all have close to ideal interaction geometries. In addition, for each group of complexes, $n_{contacts}$ shows a linear correlation with the number of carbon atoms demonstrating that $n_{contacts}$ scales linearly with interaction surface (the interaction surface scales linearly with the number of carbon atoms in these complexes, cf. Supporting Information) which is a very attractive property of this purely geometric measure. The newly introduced parameters P_{tot} and $n_{contacts}$ are a first step towards simple quantitative parameters to describe London dispersion between molecules or groups of atoms, which is demonstrated by the reasonable correlation observed between BIEs and the product of $n_{contacts}$ and the P_{tot} values of the interacting molecules (cf. Figure 8b). While P_{tot} quantifies the average strength of a dispersive contact, $n_{contacts}$ quantifies the number of contacts. Hence, in order to judge the overall interaction energy, both parameters need to be considered.

Based on these results, we propose that the reason for the weak interactions of **F** compared to **H** is their ground-state geometries, which are not ideal for intermolecular interactions. This is fully consistent with the cavity-based solubility model used to explain the solvent properties of fluorous solvents.[2,119] It is observed that molecular size plays an important role whether a solute is soluble in **F** or not. It is commonly stated in literature that, because of low intermolecular forces, **F** have large cavities in the bulk phase.[2,119] These cavities can be occupied readily by small molecules of suitable size. We would argue that the main reasons for the formation of cavities are the ground-state geometries and the high rigidity of **F**.[7] Hence, we effectively argue for an inversion in the cause-effect relationship. Not the relatively weak intermolecular interactions are the reason for the presence of cavities but rather the presence of cavities are the reason for the relatively weak intermolecular interactions. This is the case for both intermolecular complexes, in which “cavities” refers to molecular surface not used for interaction, and bulk phases, in which there are real cavities.

Mixing Behavior and Trends in Experimental Properties. The widely known *fluorophobic effect* or *fluorous effect* refers to the low miscibility of **F** with **H** in the liquid state.[8–11] Notably, the immiscibility of **F** with common organic solvents increases with carbon chain length of **F**. Additionally, the fluorous properties of **F** only begin to appear at a certain chain length. Compounds with perfluoroalkyl groups of six carbon atoms are already well soluble in typical fluorous solvents.[2] The critical solution temperature of mixtures of **5-H** and **5-F**, i.e. the temperature above which mixtures of two liquids always form one homogeneous phase, is -8 °C,[120] for mixtures of **6-H** and **6-F** it is 22.7 °C.[121] Therefore, it is reasonable to say that fluorous properties of linear **F** start to become significant for **5-F** and **6-F**, which are the two longest linear **F** investigated in this work. This also suggests that it is not the fluorine content making an organic molecule fluorous, but rather the number of carbon atoms bound to fluorine.

It is commonly argued that fluorous molecules, because of the low polarizability of fluorine, have a low propensity for interaction with any other molecule, even themselves, compared to nonfluorous molecules and therefore favor phase separation to minimize unfavorable interactions.[8] However, our relative microscopic and macroscopic BAEs of **HH**, **HF** and **FF** show that, except for **1-HF**, all the **HF** complexes have a smaller BAE than the corresponding **HH** and **FF** complexes. These observations argue against the notion that **F** are interacting weakly with any other molecule compared to **H**, i.e. indifference for interaction with anything, but rather support the view that homo-aggregation of fluorinated molecules is preferential, at least for **F** with up to six carbon atoms.

From the microscopic and macroscopic energies of mixing (cf. Table 4), the overall mixing behavior can be decomposed into the contribution of the distances and the contribution of the intrinsic dispersive

interaction ability. The distances quantify the impact of the interaction geometries on the mixing behavior. The system has a choice between one **HH**, which has close to ideal interaction geometry, plus one **FF**, which has non-ideal geometry, and two **HF**, which both have non-ideal geometry. In the absence of other influences, one ideal plus one non-ideal geometry is preferred over two non-ideal geometries. In that regard, the interaction geometries of **F** show indifference for interaction with any other molecule. On the other hand, the intrinsic dispersive interaction ability shows preferred homo-aggregation of both **H** and **F**, respectively. To put it simply, **F** have a stronger intrinsic dispersion ability, **H** have a weaker intrinsic dispersion ability, which is estimated based on their average P_{tot} measures (*vide supra*). In the absence of other influences, the system has a choice between one **HH**, which is a contact between two weaker interactors, plus one **FF**, which is a contact between two stronger interactors, and two **HF**, which is a contact between one weaker and one stronger interactor. Because the overall interaction energy is mathematically described as product of two P measures (cf. Equations 8 and 9), one strong-strong interaction plus one weak-weak interaction is generally favored over two strong-weak interactions. It is intriguing that these two very different mechanisms of unmixing favor the exact same outcome. Additionally, it is important to point out that this reasoning is based purely on enthalpic arguments. They compete with the entropy of mixing which favors mixing of **H** and **F**, which is the reason for the temperature-dependent phase separation of **H** and **F**.

We also carried out a comprehensive trend comparison of experimental bulk properties (cf. Table 5 and Table 6) of **F** and **H**. Several of the properties investigated show an inversion, i.e. they change from being smaller in **H** to being larger, or *vice versa*, when the carbon chain is elongated. All the properties showing an inversion, i.e. enthalpy of evaporation, boiling point, critical parameter ratio, surface tension, internal pressure, bulk modulus and compressibility, provide information about intermolecular interactions and the corresponding interaction geometries. They can be roughly divided into properties quantifying the interaction energy (enthalpy of evaporation, boiling point, critical parameter ratio and surface tension) and properties quantifying the change of interaction energy with volume (internal pressure, bulk modulus and compressibility). Looking more closely into the properties considered, the high compressibilities of the longer **F** have been rationalized by the presence of cavities in the bulk liquid explaining their higher gas solubilities compared to **H**. The inverted trend for **1-F** suggests less cavities which likely relates to the good interaction geometries we found in **1-FF** complexes (cf. Figure 8a). From the properties not showing an inversion, the molar heat capacity actually does not even quantify intermolecular interactions. However, we looked into it because an inversion has been suggested in the literature.[122] However, using current experimental values we could not find evidence for it. In addition, the consistently higher viscosity of **F** compared to **H** can mainly be explained by the higher roughness of **F** and is therefore not a consequence of differences in intermolecular interaction energies.[123]

To the best of our knowledge, only the boiling point inversion between **H** and **F** has been pointed out in the literature before. It was first reported by Grosse and Cady in 1947.[12] In that paper, which reported results obtained during the Manhattan Project at Columbia University during World War II, the physical properties of perfluorinated and partially fluorinated hydrocarbons were determined and documented comprehensively. To the best of our knowledge, no satisfactory explanation has been provided for the observed boiling point inversion. All the observed inversions in experimental bulk properties, including the boiling point inversion, can be explained by two synergistic mechanisms. First, we found that the dispersive interaction abilities of **F**, quantified by P_{tot}, relative to **H**, decreases with increasing carbon chain length because of a concomitant decrease in the relative molar fluorine content. Secondly, the interaction geometries of dimers of increasingly long **F** are less ideal compared

to the corresponding dimers of **H** as quantified by the trends of $n_{contacts}$ (Figure 8). **F** with a short chain length have a higher intrinsic interaction ability than the corresponding **H** and the corresponding interaction geometries are still good which results in overall stronger intermolecular interactions. Increasing the carbon chain length results in a decrease of the intrinsic interaction abilities of **F** compared to **H** and also in less ideal interaction geometries. Overall, this explains the inversions of all the bulk properties considered.

Understanding the mixing behavior of fluorous substances is critical for solving the current problems associated with perfluorooctanoic acid (PFOA) and its salts. PFOA is extremely persistent and bioaccumulative because of its chemical inertness under environmental conditions[124] and its mixing properties.[125] In humans, it accumulates in serum and has been detected in populations worldwide.[124] Furthermore, it is, including other toxicities, toxic to the liver, to reproduction and the immune system and is carcinogenic.[126] However, PFOA owes its main applications as emulsifier for the production of fluoroelastomers and fluoropolymers like polytetrafluoroethylene (PTFE)[126] or as oil and dirt repellent in textile and paper production[127] to its fluorous properties which govern its mixing properties. Because of its toxicity, PFOA was added to the restricted substances of REACH and by July 2020 will be forbidden to be produced or distributed in the European Union.[127] Therefore, good substitutes for PFOA are required, which retain its attractive properties as much as possible. Understanding the origin of the fluorous properties of PFOA is one step towards suitable substitutes which underlines the importance of our findings. They suggest that potential substitutes could be molecules with sufficient rigidity and ground-state geometries unsuitable for interaction with both themselves and other molecules.

We would like to close this section by pointing out two relatively recent experimental studies, which found stronger than expected interaction energies of perfluorinated molecules but did not put the corresponding results into the right perspective. First, in a recent study of the binding of benzenesulfonamides substituted with either alkyl or perfluoroalkyl groups to human carbon anhydrase II it was found that both groups favor binding to a similar extent both enthalpically and entropically.[128] The authors concluded that the favorable enthalpic contributions are a result of non-optimal hydration of the hydrophobic wall of human carbon anhydrase II (HCA II). However, in order to reach that conclusion, they explicitly disregarded the possibility of equally strong dispersive interactions of the alkyl and perfluoroalkyl analogues because of considerably smaller bulk polarizabilities of perfluoroalkanes.[128] However, based on our results, equally strong interactions of alkyl and perfluoroalkyl substituents with a carbon chain length of one to five with the hydrophobic pocket of HCA II cannot be excluded as explanation for the observed similarly strong enthalpic binding energy contributions. On the contrary, our results suggest they are even likely to be similar in strength. Secondly, in the recently conducted HYDROPHOBE challenge,[129] a computational challenge for reproducing experimental host-guest binding free energies in water, it was found that using state-of-the art quantum mechanical methods on the basis of PBEh-3c[130] geometries and DLPNO-CCSD(T)/CBS single point energies with TightPNO cutoff parameters resulted in significantly underestimated binding of perfluorohexane and perfluorocyclohexane. Experimentally, it was found that the perfluorinated molecules have very similar Gibbs free energies of binding, within 1 kcal mol^{-1}, compared to the unfluorinated analogues. However, the computed values showed deviations of up to 8 kcal mol^{-1}.[129] On the basis of our benchmark results (cf. Table 2), this is not surprising, as DFT-D3 methods without other means of accounting for dispersion significantly underestimate the interactions of **F**, which hints towards possible errors in the computed geometries. Additionally, TightPNO cutoff parameters for DLPNO-CCSD(T) calculations were shown not to be sufficiently accurate for **F** as well (cf. Table 2) and this would likely lead to significant underestimation of the interaction energies in the corresponding

host-guest complexes. These two recent instances of underestimated binding energies of perfluorinated molecules demonstrate the general implications of this study.

Conclusions

In this work, we report an extensive computational investigation of the interaction energies of alkane and perfluoroalkane homo- and heterodimers. We conclude that most well established computational approaches used to describe dispersion-bound systems are inappropriate to describe the interaction energies in perfluoroalkane homo- and heterodimers accurately. Therefore, we provide a systematic benchmark set of high-level computed interaction energies of alkanes and perfluoroalkanes that will likely contribute to the development of more robust (cheap) ab initio methods to describe dispersion in general, not only in fluorinated molecules, as well as to the development of accurate force fields for fluorous molecules. We also found that the B97M-V functional performs best among all tested methods and is most efficient for the estimation of the corresponding interaction energies.

Additionally, spatial energy decomposition revealed that perfluoroalkanes provide most of their intermolecular dispersion via the fluorine atoms. Not only are the fluorine atoms on the outside, but the large electronegativity difference between carbon and fluorine also results in *Umpolarisierung* so that the fluorine atoms are at least about equally polarizable as the carbon atoms in perfluoroalkanes. As a result, when both the influence of polarizabilities and ionization potentials are accounted for, perfluoroalkanes show a higher intrinsic ability for intermolecular dispersion compared to analogous alkanes, as quantified by the newly proposed P_{tot} measure. However, the higher ability for dispersion is impeded by the ground-state geometries of perfluoroalkanes, which are unsuitable for interaction with either perfluoroalkanes or alkanes, as well as their high rigidity, which make deformation of the ground-state geometries highly unfavorable. The result is that intermolecular homodimers of linear alkanes and the corresponding perfluoroalkanes with up to six carbon atoms have, except for methane and perfluoromethane, roughly equal interaction energies. Overall, we propose the unsuitable interaction geometries to be the main reason for the notion that perfluoroalkanes interact weakly with other molecules by dispersion compared to alkanes. Additionally, our study contributes to the understanding of dispersion in molecules in general. P_{tot} can be used as a simple measure to gauge the potential for dispersion of any molecule and is therefore a first stepping-stone towards the development of simple quantitative dispersion energy donor descriptors. Further work investigating the use of P measures for the quantitative description of dispersion energy donors is underway.

Moreover, as the carbon chain is elongated, the relative molar fluorine content decreases and, hence, the number of attractive fluorine-fluorine contacts per carbon atom decreases. Additionally, the geometries of perfluoroalkanes become less ideal for intermolecular interactions. These synergistic trends directly influence their intrinsic ability for dispersion and has important consequences for their bulk properties. This is apparent from the inversion of various properties of perfluoroalkanes compared to analogous alkanes. Overall, our findings contribute towards the understanding of fluorous phases in general. They implicitly propose a mechanism for the transition of an increasingly fluorinated molecule from non-fluorous behavior towards fluorous behavior. As more fluorine atoms are incorporated into a molecule, its ground-state geometry is altered favoring phase separation because of indifference. Furthermore, the growing fluorous regions of the molecule also favor self-aggregation because of stronger dispersive contacts compared to contacts with non-fluorous regions. After surpassing a critical fluorine content, the synergism between these two mechanisms make phase separation of fluorous and non-fluorous matter favorable.

Associated Content

Supporting Information

Computational details, supplementary results and discussion, mathematical derivations and raw computational data (PDF)

XYZ coordinates for all the model compounds (ZIP)

Output files of COSMO calculations (ZIP)

Atomic polarizabilities of all the atoms in the molecular complexes (ZIP)

Author Information

Corresponding Author

peter.chen@org.chem.ethz.ch

Acknowledgments

We thank Marek Bot, Eno Paenurk and Dr. Renana Poranne for helpful discussions and Prof. Ricardo Mata and Axel Wuttke for help with preparing the DID plots. The work was supported financially by the ETH Zürich, the Schweizerischer Nationalfonds, the Deutsche Forschungsgemeinschaft (SPP1807), and the ACS Petroleum Research Fund.

References

(1) O'Hagan, D. Understanding Organofluorine Chemistry. An Introduction to the C–F Bond. *Chem. Soc. Rev.* **2008**, *37* (2), 308–319. https://doi.org/10.1039/B711844A.

(2) Horvath, I. T. *Fluorous Chemistry*; Springer, 2012; Vol. 308. https://doi.org/10.1016/0302-4598(80)87026-7.

(3) Dunitz, J. D. Organic Fluorine: Odd Man Out. *ChemBioChem* **2004**, *5* (5), 614–621. https://doi.org/10.1002/cbic.200300801.

(4) Smart, B. E. Fluorine Substituent Effects (on Bioactivity). *J. Fluor. Chem.* **2001**, *109* (1), 3–11. https://doi.org/10.1016/S0022-1139(01)00375-X.

(5) Lemal, D. M. Perspective on Fluorocarbon Chemistry. *J. Org. Chem.* **2004**, *69* (1), 1–11. https://doi.org/10.1021/JO0302556.

(6) Schlosser, M.; Michel, D. About the "Physiological Size" of Fluorine Substituents: Comparison of Sensorially Active Compounds with Fluorine and Methyl Substituted Analogues. *Tetrahedron* **1996**, *52* (1), 99–108. https://doi.org/10.1016/0040-4020(95)00886-D.

(7) Eaton, D. F.; Smart, B. E. Are Fluorocarbon Chains "Stiffer" Than Hydrocarbon Chains? Dynamics of End-to-End Cyclization in a C8F16 Segment Monitored by Fluorescence. *J. Am. Chem. Soc.* **1990**, *112* (7), 2821–2823. https://doi.org/10.1021/ja00163a065.

(8) Cametti, M.; Crousse, B.; Metrangolo, P.; Milani, R.; Resnati, G. The Fluorous Effect in Biomolecular Applications. *Chem. Soc. Rev.* **2012**, *41* (1), 31–42. https://doi.org/10.1039/C1CS15084G.

(9) Johansson, G.; Percec, V.; Ungar, G.; Smith, K. Fluorophobic Effect Generates a Systematic Approach to the Synthesis of the Simplest Class of Rodlike Liquid Crystals Containing a Single Benzene Unit. *Chem. Mater.* **1997**, *9* (1), 164–175. https://doi.org/10.1021/cm960267q.

(10) Johansson, G.; Percec, V.; Ungar, G.; Zhou, J. P. Fluorophobic Effect in the Self-Assembly of Polymers and Model Compounds Containing Tapered Groups into Supramolecular Columns. *Macromolecules* **1996**, *29* (2), 646–660. https://doi.org/10.1021/ma9511558.

(11) Percec, V.; Schlueter, D.; Kwon, Y. K.; Blackwell, J.; Möller, M.; Slangen, P. J. Dramatic Stabilization of a Hexagonal Columnar Mesophase Generated from Supramolecular and Macromolecular Columns by the Semifluorination of the Alkyl Groups of Their Tapered Building Blocks. *Macromolecules* **1995**, *28* (26), 8807–8818. https://doi.org/10.1021/ma00130a013.

(12) Grosse, A. V.; Cady, G. H. Properties of Fluorocarbons. *Ind. Eng. Chem.* **1947**, *39* (3), 367–374. https://doi.org/10.1021/ie50447a627.

(13) Krafft, M. P.; Riess, J. G. Chemistry, Physical Chemistry, and Uses of Molecular Fluorocarbon-Hydrocarbon Diblocks, Triblocks, and Related Compounds-Unique "Apolar" Components for Self-Assembled Colloid and Interface Engineering. *Chem. Rev.* **2009**, *109* (5), 1714–1792. https://doi.org/10.1021/cr800260k.

(14) London, F. The General Theory of Molecular Forces. *Trans. Faraday Soc.* **1937**, *33* (8), 8–26. https://doi.org/10.1039/tf937330008b.

(15) Chattoraj, J.; Risthaus, T.; Rubner, O.; Heuer, A.; Grimme, S. A Multi-Scale Approach to Characterize Pure CH4, CF4, and CH4/CF4 Mixtures. *J. Chem. Phys.* **2015**, *142* (16), 164508. https://doi.org/10.1063/1.4919079.

(16) Biller, M. J.; Mecozzi, S. A High Level Computational Study of the CH4 /CF4 Dimer: How Does It Compare with the CH4 /CH4 and CF4 /CF4 Dimers? *Mol. Phys.* **2012**, *110* (7), 377–387. https://doi.org/10.1080/00268976.2011.648961.

(17) Tsuzuki, S.; Uchimaru, T.; Mikami, M.; Urata, S. Magnitude and Orientation Dependence of Intermolecular Interaction between Perfluoroalkanes: High Level *Ab Initio* Calculations of CF4 and C2F6 Dimers. *J. Chem. Phys.* **2002**, *116* (8), 3309–3315. https://doi.org/10.1063/1.1436468.

(18) Neese, F. The ORCA Program System. *Wiley Interdiscip. Rev. Comput. Mol. Sci.* **2012**, *2* (1), 73–78. https://doi.org/10.1002/wcms.81.

(19) Neese, F. Software Update: The ORCA Program System, Version 4.0. *Wiley Interdiscip. Rev. Comput. Mol. Sci.* **2017**, 1–6. https://doi.org/10.1002/wcms.1327.

(20) Turney, J. M.; Simmonett, A. C.; Parrish, R. M.; Hohenstein, E. G.; Evangelista, F. A.; Fermann, J. T.; Mintz, B. J.; Burns, L. A.; Wilke, J. J.; Abrams, M. L.; Russ, N. J.; Leininger, M. L.; Janssen, C. L.; Seidl, E. T.; Allen, W. D.; Schaefer, H. F.; King, R. A.; Valeev, E. F.; Sherrill, C. D.; Crawford, T. D. Psi4: An Open-Source Ab Initio Electronic Structure Program. *Wiley Interdiscip. Rev. Comput. Mol. Sci.* **2012**, *2* (4), 556–565. https://doi.org/10.1002/wcms.93.

(21) Parrish, R. M.; Burns, L. A.; Smith, D. G. A.; Simmonett, A. C.; DePrince, A. E.; Hohenstein, E. G.; Bozkaya, U.; Sokolov, A. Y.; Di Remigio, R.; Richard, R. M.; Gonthier, J. F.; James, A. M.; McAlexander, H. R.; Kumar, A.; Saitow, M.; Wang, X.; Pritchard, B. P.; Verma, P.; Schaefer, H. F.; Patkowski, K.; King, R. A.; Valeev, E. F.; Evangelista, F. A.; Turney, J. M.; Crawford, T. D.; Sherrill, C. D. Psi4 1.1: An Open-Source Electronic Structure Program Emphasizing Automation, Advanced Libraries, and Interoperability. *J. Chem. Theory Comput.* **2017**, *13* (7), 3185–3197.

https://doi.org/10.1021/acs.jctc.7b00174.

(22) Werner, H. J.; Knowles, P. J.; Knizia, G.; Manby, F. R.; Schütz, M. Molpro: A General-Purpose Quantum Chemistry Program Package. *Wiley Interdiscip. Rev. Comput. Mol. Sci.* **2012**, *2* (2), 242–253. https://doi.org/10.1002/wcms.82.

(23) Frisch, M. J.; Trucks, G. W.; Schlegel, H. B.; Scuseria, G. E.; Robb, M. A.; Cheeseman, J. R.; Scalmani, G.; Barone, V.; Mennucci, B.; Petersson, G. A.; Nakatsuji, H.; Caricato, M.; Li, X.; Hratchian, H. P.; Izmaylov, A. F.; Bloino, J.; Zheng, G.; Sonnenberg, J. L.; Hada, M.; Ehara, M.; Toyota, K.; Fukuda, R.; Hasegawa, J.; Ishida, M.; Nakajima, T.; Honda, Y.; Kitao, O.; Nakai, H.; Vreven, T.; Montgomery Jr., J. A.; Peralta, J. E.; Ogliaro, F.; Bearpark, M.; Heyd, J. J.; Brothers, E.; Kudin, K. N.; Staroverov, V. N.; Kobayashi, R.; Normand, J.; Raghavachari, K.; Rendell, A.; Burant, J. C.; Iyengar, S. S.; Tomasi, J.; Cossi, M.; Rega, N.; Millam, J. M.; Klene, M.; Knox, J. E.; Cross, J. B.; Bakken, V.; Adamo, C.; Jaramillo, J.; Gomperts, R.; Stratmann, R. E.; Yazyev, O.; Austin, A. J.; Cammi, R.; Pomelli, C.; Ochterski, J. W.; Martin, R. L.; Morokuma, K.; Zakrzewski, V. G.; Voth, G. A.; Salvador, P.; Dannenberg, J. J.; Dapprich, S.; Daniels, A. D.; Farkas, O.; Foresman, J. B.; Ortiz, J. V.; Cioslowski, J.; Fox, D. J. Gaussian09 Revision D.01. *Gaussian 09.* Gaussian Inc. Wallingford CT 2009.

(24) Baerends, E. J.; Ziegler, T.; Autschbach, J.; Bashford, D.; Berces, A.; Bickelhaupt, F. M.; Bo, C.; Boerrigter, P. M.; Cavallo, L.; Chong, D. P.; Deng, L.; Dickson, R. M.; Ellis, D. E.; van Faassen, M.; Fan, L.; Fischer, T. H.; Fonseca Guerra, C.; Franchini, M.; Ghysels, A.; Giammona, A. ADF2017. *ADF2017*. SCM, Theoretical Chemistry, Vrije Universiteit, Amsterdam, The Netherlands, http://www.scm.com.

(25) Shao, Y.; Gan, Z.; Epifanovsky, E.; Gilbert, A. T. B.; Wormit, M.; Kussmann, J.; Lange, A. W.; Behn, A.; Deng, J.; Feng, X.; Ghosh, D.; Goldey, M.; Horn, P. R.; Jacobson, L. D.; Kaliman, I.; Khaliullin, R. Z.; Kuš, T.; Landau, A.; Liu, J.; Proynov, E. I.; Rhee, Y. M.; Richard, R. M.; Rohrdanz, M. A.; Steele, R. P.; Sundstrom, E. J.; Woodcock, H. L.; Zimmerman, P. M.; Zuev, D.; Albrecht, B.; Alguire, E.; Austin, B.; Beran, G. J. O.; Bernard, Y. A.; Berquist, E.; Brandhorst, K.; Bravaya, K. B.; Brown, S. T.; Casanova, D.; Chang, C. M.; Chen, Y.; Chien, S. H.; Closser, K. D.; Crittenden, D. L.; Diedenhofen, M.; Distasio, R. A.; Do, H.; Dutoi, A. D.; Edgar, R. G.; Fatehi, S.; Fusti-Molnar, L.; Ghysels, A.; Golubeva-Zadorozhnaya, A.; Gomes, J.; Hanson-Heine, M. W. D.; Harbach, P. H. P.; Hauser, A. W.; Hohenstein, E. G.; Holden, Z. C.; Jagau, T. C.; Ji, H.; Kaduk, B.; Khistyaev, K.; Kim, J.; Kim, J.; King, R. A.; Klunzinger, P.; Kosenkov, D.; Kowalczyk, T.; Krauter, C. M.; Lao, K. U.; Laurent, A. D.; Lawler, K. V.; Levchenko, S. V.; Lin, C. Y.; Liu, F.; Livshits, E.; Lochan, R. C.; Luenser, A.; Manohar, P.; Manzer, S. F.; Mao, S. P.; Mardirossian, N.; Marenich, A. V.; Maurer, S. A.; Mayhall, N. J.; Neuscamman, E.; Oana, C. M.; Olivares-Amaya, R.; Oneill, D. P.; Parkhill, J. A.; Perrine, T. M.; Peverati, R.; Prociuk, A.; Rehn, D. R.; Rosta, E.; Russ, N. J.; Sharada, S. M.; Sharma, S.; Small, D. W.; Sodt, A.; Stein, T.; Stück, D.; Su, Y. C.; Thom, A. J. W.; Tsuchimochi, T.; Vanovschi, V.; Vogt, L.; Vydrov, O.; Wang, T.; Watson, M. A.; Wenzel, J.; White, A.; Williams, C. F.; Yang, J.; Yeganeh, S.; Yost, S. R.; You, Z. Q.; Zhang, I. Y.; Zhang, X.; Zhao, Y.; Brooks, B. R.; Chan, G. K. L.; Chipman, D. M.; Cramer, C. J.; Goddard, W. A.; Gordon, M. S.; Hehre, W. J.; Klamt, A.; Schaefer, H. F.; Schmidt, M. W.; Sherrill, C. D.; Truhlar, D. G.; Warshel, A.; Xu, X.; Aspuru-Guzik, A.; Baer, R.; Bell, A. T.; Besley, N. A.; Chai, J. Da; Dreuw, A.; Dunietz, B. D.; Furlani, T. R.; Gwaltney, S. R.; Hsu, C. P.; Jung, Y.; Kong, J.; Lambrecht, D. S.; Liang, W.; Ochsenfeld, C.; Rassolov, V. A.; Slipchenko, L. V.; Subotnik, J. E.; Van Voorhis, T.; Herbert, J. M.; Krylov, A. I.; Gill, P. M. W.; Head-Gordon, M. Advances in Molecular Quantum Chemistry Contained in the Q-Chem 4 Program Package. *Mol. Phys.* **2015**, *113* (2), 184–215. https://doi.org/10.1080/00268976.2014.952696.

(26) Mahlanen, R.; Jalkanen, J.-P.; Pakkanen, T. A. Potential Energy Surfaces of CF4, CCl4 and CBr4 Dimers. *Chem. Phys.* **2005**, *313* (1), 271–277. https://doi.org/10.1016/j.chemphys.2005.01.018.

(27) Tsuzuki, S.; Uchimaru, T.; Mikami, M.; Urata, S. Magnitude and Orientation Dependence of Intermolecular Interaction of Perfluoropropane Dimer Studied by High-Level Ab Initio Calculations: Comparison with Propane Dimer. *J. Chem. Phys.* **2004**, *121* (20), 9917–9924. https://doi.org/10.1063/1.1809603.

(28) Kozuch, S.; Martin, J. M. L. Spin-Component-Scaled Double Hybrids: An Extensive Search for the Best Fifth-Rung Functionals Blending DFT and Perturbation Theory. *J. Comput. Chem.* **2013**, *34* (27), 2327–2344. https://doi.org/10.1002/jcc.23391.

(29) Riplinger, C.; Neese, F. An Efficient and near Linear Scaling Pair Natural Orbital Based Local Coupled Cluster Method. *J. Chem. Phys.* **2013**, *138* (3), 034106. https://doi.org/10.1063/1.4773581.

(30) Riplinger, C.; Sandhoefer, B.; Hansen, A.; Neese, F. Natural Triple Excitations in Local Coupled Cluster Calculations with Pair Natural Orbitals. *J. Chem. Phys.* **2013**, *139* (13), 134101. https://doi.org/10.1063/1.4821834.

(31) Liakos, D. G.; Neese, F. Is It Possible to Obtain Coupled Cluster Quality Energies at near Density Functional Theory Cost? Domain-Based Local Pair Natural Orbital Coupled Cluster vs Modern Density Functional Theory. *J. Chem. Theory Comput.* **2015**, *11* (9), 4054–4063. https://doi.org/10.1021/acs.jctc.5b00359.

(32) Adler, T. B.; Knizia, G.; Werner, H. J. A Simple and Efficient CCSD(T)-F12 Approximation. *J. Chem. Phys.* **2007**, *127* (22), 221106. https://doi.org/10.1063/1.2817618.

(33) Knizia, G.; Adler, T. B.; Werner, H. J. Simplified CCSD(T)-F12 Methods: Theory and Benchmarks. *J. Chem. Phys.* **2009**, *130* (5), 054104. https://doi.org/10.1063/1.3054300.

(34) Mardirossian, N.; Head-Gordon, M. Mapping the Genome of Meta-Generalized Gradient Approximation Density Functionals: The Search for B97M-V. *J. Chem. Phys.* **2015**, *142* (7), 074111. https://doi.org/10.1063/1.4907719.

(35) Mardirossian, N.; Head-Gordon, M. ω B97M-V: A Combinatorially Optimized, Range-Separated Hybrid, Meta-GGA Density Functional with VV10 Nonlocal Correlation. *J. Chem. Phys.* **2016**, *144* (21), 214110. https://doi.org/10.1063/1.4952647.

(36) Johnson, E. R.; Becke, A. D. A Post-Hartree-Fock Model of Intermolecular Interactions. *J. Chem. Phys.* **2005**, *123* (2), 024101. https://doi.org/10.1063/1.1949201.

(37) Johnson, E. R.; Becke, A. D. A Post-Hartree-Fock Model of Intermolecular Interactions: Inclusion of Higher-Order Corrections. *J. Chem. Phys.* **2006**, *124* (17), 174104. https://doi.org/10.1063/1.2190220.

(38) Becke, A. D.; Johnson, E. R. Exchange-Hole Dipole Moment and the Dispersion Interaction. *J. Chem. Phys.* **2005**, *122*, 154104.

(39) Becke, A. D.; Johnson, E. R. Exchange-Hole Dipole Moment and the Dispersion Interaction Revisited. *J. Chem. Phys.* **2007**, *127* (15), 154104. https://doi.org/10.1063/1.2795701.

(40) Moller, C.; Plesset, M. S. Note on an Approximation Treatment for Many-Electron Systems. *Phys. Rev.* **1934**, *46* (7), 618–622.

(41) Feyereisen, M.; Fitzgerald, G.; Komornicki, A. Use of Approximate Integrals in Ab Initio Theory. An Application in MP2 Energy Calculations. *Chem. Phys. Lett.* **1993**, *208* (5–6), 359–363. https://doi.org/10.1016/0009-2614(93)87156-W.

(42) Vahtras, O.; Almlöf, J.; Feyereisen, M. W. Integral Approximations for LCAO-SCF Calculations.

Chem. Phys. Lett. **1993**, *213* (5–6), 514–518. https://doi.org/10.1016/0009-2614(93)89151-7.

(43) Moszyński, R.; Jeziorski, B.; Szalewicz, K. Many-Body Theory of Exchange Effects in Intermolecular Interactions - 2Nd-Quantization Approach and Comparison With Full Configuration-Interaction Results. *J. Chem. Phys.* **1994**, *100* (1994), 1312–1325.

(44) Rybak, S.; Jeziorski, B.; Szalewicz, K. Many-body Symmetry-adapted Perturbation Theory of Intermolecular Interactions. H_2O and HF Dimers. *J. Chem. Phys.* **1991**, *95* (9), 6576–6601. https://doi.org/10.1063/1.461528.

(45) Jeziorski, B.; Jeziorski, B.; Moszynski, R.; Moszynski, R.; Szalewicz, K.; Szalewicz, K. Perturbation Theory Approach to Intermolecular Potential Energy Surfaces of van Der Waals Complexes. *Chem. Rev.* **1994**, *94* (7), 1887–1930. https://doi.org/10.1021/cr00031a008.

(46) Szalewicz, K. Symmetry-Adapted Perturbation Theory of Intermolecular Forces. *Wiley Interdiscip. Rev. Comput. Mol. Sci.* **2012**, *2* (2), 254–272. https://doi.org/10.1002/wcms.86.

(47) Schneider, W. B.; Bistoni, G.; Sparta, M.; Saitow, M.; Riplinger, C.; Auer, A. A.; Neese, F. Decomposition of Intermolecular Interaction Energies within the Local Pair Natural Orbital Coupled Cluster Framework. *J. Chem. Theory Comput.* **2016**, *12* (10), 4778–4792. https://doi.org/10.1021/acs.jctc.6b00523.

(48) Bistoni, G.; Auer, A. A.; Neese, F. Understanding the Role of Dispersion in Frustrated Lewis Pairs and Classical Lewis Adducts: A Domain-Based Local Pair Natural Orbital Coupled Cluster Study. *Chem. - A Eur. J.* **2017**, *23* (4), 865–873. https://doi.org/10.1002/chem.201604127.

(49) Wuttke, A.; Mata, R. A. Visualizing Dispersion Interactions through the Use of Local Orbital Spaces. *J. Comput. Chem.* **2017**, *38* (1), 15–23. https://doi.org/10.1002/jcc.24508.

(50) Hättig, C.; Jansen, G.; Hess, B. A.; Ángyán, J. G. Topologically Partitioned Dynamic Polarizabilities Using the Theory of Atoms in Molecules. *Can. J. Chem.* **1996**, *74* (6), 976–987. https://doi.org/10.1139/v96-108.

(51) Krawczuk, A.; Pérez, D.; MacChi, P. PolaBer: A Program to Calculate and Visualize Distributed Atomic Polarizabilities Based on Electron Density Partitioning. *J. Appl. Crystallogr.* **2014**, *47* (4), 1452–1458. https://doi.org/10.1107/S1600576714010838.

(52) Keith, T. A. AIMAll (Version 17.11.14). Todd A. Keith, TK Gristmill Software, Overland Park KS, USA, 2017 (aim.tkgristmill.com).

(53) Politzer, P.; Jin, P.; Murray, J. S. Atomic Polarizability, Volume and Ionization Energy. *J. Chem. Phys.* **2002**, *117* (18), 8197–8202. https://doi.org/10.1063/1.1511180.

(54) Schulman, J. M.; Musher, J. I. Hydrogen-Atom Polarizability as a Hartree–Fock Perturbation Expansion: A Geometric Approximation to Atomic Polarizabilities. *J. Chem. Phys.* **1968**, *49* (11), 4845. https://doi.org/10.1063/1.1669968.

(55) *CRC Handbook of Chemistry and Physics*, 98th ed.; Rumble, J. R., Ed.; CRC Press/Taylor & Francis: Boca Raton, FL, 2017.

(56) Eisenschitz, R.; London, F. Über Das Verhältnis Der van Der Waalsschen Kräfte Zu Den Homöopolaren Bindungskräften. *Zeitschrift für Phys.* **1930**, *60* (7–8), 491–527. https://doi.org/10.1007/BF01341258.

(57) Grimme, S.; Hansen, A.; Brandenburg, J. G.; Bannwarth, C. Dispersion-Corrected Mean-Field Electronic Structure Methods. *Chem. Rev.* **2016**, *116* (9), 5105–5154. https://doi.org/10.1021/acs.chemrev.5b00533.

(58) Contreras-Garcia, J.; Johnson, E. R.; Keinan, S.; Chaudret, R.; Piquemal, J. P.; Beratan, D. N.; Yang, W. NCIPLOT: A Program for Plotting Noncovalent Interaction Regions. *J. Chem. Theory Comput.* **2011**, *7* (3), 625–632. https://doi.org/10.1021/ct100641a.

(59) Flory, P. J. Thermodynamics of High Polymer Solutions. *J. Chem. Phys.* **1942**, *10* (51), 51–61. https://doi.org/10.1063/1.1723621.

(60) Huggins, M. L. Thermodynamic Properties of Solutions of Long-Chain Compounds. *Ann. N.Y. Acad. Sci.* **1942**, *43* (828), 1–32.

(61) Dantzler Siebert, E. M.; Knobler, C. M. Interaction Virial Coefficients in Hydrocarbon-Fluorocarbon Mixtures. *J. Phys. Chem.* **1971**, *75* (25), 3863–3870. https://doi.org/10.1021/j100848a049.

(62) Dantzler, E. M.; Knobler, C. M.; Windsor, M. L. Interaction Virial Coefficients in Hydrocarbon Mixtures. *J. Phys. Chem.* **1968**, *72* (2), 684. https://doi.org/10.1021/j100694a014.

(63) Dantzler, E. M.; Knobler, C. M. Interaction Virial Coefficients in Fluorocarbon Mixtures. *J. Phys. Chem.* **1969**, *73* (5), 1335–1341. https://doi.org/10.1021/j100694a014.

(64) Hermann, J.; DiStasio, R. A.; Tkatchenko, A. First-Principles Models for van Der Waals Interactions in Molecules and Materials: Concepts, Theory, and Applications. *Chem. Rev.* **2017**, *117* (6), 4714–4758. https://doi.org/10.1021/acs.chemrev.6b00446.

(65) Hohenstein, E. G.; Sherrill, C. D. Wavefunction Methods for Noncovalent Interactions. *Wiley Interdiscip. Rev. Comput. Mol. Sci.* **2012**, *2* (2), 304–326. https://doi.org/10.1002/wcms.84.

(66) Burns, L. A.; Marshall, M. S.; Sherrill, C. D. Appointing Silver and Bronze Standards for Noncovalent Interactions: A Comparison of Spin-Component-Scaled (SCS), Explicitly Correlated (F12), and Specialized Wavefunction Approaches. *J. Chem. Phys.* **2014**, *141* (23), 234111. https://doi.org/10.1063/1.4903765.

(67) Mardirossian, N.; Head-Gordon, M. Thirty Years of Density Functional Theory in Computational Chemistry: An Overview and Extensive Assessment of 200 Density Functionals. *Mol. Phys.* **2017**, *8976* (July), 1–58. https://doi.org/10.1080/00268976.2017.1333644.

(68) Johnson, E. R.; Mackie, I. D.; DiLabio, G. A. Dispersion Interactions in Density-Functional Theory. *J. Phys. Org. Chem.* **2009**, *22* (12), 1127–1135. https://doi.org/10.1002/poc.1606.

(69) Goerigk, L.; Kruse, H.; Grimme, S. Benchmarking Density Functional Methods against the S66 and S66x8 Datasets for Non-Covalent Interactions. *ChemPhysChem* **2011**, *12* (17), 3421–3433. https://doi.org/10.1002/cphc.201100826.

(70) Mardirossian, N.; Head-Gordon, M. How Accurate Are the Minnesota Density Functionals for Noncovalent Interactions, Isomerization Energies, Thermochemistry, and Barrier Heights Involving Molecules Composed of Main-Group Elements? *J. Chem. Theory Comput.* **2016**, *12* (9), 4303–4325. https://doi.org/10.1021/acs.jctc.6b00637.

(71) Otero-de-la-Roza, A.; Johnson, E. R. Non-Covalent Interactions and Thermochemistry Using XDM-Corrected Hybrid and Range-Separated Hybrid Density Functionals Non-Covalent Interactions and Thermochemistry Using XDM-Corrected Hybrid and Range-Separated Hybrid Density Functionals. *J. Chem. Phys.* **2013**, *138*, 204109. https://doi.org/10.1063/1.4807330.

(72) Kannemann, F. O.; Becke, A. D. Van Der Waals Interactions in Density-Functional Theory: Intermolecular Complexes. *J. Chem. Theory Comput.* **2010**, *6*, 1081–1088.

(73) Calbo, J.; Ortí, E.; Sancho-García, J. C.; Aragó, J. The Nonlocal Correlation Density Functional

VV10: A Successful Attempt to Accurately Capture Noncovalent Interactions. *Annu. Rep. Comput. Chem.* **2015**, *11*, 37–102. https://doi.org/10.1016/bs.arcc.2015.09.002.

(74) Otero-De-La-Roza, A.; Johnson, E. R. Predicting Energetics of Supramolecular Systems Using the XDM Dispersion Model. *J. Chem. Theory Comput.* **2015**, *11* (9), 4033–4040. https://doi.org/10.1021/acs.jctc.5b00044.

(75) Goerigk, L.; Grimme, S. A General Database for Main Group Thermochemistry, Kinetics, and Noncovalent Interactions - Assessment of Common and Reparameterized (Meta-)GGA Density Functionals. *J. Chem. Theory Comput.* **2010**, *6* (1), 107–126. https://doi.org/10.1021/ct900489g.

(76) Risthaus, T.; Grimme, S. Benchmarking of London Dispersion-Accounting Density Functional Theory Methods on Very Large Molecular Complexes. *J. Chem. Theory Comput.* **2013**, *9* (3), 1580–1591. https://doi.org/10.1021/ct301081n.

(77) Goerigk, L.; Grimme, S. Double-Hybrid Density Functionals. *Wiley Interdiscip. Rev. Comput. Mol. Sci.* **2014**, *4* (6), 576–600. https://doi.org/10.1002/wcms.1193.

(78) Goerigk, L.; Grimme, S. A Thorough Benchmark of Density Functional Methods for General Main Group Thermochemistry, Kinetics, and Noncovalent Interactions. *Phys. Chem. Chem. Phys.* **2011**, *13*, 6670–6688. https://doi.org/10.1039/C0CP02984J.

(79) Grimme, S. Supramolecular Binding Thermodynamics by Dispersion-Corrected Density Functional Theory. *Chem. Eur. J.* **2012**, *18* (32), 9955–9964. https://doi.org/10.1002/chem.201200497.

(80) Calbo, J.; Ortí, E.; Sancho-García, J. C.; Aragó, J. Accurate Treatment of Large Supramolecular Complexes by Double-Hybrid Density Functionals Coupled with Nonlocal van Der Waals Corrections. *J. Chem. Theory Comput.* **2015**, *11* (3), 932–939. https://doi.org/10.1021/acs.jctc.5b00002.

(81) Grimme, S. Accurate Description of van Der Waals Complexes by Density Functional Theory Including Empirical Corrections. *J. Comput. Chem.* **2004**, *25* (12), 1463–1473. https://doi.org/10.1002/jcc.20078.

(82) Grimme, S.; Antony, J.; Ehrlich, S.; Krieg, H. A Consistent and Accurate Ab Initio Parametrization of Density Functional Dispersion Correction (DFT-D) for the 94 Elements H-Pu. *J. Chem. Phys.* **2010**, *132* (15), 154104. https://doi.org/10.1063/1.3382344.

(83) Becke, A. D.; Johnson, E. R. A Density-Functional Model of the Dispersion Interaction. *J. Chem. Phys.* **2005**, *123* (15), 154101. https://doi.org/10.1063/1.2065267.

(84) Steinmann, S. N.; Corminboeuf, C. A System-Dependent Density-Based Dispersion Correction. *J. Chem. Theory Comput.* **2010**, *6* (7), 1990–2001. https://doi.org/10.1021/ct1001494.

(85) Steinmann, S. N.; Corminboeuf, C. Comprehensive Benchmarking of a Density-Dependent Dispersion Correction. *J. Chem. Theory Comput.* **2011**, *7* (11), 3567–3577. https://doi.org/10.1021/ct200602x.

(86) Steinmann, S. N.; Corminboeuf, C. A Generalized-Gradient Approximation Exchange Hole Model for Dispersion Coefficients. *J. Chem. Phys.* **2011**, *134* (4), 044117. https://doi.org/10.1063/1.3545985.

(87) Vydrov, O. A.; Van Voorhis, T. Nonlocal van Der Waals Density Functional: The Simpler the Better. *J. Chem. Phys.* **2010**, *133* (24), 244103. https://doi.org/10.1063/1.3521275.

(88) Zhao, Y.; Truhlar, D. G. The M06 Suite of Density Functionals for Main Group Thermochemistry, Thermochemical Kinetics, Noncovalent Interactions, Excited States, and Transition Elements: Two New Functionals and Systematic Testing of Four M06-Class Functionals and 12 Other Function. *Theor. Chem. Acc.* **2008**, *120* (1–3), 215–241. https://doi.org/10.1007/s00214-007-0310-x.

(89) Zhao, Y.; Truhlar, D. G. A New Local Density Functional for Main-Group Thermochemistry, Transition Metal Bonding, Thermochemical Kinetics, and Noncovalent Interactions. *J. Chem. Phys.* **2006**, *125* (19), 194101. https://doi.org/10.1063/1.2370993.

(90) Lee, K.; Murray, É. D.; Kong, L.; Lundqvist, B. I.; Langreth, D. C. Higher-Accuracy van Der Waals Density Functional. *Phys. Rev. B - Condens. Matter Mater. Phys.* **2010**, *82* (8), 3–6. https://doi.org/10.1103/PhysRevB.82.081101.

(91) Řezáč, J.; Šimová, L.; Hobza, P. CCSD[T] Describes Noncovalent Interactions Better than the CCSD(T), CCSD(TQ), and CCSDT Methods. *J. Chem. Theory Comput.* **2013**, *9* (1), 364–369. https://doi.org/10.1021/ct3008777.

(92) Burns, L. A.; Marshall, M. S.; Sherrill, C. D. Comparing Counterpoise-Corrected, Uncorrected, and Averaged Binding Energies for Benchmarking Noncovalent Interactions. *J. Chem. Theory Comput.* **2014**, *10* (1), 49–57. https://doi.org/10.1021/ct400149j.

(93) Řezáč, J.; Riley, K. E.; Hobza, P. Benchmark Calculations of Noncovalent Interactions of Halogenated Molecules. *J. Chem. Theory Comput.* **2012**, *8* (11), 4285–4292. https://doi.org/10.1021/ct300647k.

(94) Jurecka, P.; Sponer, J.; Cerný, J.; Hobza, P. Benchmark Database of Accurate (MP2 and CCSD(T) Complete Basis Set Limit) Interaction Energies of Small Model Complexes, DNA Base Pairs, and Amino Acid Pairs. *Phys. Chem. Chem. Phys.* **2006**, *8* (17), 1985–1993. https://doi.org/10.1039/b600027d.

(95) Cheng, L.; Gauss, J.; Ruscic, B.; Armentrout, P. B.; Stanton, J. F. Bond Dissociation Energies for Diatomic Molecules Containing 3d Transition Metals: Benchmark Scalar-Relativistic Coupled-Cluster Calculations for 20 Molecules. *J. Chem. Theory Comput.* **2017**, *13* (3), 1044–1056. https://doi.org/10.1021/acs.jctc.6b00970.

(96) Liakos, D. G.; Sparta, M.; Kesharwani, M. K.; Martin, J. M. L.; Neese, F. Exploring the Accuracy Limits of Local Pair Natural Orbital Coupled-Cluster Theory. *J. Chem. Theory Comput.* **2015**, *11* (4), 1525–1539. https://doi.org/10.1021/ct501129s.

(97) Minenkov, Y.; Chermak, E.; Cavallo, L. Accuracy of DLPNO-CCSD (T) Method for Non-Covalent Bond Dissociation Enthalpies from Coinage Metal Cation Complexes. *J. Chem. Theory Comput.* **2015**, *11* (10), 1–65.

(98) Liakos, D. G.; Neese, F. Domain Based Pair Natural Orbital Coupled Cluster Studies on Linear and Folded Alkane Chains. *J. Chem. Theory Comput.* **2015**, *11* (5), 2137–2143. https://doi.org/10.1021/acs.jctc.5b00265.

(99) Paulechka, E.; Kazakov, A. Efficient DLPNO-CCSD(T)-Based Estimation of Formation Enthalpies for C-, H-, O-, and N-Containing Closed-Shell Compounds Validated Against Critically Evaluated Experimental Data. *J. Phys. Chem. A* **2017**, *121* (22), 4379–4387. https://doi.org/10.1021/acs.jpca.7b03195.

(100) Phipps, M. J. S.; Fox, T.; Tautermann, C. S.; Skylaris, C.-K. Energy Decomposition Analysis Approaches and Their Evaluation on Prototypical Protein–drug Interaction Patterns. *Chem. Soc. Rev.* **2015**, *44* (10), 3177–3211. https://doi.org/10.1039/C4CS00375F.

(101) De Silva, P.; Corminboeuf, C. Simultaneous Visualization of Covalent and Noncovalent Interactions Using Regions of Density Overlap. *J. Chem. Theory Comput.* **2014**, *10* (9), 3745–3756. https://doi.org/10.1021/ct500490b.

(102) Johnson, E. R.; Keinan, S.; Mori-Sánchez, P.; Contreras-García, J.; Cohen, A. J.; Yang, W. Revealing Noncovalent Interactions. *J. Am. Chem. Soc.* **2010**, *132* (18), 6498–6506. https://doi.org/10.1021/ja100936w.

(103) Krawczuk-Pantula, A.; Perez, D.; Macchi, P. Distributed Atomic Polarizabilities from Electron Density. 1. Motivations and Theory. *Trans. Amer. Cryst. Ass.* **2012**, *42*, 1–25.

(104) Tkatchenko, A.; Scheffler, M. Accurate Molecular van Der Waals Interactions from Ground-State Electron Density and Free-Atom Reference Data. *Phys. Rev. Lett.* **2009**, *102* (7), 6–9. https://doi.org/10.1103/PhysRevLett.102.073005.

(105) Caldeweyher, E.; Bannwarth, C.; Grimme, S. Extension of the D3 Dispersion Coefficient Model. *J. Chem. Phys.* **2017**, *147* (3), 034112. https://doi.org/10.1063/1.4993215.

(106) Sanderson, R. T. Principles of Electronegativity Part I. General Nature. *J. Chem. Educ.* **1988**, *65* (2), 112. https://doi.org/10.1021/ed065p112.

(107) Sanderson, R. T. Principles of Electronegativity Part II. Applications. *J. Chem. Educ.* **1988**, *65* (3), 227. https://doi.org/10.1021/ed065p227.

(108) Parr, R. G.; Donnelly, R. A.; Levy, M.; Palke, W. E. Electronegativity: The Density Functional Viewpoint. *J. Chem. Phys.* **1978**, *68* (8), 3801–3807. https://doi.org/10.1063/1.436185.

(109) Geerlings, P.; De Proft, F.; Langenaeker, W. Conceptual Density Functional Theory. *Chem. Rev.* **2003**, *103* (5), 1793–1874. https://doi.org/10.1021/cr990029p.

(110) Proft, F. De; Ayers, P. W.; Geerlings, P. *The Conceptual Density Functional Theory Perspective of Bonding. In The Chemical Bond*; Frenking, G., Shaik, S., Eds.; 2014. https://doi.org/10.1002/9783527664696.ch7.

(111) Nagle, J. K. Atomic Polarizability and Electronegativity. *J. Am. Chem. Soc.* **1990**, *112* (12), 4741–4747. https://doi.org/10.1021/ja00168a019.

(112) Pearson, R. G. Chemical Hardness and Density Functional Theory. *J. Chem. Sci.* **2005**, *117* (5), 369–377. https://doi.org/10.1007/BF02708340.

(113) Parr, R. G.; Pearson, R. G. Absolute Hardness: Companion Parameter to Absolute Electronegativity. *J. Am. Chem. Soc.* **1983**, *105* (26), 7512–7516. https://doi.org/10.1021/ja00364a005.

(114) Pearson, R. G. Hard and Soft Acids and Bases, HSAB, Part 1: Fundamental Principles. *J. Chem. Educ.* **1968**, *45* (9), 581. https://doi.org/10.1021/ed045p581.

(115) Pearson, R. G. Hard and Soft Acids and Bases, HSAB, Part II: Underlying Theories. *J. Chem. Educ.* **1968**, *45* (10), 643. https://doi.org/10.1021/ed045p643.

(116) Grimme, S.; Huenerbein, R.; Ehrlich, S. On the Importance of the Dispersion Energy for the Thermodynamic Stability of Molecules. *ChemPhysChem* **2011**, *12* (7), 1258–1261. https://doi.org/10.1002/cphc.201100127.

(117) Wagner, J. P.; Schreiner, P. R. London Dispersion in Molecular Chemistry - Reconsidering Steric Effects. *Angew. Chem. Int. Ed.* **2015**, *54* (42), 12274–12296. https://doi.org/10.1002/anie.201503476.

(118) McKinnon, J. J.; Jayatilaka, D.; Spackman, M. A. Towards Quantitative Analysis of Intermolecular Interactions with Hirshfeld Surfaces. *Chem. Commun.* **2007**, No. 37, 3814–3816. https://doi.org/10.1039/b704980c.

(119) Gladysz, J. A.; Emnet, C. Fluorous Solvents and Related Media. In *Handbook of Fluorous Chemistry*; Gladysz, J. A., Curran, D. P., Horvath, I. T., Eds.; WILEY-VCH Verlag: Weinheim, Germany, 2005; pp 11–23. https://doi.org/10.1002/3527603905.ch3.

(120) Simons, J. H.; Dunlap, R. D. The Properties of N-Pentforane and Its Mixtures with n-Pentane. *J. Chem. Phys.* **1950**, *18* (3), 335–346. https://doi.org/10.1063/1.1747628.

(121) Bedford, R. G.; Dunlap, R. D. Solubilities and Volume Changes Attending Mixing for the System: Perfluoro-n-Hexane–n-Hexane. *J. Am. Chem. Soc.* **1958**, *80* (2), 282–285. https://doi.org/10.1021/ja01535a007.

(122) Campos-Vallette, M.; Campos-Vallette, M.; Diaz-Fleming, G. Some Physical and Thermodynamic Properties of N-Cnf2n+2 Compounds with n = 4-8. *Semina: Ciências Agrárias*. 1983, pp 405–409. https://doi.org/10.5433/1679-0359.1983v4n14p405.

(123) Morgado, P.; Laginhas, C. M. C.; Lewis, J. Ben; McCabe, C.; Martins, L. F. G.; Filipe, E. J. M. Viscosity of Liquid Perfluoroalkanes and Perfluoroalkylalkane Surfactants. *J. Phys. Chem. B* **2011**, *115* (29), 9130–9139. https://doi.org/10.1021/jp201364k.

(124) Post, G. B.; Cohn, P. D.; Cooper, K. R. Perfluorooctanoic Acid (PFOA), an Emerging Drinking Water Contaminant: A Critical Review of Recent Literature. *Environ. Res.* **2012**, *116*, 93–117. https://doi.org/10.1016/j.envres.2012.03.007.

(125) Prevedouros, K.; Cousins, I. T.; Buck, R. C.; Korzeniowski, S. H. Sources, Fate and Transport of Perfluorocarboxylates. *Environ. Sci. Technol.* **2006**, *40* (1), 32–44. https://doi.org/10.1021/es0512475.

(126) Lau, C.; Anitole, K.; Hodes, C.; Lai, D.; Pfahles-Hutchens, A.; Seed, J. Perfluoroalkyl Acids: A Review of Monitoring and Toxicological Findings. *Toxicol. Sci.* **2007**, *99* (2), 366–394. https://doi.org/10.1093/toxsci/kfm128.

(127) L 150. *Off. J. Eur. Union* **2017**, *60* (L150), 1–19.

(128) Mecinović, J.; Snyder, P. W.; Mirica, K. A.; Bai, S.; MacK, E. T.; Kwant, R. L.; Moustakas, D. T.; Héroux, A.; Whitesides, G. M. Fluoroalkyl and Alkyl Chains Have Similar Hydrophobicities in Binding to the "Hydrophobic Wall" of Carbonic Anhydrase. *J. Am. Chem. Soc.* **2011**, *133* (35), 14017–14026. https://doi.org/10.1021/ja2045293.

(129) Assaf, K. I.; Florea, M.; Antony, J.; Henriksen, N. M.; Yin, J.; Hansen, A.; Qu, Z.; Sure, R.; Klapstein, D.; Gilson, M. K.; Grimme, S.; Nau, W. M. The Hydrophobe Challenge: A Joint Experimental and Computational Study on the Binding of Hydrocarbons to Cucurbiturils. *J. Phys. Chem. B* **2017**, *121* (49), 11144–11162. https://doi.org/10.1021/acs.jpcb.7b09175.

(130) Grimme, S.; Brandenburg, J. G.; Bannwarth, C.; Hansen, A. Consistent Structures and Interactions by Density Functional Theory with Small Atomic Orbital Basis Sets. *J. Chem. Phys.* **2015**, *143* (5), 054107. https://doi.org/10.1063/1.4927476.

For Table of Contents Only:

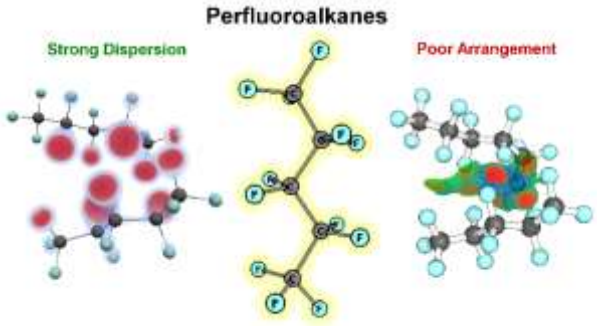

Electronic Supporting Information for

Origin of the Immiscibility of Alkanes and Perfluoroalkanes

Robert Pollice and Peter Chen*

Laboratorium für Organische Chemie, ETH Zürich, Vladimir-Prelog-Weg 2, 8093 Zürich, Switzerland

E-mail: peter.chen@org.chem.ethz.ch

Contents

1 Computational Methods

The following programs were employed for all the computations in this study:

- Orca (versions 3.0.3 and 4.0.1)[1,2]
- PSI4 (versions 1.1 and 1.2)[3,4]
- Molpro (version 2015.1.18)[5]
- Gaussian (version 09, revision D.01)[6]
- ADF (version 2016)[7]
- Q-Chem (version 4.3)[8]
- postg[9,10]
- BootD3[11,12]
- xtb (version 5.8)[13]
- Paraview (version 5.5.0-RC3)[14,15]
- PolaBer (version 0.02)[16]
- AIMAll (version 17.11.14)[17]
- multiwfn (version 3.4.1)[18]
- NCIPLOT (version 3.0)[19,20]
- PyMol (version 1.8.4)[21]
- Chemcraft (version 1.8, build 536b)[22]
- Python (version 3.6.0)[23]

1.1 Geometry Optimizations for Benchmarking

Geometry optimizations were performed in Orca (version 3.0.3) using the DSD-PBEP86[24]/def2-TZVP-spd[25,26] level of theory employing the RIJCOSX[27,28] approximation in conjunction with the def2-TZVP/J[29] and def2-TZVP/C[30] fitting basis sets. We performed systematic exploration of the conformational space of the intermolecular complexes by starting DFT geometry optimizations from various initial geometries having distinct spatial arrangements

of the interacting molecules. The exploration was performed starting from **1-HH**, **1-HF** and **1-FF** by increasing the carbon chains of the interacting molecules by one and finding the most stable intermolecular complexes for **2-HH**, **2-HF** and **2-FF** by systematically varying the position of the newly introduced groups and the spatial arrangement of the two interacting molecules. In addition, in a second cycle, we started from the most stable intermolecular complexes for **6-HH**, **6-HF** and **6-FF** and systematically reduced the carbon chain length by successively removing distinct end groups from the complexes. That way, the conformational space was explored step-by-step by systematically changing the carbon chain length from one to six and from six to one and performing conformational exploration at every step. The most stable conformers, judged on the basis of DSD-PBEP86/def2-QZVP single point energies, were selected for benchmarking. For **HH** and **FF**, the two lowest energy conformers in each class of complexes was selected for further benchmarking. For **HF**, except for **1-HF** for which we selected only two conformers, the four lowest energy conformers in each class of complexes was selected for benchmarking.

1.2 Single Points

Wavefunction Theory (WFT) methods and Density Function Theory (DFT) methods were used for single point calculations. Single point calculations were performed using DSD-PBEP86/def2-TZVP-spd geometries. Two-point complete basis set (CBS) extrapolations were performed using two single point energies calculated using the either the cc-pVTZ[31] and cc-pVQZ[31] or the aug-cc-pVTZ[32] and aug-cc-pVQZ[32] basis sets and are abbreviated herein as CBS(34) and CBS(aug34), respectively. For DLPNO-CCSD(T) calculations, we also used the following non-standard sets of thresholds together with the TightPNO[33] keyword in Orca:

- VeryTightPNO:[34] TCutPNO = $1 \cdot 10^{-8}$, TCutPairs = $1 \cdot 10^{-6}$, TCutMKN = $1 \cdot 10^{-4}$
- ExtremePNO: TCutPNO = $1 \cdot 10^{-9}$, TCutPairs = $1 \cdot 10^{-7}$, TCutMKN = $1 \cdot 10^{-5}$

1.2.1 Semiempirical Methods

GFN-xTB[13] and GFN2-xTB[35] calculations were performed using xtb (version 5.8).

1.2.2 WFT

Method	Basis set	Software	Comments
CCSD(T)-F12[36,37]	cc-pVTZ-F12[38]	Molpro	_
CCSD(T)-F12[36,37]	cc-pVDZ-F12[38]	Molpro	_
CCSD(T)[39,40]	CBS(34)	Molpro	_
CCSD(T)[39,40]	aug-cc-pVDZ[32]	Molpro	CBS(aug34) extrapolation was performed using Orca (version 4.0.1) with RI-MP2.[41,42]
CCSD(T)[39,40]	aug-cc-pVDZ[32]	Molpro	CBS(aug34) extrapolation was performed using Orca (version 4.0.1) with LPNO-CEPA/1.[43]
DLPNO-CCSD(T)[44,45]	CBS(34)	Orca 4.0.1	The NormalPNO,[33] TightPNO,[33] VeryTightPNO and ExtremePNO sets of threshold parameters were used, respectively. The RI-JK[46] approximation for HF calculations was used.
MP2[47]	CBS(34)	Orca 4.0.1	_
RI-MP2[41,42]	CBS(34)	Orca 4.0.1	The RI-JK[46] approximation for HF calculations was used.
RI-SCS-MP2[41,42,48]	CBS(34)	Orca 4.0.1	The RI-JK[46] approximation for HF calculations was used.
RI-MP3[41,42,49,50]	CBS(34)	Orca 4.0.1	The RI-JK[46] approximation for HF calculations was used.

1.2.3 DFT

Method	Basis set	Software	Comments
B97M-V [51]	def2-QZVP [25]	PSI4 1.2	The RI-J [52–54] approximation with the def2/JK [55] fitting basis set was used.
ωB97M-V [56]	def2-QZVP [25]	PSI4 1.2	The RI-JK [46] approximation with the def2/JK [55] fitting basis set was used.
B3LYP [57–59]-XDM [60–64]	aug-cc-pVTZ [32]	Gaussian, postg	–
PBE [65]-XDM [60–64]	aug-cc-pVTZ [32]	Gaussian, postg	–
DSD-PBEP86 [24]	def2-QZVP [25]	Orca 3.0.3	The RIJCOSX [27,28] approximation with the def2-TZVP/J [29] and def2-TZVP/C [30] fitting basis sets was used.
BLYP [57,58]-XDM [60–64]	aug-cc-pVTZ [32]	Gaussian, postg	–
M06L [66]	def2-QZVP [25]	Orca 4.0.1	The RI-J [52–54] approximation with the def2/J [55] fitting basis set was used.
B3LYP [57–59]-NL [67,68]	def2-QZVP [25]	Orca 4.0.1	The RIJCOSX [27,28] approximation with the def2-TZVP/J [29] fitting basis set was used.
PBE [65]-D3(BJ) [11,69]	def2-QZVP [25]	Orca 4.0.1	The RI-J [52–54] approximation with the def2/J [55] fitting basis set was used.
M06-2X [70]-D3(ZERO) [11,69]	def2-QZVP [25]	Orca 4.0.1	The RIJCOSX [27,28] approximation with the def2-TZVP/J [29] fitting basis set was used.
BLYP [57,58]-NL [67,68]	def2-QZVP [25]	Orca 4.0.1	The RI-J [52–54] approximation with the def2/J [55] fitting basis set was used.
B3LYP [57–59]-dDsC [71–73]	QZ4P [74]	ADF	Density fitting was performed using the RI approximation [74,75] with the QZ4P [74] fitting basis set.

Method	Basis set	Software	Comments
M06L[66]-D3(ZERO)[11,69]	def2-QZVP[25]	Orca 4.0.1	The RI-J[52–54] approximation with the def2/J[55] fitting basis set was used.
B2PLYP[76]-D3[11,69]	def2-QZVP[25]	Orca 4.0.1	The RIJCOSX[27,28] approximation with the def2-TZVP/J[29] and def2-TZVP/C[30] fitting basis sets were used.
TPSS[77]-D3(BJ)[11,69]	def2-QZVP[25]	Orca 4.0.1	The RI-J[52–54] approximation with the def2/J[55] fitting basis set was used.
B3LYP[57–59]-D3(BJ)[11,69]	def2-QZVP[25]	Orca 4.0.1	The RIJCOSX[27,28] approximation with the def2-TZVP/J[29] fitting basis set was used.
ωB97X-D3(BJ)[11,69,78]	def2-QZVP[25]	Orca 4.0.1	The RIJCOSX[27,28] approximation with the def2-TZVP/J[29] fitting basis set was used.
rPW86PW92-vdW-DF10[79]	pc-3[80–82]	Q-Chem	–
PBE[65]-dDsC[71–73]	QZ4P[74]	ADF	Density fitting was performed using the RI approximation[75] with the QZ4P[74] fitting basis set.
BLYP[57,58]-D3(BJ)[11,69]	def2-QZVP[25]	Orca 4.0.1	The RI-J[52–54] approximation with the def2/J[55] fitting basis set was used.
M06-2X[70]	def2-QZVP[25]	Orca 4.0.1	The RIJCOSX[27,28] approximation with the def2-TZVP/J[29] fitting basis set was used.
B97-D3(BJ)[11,69,83]	def2-QZVP[25]	Orca 4.0.1	The RI-J[52–54] approximation with the def2/J[55] fitting basis set was used.

1.3 Energy Decomposition Schemes

Method	Basis set	Software	Comments
sSAPT0[84]	jun-cc-pVDZ[85,86]	PSI4 1.1	The RI-JK[46] approximation for HF calculations was used with the jun-cc-pVDZ/JK[87] fitting basis set.
SAPT2+[84]	aug-cc-pVDZ[32]	PSI4 1.1	The RI-JK[46] approximation for HF calculations was used with the aug-cc-pVDZ/JK[46] fitting basis set.
SAPT2+(3)δMP2[84]	aug-cc-pVTZ[32]	PSI4 1.1	The RI-JK[46] approximation for HF calculations was used with the aug-cc-pVTZ/JK[46] fitting basis set.
SAPT2+(CCD)δMP2[84]	aug-cc-pVTZ[32]	PSI4 1.1	The RI-JK[46] approximation for HF calculations was used with the aug-cc-pVTZ/JK[46] fitting basis set.
LED[88]-DLPNO-CCSD(T)[44,45]	cc-pVQZ[31]	Orca 4.0.1	The RI-JK[46] approximation for HF calculations was used with the cc-pVQZ/JK[46] fitting basis set. TightPNO[33] thresholds were used.

1.4 Visual Analyses

Method	Level of Theory	Software	Comments
DID[89]	LMP2[90]/aug-cc-pVTZ	Molpro	The cc-pVTZ basis set was used on H atoms. The RI-JK[46] approximation for HF calculations was used with the automatically generated JKFIT basis set. Visualization was performed using Paraview.
PolaBer[16]	MP2[91]/def2-TZVPPD[25,92]	PolaBer, Orca 4.0.1	Calculations were performed once in the absence and in the presence of electric fields of 0.005 a.u. in the positive and negative directions of the cartesian coordinate axes, respectively.

Method	Level of Theory	Software	Comments
NCIPLOT[19,20]	MP2[91]/def2-TZVPPD[25,92]	NCIPLOT, Orca 4.0.1	The intermolecular cut-off used was 0.9 to neglect intramolecular interactions. The density cut-off was 0.1. The reduced density gradient cut-off was 2.0. The density cut-off in the cube files was 0.007, the RDG cut-off in the cube files was 0.5. Visualization was performed using PyMol.

1.5 Additional Analyses

Van der Waals surfaces were calculated with an isovalue of 0.001 using MP2[91]/def2-TZVPPD[25,92] densities in multiwfn. COSMO[93] surfaces were calculated using ADF and the corresponding volumes and surfaces were obtained from the corresponding COSMO-RS module.[94] Additional calculations including the simple interaction models, the Q values, the P values and the $n_{contacts}$ were performed using python.

2 Supplementary Results and Discussion

In this section, additional results, that did not fit into the main manuscript, are presented and discussed.

2.1 Benchmarking

2.1.1 Structures of the Complexes

Figures S1-S46 show the final structures of all the intermolecular complexes. The corresponding XYZ files are provided in the additional supporting material. For benchmarking of the DFT and WFT methods (cf. Table 2), the following types of complexes were used: **1-HH**, **1-HF**, **1-FF**, **2-HH**, **2-HF**, **2-FF**, **3-HH**, **3-HF**, **3-FF**, **4-HH** and **4-FF**.

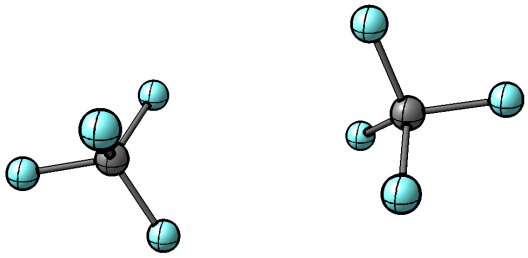

Figure S1: Final structure of complex **1-FF1**.

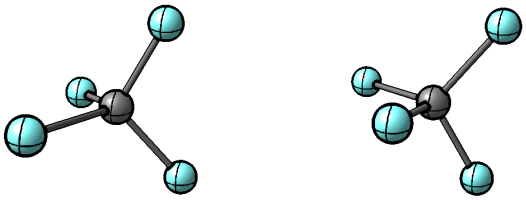

Figure S2: Final structure of complex **1-FF2**.

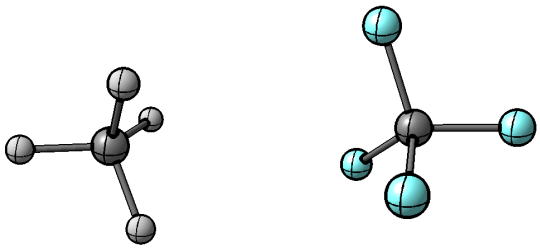

Figure S3: Final structure of complex **1-HF1**.

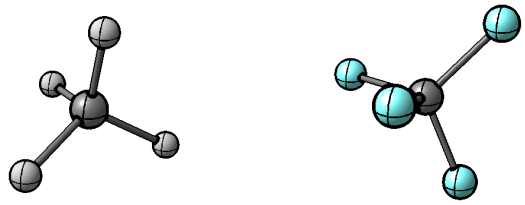

Figure S4: Final structure of complex **1-HF2**.

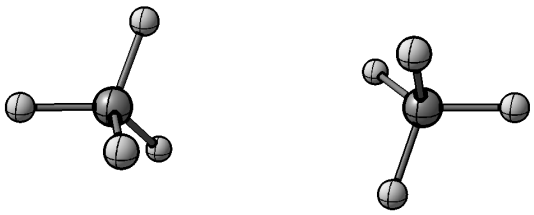

Figure S5: Final structure of complex **1-HH1**.

Figure S6: Final structure of complex **1-HH2**.

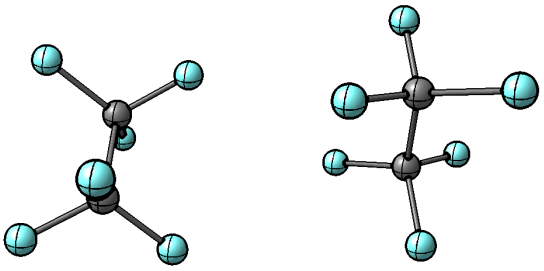

Figure S7: Final structure of complex **2-FF1**.

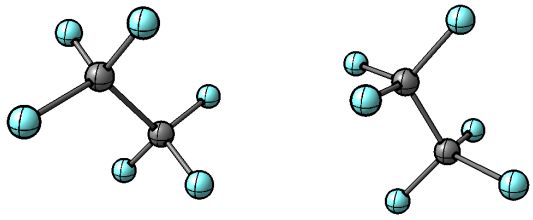

Figure S8: Final structure of complex **2-FF2**.

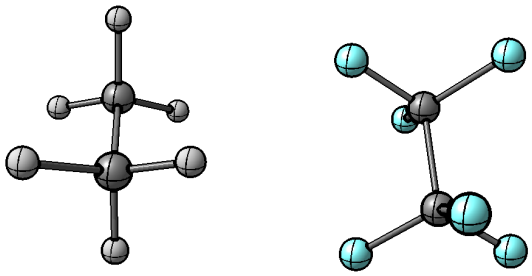

Figure S9: Final structure of complex **2-HF1**.

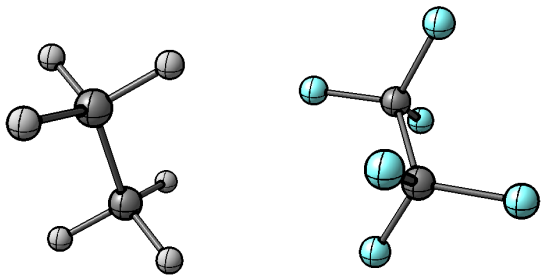

Figure S10: Final structure of complex **2-HF2**.

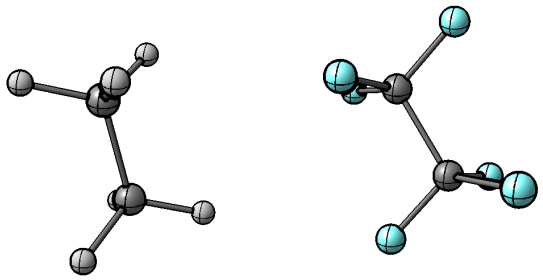

Figure S11: Final structure of complex **2-HF3**.

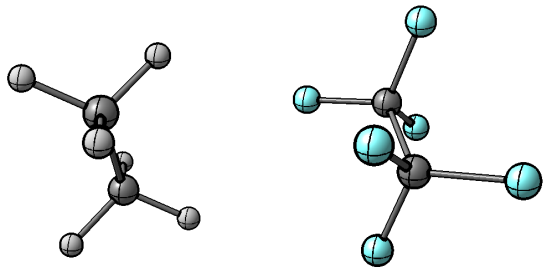

Figure S12: Final structure of complex **2-HF4**.

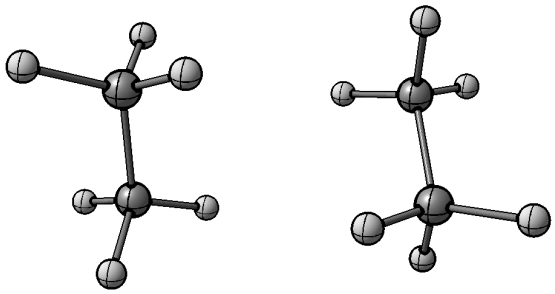

Figure S13: Final structure of complex **2-HH1**.

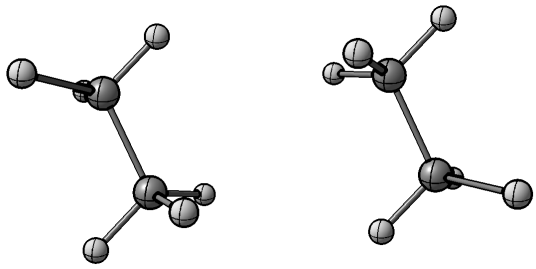

Figure S14: Final structure of complex **2-HH2**.

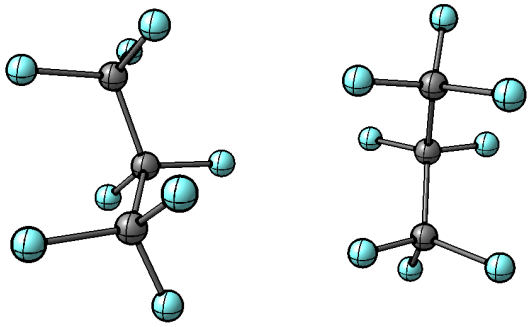

Figure S15: Final structure of complex **3-FF1**.

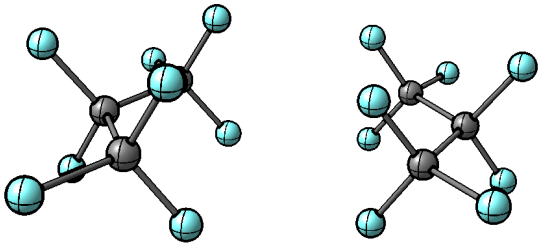

Figure S16: Final structure of complex **3-FF2**.

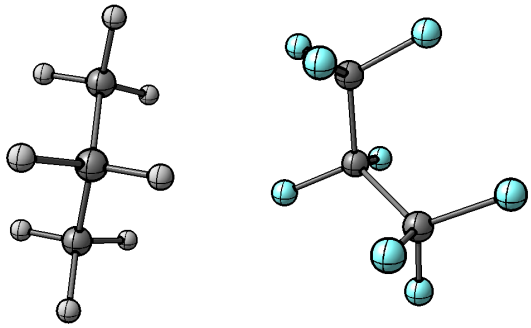

Figure S17: Final structure of complex **3-HF1**.

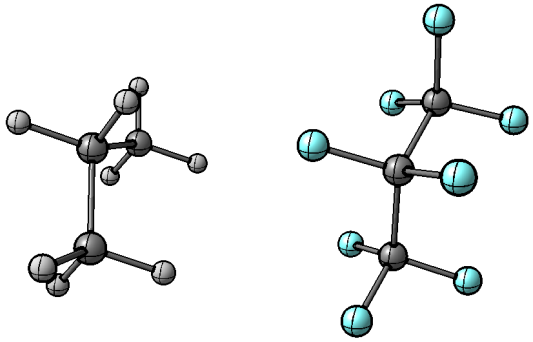

Figure S18: Final structure of complex **3-HF2**.

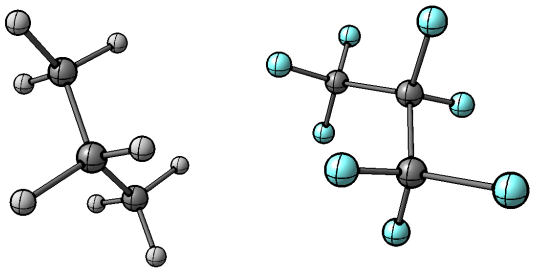

Figure S19: Final structure of complex **3-HF3**.

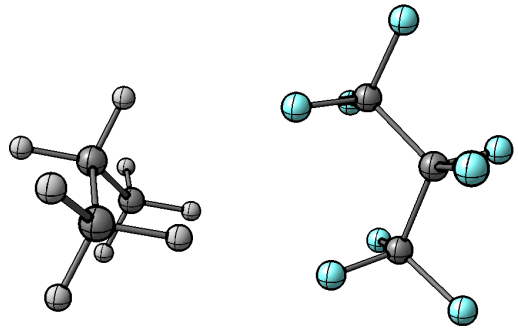

Figure S20: Final structure of complex **3-HF4**.

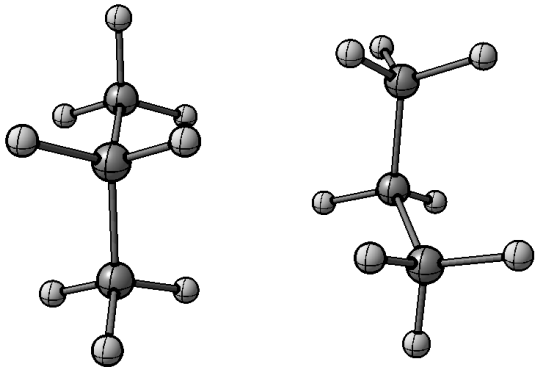

Figure S21: Final structure of complex **3-HH1**.

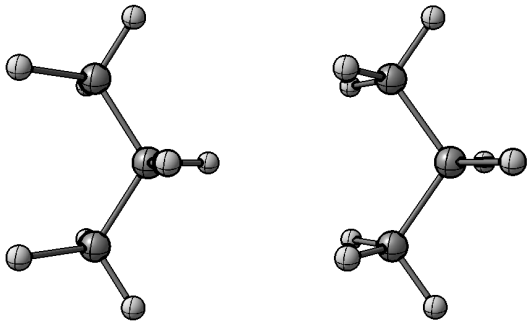

Figure S22: Final structure of complex **3-HH2**.

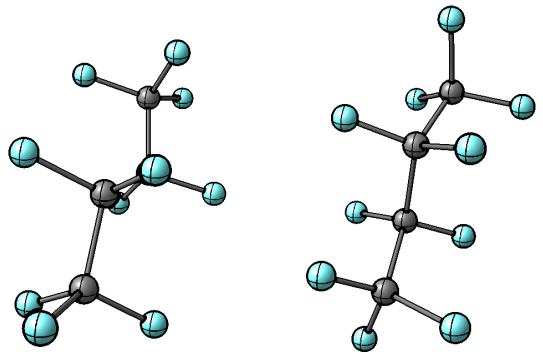

Figure S23: Final structure of complex **4-FF1**.

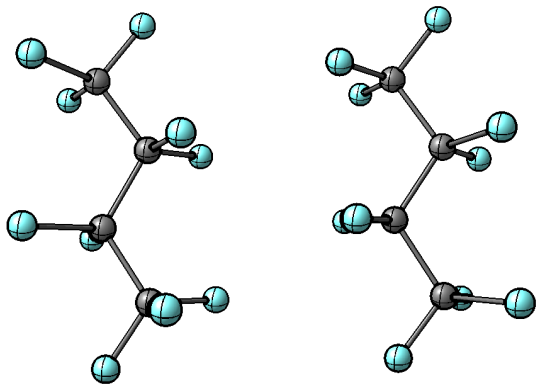

Figure S24: Final structure of complex **4-FF2**.

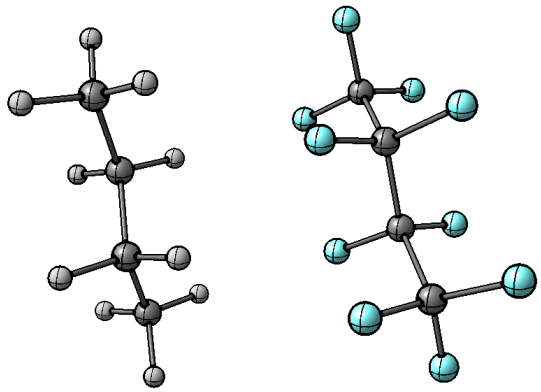

Figure S25: Final structure of complex **4-HF1**.

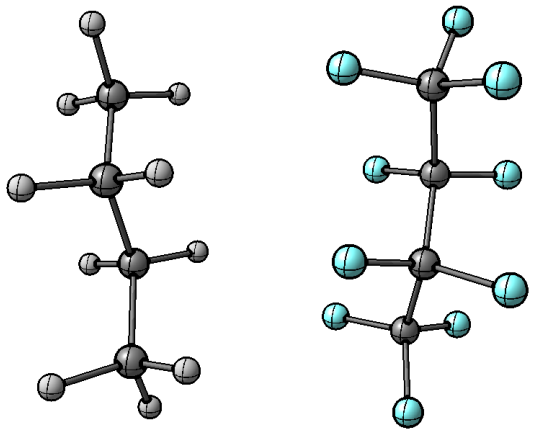

Figure S26: Final structure of complex **4-HF2**.

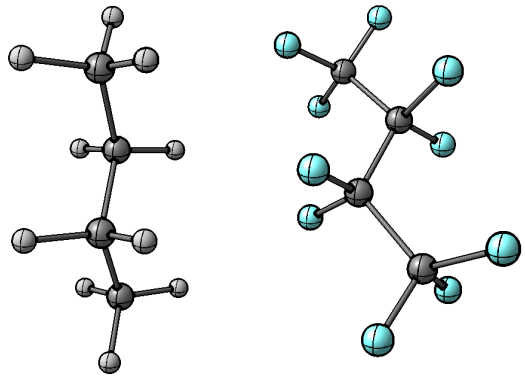

Figure S27: Final structure of complex **4-HF3**.

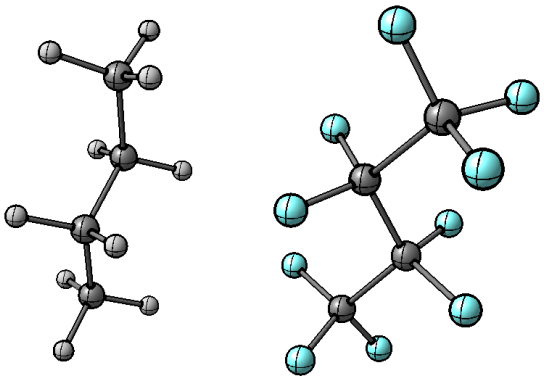

Figure S28: Final structure of complex **4-HF4**.

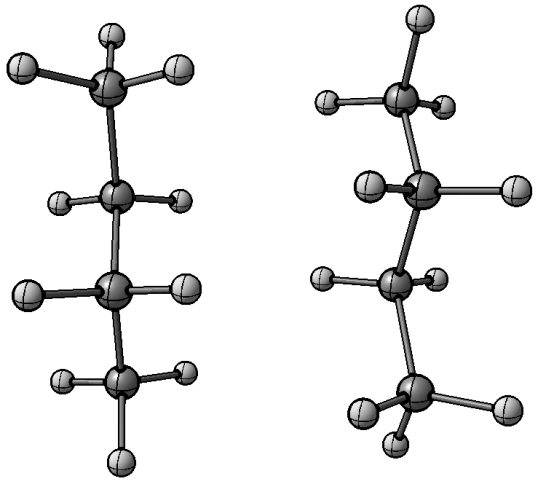

Figure S29: Final structure of complex **4-HH1**.

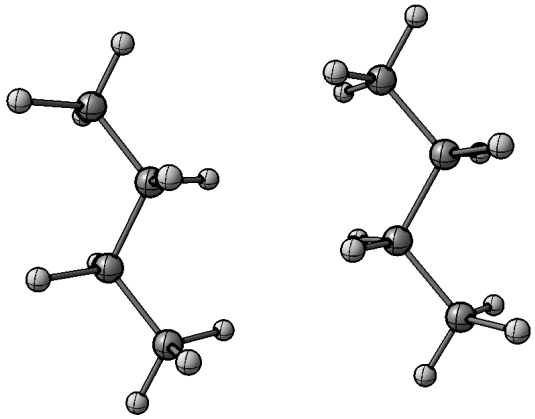

Figure S30: Final structure of complex **4-HH2**.

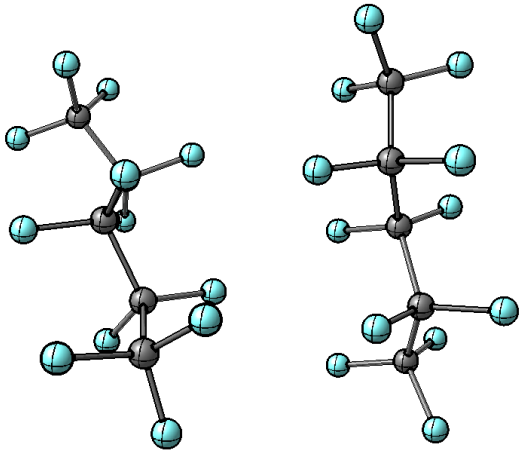

Figure S31: Final structure of complex **5-FF1**.

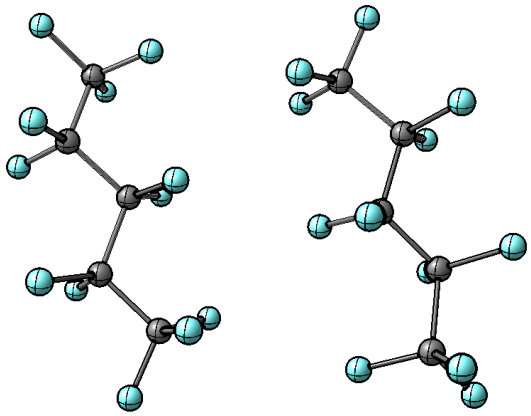

Figure S32: Final structure of complex **5-FF2**.

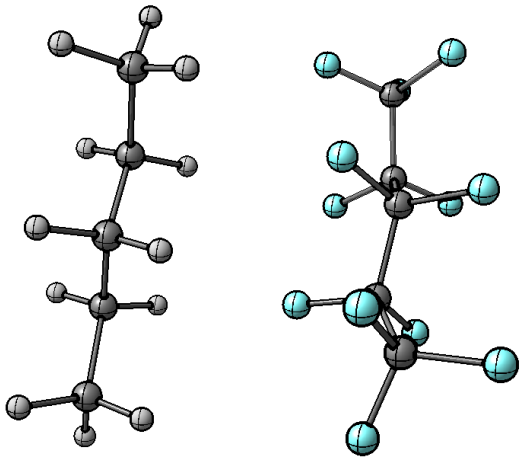

Figure S33: Final structure of complex **5-HF1**.

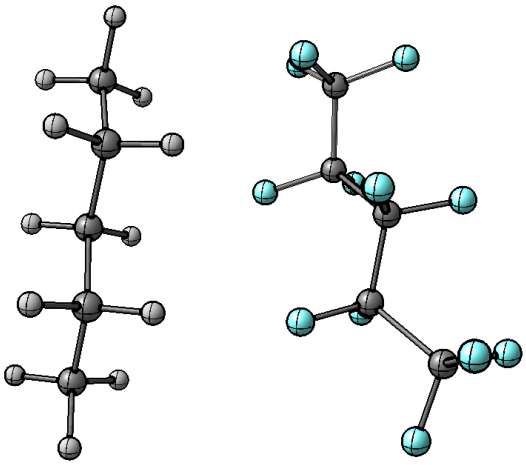

Figure S34: Final structure of complex **5-HF2**.

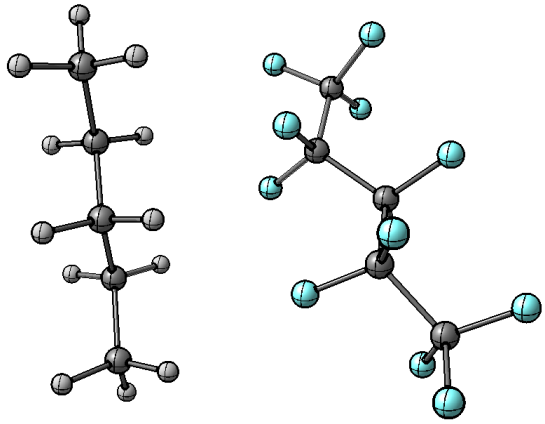

Figure S35: Final structure of complex **5-HF3**.

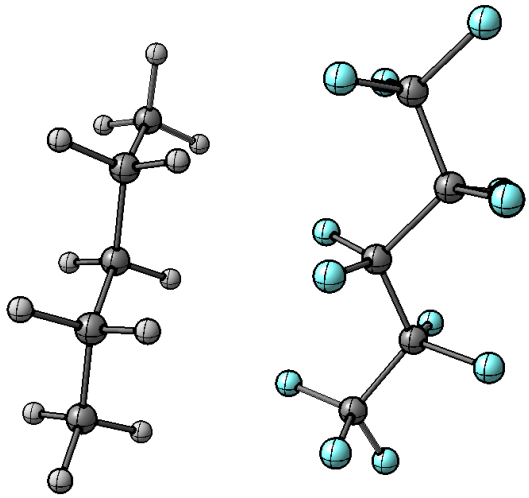

Figure S36: Final structure of complex **5-HF4**.

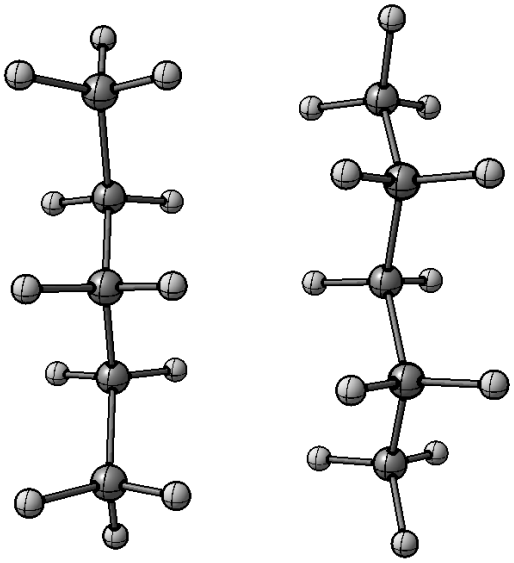

Figure S37: Final structure of complex **5-HH1**.

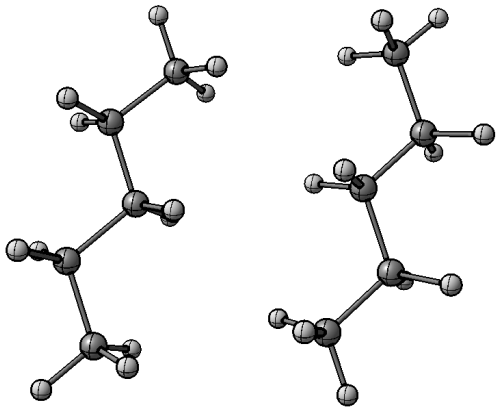

Figure S38: Final structure of complex **5-HH2**.

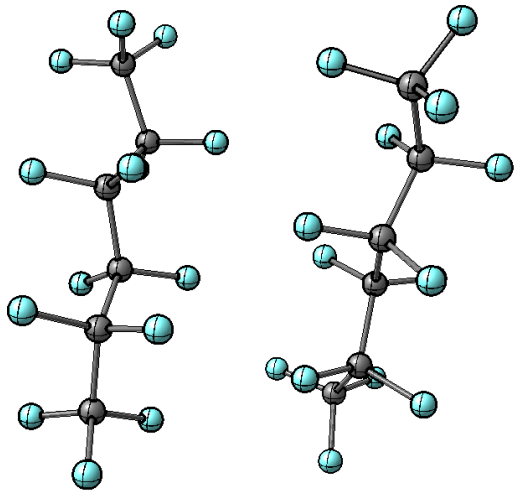

Figure S39: Final structure of complex **6-FF1**.

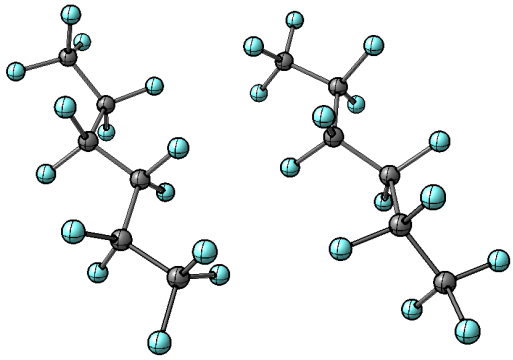

Figure S40: Final structure of complex **6-FF2**.

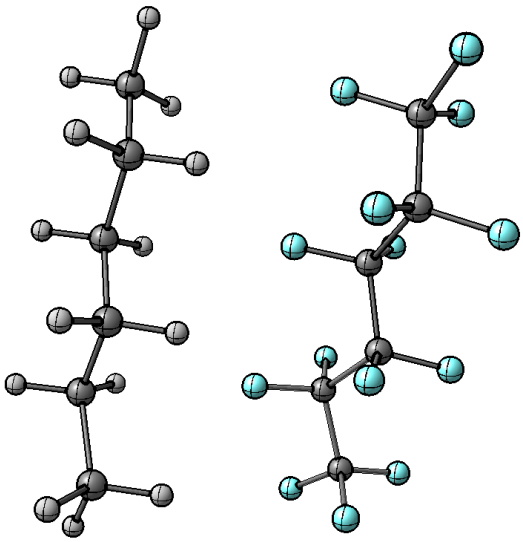

Figure S41: Final structure of complex **6-HF1**.

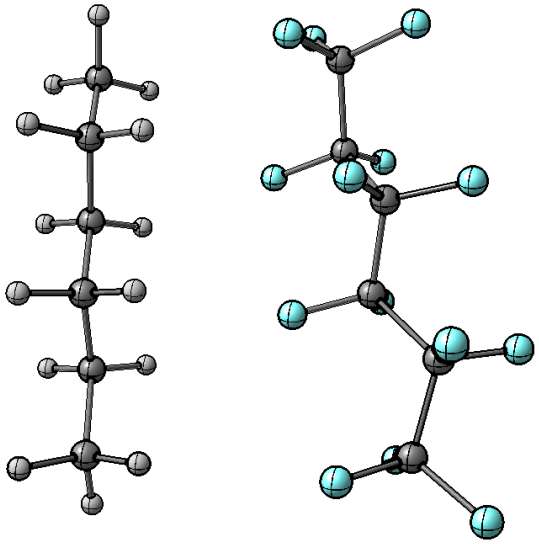

Figure S42: Final structure of complex **6-HF2**.

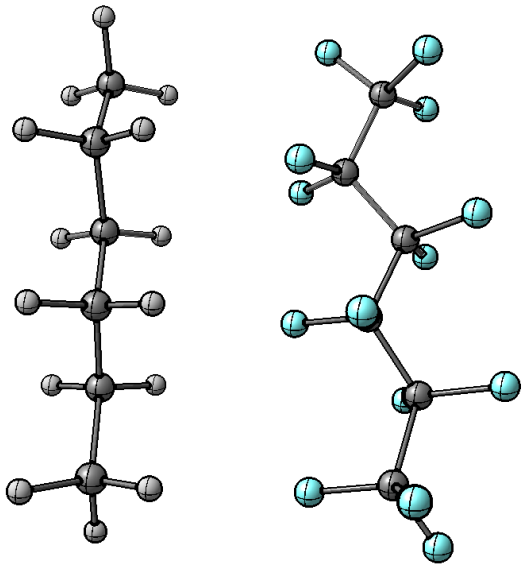

Figure S43: Final structure of complex **6-HF3**.

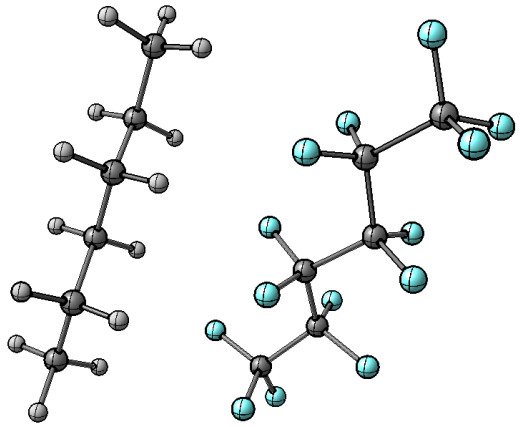

Figure S44: Final structure of complex **6-HF4**.

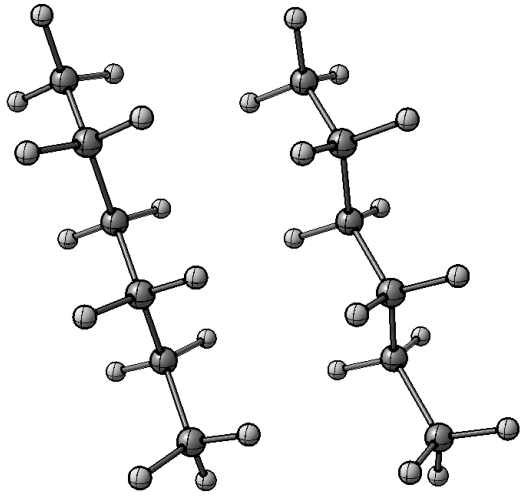

Figure S45: Final structure of complex **6-HH1**.

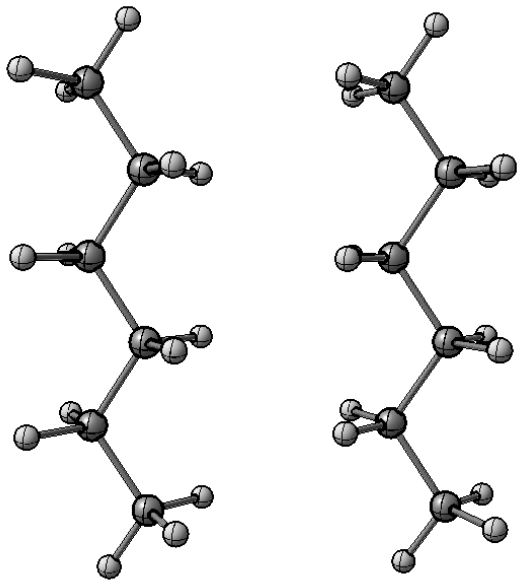

Figure S46: Final structure of complex **6-HH2**.

2.1.2 Discussion

Systematic benchmark data for perfluoroalkane dimers of increasing carbon chain length is sparse. The only high-level benchmark data set that comes closest includes several halogenated small molecules, the most similar type of interaction energy computed being the molecular complex of trifluoromethane and methane.[95] To the best of our knowledge, no CCSD(T) benchmark interaction energies estimated at the CBS limit of perfluoroalkane dimers larger than perfluoromethane have been reported before, probably because of the extremely high computational demands of these calculations.

The working horse for our benchmark data is the explicitly correlated CCSD(T)-F12 method. It provides BIEs close to the CBS limit already using the cc-pVDZ-F12 (VDZ-F12) basis set and therefore CCSD(T)-F12/VDZ-F12 is the most efficient benchmark method for the systems under investigation. We compared the VDZ-F12 numbers to the corresponding cc-pVTZ-F12 (VTZ-F12) numbers for methanes and ethanes and obtained almost the same results (vide supra). Explicitly correlated coupled cluster methods[36,37,96–98] represent, at the moment, the best alternative to CBS extrapolation schemes and are in conjunction with

CCSD(T) computationally more affordable than CBS from triple- and quadruple-zeta basis set results.

Our benchmark results (cf. Table 2) also show that while for **HH** and **HF** systems TightPNO-DLPNO-CCSD(T) is almost converged to the canonical CCSD(T) results, using tighter cutoff parameters results only in slow convergence of the DLPNO-CCSD(T) results towards our CCSD(T)-F12/VDZ benchmark energies for **FF** complexes. The problems of DLPNO-CCSD(T) in reproducing the benchmark interaction energies of perfluoroalkane complexes likely stem (at least to a significant extent) from the large contribution of the so-called weak pairs, which are treated using Local-MP2 and not further considered in the CCSD step.[99] It should be noted that it has been shown before that for the accurate description of the interaction energies of some specific systems tighter cutoff thresholds than the standard TightPNO settings are necessary.[34,100,101] The drawback is that these tighter cutoff thresholds make the corresponding DLPNO-CCSD(T) computations much less affordable for increasingly large systems.

Additionally, it is also interesting to note that the commonly employed CBS extrapolation schemes used on top of CCSD(T) single points are not reproducing BIEs in **HF** and **FF** systems properly. Neither using MP2 nor using LPNO-CEPA/1 for extrapolation provides comparable numbers to either CCSD(T)-F12 or CCSD(T)/CBS(34) (tested on methanes and ethanes). However, using MP2 for estimating the CBS correction to be added on top of CCSD(T) single points is commonly used for benchmark calculations.[95,102] Extrapolation using LPNO-CEPA/1 has been proposed recently as alternative but has not yet been commonly applied.[103]

Looking at the performance of the various DFT methods, M06L performs acceptable across the whole series of molecules but still shows larger deviations for **HF** and **FF**. The behavior of dDsC does not show a clear tendency as it significantly underestimates the BIEs in both **HF** and **FF** in conjunction with B3LYP but significantly overestimates the same BIEs in conjunction with PBE. While D3 performs well for **HH**, it shows significant de-

viations for **HF** already and even bigger deviations for **FF** complexes underestimating the dispersive contributions in these systems. It should be noted that it has been observed before that the standard D3 parametrization is inappropriate to describe the interaction of **1-FF**.[104] We also used the recently developed program BootD3[12] to test the uncertainties in the D3 dispersion contribution to the interaction energies. We obtained low uncertainties (i.e. generally below 10 %) with respect to the overall interaction energies. Therefore, uncertainties in the D3 correction cannot explain the large deviations from the benchmark values observed. The likely reason for the failure of D3 in perfluoroalkanes is the neglect of the change in polarizability due to the strongly polarized C—F bonds. This effect is taken into account, at least to some extent, in the XDM correction and it is very strong in perfluoroalkanes as can be seen from the computed atomic polarizabilities in **1-F** (cf. Table 3). It should be noted that this shortcoming of D3 is known and D4 has been developed to alleviate this problem.[105] At the time this manuscript was prepared, we could only test the D4 correction as part of the semiempirical GFN2-xTB method.[35] On the basis of our benchmarks, GFN2-xTB is a significant improvement over GFN-xTB.[13] However, the performance of D4 in conjunction with DFT remains to be tested in the near future. VV10, abbreviated as either NL or V herein, on the other hand, in B97M-V and ωB97M-V, provides the most robust and efficient methods to predict BIEs of complexes of alkanes and perfluoroalkanes. On the other hand, in conjuction with BLYP and B3LYP it results in significant overestimation of the BIEs of **HF** and **FF**. This suggests that VV10 needs to be included in the overall functional parametrization rather than being used as correction on top of a given functional to obtain accurate results.

Having discussed the computational methods used to obtain accurate BIEs of our model complexes, we can now shift our attention to comparing the BIEs of **HH**, **HF** and **FF** complexes having the same carbon chain length (cf. Figure 13). Looking at the actual CCSD(T)-F12 numbers and the estimated CCSD(T)-F12 numbers we observe that from carbon chains of one to three the **FF** complexes have a stronger BIE than the correspond-

ing **HH** complexes. The estimated CCSD(T)-F12 numbers suggest that with carbon chain lengths of four and longer the relative BIEs invert so that the corresponding **HH** complexes have a stronger BIE. Interestingly, this change in the relative BIEs parallels the experimentally observed inversion of relative boiling points of alkanes and perfluoroalkanes at a carbon chain length of four (cf. Figure 14). The boiling point is a measure of the strength of intermolecular interactions so it is expected to somewhat reflect the BIEs of intermolecular complexes. The inversion of relative BIEs also reflects the trend observed in the experimental average attraction energies obtained from critical parameters (cf. Figure 15). The inversion in relative average attraction energies is observed already at a carbon chain length of two but the general trend is comparable.

From the benchmarked methods, only relative BIEs from B97M-V show the inversion at a carbon chain length of four, the third, fourth and fifth best methods according to our benchmarking, i.e. ωB97M-V/def2-QZVP, B3LYP-XDM/aug-cc-pVTZ and VeryTight-DLPNO-CCSD(T)/CBS(34) would predict the inversion of BIEs already at a carbon chain length of two. It can be concluded that **H** and **F** homodimers with carbon chain lengths between one and six show similar BIEs. Overall, the benchmarking performed was necessary in order to be able to evaluate the relative BIEs of **HH**, **HF** and **FF** properly. We find that the BIEs of the homodimers of alkanes and perfluoroalkanes having the same number of carbon atoms are similar (cf. Figure 13a) from one to six carbon atoms. Except for **1-HF**, we find that the corresponding heterodimers have weaker BIEs than either of the homodimers.

Another important aspect are the geometries we chose for our benchmark data set. DSD-PBEP86 is a double-hybrid functional and was selected on the basis of available benchmarks for "ordinary" organic molecules.[24] While it is not the best functional to predict the BIEs of our model complexes (in our ranking of computational methods it is only the 11th rank), the rigid energy scans performed using Tight-LED-DLPNO-CCSD(T)/QZ show minima in the BIE at about the same intermolecular separations (vide supra) which suggests the interaction

geometries to be adequate. Additionally, when looking at our ranking, the only better ranked methods to predict the BIEs, which could have been used for efficient geometry optimization as well, are MP2, PBE-XDM, B3LYP-XDM, B97M-V and ωB97M-V. For future computations, B97M-V geometries might be a cost-effective alternative to DSD-PBEP86 geometries as the additional cost of the HF and MP2 single points performed during the DSD-PBEP86 calculations are computationally more expensive than the additional cost of the VV10 correction in B97M-V.

2.1.3 Benchmarking WFT Methods

Using the optimized geometries we computed the interaction energies of the molecular complexes of the methane and ethane systems using high-level wavefunction methods. We used CCSD(T)-F12/VTZ as benchmark and compared several alternative methods against it. The corresponding results are summarized in Table S1.

One would expect the canonical coupled cluster methods CCSD(T)-F12 and CCSD(T)/CBS(34), which are extrapolated to the complete basis set limit, to be most accurate. On the basis of literature benchmarks[36,37] we selected CCSD(T)-F12/VTZ as reference method and were looking for a cheaper method that reproduces the corresponding interaction energies best. CCSD(T)-F12/VDZ shows only minor deviations from the reference method at much less computational cost (cf. Table S1). Using CCSD(T)-F12/VDZ we were able to perform benchmark calculations for most of our molecular complexes under study except for **FF** with a carbon chain length of four or higher, and **HF** with a carbon chain legnth of five or six.

We compared the corresponding CCSD(T)-F12/VDZ interaction energies to DLPNO-CCSD(T) results using various sets of cut-off thresholds. While many data points agree very well to the benchmark data, some selected data points show considerable deviations. We investigated these deviations further by analyzing all the data points of the corresponding subsystems **HH**, **HF** and **FF** separately (Figures S47-S49).

Table S1: Benchmark of various wavefunction methods against CCSD(T)-F12/VTZ as reference for methane and ethane systems (MP3/CBS(34) numbers are only based on methane systems). CCSD(T)-F12/VDZ compares best and is still affordable for most of the complexes studied in this work.

Method	MAD [kcal mol^{-1}]	MAD$_{rel}$ [%]	MSD [kcal mol^{-1}]	MSD$_{rel}$ [%]
CCSD(T)-F12/VDZ	0.02(1)	2(1)	0.02(1)	2(1)
CCSD(T)/CBS(34)	0.03(3)	3(3)	0.02(3)	2(4)
SAPT2(CCD)δMP2/aTZ	0.03(3)	3(3)	0.02(4)	2(4)
SAPT2+(3)δMP2/aTZ	0.06(3)	6(3)	0.06(3)	6(3)
CCSD(T)/CBS(LPNO-CEPA/1)	0.07(4)	8(4)	-0.05(6)	-4(8)
CCSD(T)/CBS(MP2)	0.13(9)	14(9)	-0.13(9)	-14(9)
MP2/CBS(34)	0.13(8)	14(7)	0.12(10)	13(9)
MP3/CBS(34)	0.14(10)	20(10)	0.14(10)	20(10)

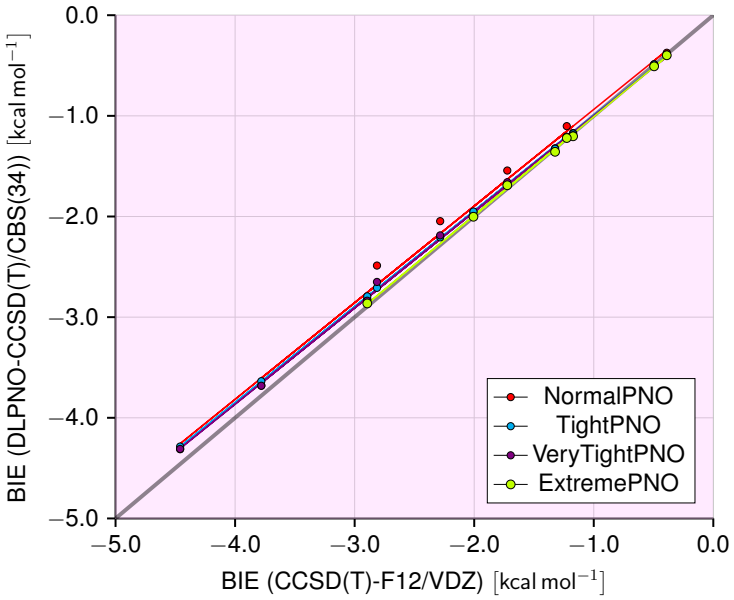

Figure S47: Interaction energies of molecular complexes from DLPNO-CCSD(T)/CBS using various cut-off thresholds against CCSD(T)-F12/VDZ as reference in **HH** complexes. Linear regressions illustrate the systematic deviations observed from the reference as a function of interaction energies.

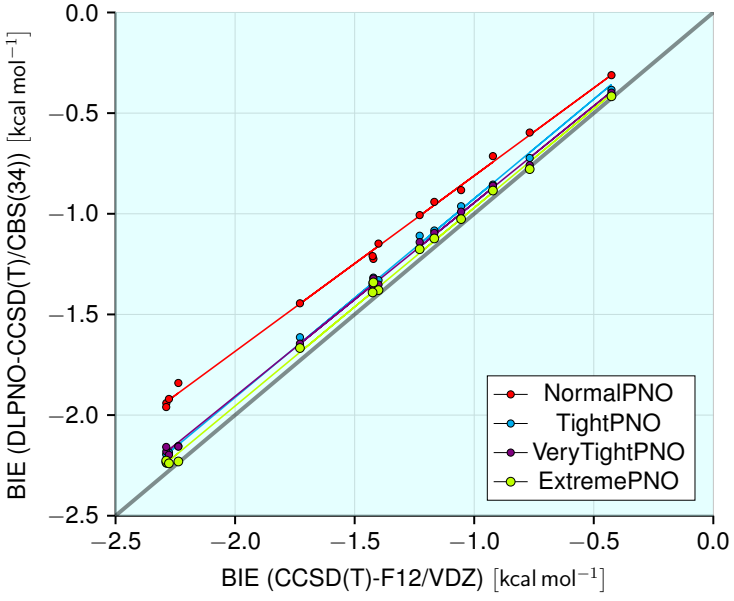

Figure S48: Interaction energies of molecular complexes from DLPNO-CCSD(T)/CBS using various cut-off thresholds against CCSD(T)-F12/VDZ as reference in **HF** complexes. Linear regressions illustrate the systematic deviations observed from the reference as a function of interaction energies.

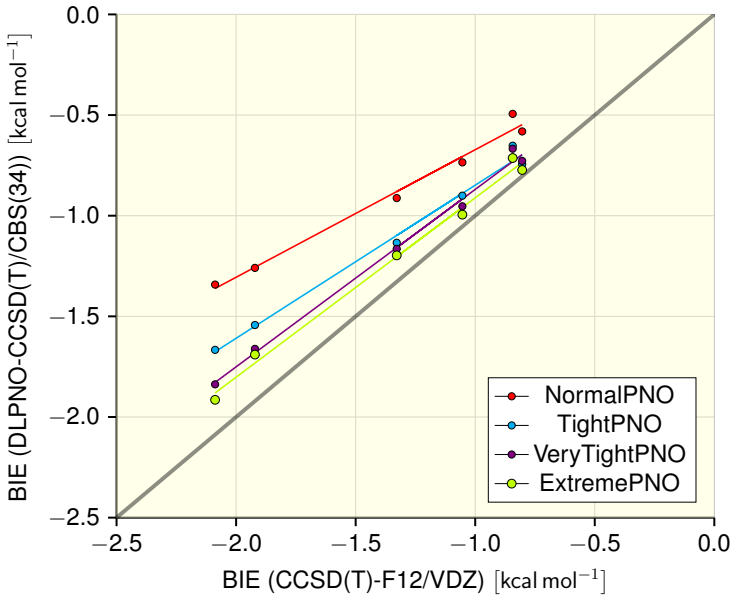

Figure S49: Interaction energies of molecular complexes from DLPNO-CCSD(T)/CBS using various cut-off thresholds against CCSD(T)-F12/VDZ as reference in **FF** complexes. Linear regressions illustrate the systematic deviations observed from the reference as a function of interaction energies.

Figures S47-S49 show that the data points with significant deviations are the **FF** subsystems. Additionally, the deviations are systematic as they approximately show linear scaling with interaction energy size. The corresponding linear regressions assessing the extent of the systematic deviations are shown in Table S2.

The parameters of the linear regressions from Table S2 can be interpreted as quantitative measure of the systematic deviations between DLPNO-CCSD(T)/CBS(34) and CCSD(T)-F12/VDZ interaction energies. The slope (k) is a measure of what percentage of the benchmark interaction energy is recovered by the DLPNO approach as the interaction energy increases (ideal would be a slope of one). The intercept (d) is a measure of the additional offset of all the interaction energies relative to the benchmark energies (ideal would be an intercept of zero). Table S2 demonstrates that all the intercepts are small but shows significant deviations of the slopes from one for the **FF** subsystems. This shows that DLPNO-CCSD(T)/CBS(34) methods significantly underestimate the interaction of **F** with each other.

Table S2: Systematic deviations of interaction energies of molecular complexes from DLPNO-CCSD(T)/CBS using various cut-off thresholds against CCSD(T)-F12/VDZ as reference divided into the three subclasses **HH**, **HF** and **FF**. Systematic deviations are negligible for **HH**, small for **HF** but significant for **FF**.

$$\text{BIE(DLPNO-CCSD(T)/CBS(34)} = \text{k} \cdot \text{BIE(CCSD(T)-F12/VDZ)} + \text{d}$$

Truncation	**HH**		**HF**		**FF**	
	k	**d [kcal mol^{-1}]**	**k**	**d [kcal mol^{-1}]**	**k**	**d [kcal mol^{-1}]**
NormalPNO	0.96(2)	0.02(5)	0.87(1)	0.06(2)	0.63(4)	-0.04(6)
TightPNO	0.952(4)	-0.039(9)	0.99(1)	0.06(1)	0.76(4)	-0.09(6)
VeryTightPNO	0.956(9)	-0.04(2)	0.962(9)	0.02(1)	0.88(3)	0.01(5)
ExtremePNO	0.98(1)	-0.03(2)	0.98(1)	0.01(2)	0.89(4)	-0.02(6)

It should be noted that while using increasingly tight cut-off thresholds remedies the problem, even ExtremePNO systematically underestimates the interaction by 11% (cf. Table S2). Additionally, we used the correlation of VeryTightPNO-DLPNO-CCSD(T)/CBS(34) against CCSD(T)-F12/VDZ to estimate benchmark interaction energies for **HF** complexes with five and six carbon atoms and **FF** complexes with four, five and six carbon atoms because the corresponding CCSD(T)-F12/VDZ calculations were too prohibitively expensive. These estimates agree reasonably well with the corresponding B97M-V BIEs.

2.1.4 Rigid Geometry Scans

To assess the performance of DSD-PBEP86/def2-TZVP(spd) in the geometry optimizations for our test systems we performed rigid geometry scans in which we systematically changed the distance between the interacting molecules but did not allow for geometry relaxation. We used both RI-MP2/CBS(34) and LED-DLPNO-CCSD(T)/QZ for the rigid distance scans. RI-MP2/CBS(34) was used for all the complexes studied, LED-DLPNO-CCSD(T)/QZ was used for complexes with one to three carbon atoms in the interacting molecules. The corresponding results are illustrated in Figures S50-S95. The interaction energy minima of both RI-MP2 and LED-DLPNO-CCSD(T)/QZ coincide well with the optimized intermolecular separation in the DSD-PBEP86 geometries. The good agreement between the interaction energy minima of LED-DLPNO-CCSD(T)/QZ, RI-MP2 and DSD-PBEP86/def2-TZVP(spd)

suggests that these geometries are sufficiently accurate for all the molecular complexes under study.

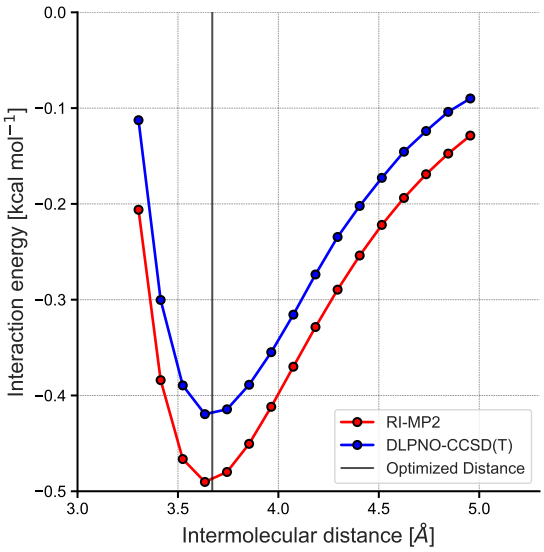

Figure S50: Rigid geometry scan of **1-HH1** and comparison to the optimized intermolecular separation.

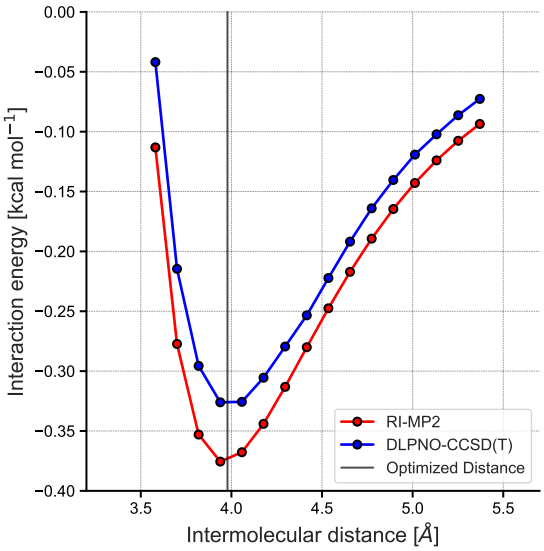

Figure S51: Rigid geometry scan of **1-HH2** and comparison to the optimized intermolecular separation.

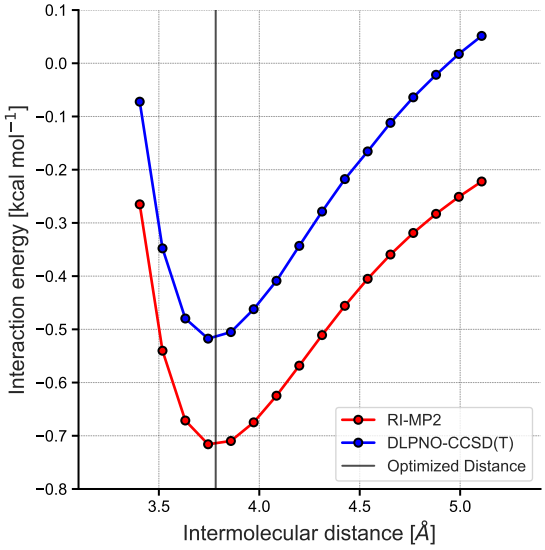

Figure S52: Rigid geometry scan of **1-HF1** and comparison to the optimized intermolecular separation.

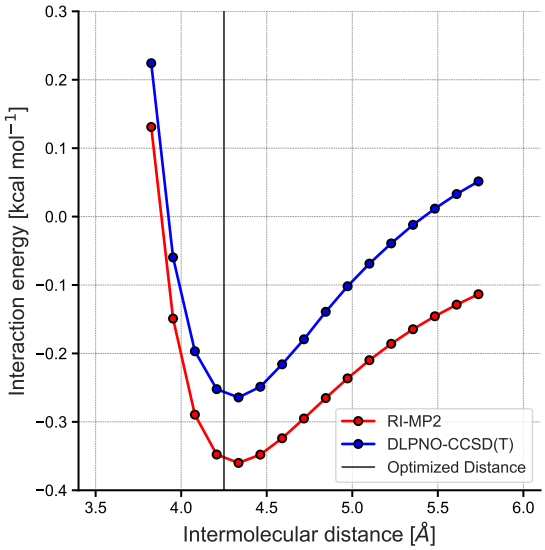

Figure S53: Rigid geometry scan of **1-HF2** and comparison to the optimized intermolecular separation.

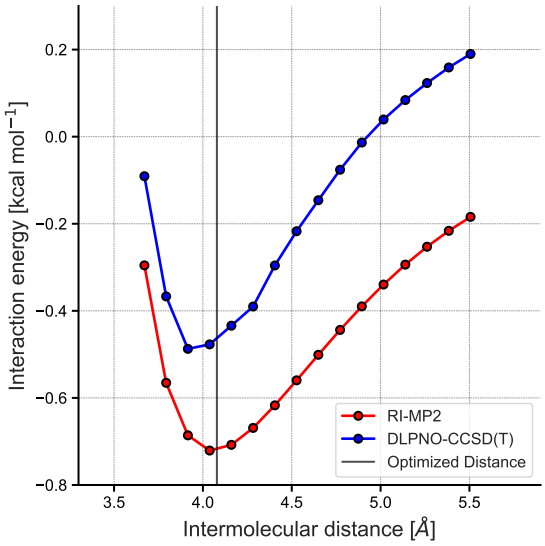

Figure S54: Rigid geometry scan of **1-FF1** and comparison to the optimized intermolecular separation.

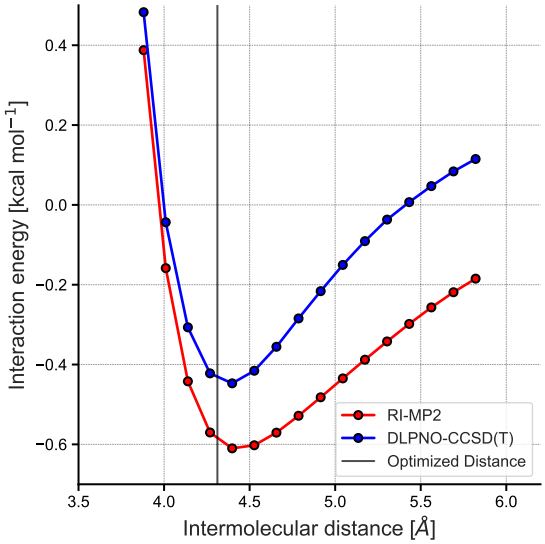

Figure S55: Rigid geometry scan of **1-FF2** and comparison to the optimized intermolecular separation.

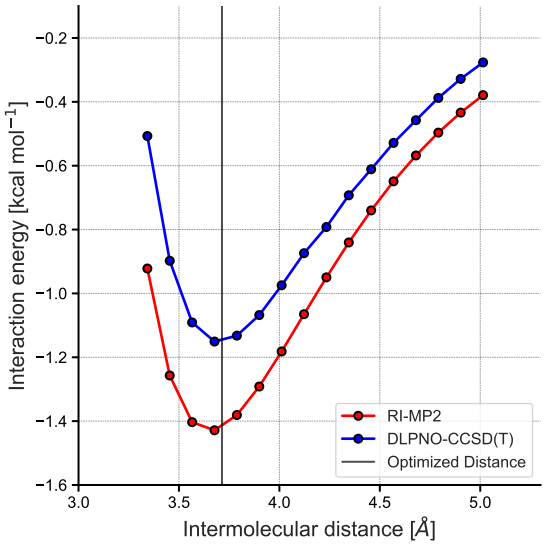

Figure S56: Rigid geometry scan of **2-HH1** and comparison to the optimized intermolecular separation.

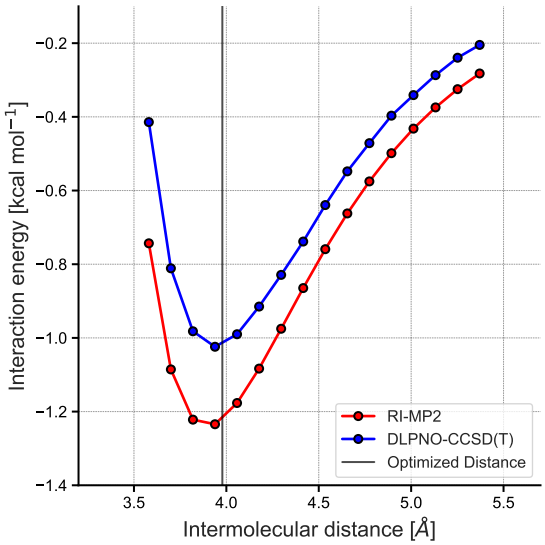

Figure S57: Rigid geometry scan of **2-HH2** and comparison to the optimized intermolecular separation.

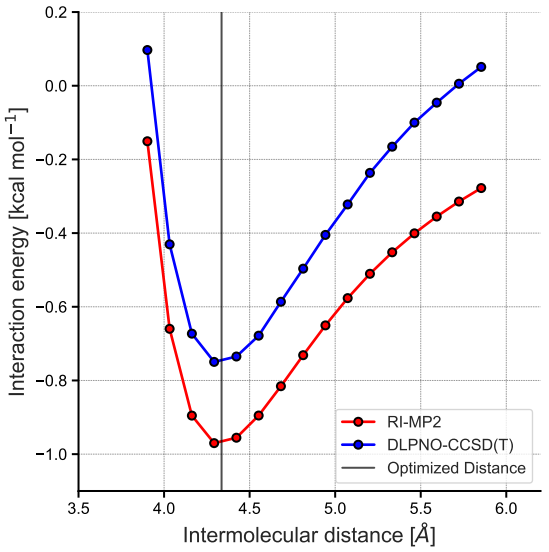

Figure S58: Rigid geometry scan of **2-HF1** and comparison to the optimized intermolecular separation.

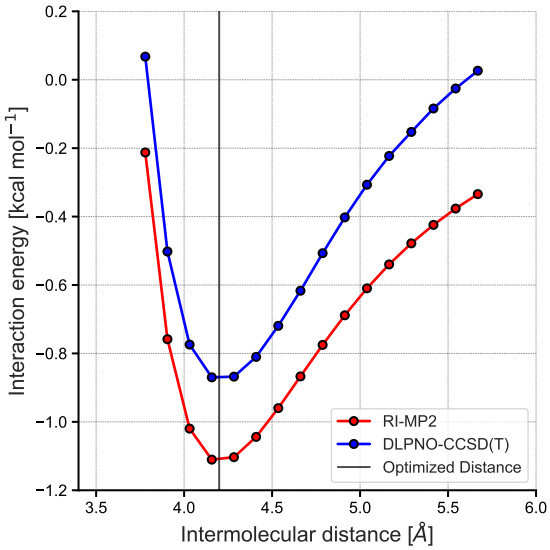

Figure S59: Rigid geometry scan of **2-HF2** and comparison to the optimized intermolecular separation.

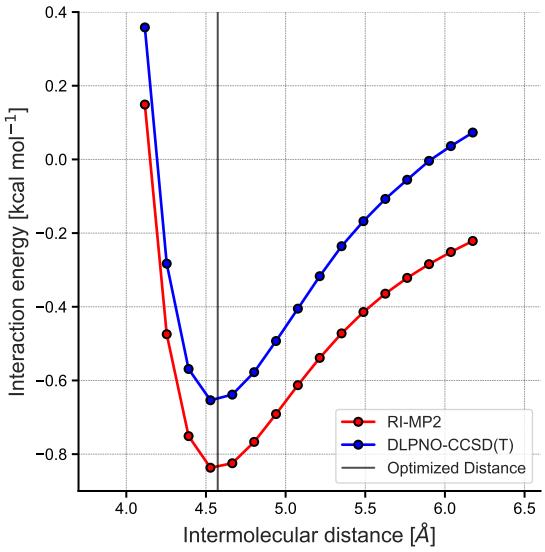

Figure S60: Rigid geometry scan of **2-HF3** and comparison to the optimized intermolecular separation.

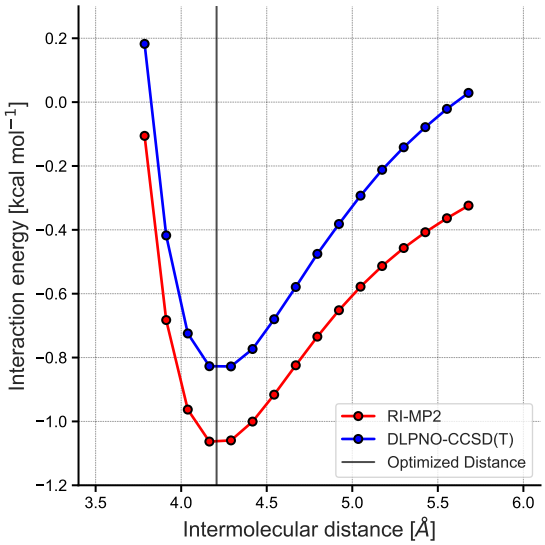

Figure S61: Rigid geometry scan of **2-HF4** and comparison to the optimized intermolecular separation.

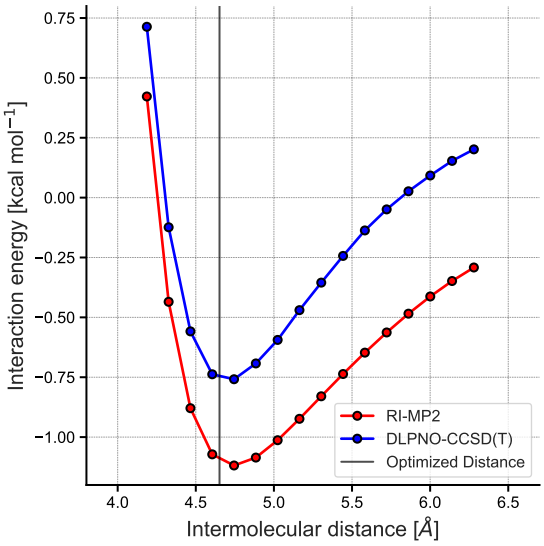

Figure S62: Rigid geometry scan of **2-FF1** and comparison to the optimized intermolecular separation.

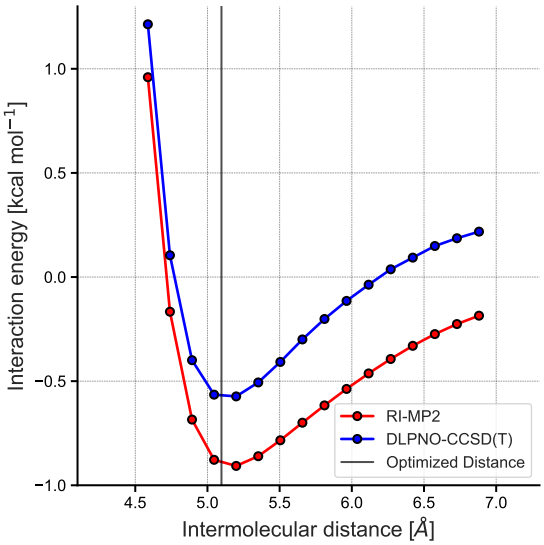

Figure S63: Rigid geometry scan of **2-FF2** and comparison to the optimized intermolecular separation.

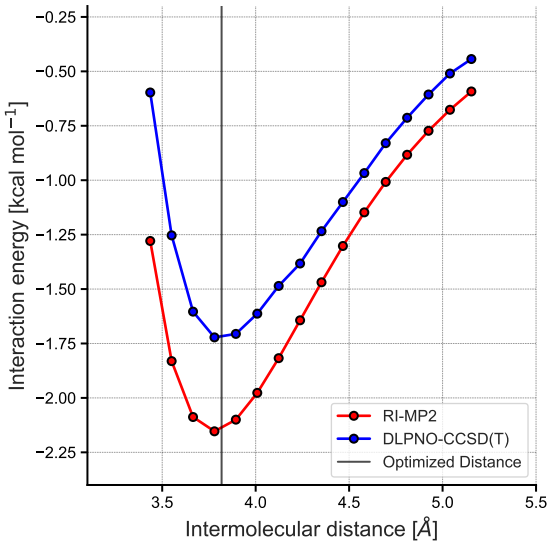

Figure S64: Rigid geometry scan of **3-HH1** and comparison to the optimized intermolecular separation.

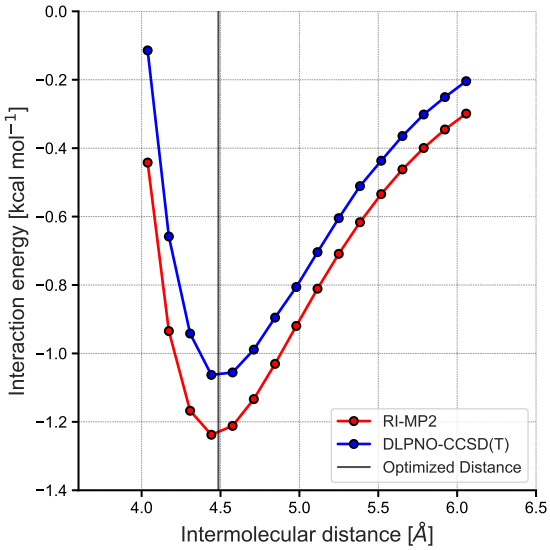

Figure S65: Rigid geometry scan of **3-HH2** and comparison to the optimized intermolecular separation.

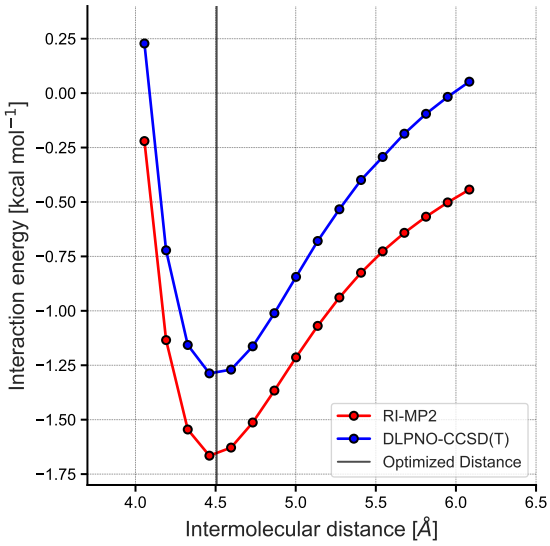

Figure S66: Rigid geometry scan of **3-HF1** and comparison to the optimized intermolecular separation.

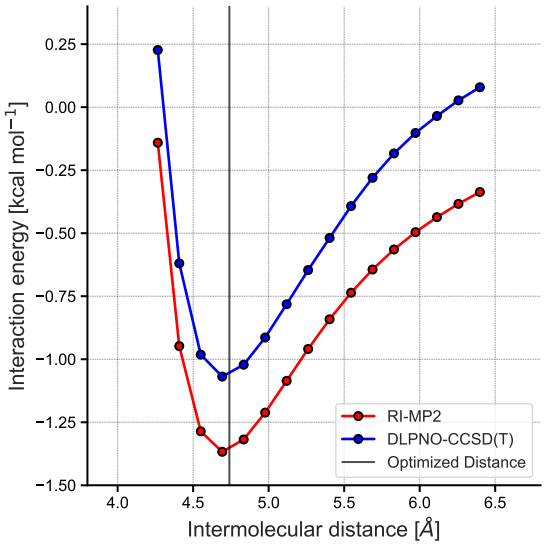

Figure S67: Rigid geometry scan of **3-HF2** and comparison to the optimized intermolecular separation.

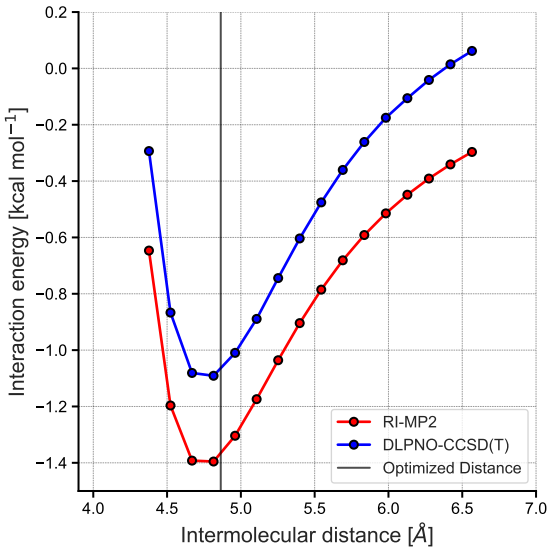

Figure S68: Rigid geometry scan of **3-HF3** and comparison to the optimized intermolecular separation.

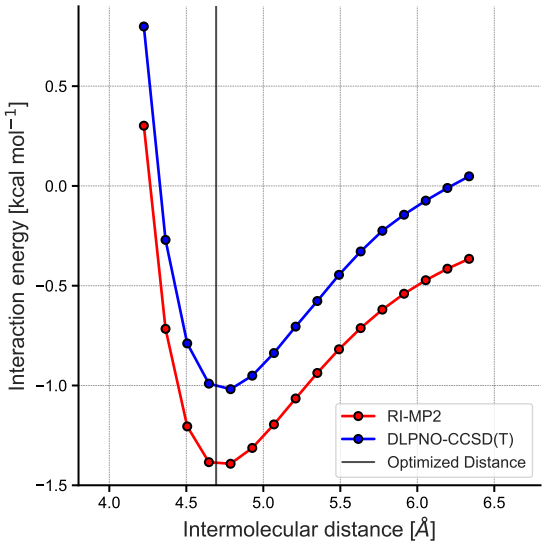

Figure S69: Rigid geometry scan of **3-HF4** and comparison to the optimized intermolecular separation.

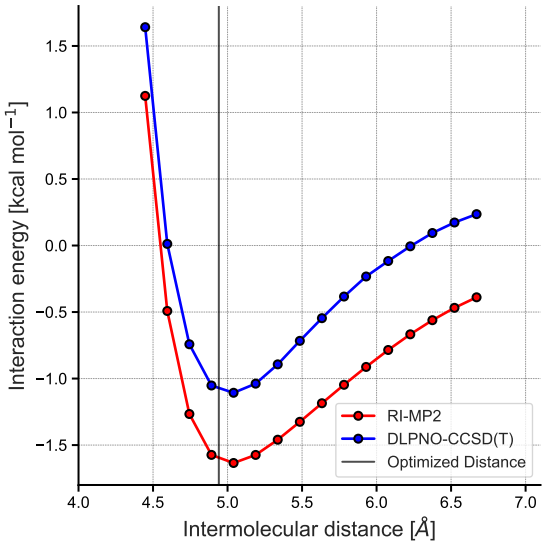

Figure S70: Rigid geometry scan of **3-FF1** and comparison to the optimized intermolecular separation.

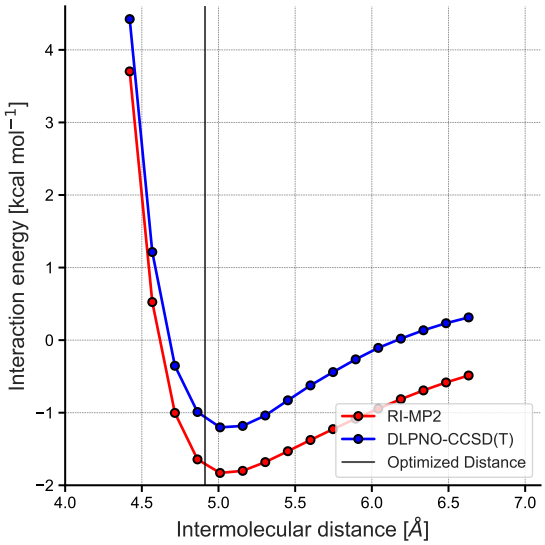

Figure S71: Rigid geometry scan of **3-FF2** and comparison to the optimized intermolecular separation.

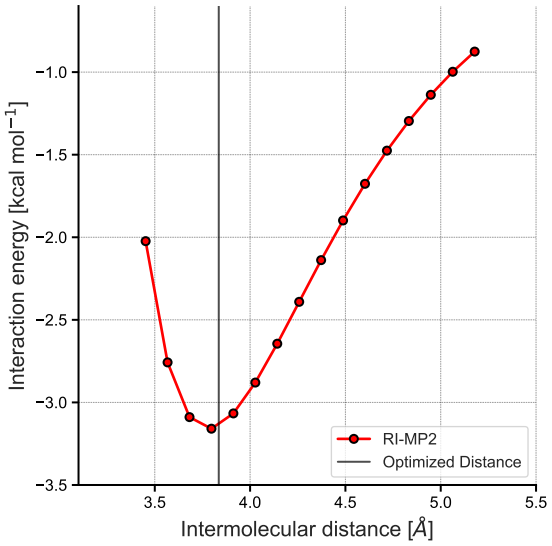

Figure S72: Rigid geometry scan of **4-HH1** and comparison to the optimized intermolecular separation.

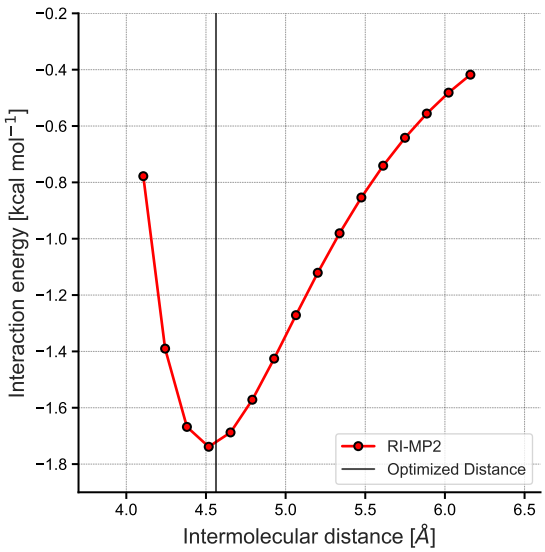

Figure S73: Rigid geometry scan of **4-HH2** and comparison to the optimized intermolecular separation.

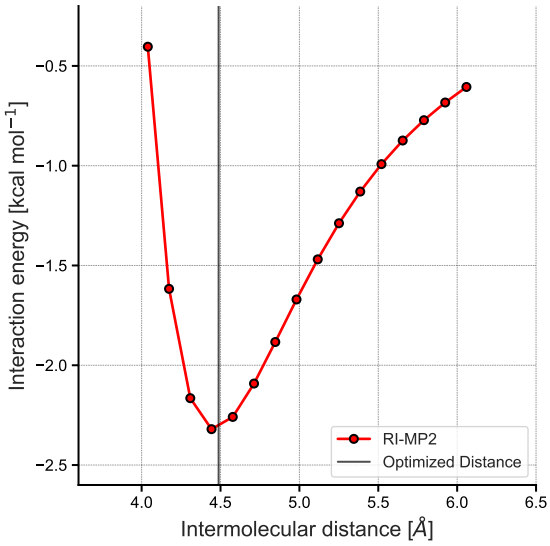

Figure S74: Rigid geometry scan of **4-HF1** and comparison to the optimized intermolecular separation.

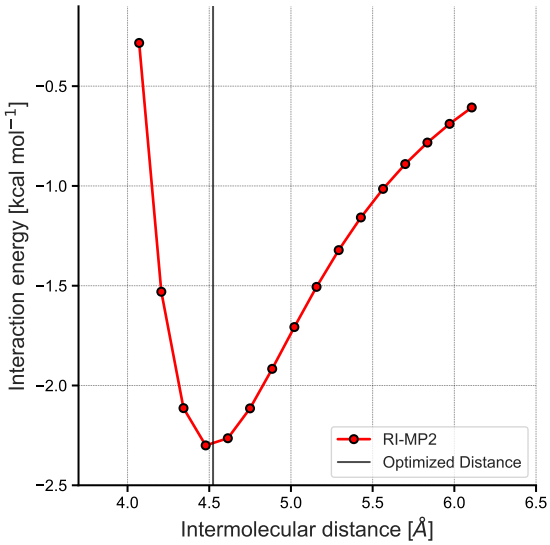

Figure S75: Rigid geometry scan of **4-HF2** and comparison to the optimized intermolecular separation.

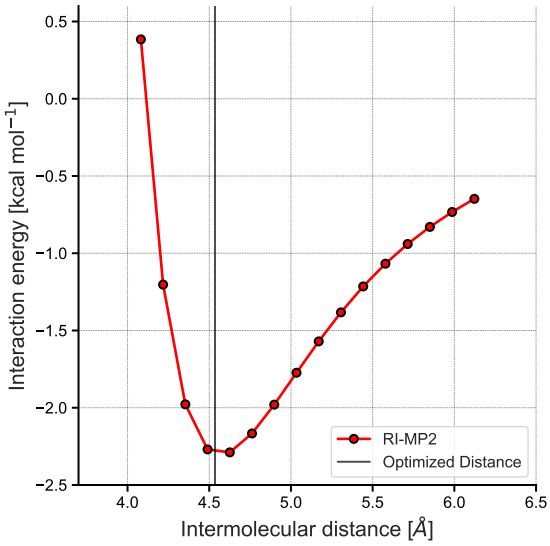

Figure S76: Rigid geometry scan of **4-HF3** and comparison to the optimized intermolecular separation.

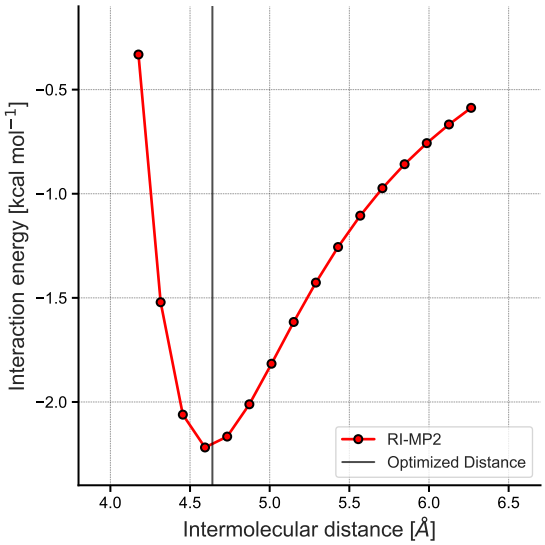

Figure S77: Rigid geometry scan of **4-HF4** and comparison to the optimized intermolecular separation.

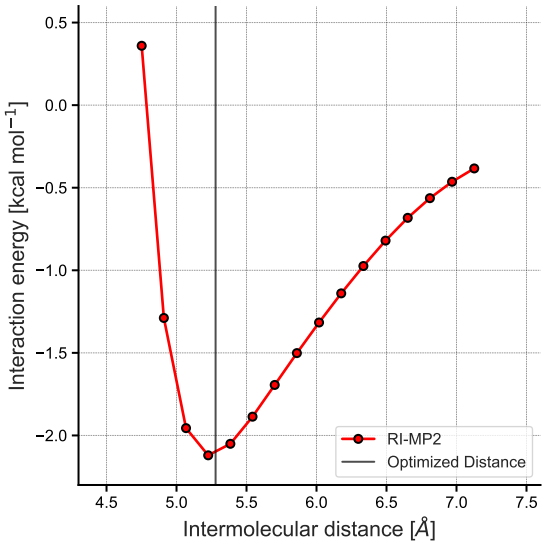

Figure S78: Rigid geometry scan of **4-FF1** and comparison to the optimized intermolecular separation.

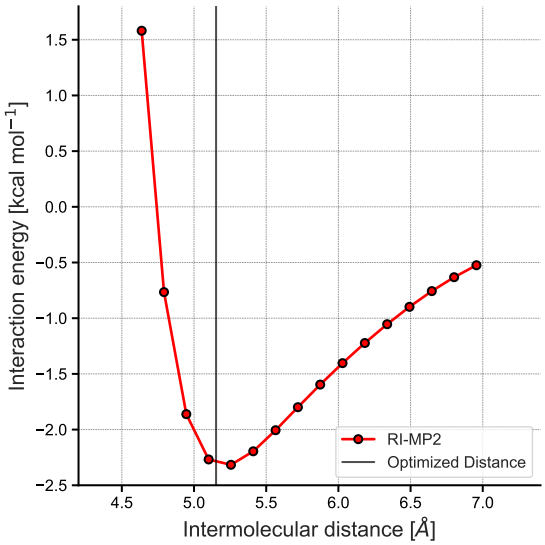

Figure S79: Rigid geometry scan of **4-FF2** and comparison to the optimized intermolecular separation.

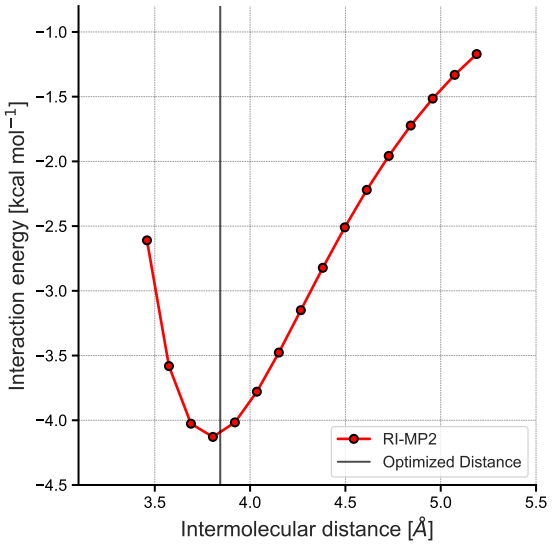

Figure S80: Rigid geometry scan of **5-HH1** and comparison to the optimized intermolecular separation.

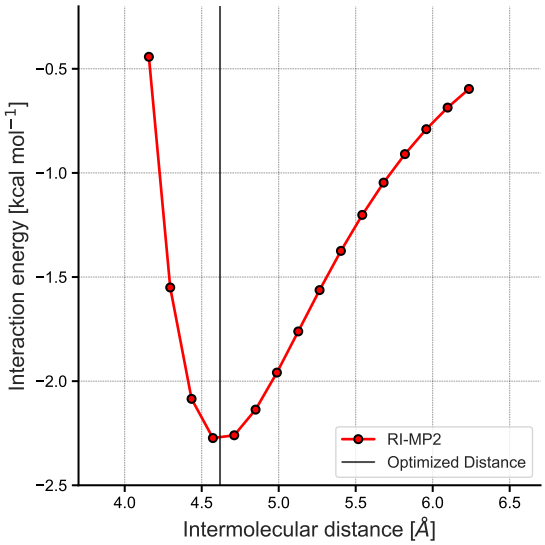

Figure S81: Rigid geometry scan of **5-HH2** and comparison to the optimized intermolecular separation.

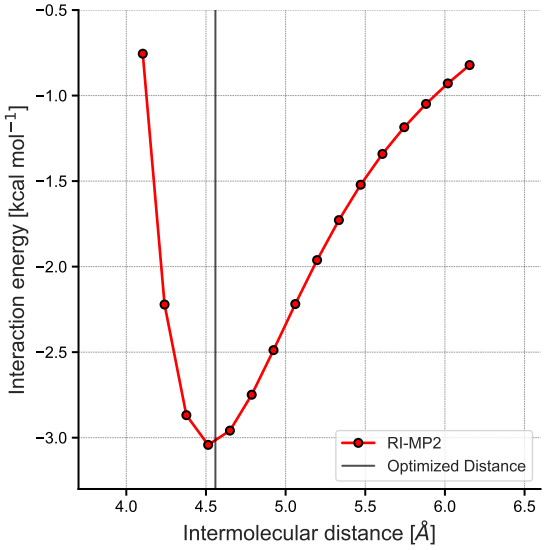

Figure S82: Rigid geometry scan of **5-HF1** and comparison to the optimized intermolecular separation.

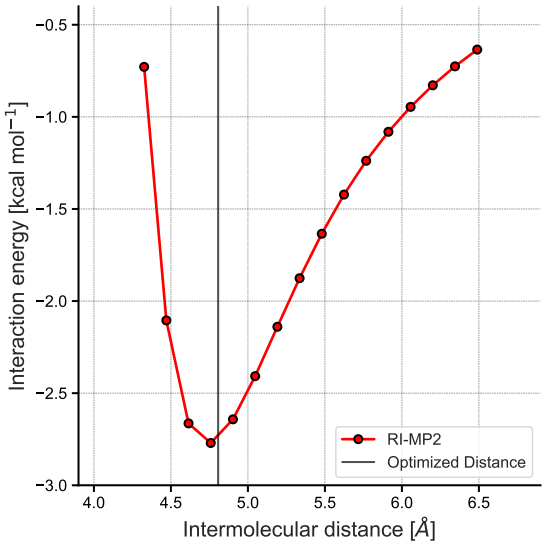

Figure S83: Rigid geometry scan of **5-HF2** and comparison to the optimized intermolecular separation.

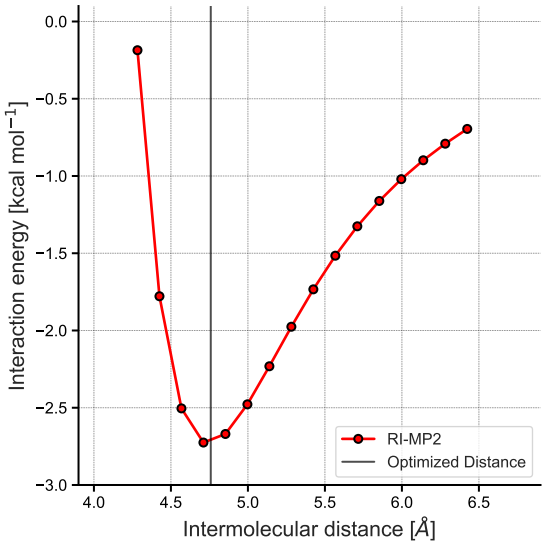

Figure S84: Rigid geometry scan of **5-HF3** and comparison to the optimized intermolecular separation.

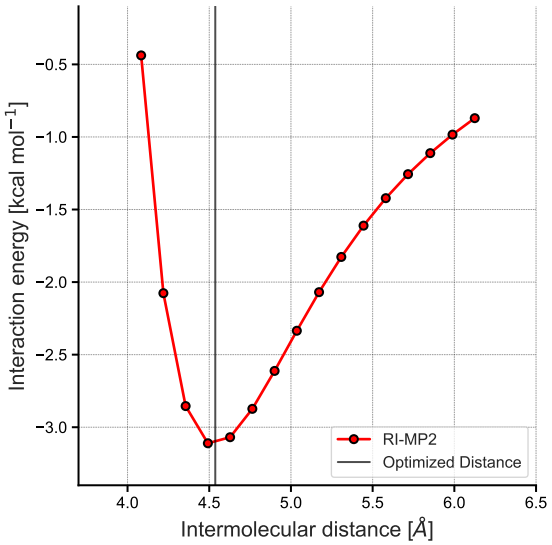

Figure S85: Rigid geometry scan of **5-HF4** and comparison to the optimized intermolecular separation.

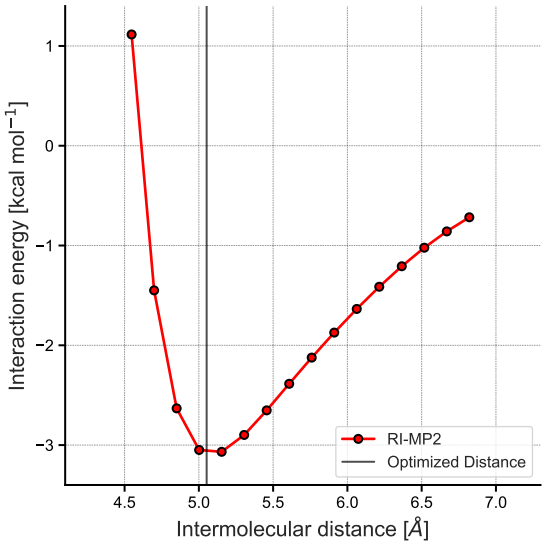

Figure S86: Rigid geometry scan of **5-FF1** and comparison to the optimized intermolecular separation.

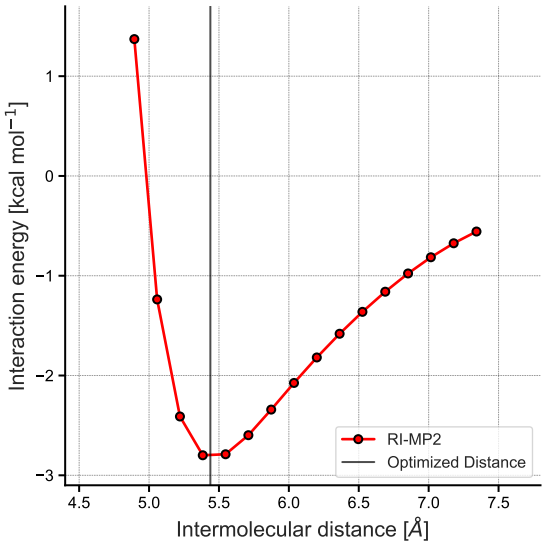

Figure S87: Rigid geometry scan of **5-FF2** and comparison to the optimized intermolecular separation.

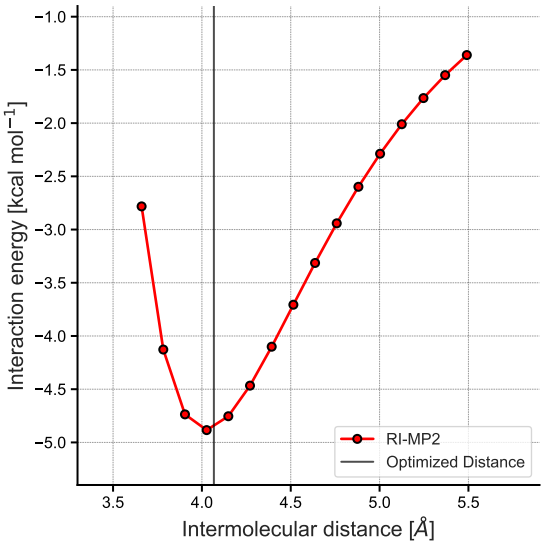

Figure S88: Rigid geometry scan of **6-HH1** and comparison to the optimized intermolecular separation.

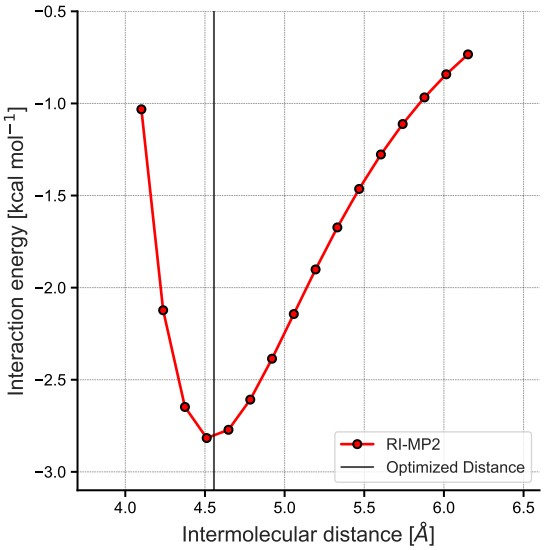

Figure S89: Rigid geometry scan of **6-HH2** and comparison to the optimized intermolecular separation.

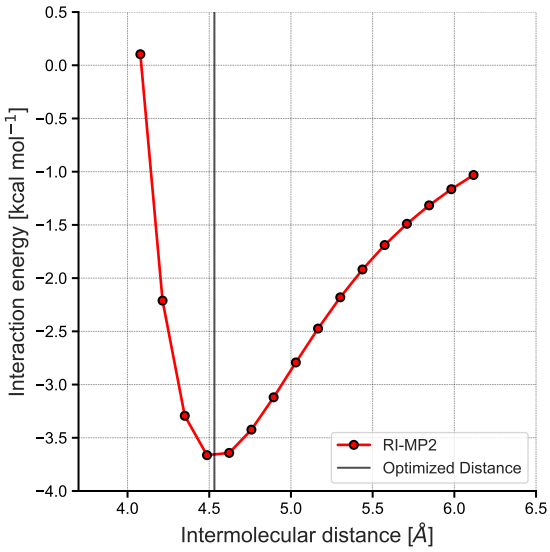

Figure S90: Rigid geometry scan of **6-HF1** and comparison to the optimized intermolecular separation.

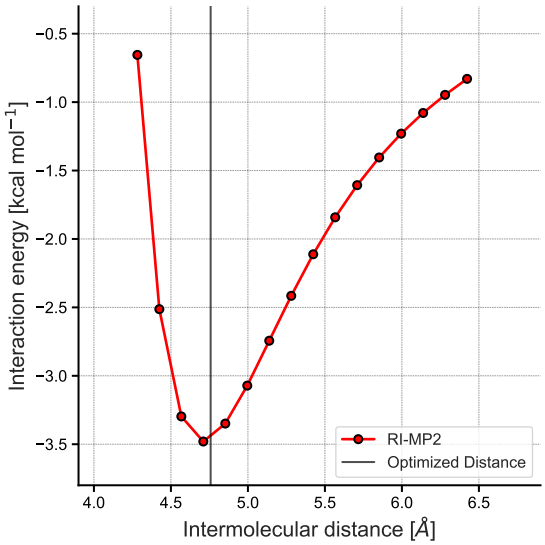

Figure S91: Rigid geometry scan of **6-HF2** and comparison to the optimized intermolecular separation.

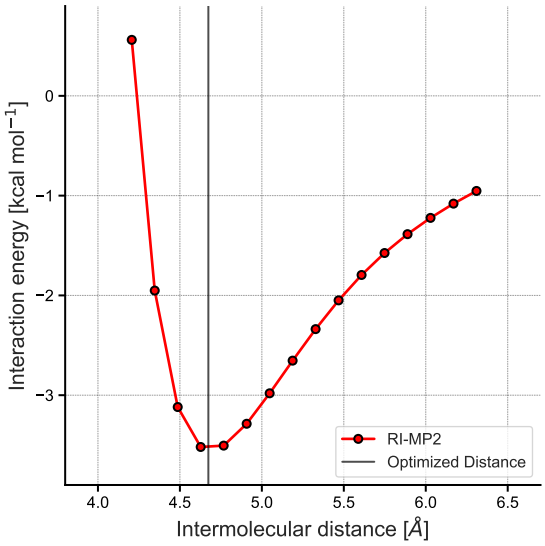

Figure S92: Rigid geometry scan of **6-HF3** and comparison to the optimized intermolecular separation.

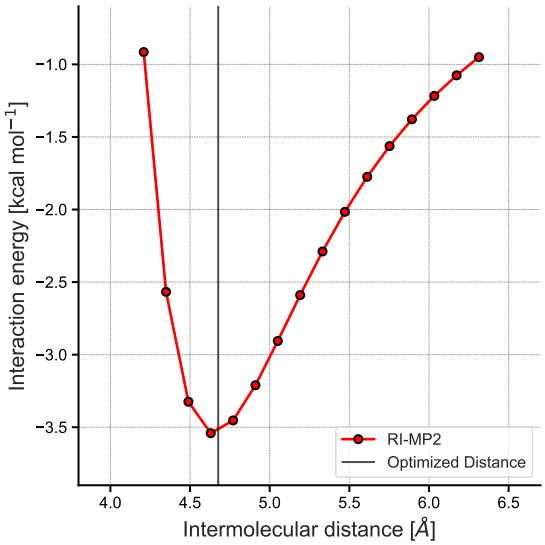

Figure S93: Rigid geometry scan of **6-HF4** and comparison to the optimized intermolecular separation.

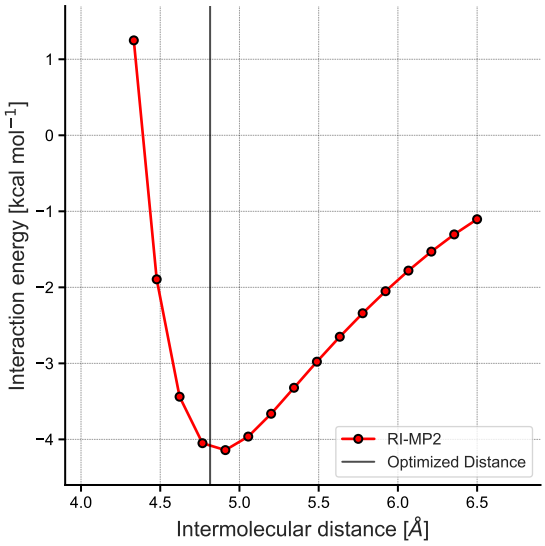

Figure S94: Rigid geometry scan of **6-FF1** and comparison to the optimized intermolecular separation.

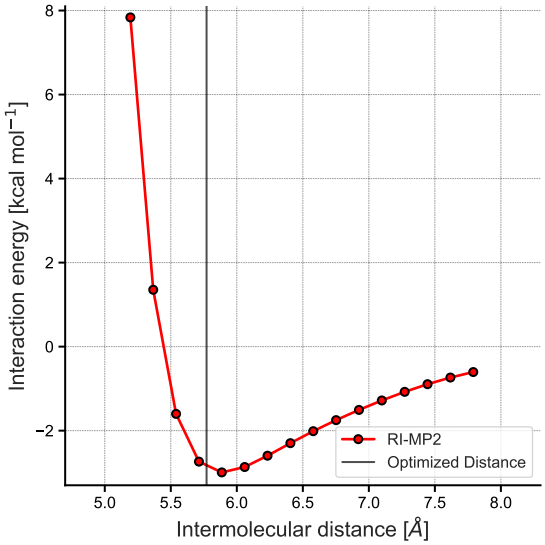

Figure S95: Rigid geometry scan of **6-FF2** and comparison to the optimized intermolecular separation.

2.1.5 Deformation Energies

Deformation energies (E_{def}) were estimated on the basis of the DSD-PBEP86/def2-TZVP(spd) geometries using the benchmark method CCSD(T)-F12/VDZ and the best-performing methods in the benchmarks for which results for all molecules under study were obtained (i.e. B97M-V/def2-QZVP, B3LYP-XMD/aug-cc-pVTZ and VeryTightPNO-DLPNO-CCSD(T)/CBS(3-4)). CCSD(T)-F12/VDZ values show that, on average, deformation energies amount only to about $(1 \pm 2)\,\%$ of the BIEs. Similarly, B97M-V predicts $(3 \pm 3)\,\%$, B3LYP-XDM predicts $(2 \pm 3)\,\%$ and VeryTightPNO-DLPNO-CCSD(T) predicts $(3 \pm 3)\,\%$. This shows that for these complexes, E_{def} can be neglected without introducing too big errors because the error is on the same order of magnitude as the error in the computational methods or smaller than that, but not larger.

2.2 Energy Decomposition Analysis

2.2.1 Dispersion

We looked closer into the sum of the exchange and dispersion components and its importance in **HH**, **HF** and **FF** complexes, respectively. Figure S96 shows this sum as a function of the overall BIE for the three different classes of complexes. It illustrates that the sum of exchange and dispersion is larger in **FF** systems than in **HF** and **HH**. Figure S97 shows views across the interaction surface of exemplary complexes (labelled in Figure S96) of each class.

2.2.2 Electrostatics

We also looked closer into the electrostatics component and its importance in **HH**, **HF** and **FF** complexes, respectively. Figure S98 shows the electrostatics contribution as a function of the overall BIE for the three different classes of complexes. It illustrates that while the sum of exchange and dispersion was larger in **FF** systems than in **HF** and **HH** (*vide supra*), the

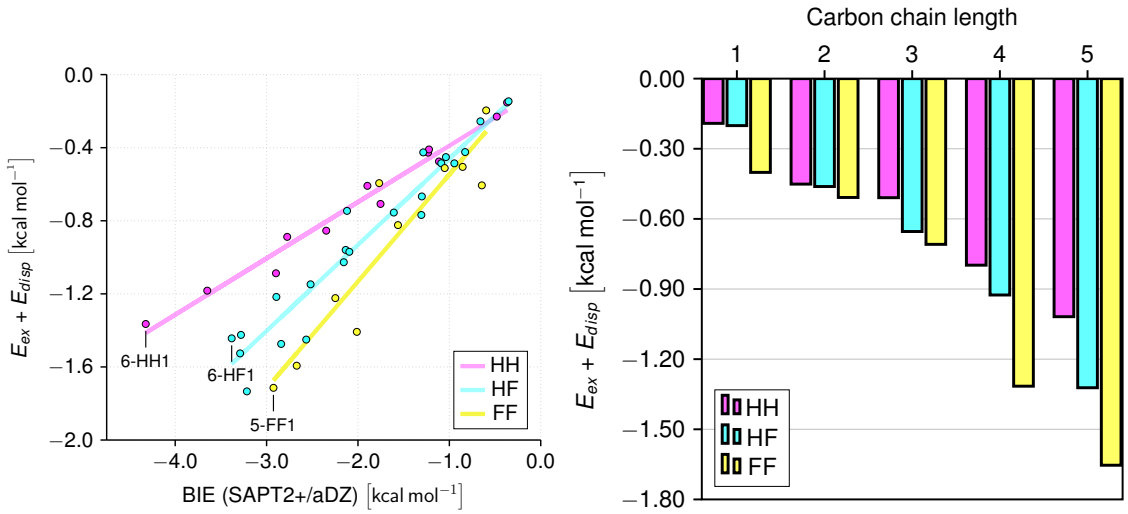

Figure S96: Sum of Pauli exchange and dispersion of the molecular complexes divided into the three subclasses **HH**, **HF** and **FF**. Left: Sum of Pauli exchange and dispersion plotted against overall interaction energies. Right: Sum of Pauli exchange and dispersion plotted against number of carbon atoms in the interacting molecules. Overall, the relative importance of dispersion increases when going from **HH** via **HF** to **FF**.

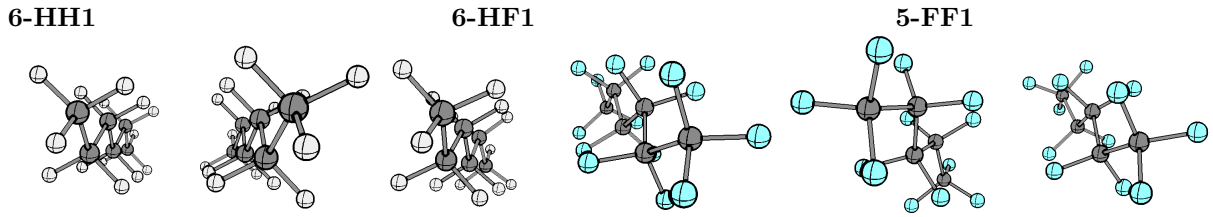

Figure S97: View along the interacting fragments of the labelled complexes **6-HH1**, **6-HF1** and **5-FF1**, respectively.

corresponding ordering in the electrostatic contribution is reversed. It is striking that **HF** complexes do not show a larger contribution to the electrostatic component compared to the homomolecular complexes. It can be rationalized because the fluorine atoms of **F** prefer to maximize contacts with the carbon atoms of **H** to optimize attractive dispersion. However, these types of atoms are negatively polarized which results in a repulsive component to the overall electrostatics. Electrostatics could be maximized by increasing contacts of the fluorine atoms of **F** with the hydrogen atoms of **H** which, however, is not ideal for optimizing dispersion. This showcases that dispersion dominates the interaction and, hence, also the interaction geometries in all the intermolecular complexes studied.

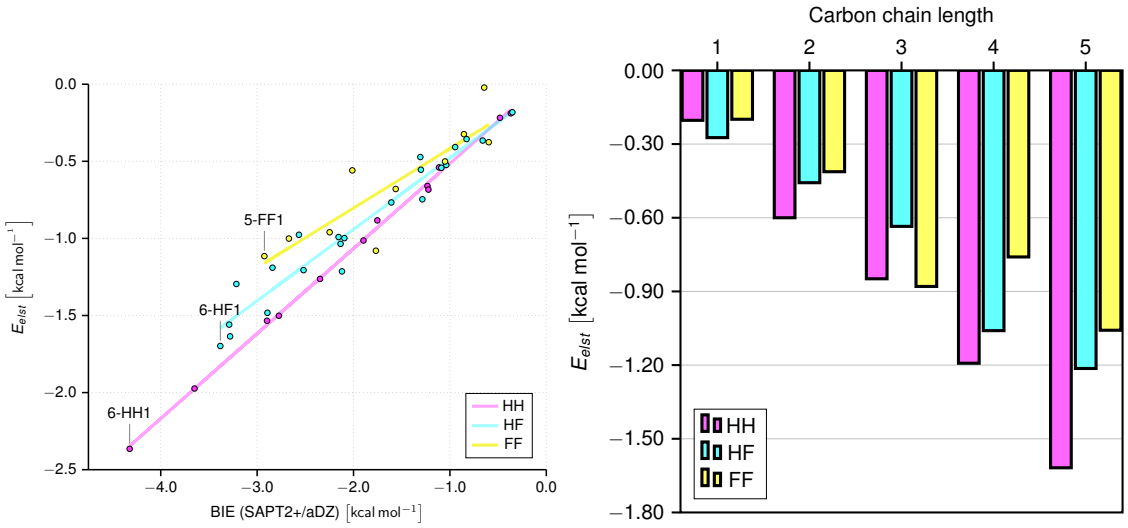

Figure S98: Electrostatics from SAPT of the molecular complexes divided into the three subclasses **HH**, **HF** and **FF**. Left: Electrostatics plotted against the BIE. Right: Electrostatics plotted against the number of carbon atoms.

2.2.3 Comparison of SAPT2+ and LED

We also looked into both the BIE and the dispersion energy obtained from LED-DLPNO-CCSD(T)/QZ calculations and compared them to the results of the SAPT2+/aDZ calculations. The numbers showed equivalent trends compared to the energies from SAPT (Figure S99) which provides mutual support for the adequacy of these two method to discern the importance of dispersion in the overall interaction.

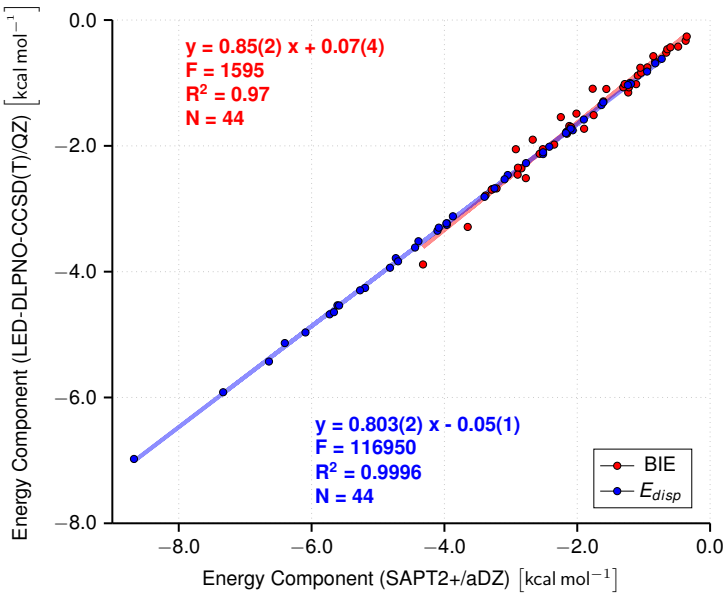

Figure S99: Comparison of interaction energies and dispersion energy components of molecular complexes obtained from SAPT2+/aDZ and LED-TightPNO-DLPNO-CCSD(T)/QZ, respectively. Systematic differences in the magnitudes are observed but trends are equivalent.

2.2.4 LED Decomposition

The decomposition of dispersion into contributions of atoms and bonds in complexes of **H** and **F** was performed using four distinct LED jobs (cf. Figure S100). First, LED was performed using two fragments corresponding to the two interacting molecules (job 1). Secondly, two LED jobs were performed with three fragments each (job 2 and job 3). In job 2 the hydrogen or fluorine atoms of the first interacting molecule were considered as a separate fragment from the corresponding carbon backbone. In job 3 the hydrogen or fluorine atoms of the second interacting molecule were considered as a separate fragment from the corresponding carbon backbone. In job 4 the hydrogen or fluorine atoms of both interacting molecules were considered as a separate fragment from the corresponding carbon backbone.

The results of these four LED jobs were evaluated to get nine different dispersion contributions. The corresponding formulas used for evaluation of the data are derived in this section. First, the parameters used are defined:

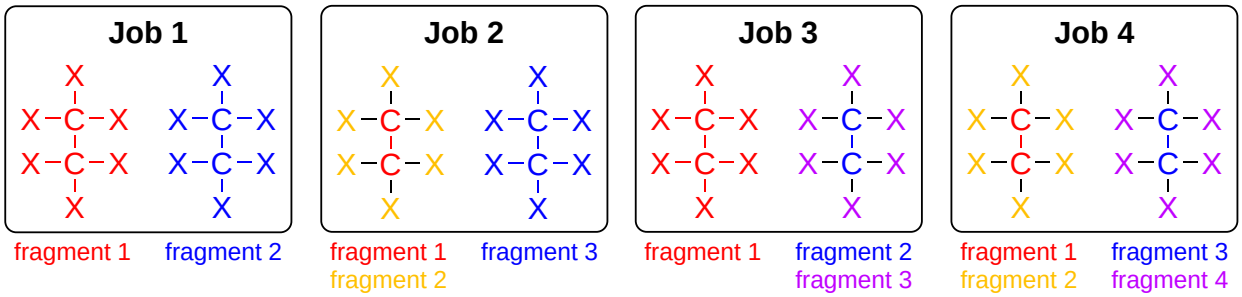

Figure S100: Required LED jobs to decompose the overall intermolecular dispersion into contributions from atoms and bonds.

$D(n, A-B)$	...	Intermolecular dispersion obtained from job n between fragments A and B
D_{tot}	...	Total intermolecular dispersion
$D(C1-C2)$	...	Dispersion between carbon chain C1 and carbon chain C2
$D(C1-X2)$	...	Dispersion between carbon chain C1 and atoms X2 (X = H,F)
$D(X1-C2)$	...	Dispersion between atoms X1 (X = H,F) and carbon chain C2
$D(X1-X2)$	...	Dispersion between atoms X1 and atoms X2 (X = H,F)
$D(C1-CX2)$	...	Dispersion between carbon chain C1 and CX2 bonds (X = H,F)
$D(CX1-C2)$	...	Dispersion between CX1 bonds (X = H,F) and carbon chain C2
$D(X1-CX2)$	...	Dispersion between atoms X1 and CX2 bonds (X = H,F)
$D(CX1-X2)$	...	Dispersion between CX1 bonds and atoms X2 (X = H,F)
$D(CX1-CX2)$	...	Dispersion between CX1 bonds and CX2 bonds (X = H,F)

The total dispersion energy is the sum of all its components (abbreviated as D_{ij} for simplification):

$$D_{tot} = \sum_i \sum_j D_{ij} \tag{S1}$$

The following equations show which contributions are obtained from the 4 jobs:

$$D(1, 1-2) = D_{tot} \tag{S2}$$

$$D(2, 1-3) = D(C1-C2) + D(C1-X2) + D(C1-CX2) \tag{S3}$$

$$D(2,2-3) = D(X1-C2) + D(X1-X2) + D(X1-CX2) \tag{S4}$$

$$D(3,1-2) = D(C1-C2) + D(X1-C2) + D(CX1-C2) \tag{S5}$$

$$D(3,1-3) = D(C1-X2) + D(X1-X2) + D(CX1-X2) \tag{S6}$$

$$D(4,1-3) = D(C1-C2) \tag{S7}$$

$$D(4,1-4) = D(C1-X2) \tag{S8}$$

$$D(4,2-3) = D(X1-C2) \tag{S9}$$

$$D(4,2-4) = D(X1-X2) \tag{S10}$$

Overall, we have ten independent linear equations and ten unknown parameters. Therefore, it should be possible to solve this system of equations for all unknown parameters. Five out of the ten unknown parameters are directly obtained from the jobs. Four additional parameters are obtained from equations S3-S6 by inserting the respective terms obtained from equations S7-S10. The last parameter is obtained from the energy balance in equation S1 by inserting all the other nine parameters. Using these equations, we obtained the overall intermolecular dispersion between the interacting molecules, as well as, nine distinct contributions to the overall intermolecular dispersion from interactions between different atoms and bonds with each other. The corresponding results of this decomposition are shown in the main text and in the following section.

2.2.5 Additional LED Results

The relative contribution of the F1-F2 dispersive interaction correlates linearly with the relative molar fluorine content (cf. Figure S101). Plotting the ratio of the relative contributions of C1 and C2 of **FF** and **HH** against the relative molar carbon content also results in a linear regression (Figure S101). In other words, the smaller the relative number of fluorine atoms compared to the number of carbon atoms the smaller the number of favorable intermolecular fluorine-fluorine interactions. Since these dispersive interactions are most attractive, **FF** with longer carbon chains have lower BIEs normalized by the number of carbons compared to **FF** with shorter carbon chains. However, the relative carbon content levels at longer carbon chain lengths and, hence, this effect is most pronounced in the short and intermediate **H** and **F**.

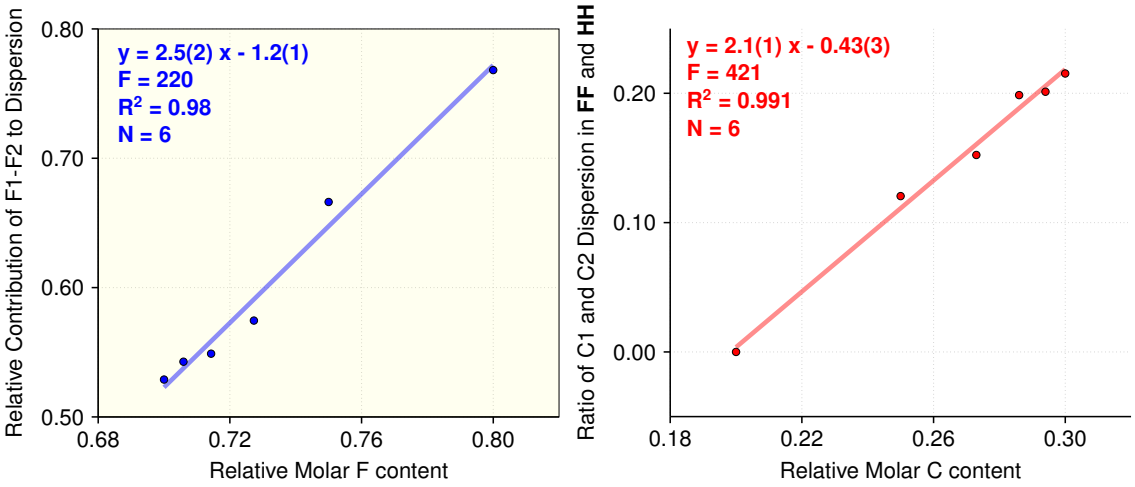

Figure S101: Left: Relative contribution of fluorine-fluorine interactions (F1-F2) in **FF** towards dispersion from LED-TightPNO-DLPNO-CCSD(T)/QZ as a function of the relative molar fluorine content. The relative importance of F1-F2 decreases with the fluorine content as the carbon chain is elongated. Right: Ratio of the contributions of C1 and C2 in **FF** and **HH**, respectively, towards dispersion from LED-TightPNO-DLPNO-CCSD(T)/QZ as a function of the relative molar carbon content.

Figures S102-S116 show the decomposition of LED-DLPNO-CCSD(T) dispersion energies into contributions of interactions between atoms and bonds for **HH**, **HF** and **FF** with two to six carbon atoms in the respective interacting molecules. They show that that the results are

relatively stable with respect to the number of carbon atoms. The most striking difference is observed in the relative contribution of F1-F2 in **FF** as discussed in the main text.

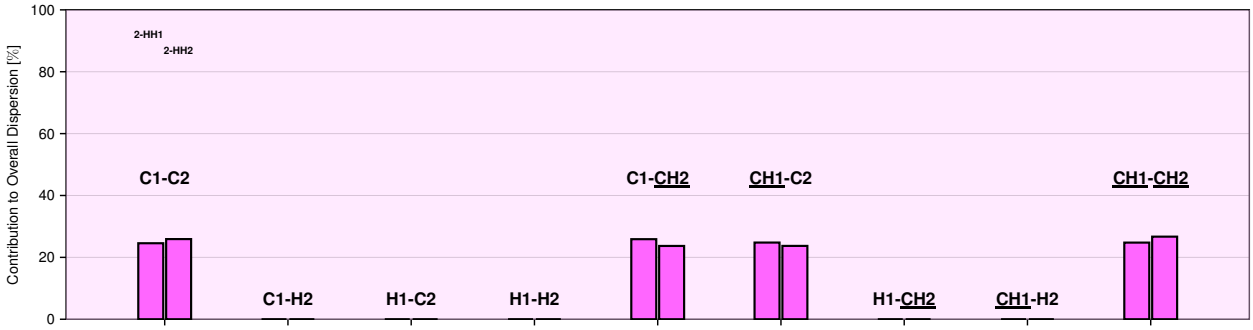

Figure S102: Decomposition of dispersion obtained from LED-TightPNO-DLPNO-CCSD(T)/QZ into contributions of atoms and bonds for **2-HH** complexes.

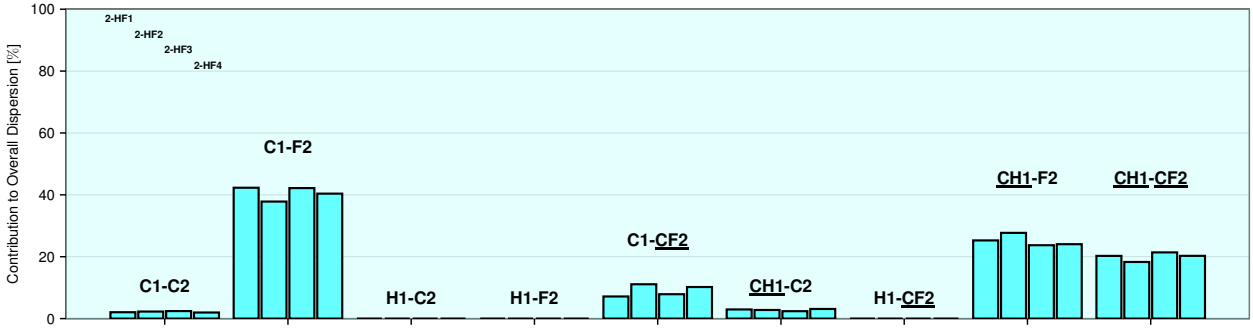

Figure S103: Decomposition of dispersion obtained from LED-TightPNO-DLPNO-CCSD(T)/QZ into contributions of atoms and bonds for **2-HF** complexes.

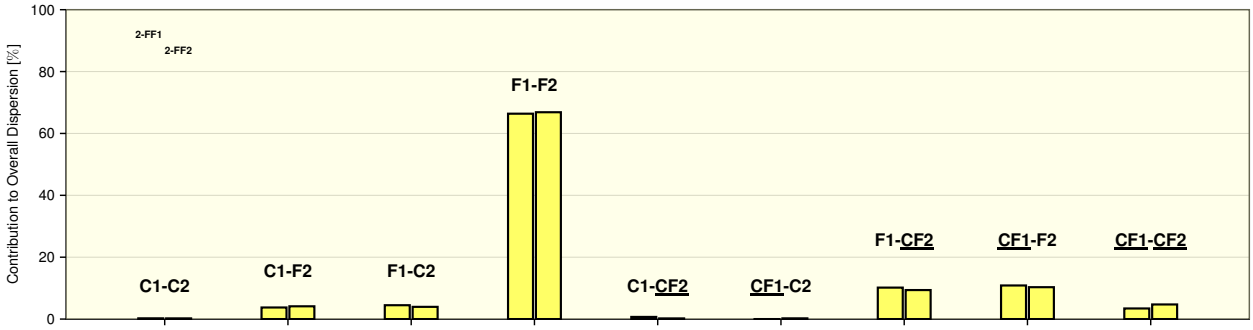

Figure S104: Decomposition of dispersion obtained from LED-TightPNO-DLPNO-CCSD(T)/QZ into contributions of atoms and bonds for **2-FF** complexes.

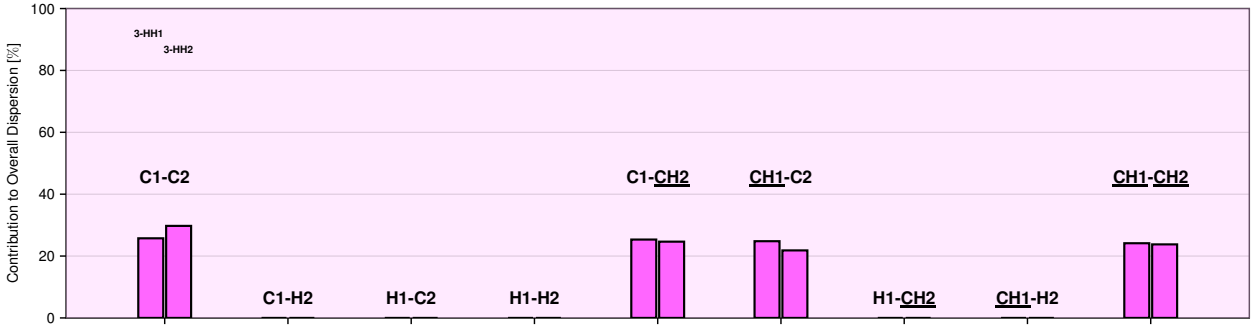

Figure S105: Decomposition of dispersion obtained from LED-TightPNO-DLPNO-CCSD(T)/QZ into contributions of atoms and bonds for **3-HH** complexes.

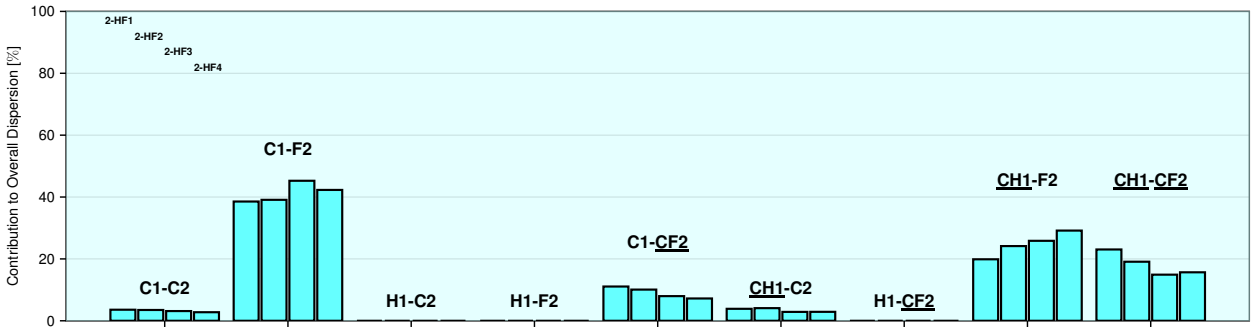

Figure S106: Decomposition of dispersion obtained from LED-TightPNO-DLPNO-CCSD(T)/QZ into contributions of atoms and bonds for **3-HF** complexes.

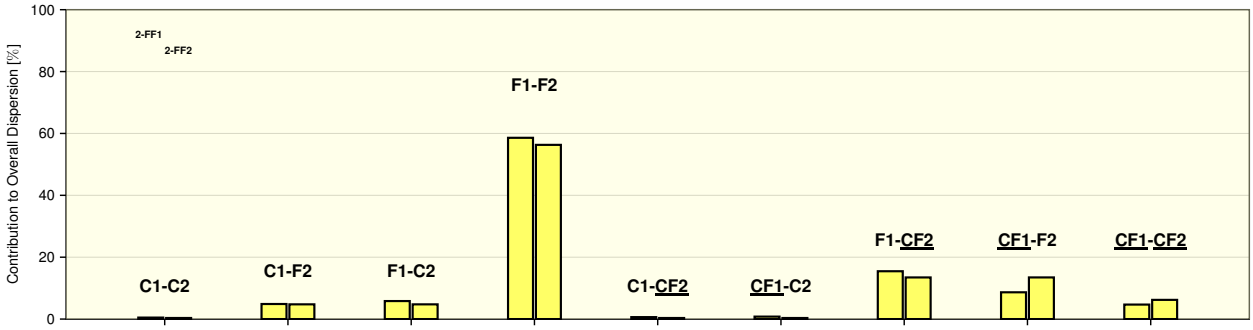

Figure S107: Decomposition of dispersion obtained from LED-TightPNO-DLPNO-CCSD(T)/QZ into contributions of atoms and bonds for **3-FF** complexes.

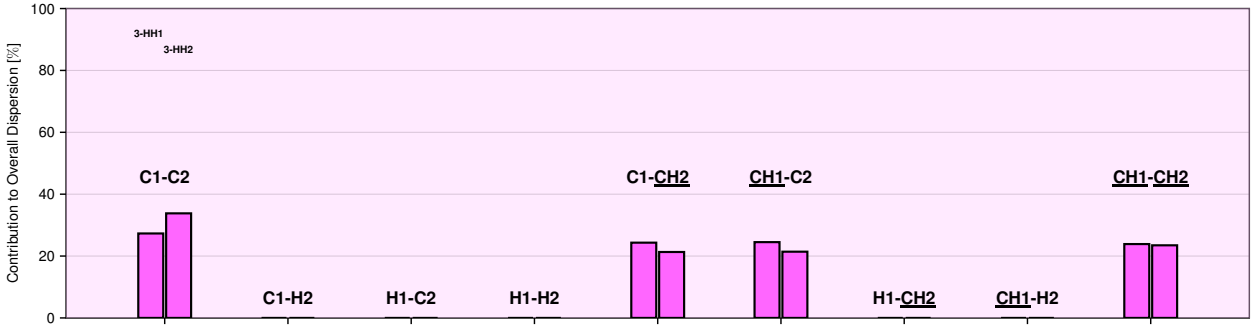

Figure S108: Decomposition of dispersion obtained from LED-TightPNO-DLPNO-CCSD(T)/QZ into contributions of atoms and bonds for **4-HH** complexes.

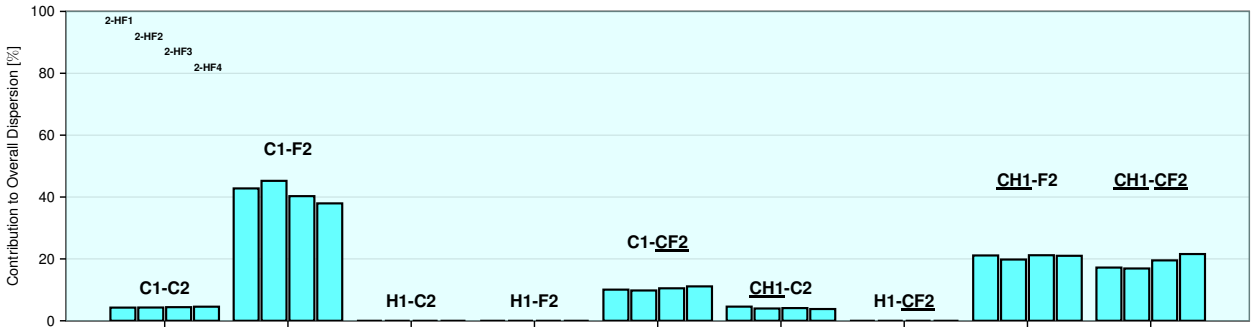

Figure S109: Decomposition of dispersion obtained from LED-TightPNO-DLPNO-CCSD(T)/QZ into contributions of atoms and bonds for **4-HF** complexes.

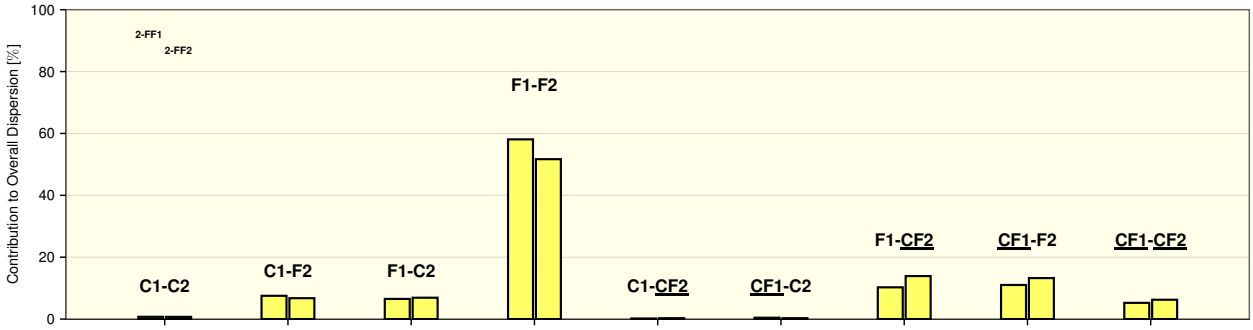

Figure S110: Decomposition of dispersion obtained from LED-TightPNO-DLPNO-CCSD(T)/QZ into contributions of atoms and bonds for **4-FF** complexes.

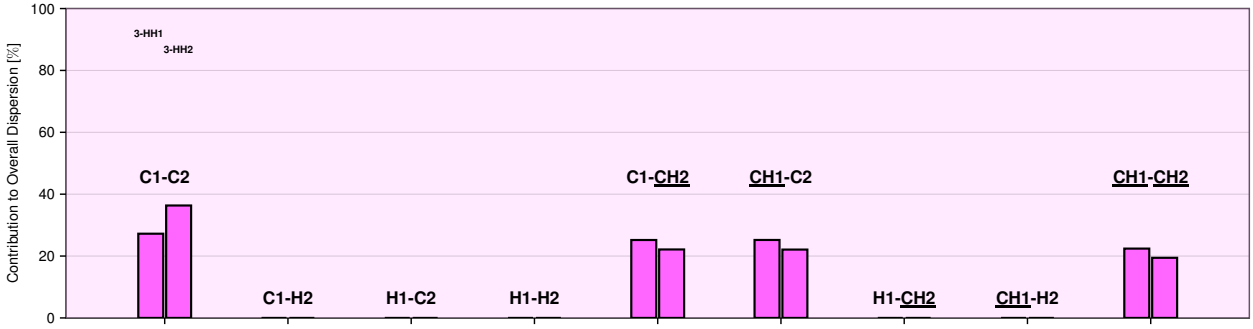

Figure S111: Decomposition of dispersion obtained from LED-TightPNO-DLPNO-CCSD(T)/QZ into contributions of atoms and bonds for **5-HH** complexes.

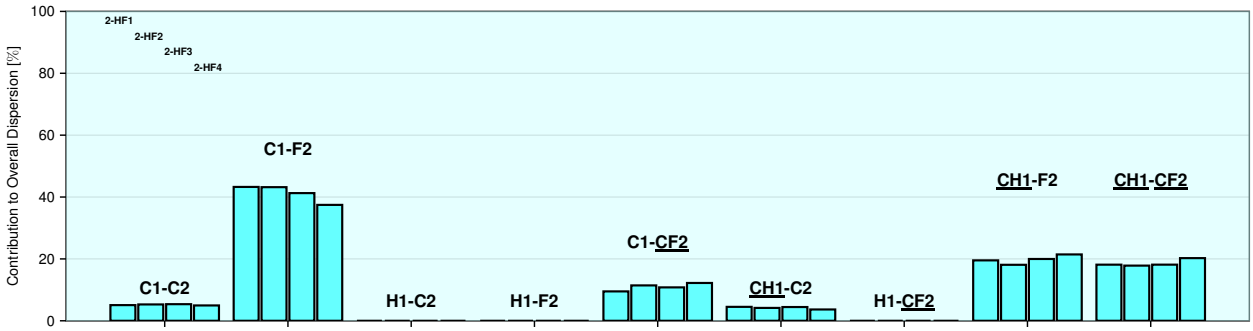

Figure S112: Decomposition of dispersion obtained from LED-TightPNO-DLPNO-CCSD(T)/QZ into contributions of atoms and bonds for **5-HF** complexes.

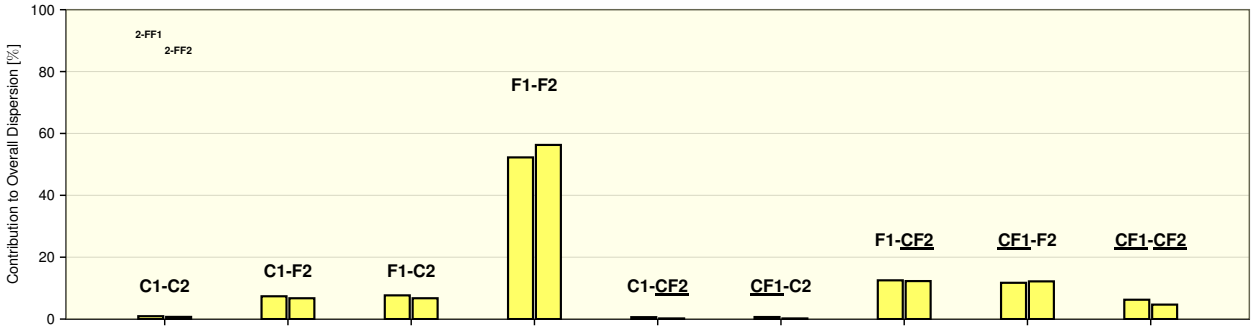

Figure S113: Decomposition of dispersion obtained from LED-TightPNO-DLPNO-CCSD(T)/QZ into contributions of atoms and bonds for **5-FF** complexes.

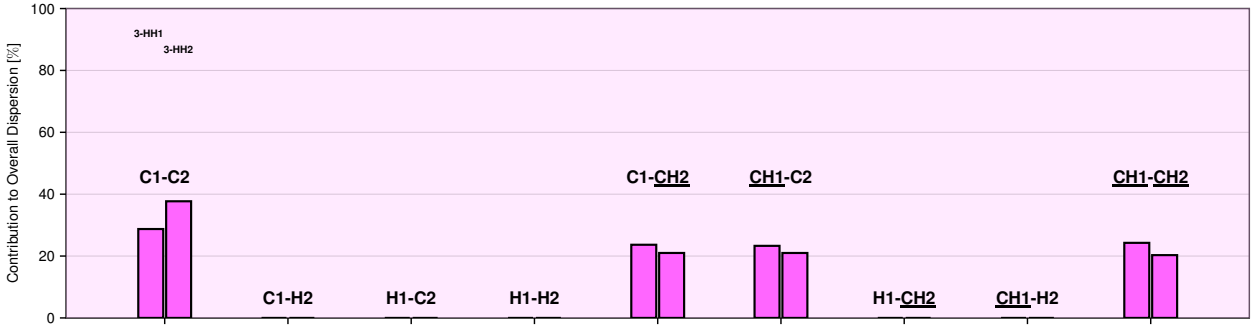

Figure S114: Decomposition of dispersion obtained from LED-TightPNO-DLPNO-CCSD(T)/QZ into contributions of atoms and bonds for **6-HH** complexes.

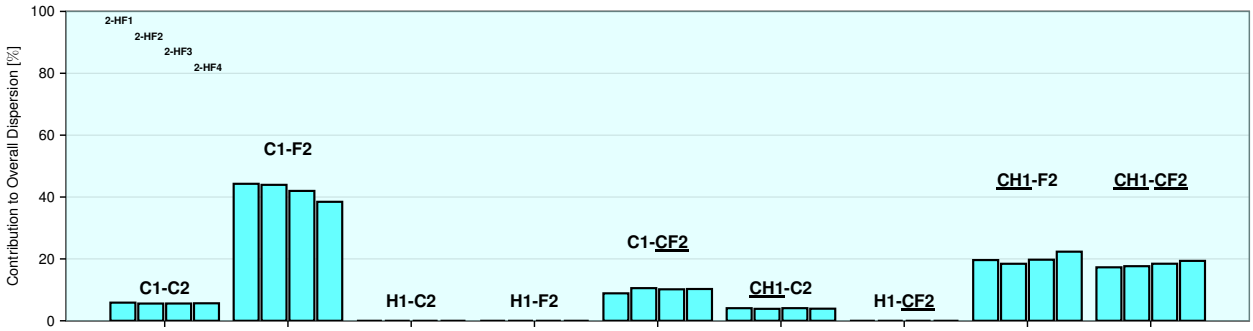

Figure S115: Decomposition of dispersion obtained from LED-TightPNO-DLPNO-CCSD(T)/QZ into contributions of atoms and bonds for **6-HF** complexes.

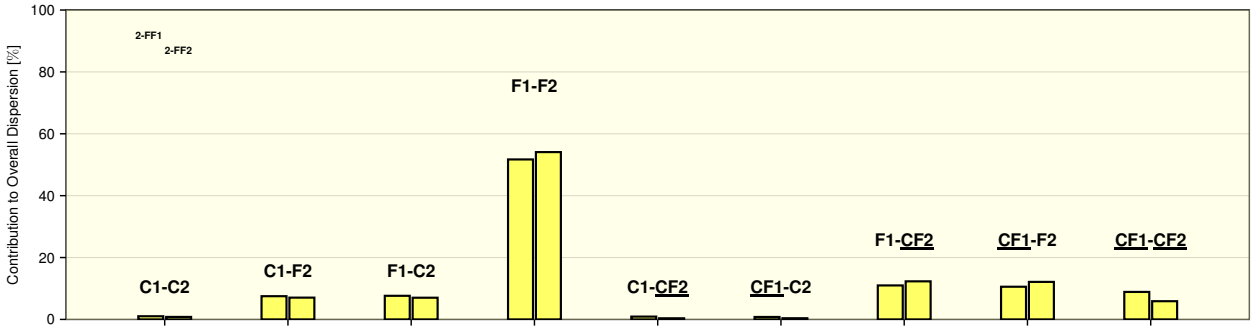

Figure S116: Decomposition of dispersion obtained from LED-TightPNO-DLPNO-CCSD(T)/QZ into contributions of atoms and bonds for **6-FF** complexes.

2.2.6 Additional DID Plots

Figures S117-S131 show additional DID plots of the complexes investigated in this study. Qualitatively, they all illustrate that dispersion in **F** comes mainly from fluorine atoms and in **H** it is distributed between the carbon atoms and the carbon-hydrogen bonds. Additionally, they also show that the results are relatively stable with respect to the number of carbon atoms in the interacting complexes.

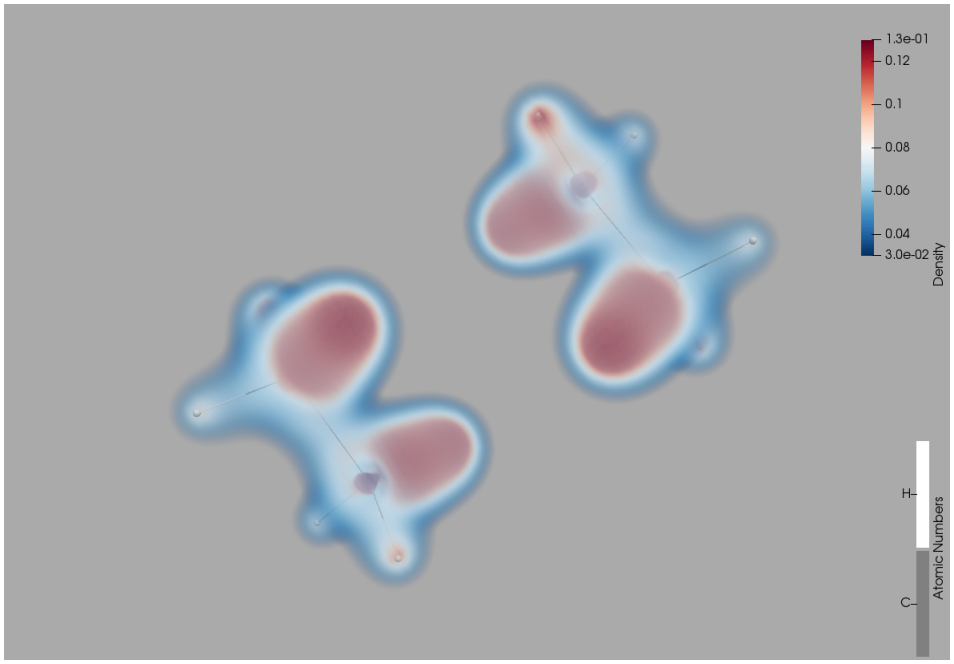

Figure S117: DID plot of **2-HH1**.

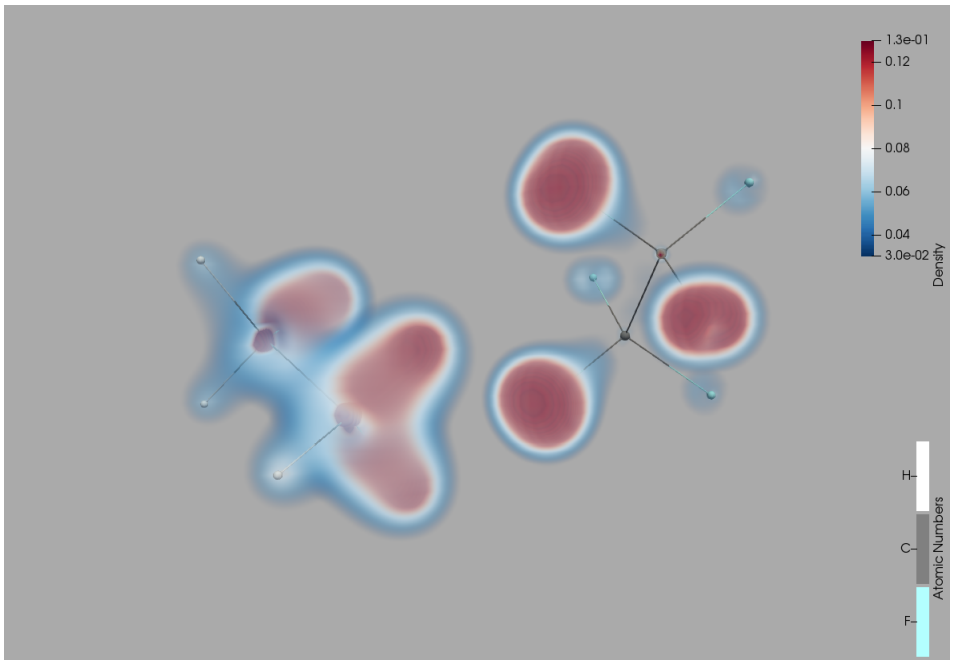

Figure S118: DID plot of **2-HF2**.

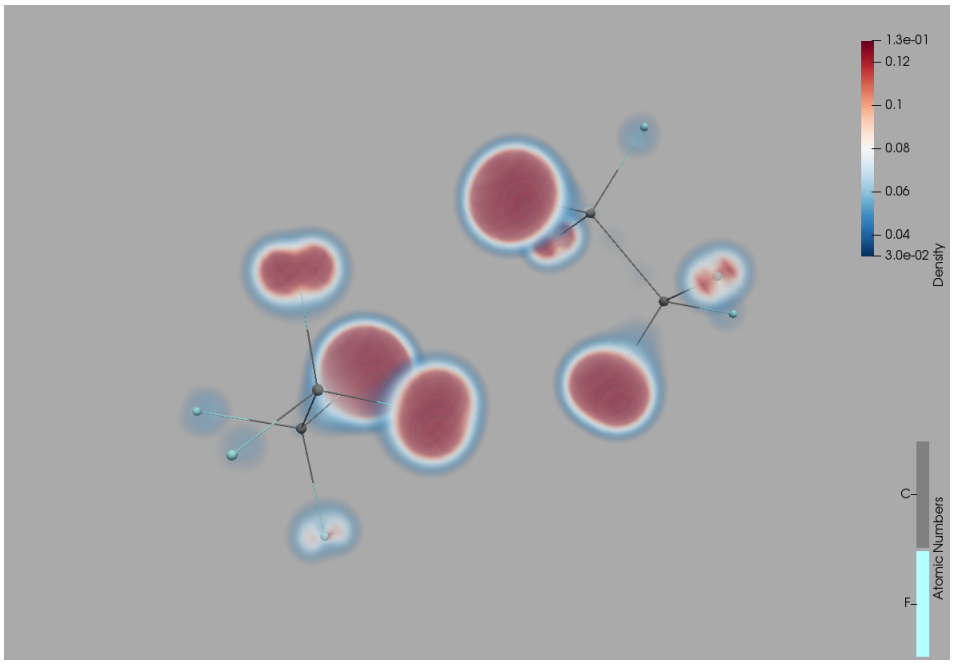

Figure S119: DID plot of **2-FF1**.

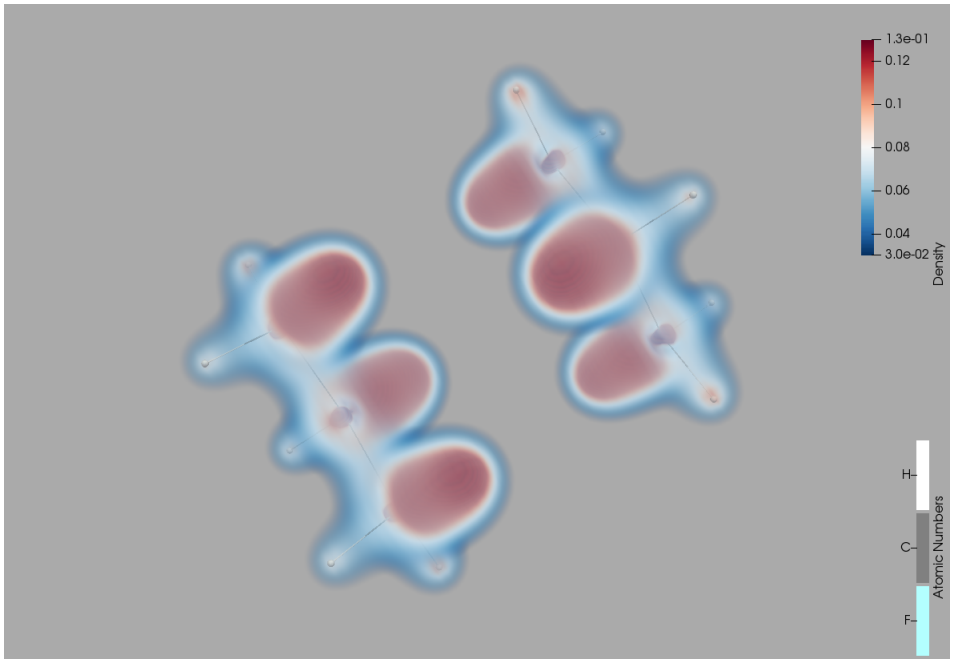

Figure S120: DID plot of **3-HH1**.

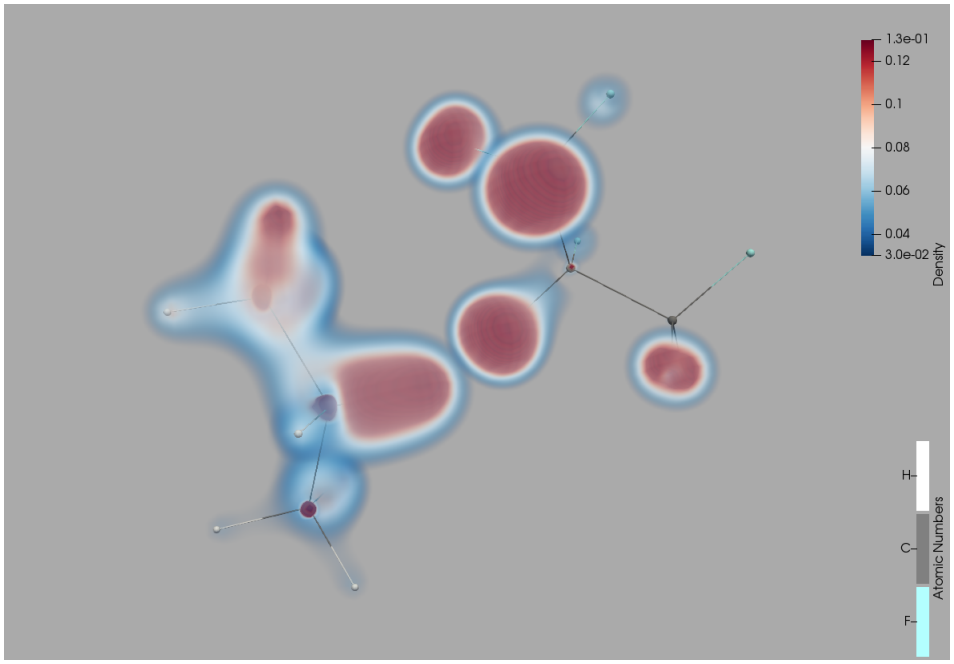

Figure S121: DID plot of **3-HF1**.

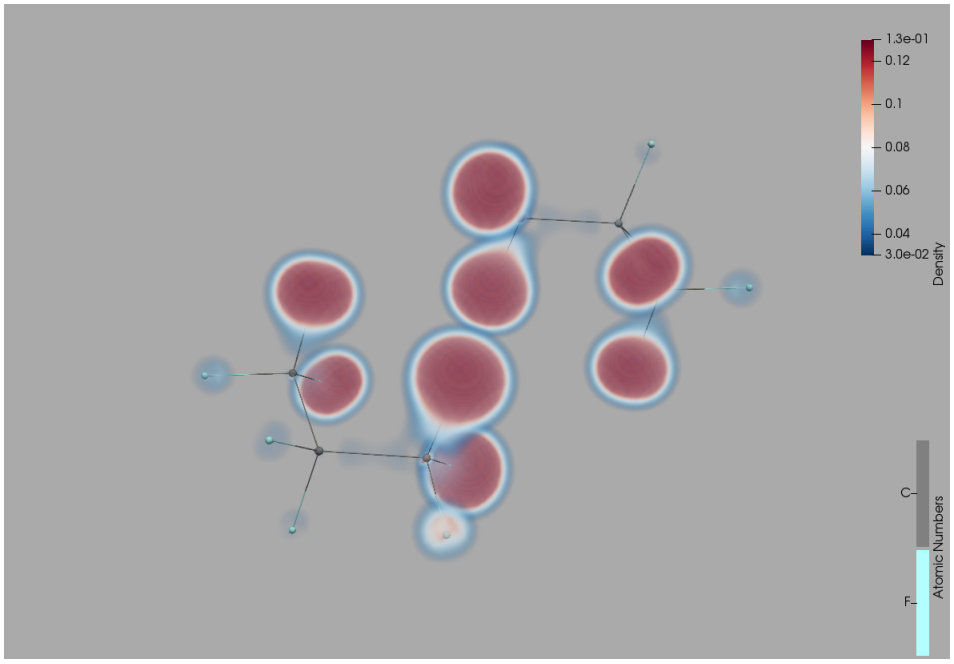

Figure S122: DID plot of **3-FF2**.

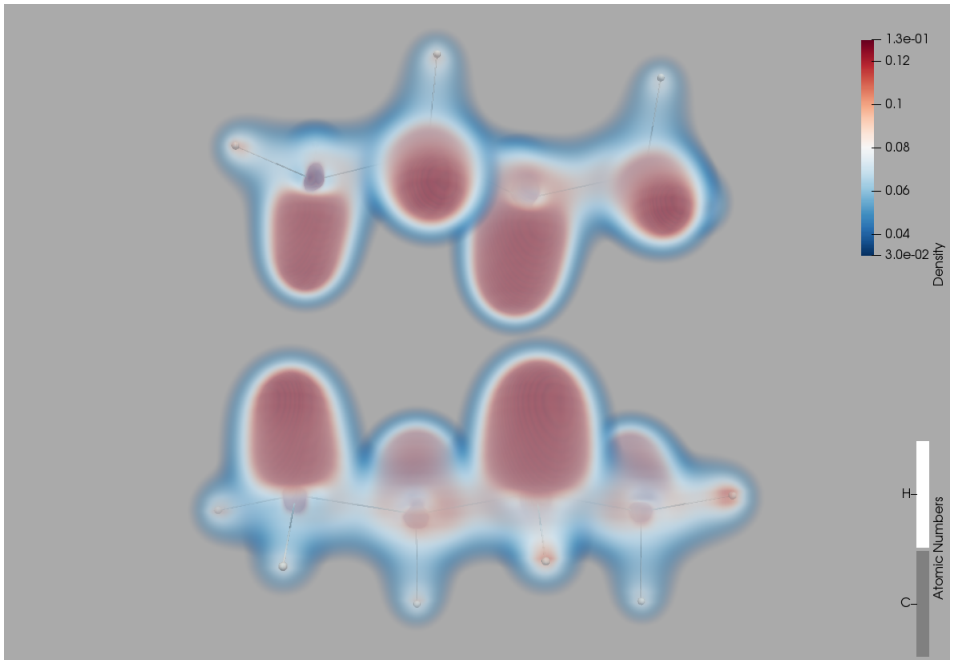

Figure S123: DID plot of **4-HH1**.

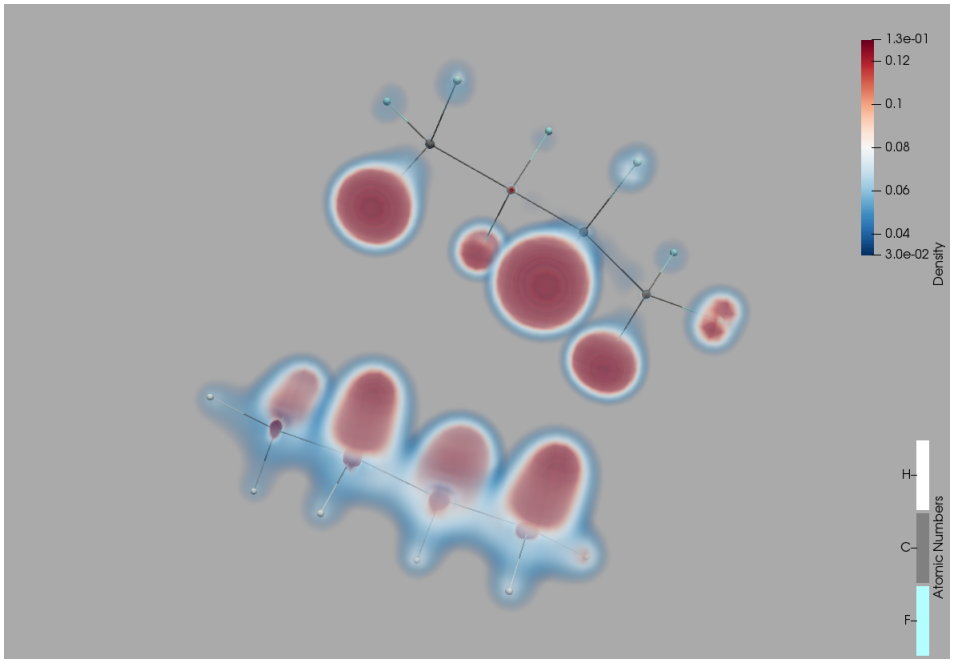

Figure S124: DID plot of **4-HF2**.

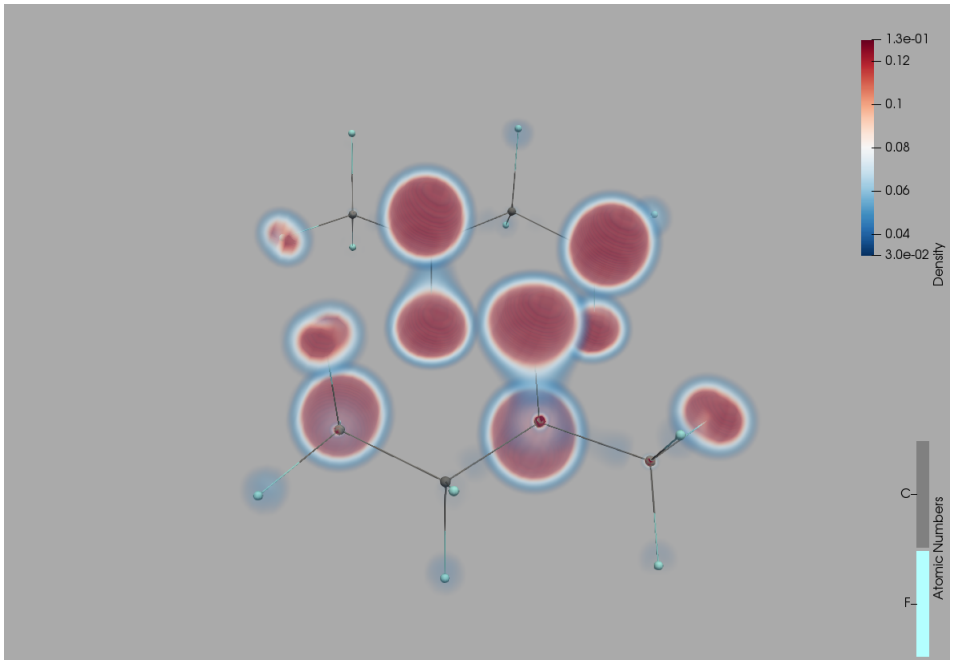

Figure S125: DID plot of **4-FF2**.

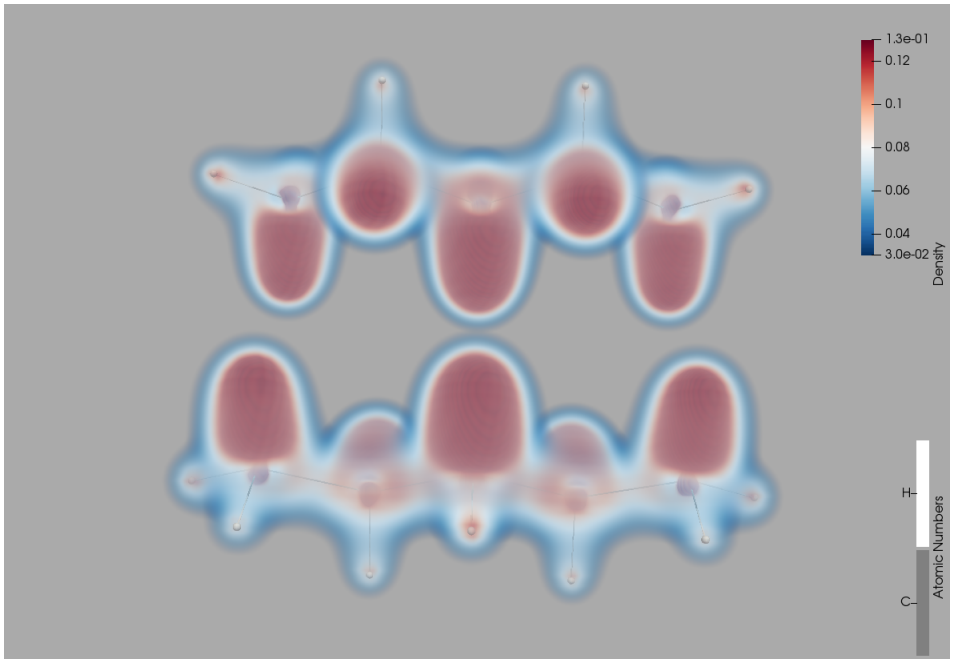

Figure S126: DID plot of **5-HH1**.

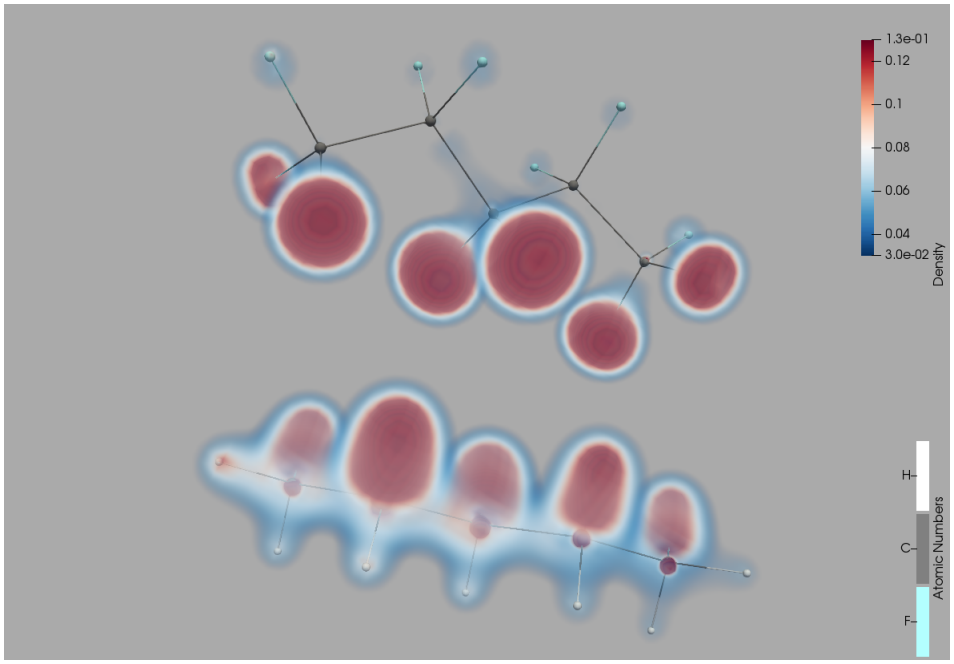

Figure S127: DID plot of **5-HF4**.

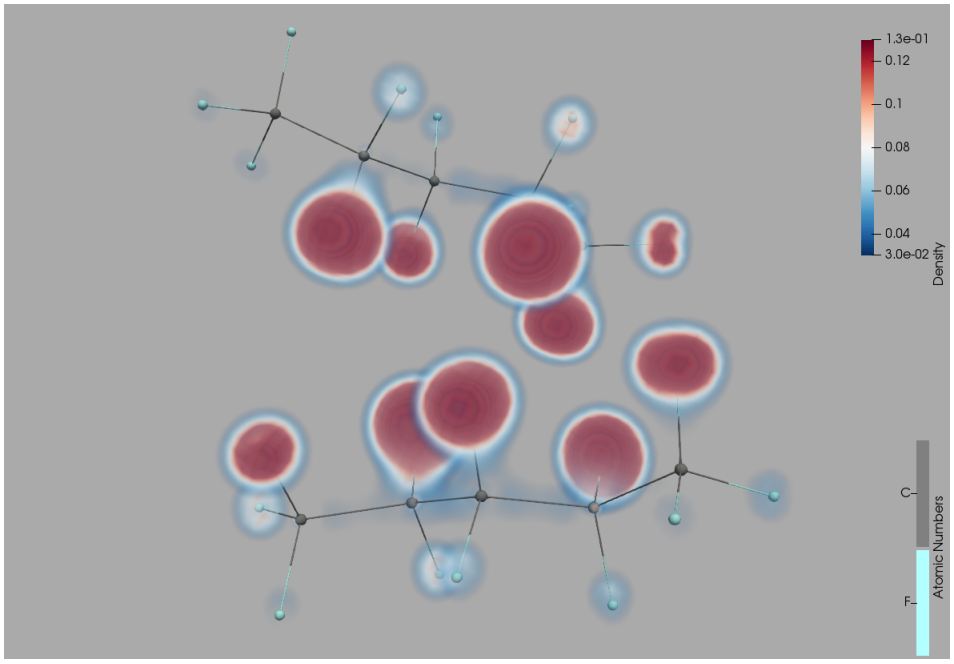

Figure S128: DID plot of **5-FF1**.

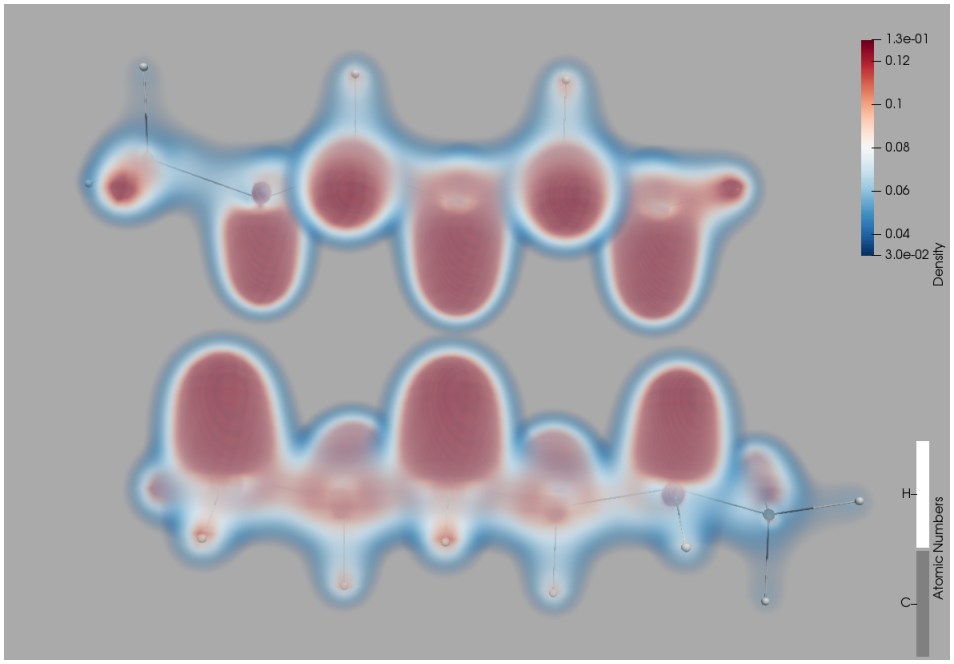

Figure S129: DID plot of **6-HH1**.

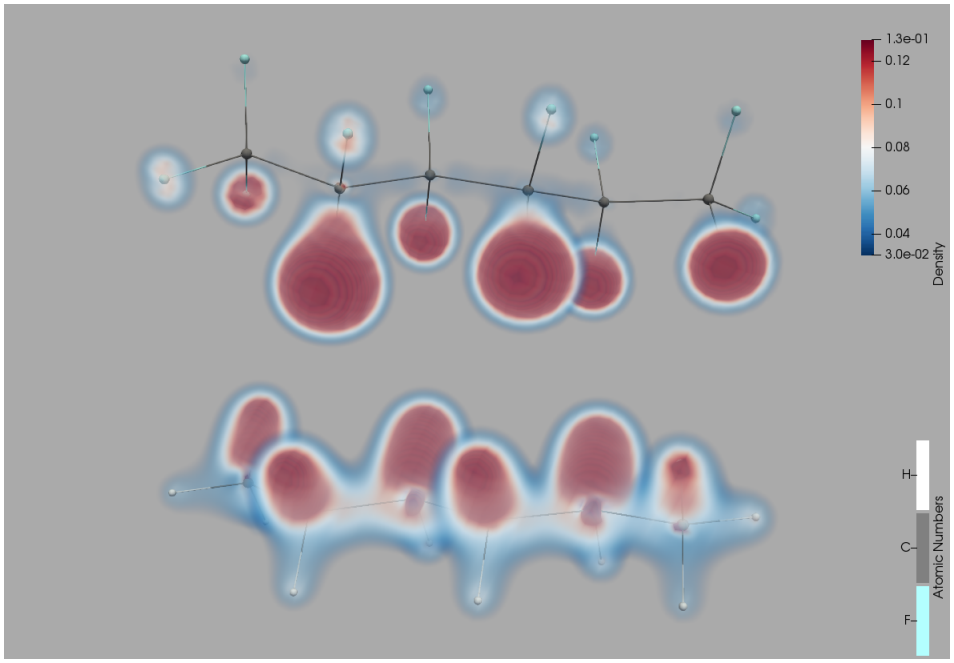

Figure S130: DID plot of **6-HF1**.

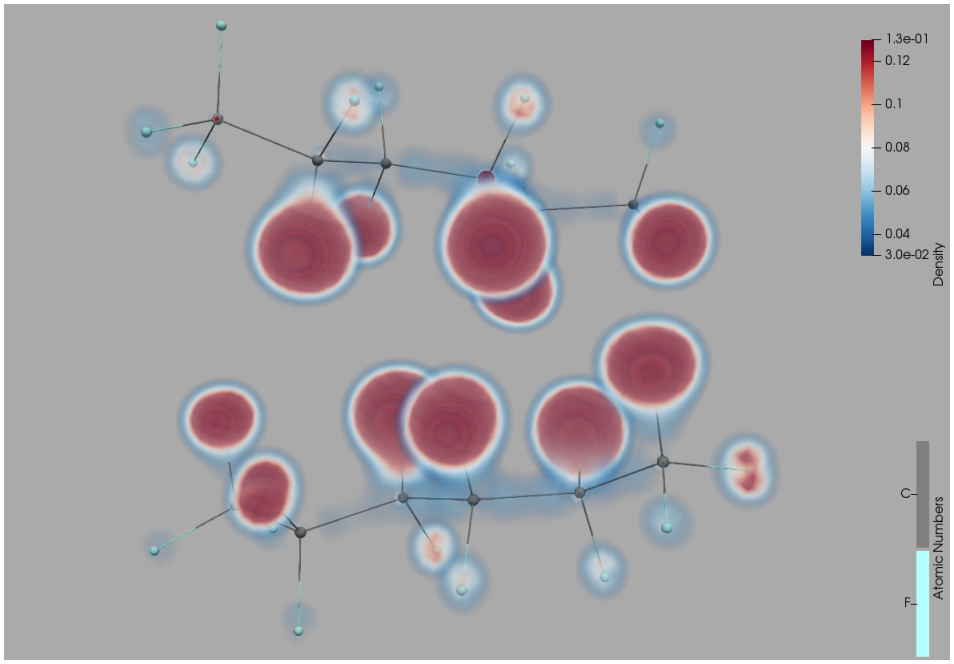

Figure S131: DID plot of **6-FF1**.

2.3 Simple Interaction Models

2.3.1 Molecular London Dispersion Model

For the molecular London dispersion model, ionization potentials I_1 and I_2 and polarizabilities α_1 and α_2 of the separate molecules with index 1 and 2 are required, as well as the intermolecular distance R. While it seems obvious to use the molecular ionization potentials and polarizabilities to describe intermolecular dispersion in this admittedly crude model, the choice of intermolecular distance to use between the molecules is not straightforward. Using MP2/CBS(34) ionization potentials and MP2/def2-TZVPD polarizabilities together with the average distance of the two carbon chains in each molecular complex resulted in the estimated London dispersion energies shown in Figure S132. It can be directly seen, when the estimated London dispersion energies are compared to CCSD(T)-F12 BIEs, that **HH**, **HF** and **FF** are not uniformly estimated and the three subclasses show three separate linear regression functions.

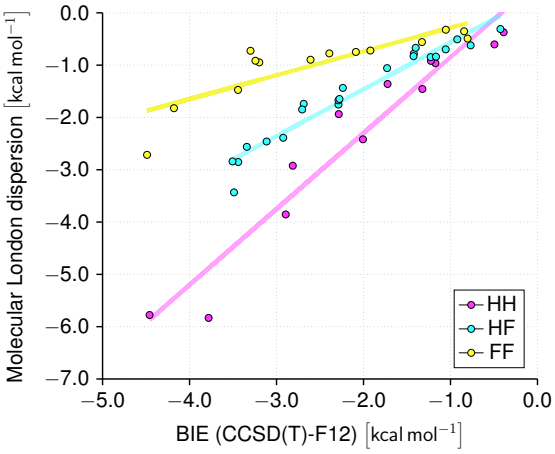

Figure S132: Intermolecular dispersion estimated with the London dispersion formula (cf. Equation 6 in the main text) using molecular ionization potentials and molecular polarizabilities compared to CCSD(T)-F12 BIEs. The average distance between the carbon chains of the interacting molecules was used.

2.3.2 Atom-pairwise London Dispersion Models

We used two atom-pairwise London dispersion models to fit interaction parameters of **HH**, **HF** and **FF** and to estimate the corresponding BIEs. The idea was to find the best set of atom-type dependent parameters for the atomic ionization potentials to best reproduce the benchmark interaction energies (CCSD(T)-F12 level of theory). We performed this optimization using two different approaches. For the first, we used the London dispersion formula, as is, (cf. Equation 6 in the main text) and optimized atomic ionization potentials. For the second we used an approximation of the London dispersion formula explained in the main text simplifying the ionization potential pre-factor (which we term A_{12}) as product of atom-type dependent pre-factors A_1 and A_2 (cf. right-hand side of Equation 8 in the main text) and therefore we optimized the atomic pre-factors A. The most basic assumption of all our simple interaction models is that the overall BIE of our model complexes can be approximated by accounting only for dispersion. This assumption is plausible on the basis of the results of the energy decomposition analyses employed. For the first model, we used the London dispersion formula, as is,[106,107] and computed the overall BIE as sum of atom-pairwise terms:

$$\mathrm{BIE} \approx \sum_i \sum_j -\frac{3}{2} \frac{I_i I_j}{I_i + I_j} \frac{\alpha_i \alpha_j}{R_{ij}^6} \tag{S11}$$

We used the optimized geometries at the DSD-PBEP86/def2-TZVP(spd) level of theory to determine the atom-pairwise interaction distances R_{ij} and we determined the atomic polarizabilities α_i using PolaBer on the basis of MP2/def2-TZVPD densities. We assumed that the ionization potentials are atom-type dependent parameters and, hence, the model had three adjustable parameters (i.e. I_H, I_C and I_F). These parameters were determined by minimizing the MAD between the estimated BIEs and the benchmark BIEs at the CCSD(T)-F12/VDZ level of theory. After finding the best set of parameters, we compared the estimated BIEs to the benchmark BIEs. The corresponding results are illustrated in Figure S133.

The MAD_{rel} of the fitted values is only $(5 \pm 4)\,\%$ and is therefore comparable to the best benchmarked DFT and WFT methods (cf. main text). It is also slightly better than the second atom-pairwise London dispersion model (vide infra).

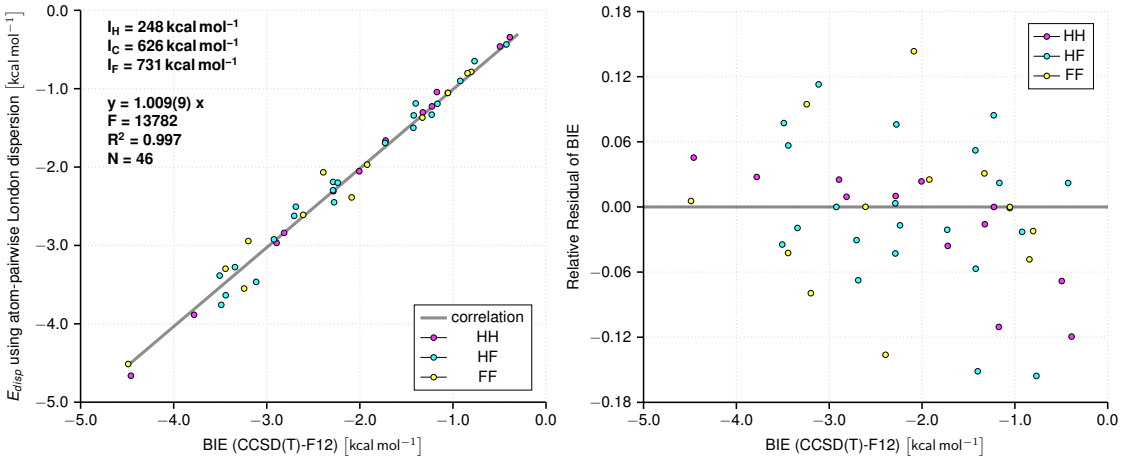

Figure S133: Intermolecular dispersion estimated using atom-pairwise London dispersion by optimizing atom-type dependent ionization potentials. Left: Results compared to reference data with the corresponding correlation. Right: Residual plot.

For the second model, we used an approximation of the London dispersion formula to describe the overall BIE of the complexes using instead of ionization potentials atom-type dependent pre-factors A:

$$\mathrm{BIE} \approx \sum_i \sum_j -\frac{3}{2} \frac{A_i \alpha_i A_j \alpha_j}{R_{ij}^6} \tag{S12}$$

These atom-type dependent pre-factors formally have the dimension of the square-root of energy. The advantage of these pre-factors is that the dispersion can be formally decomposed into a product of two values which is only dependent on one of the interacting molecules each. The motivation for pursuing this approach is explained in detail in the main text. We used again optimized geometries at the DSD-PBEP86/def2-TZVP(spd) level of theory to determine the atom-pairwise interaction distances R_{ij} and we also used the atomic polarizabilities α_i obtained from PolaBer on the basis of MP2/def2-TZVPD densities. In this model we optimized the atom-type dependent pre-factors as three adjustable parameters

(i.e. A_H, A_C and A_F). These parameters were again determined by minimizing the MAD between the estimated BIEs and the benchmark BIEs at the CCSD(T)-F12/VDZ level of theory. After finding the best set of parameters, we compared the estimated BIEs to the benchmark BIEs. The corresponding results are illustrated in Figure S134.

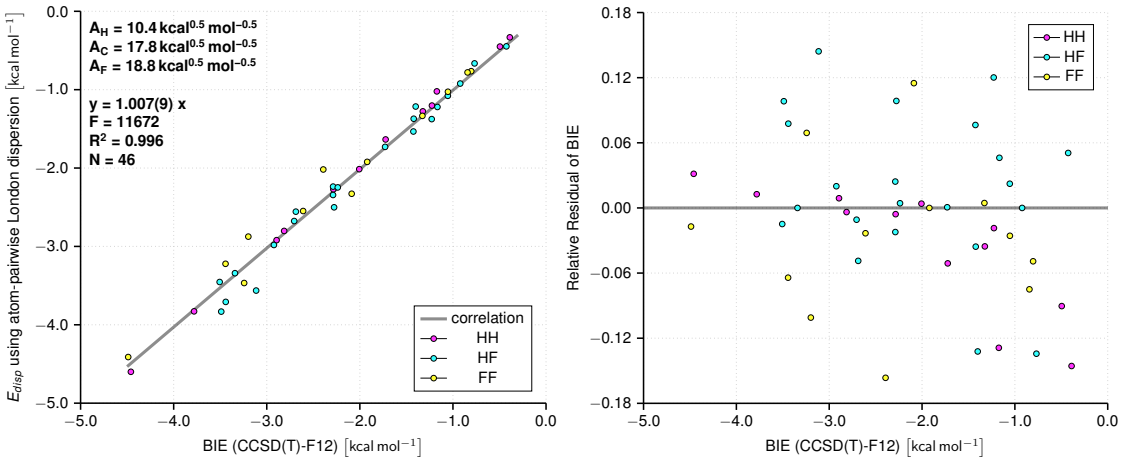

Figure S134: Intermolecular dispersion estimated using atom-pairwise London dispersion by optimizing atom-type dependent pre-factors A. Left: Results compared to reference data with the corresponding correlation. Right: Residual plot.

2.3.3 Atom-type Energy Decomposition

We also used the atom-pairwise London dispersion model to perform a decomposition of the overall dispersion into contributions of interactions between specific types of atoms. In that regard, it is similar to the decomposition into contributions of atoms and bonds we carried out using LED (vide supra). Hence, we obtain the following six energetic contributions:

D_{tot}	...	Total intermolecular dispersion
$D(C-C)$	...	Dispersion between two carbon atoms
$D(C-H)$	...	Dispersion between a carbon atom and a hydrogen atom
$D(H-H)$	...	Dispersion between two hydrogen atoms
$D(C-F)$	...	Dispersion between one carbon and one fluorine atom
$D(H-F)$	...	Dispersion between one hydrogen and one fluorine atom
$D(F-F)$	...	Dispersion between two fluorine atoms

The corresponding results for all the molecular complexes studied are illustrated in Fig-

ures S135-S152. The main difference between the LED decomposition into atoms and bonds and the decomposition performed using the atom-pairwise London dispersion model is that in the former the dispersion is also decomposed into contributions of bonds. In the atom-pairwise model the contributions of the bonds are distributed between the respective atomic contributions. This can be gleaned from the results of the complexes of **1-H** and **1-F**. In **1-HH** the contributions of the C-H bonds are distributed among the C-H and the H-H contributions. In **1-HF** the contributions of the C-H and C-F bonds are mainly distributed between the C-F and H-F contributions. In **1-FF** the contributions of the C-F bonds are mainly distributed between the C-F and F-F contributions.

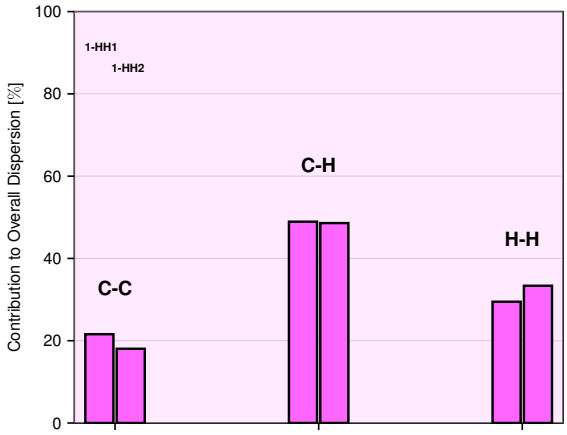

Figure S135: Decomposition of dispersion obtained from the atom-pairwise London dispersion model into contributions of interactions between types of atoms for **1-HH** complexes.

Additionally, we investigated the relative contribution of F-F in **FF** as a function of the relative molar fluorine content, as well as, the relative contribution of C-C in **HH** as a function of the relative molar carbon content (cf. Figure S153). In both cases we obtain reasonable linear correlations. These results indicate the direct impact of the relative molar carbon content on the dispersion interaction pattern. They also support the findings from LED.

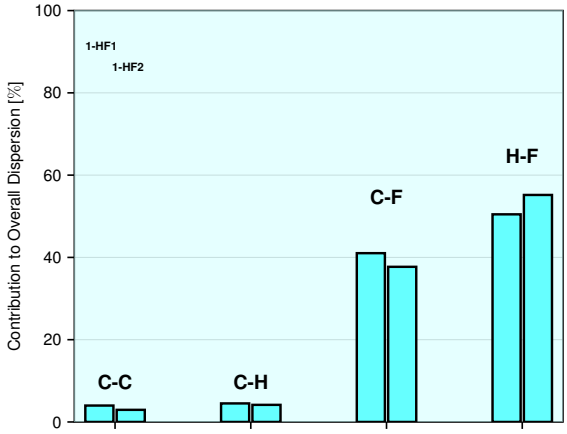

Figure S136: Decomposition of dispersion obtained from the atom-pairwise London dispersion model into contributions of interactions between types of atoms for **1-HF** complexes.

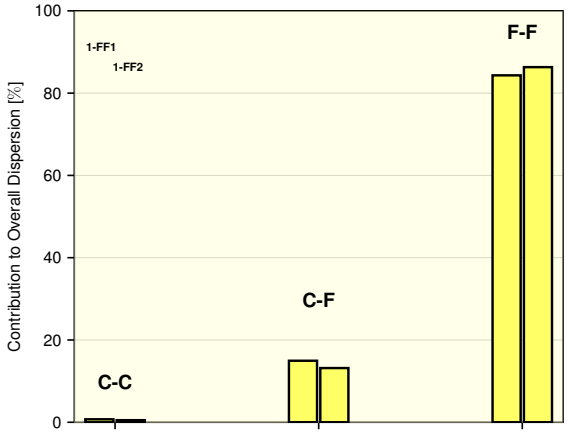

Figure S137: Decomposition of dispersion obtained from the atom-pairwise London dispersion model into contributions of interactions between types of atoms for **1-FF** complexes.

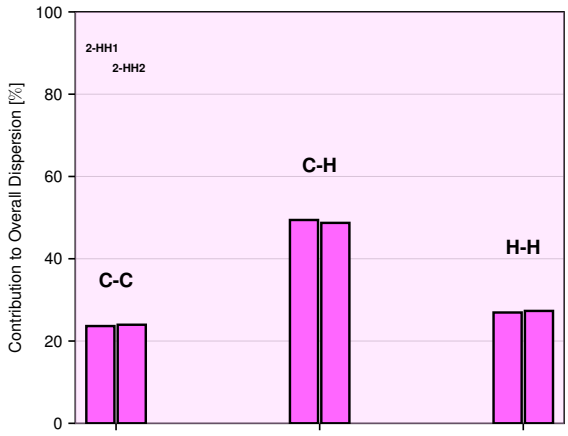

Figure S138: Decomposition of dispersion obtained from the atom-pairwise London dispersion model into contributions of interactions between types of atoms for **2-HH** complexes.

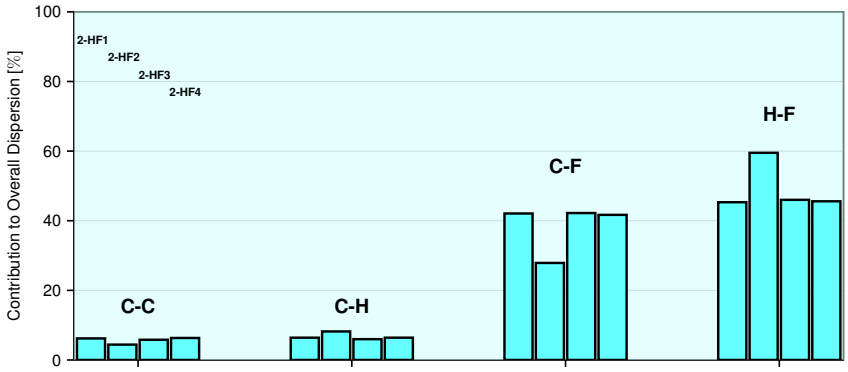

Figure S139: Decomposition of dispersion obtained from the atom-pairwise London dispersion model into contributions of interactions between types of atoms for **2-HF** complexes.

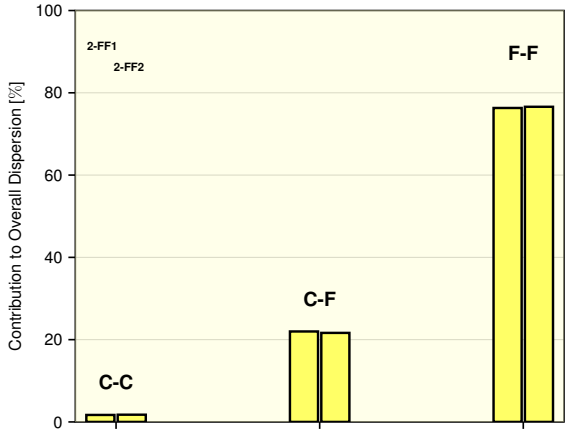

Figure S140: Decomposition of dispersion obtained from the atom-pairwise London dispersion model into contributions of interactions between types of atoms for **2-FF** complexes.

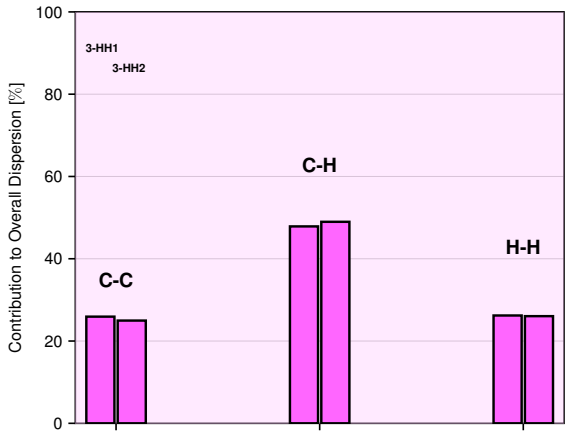

Figure S141: Decomposition of dispersion obtained from the atom-pairwise London dispersion model into contributions of interactions between types of atoms for **3-HH** complexes.

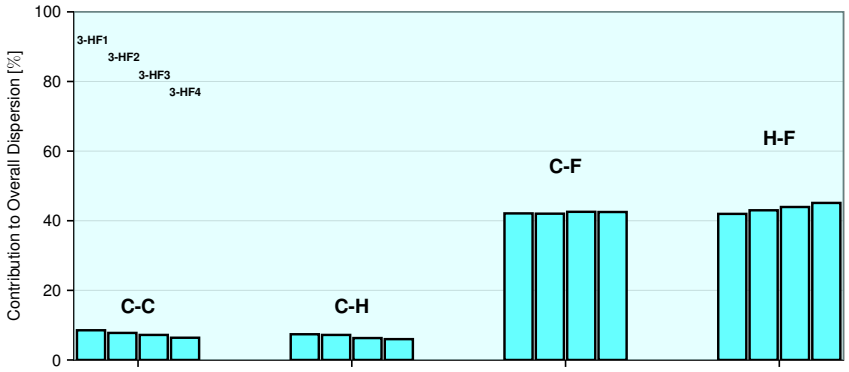

Figure S142: Decomposition of dispersion obtained from the atom-pairwise London dispersion model into contributions of interactions between types of atoms for **3-HF** complexes.

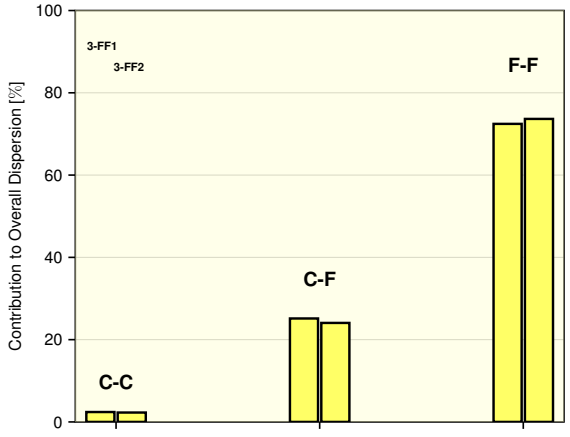

Figure S143: Decomposition of dispersion obtained from the atom-pairwise London dispersion model into contributions of interactions between types of atoms for **3-FF** complexes.

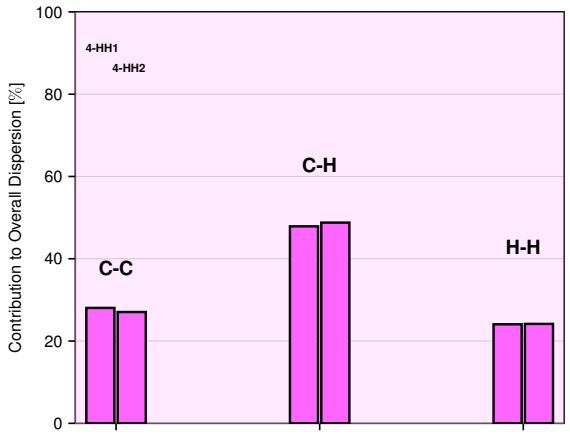

Figure S144: Decomposition of dispersion obtained from the atom-pairwise London dispersion model into contributions of interactions between types of atoms for **4-HH** complexes.

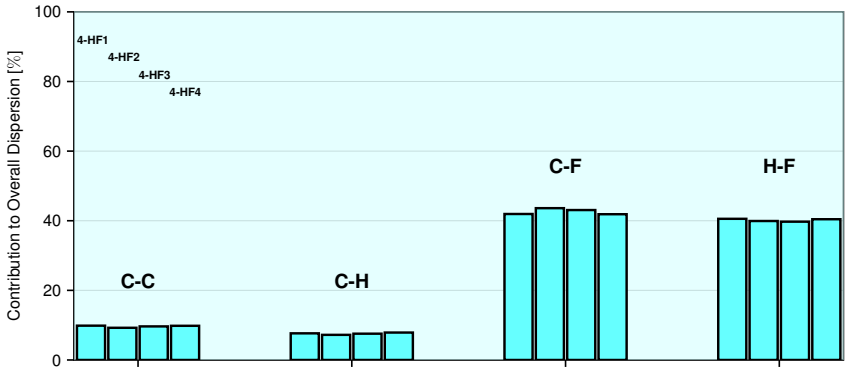

Figure S145: Decomposition of dispersion obtained from the atom-pairwise London dispersion model into contributions of interactions between types of atoms for **4-HF** complexes.

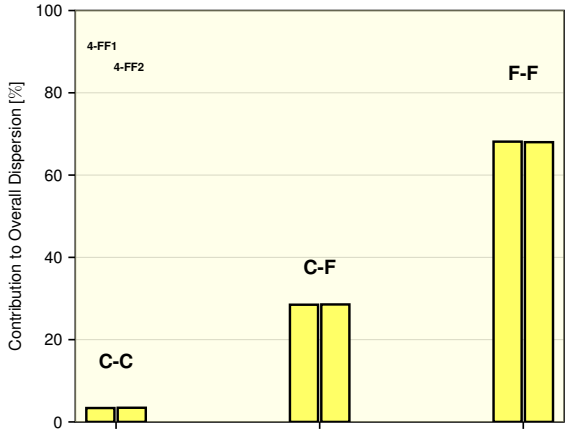

Figure S146: Decomposition of dispersion obtained from the atom-pairwise London dispersion model into contributions of interactions between types of atoms for **4-FF** complexes.

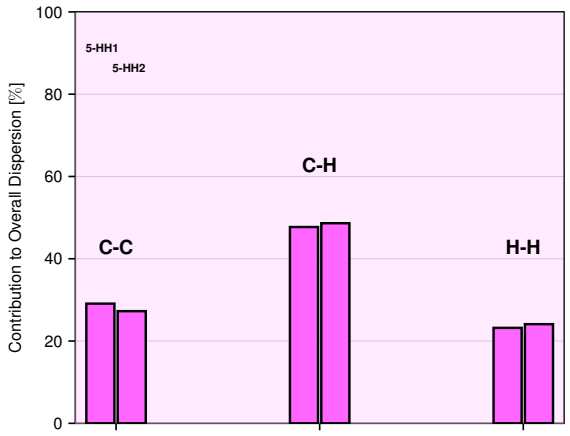

Figure S147: Decomposition of dispersion obtained from the atom-pairwise London dispersion model into contributions of interactions between types of atoms for **5-HH** complexes.

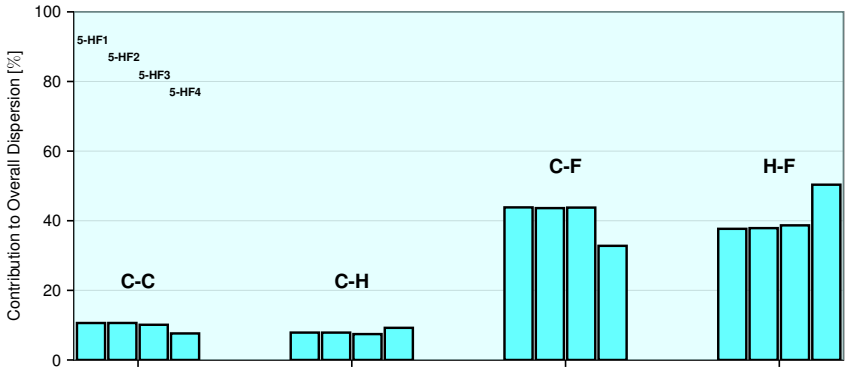

Figure S148: Decomposition of dispersion obtained from the atom-pairwise London dispersion model into contributions of interactions between types of atoms for **5-HF** complexes.

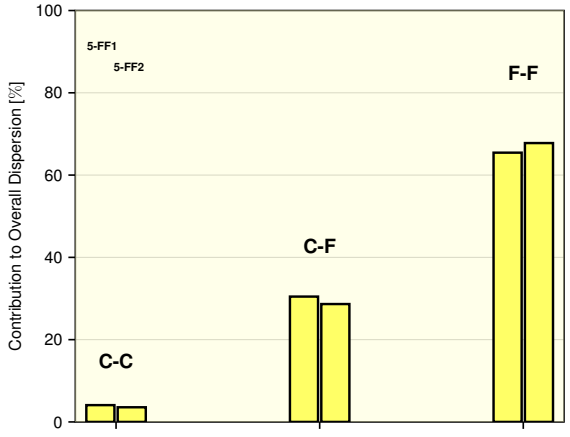

Figure S149: Decomposition of dispersion obtained from the atom-pairwise London dispersion model into contributions of interactions between types of atoms for **5-FF** complexes.

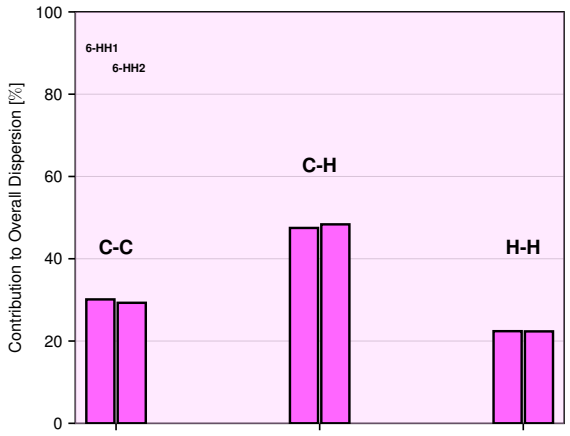

Figure S150: Decomposition of dispersion obtained from the atom-pairwise London dispersion model into contributions of interactions between types of atoms for **6-HH** complexes.

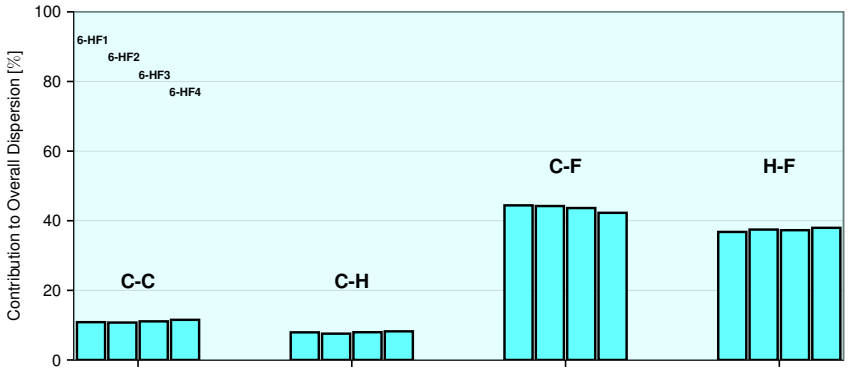

Figure S151: Decomposition of dispersion obtained from the atom-pairwise London dispersion model into contributions of interactions between types of atoms for **6-HF** complexes.

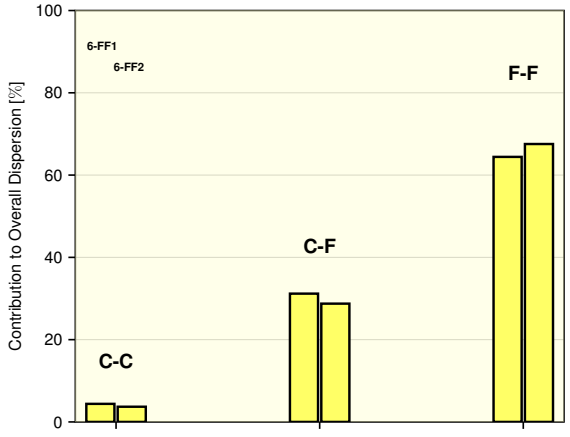

Figure S152: Decomposition of dispersion obtained from the atom-pairwise London dispersion model into contributions of interactions between types of atoms for **6-FF** complexes.

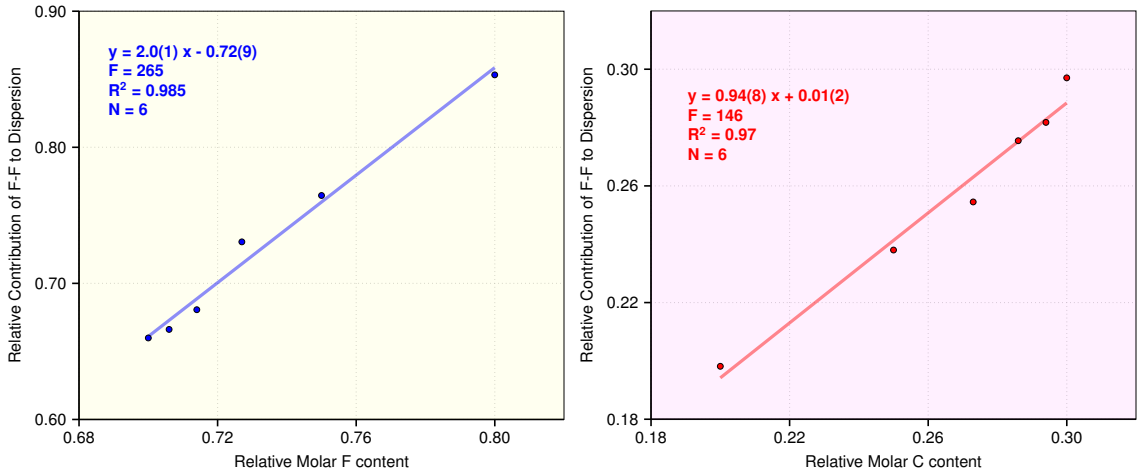

Figure S153: Left: Relative contribution of F-F in **FF** as a function of the relative molar fluorine content. Right: Relative contribution of C-C in **HH** as a function of the relative molar carbon content from the atom-pairwise London dispersion interaction model.

2.3.4 Correlation of BIE with Interaction Surface

Furthermore, we were also interested whether alternative simple interaction models could be applied to predicting the interaction energies of **F**. One common approximation is to regard it as interaction between exposed surfaces. Therefore, we computed the interaction surface area of all the molecular complexes using COSMO calculations and plotted the BIEs at the VeryTightPNO-DLPNO-CCSD(T)/CBS level of theory as well as the dispersion energy components at the LED-TightPNO-DLPNO-CCSD(T)/QZ level of theory against the corresponding interaction surface areas (cf. Figure S154). It can be seen that in both cases for each of the subsystems the BIE gets increasingly favorable as the interaction surface is increased and that reasonable linear correlations are observed.

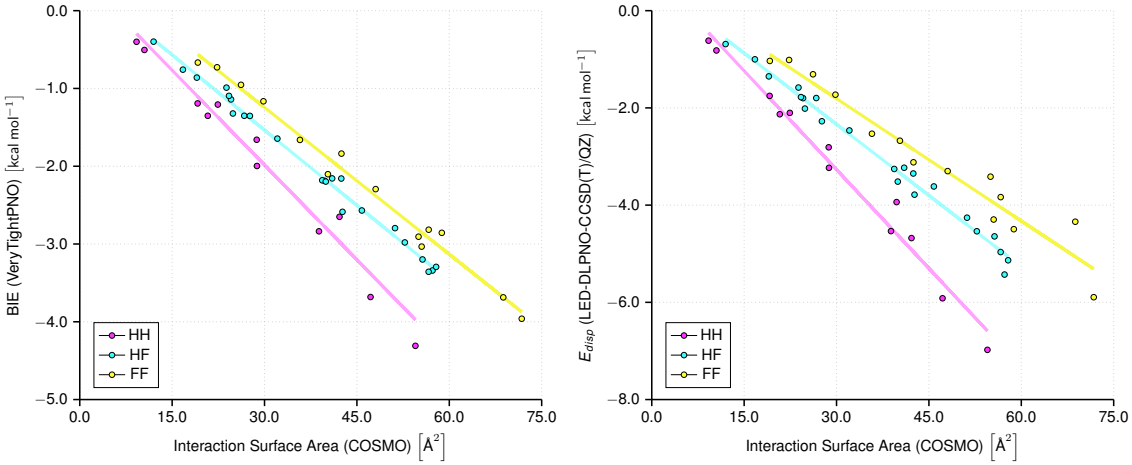

Figure S154: Left: Interaction energies obtained from VeryTightPNO-DLPNO-CCSD(T)/CBS calculations plotted against the corresponding interaction surface areas. Right: Dispersion energy components of molecular complexes obtained from LED-TightPNO-DLPNO-CCSD(T)/QZ calculations plotted against the corresponding interaction surface areas. Within each of the three subclasses of molecular complexes, a linear correlation is observed.

2.4 Interaction Descriptors

2.4.1 Q Measure and P Measure

Q_{atom} values were calculated as follows: For every point on the van der Waals surface (obtained from MP2/def2-TZVPD densities) the distance to one specific atom was calculated. The atomic polarizability (obtained using PolaBer) was divided by the third power of that distance to obtain the Q_{atom} value with respect to that specific point in space. The largest Q_{atom} on the van der Waals surface was then the maximum Q_{atom}. To obtain Q_{tot}, for every point on the van der Waals surface the sum of all Q_{atom} values of the molecule was calculated. Q_{tot} was obtained as average of all these sums with respect to all points on the van der Waals surface. The corresponding P values were calculated analogously with the difference that multiplication by the respective atom-type dependent pre-factor A was carried out as well.

Figure S155 shows the correlation between the relative P_{tot} value of **F** with respect to the corresponding **H** and the ratio of the relative contributions of C1 and C2 of **FF** and **HH** from LED. This correlation suggests that the change in the relative importance of the interactions

of the different atoms and bonds in the molecules is related to the change in the dispersive interaction capabilities of **H** with respect to **F**. The relative P_{tot} value of **F** with respect to the corresponding **H** as a function of the relative molar carbon content is illustrated in Figure S155. The linear correlation observed illustrates that the dispersive interaction capability of **F** relative to **H** decreases with increasing carbon chain length because of a concomitant decreasing relative molar fluorine content.

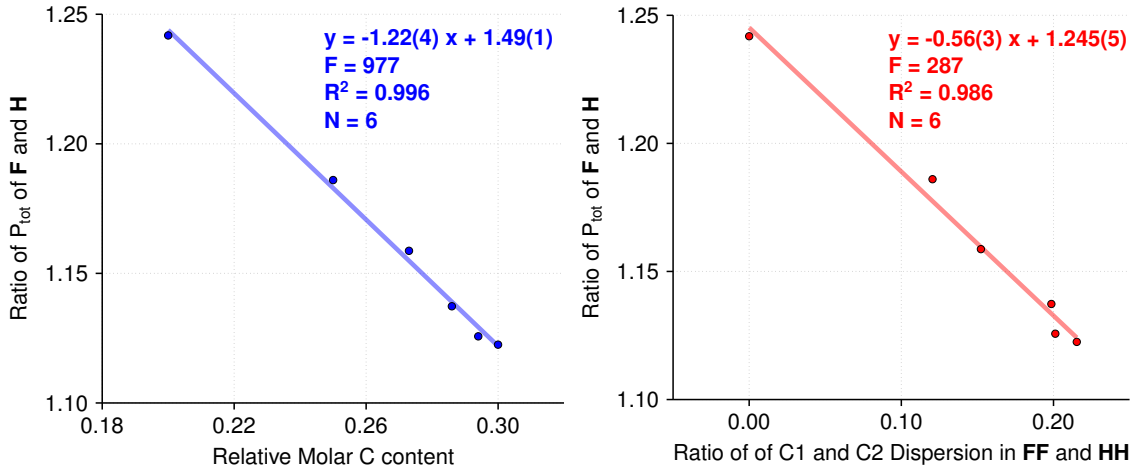

Figure S155: Correlation between the ratio of P_{tot} values of **F** and **H**. Left: the relative molar carbon content; Right: the ratio of the relative contributions of C1 and C2 of **FF** and **HH** from LED.

2.5 Interaction Geometries

2.5.1 Interaction Surface Areas

We applied the geometric interaction model of cuboids (vide infra) to assess how well the interaction geometries of **HF** and **FF** compared to **HH** are. To do that, we determined the correlation of the molecular surfaces of **H** and **F**, respectively, with the number of carbon atoms. For that, we used the COSMO surfaces (S) of these molecules. The corresponding results are illustrated in Figure S156.

Consequently, we looked at the correlation of the COSMO interaction surfaces (S_{int}) of **HH**, **HF** and **FF** against the number of carbon atoms. The COSMO interaction surfaces

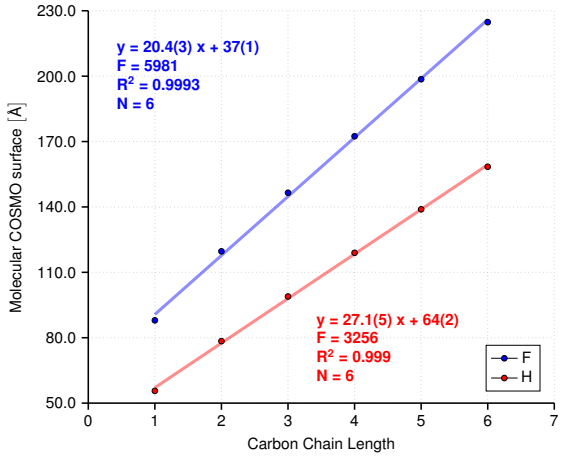

Figure S156: Molecular COSMO surface as a function of the number of carbon atoms for **H** and **F**.

were determined as difference of the molecular COSMO surfaces of the complexes and the respective monomers. Figure S157 shows the correlation of the COSMO interaction surfaces against the number of carbon atoms for the three classes of complexes. For each number of carbon atoms we used the complex with the largest COSMO interaction surface for the correlation. The corresponding statistical parameters are summarized in Table S3.

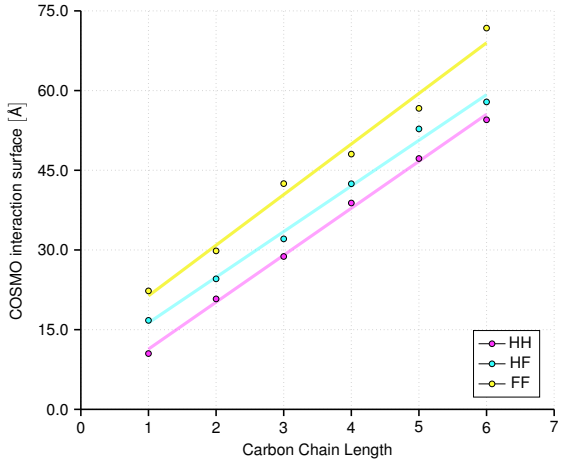

Figure S157: COSMO interaction surface as a function of the number of carbon atoms for **HH**, **HF** and **FF**.

From these correlations we can compare the interaction surfaces of **HH**, **HF** and **FF**. We assume that the interaction surface in **HH** is ideal. This assumption is based on the results of the NCI plots. On the basis of the interaction models of cuboids (vide infra) we

Table S3: Statistical parameters of the correlation of the COSMO interaction surface with the number of carbon atoms for **HH**, **HF** and **FF**.

$S_{int} = k \cdot n(C) + d$

Parameter	**HH**	**HF**	**FF**
k [Å]	8.8(2)	8.6(4)	9.5(6)
d [Å]	2.5(9)	8(1)	12(2)
F	1590	585	249
R^2	0.997	0.993	0.8
N	6	6	6

know that the ratio of the slope of the total surfaces of **H** and **F** as a function of the number of carbon atoms should correspond to the ratio of the slope of the interaction surfaces of **HH** and **FF** as a function of the number of carbon atoms if both are ideal. Hence, we need to compare the ratios of the molecular COSMO surfaces of **H** and **F** and the ratios of the COSMO interaction surfaces of **HH** and **FF**. The ratio of the slopes of the molecular COSMO surfaces of **F** and **H** is 1.32. The ratio of the slopes of the COSMO interaction surfaces of **FF** and **HH** is 1.1. Hence, the interaction surface in **FF** is 81 % of what the ideal interaction surface estimated on the basis of the cuboid model should be. In addition, using the heteromolecular cuboid model (vide infra) we estimated that the ideal ratio of the slopes of the interaction surfaces of **HF** and **HH** should be 1.14. However, the ratio of the slopes of the COSMO interaction surfaces of **HF** and **HH** is 0.97, i.e. it is 85 % of what the ideal ratio is estimated to be. Overall, this suggests that the interaction surfaces in **HF** and **FF** are not ideal compared to the interaction surfaces in **HH**.

For the computation of $n_{contacts}$ we used the recalculated van der Waals radii of Alvarez.[108] Hence, we used 1.20 Å for hydrogen, 1.77 Å for carbon and 1.46 Å for fluorine. Table S4 gives the statistical parameters of $n_{contacts}$ as a function of the carbon chain length for **HH**, **HF** and **FF** (cf. main text).

Table S4: Statistical parameters of the correlation of $n_{contacts}$ with the number of carbon atoms for **HH**, **HF** and **FF**.

$n_{contacts} = k \cdot n(C) + d$

Parameter	HH	HF	FF
k	8.2(1)	5.0(3)	4.5(4)
d	-3.1(5)	0.3(6)	1(2)
F	4159	908	112
R^2	0.999	0.996	0.97
N	6	6	6

2.6 Predicted Microscopic and Macroscopic Mixing Behavior

2.6.1 Average Coordination Number

In order to estimate macroscopic BIEs on the basis of Flory-Huggins solution theory,[109,110] we needed to estimate the average coordination number of one molecule of the liquid in the bulk liquid. To do that, we assumed that the interaction geometries in the dimers we investigated in this work are akin to the interaction geometries in the liquid phase. Hence, we determined the average coordination number as ratio of the sum of the molecular COSMO surfaces of the interacting molecules in the molecular complex and the corresponding COSMO interaction surface in the molecular complex divided by two. The macroscopic interaction energies are then the product of the BIE of one intermolecular complex and the average coordination number.

2.7 Trends in Experimental Properties

2.7.1 Boiling Points of Alkanes and Perfluoroalkanes

When looking at the boiling points of **H** and **F** as a function of carbon chain length, linear **F** with a carbon chain length up to three have a higher boiling point compared to the corresponding **H**.[111,112] Linear **F** with a longer carbon chain have a lower boiling point compared to the corresponding **H** (cf. Figure S158). Hence, there is a crossover in the boiling point curves between **H** and **F**. As the boiling point is a measure of the strength of

intermolecular interactions, the relative boiling point inversion indicates that the strength of the intermolecular interactions in **H** increase to a greater extent with carbon chain length than they do in **F**. When the boiling point difference between **H** and the corresponding **F** is plotted against the relative molar carbon content, a linear correlation is observed (cf. Figure S158).

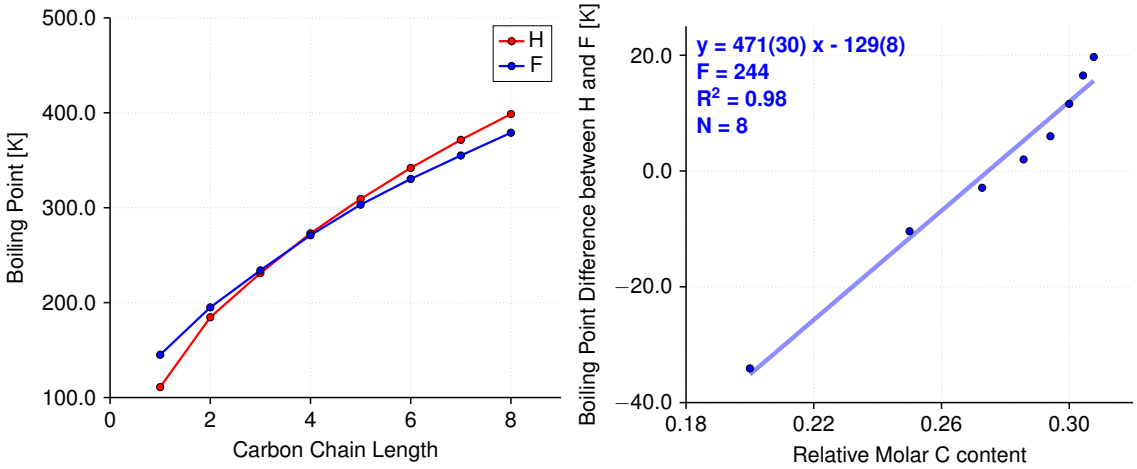

Figure S158: Left: Boiling points of **H** and **F** as a function of the respective carbon chain length. **H** have a higher boiling point at carbon chain lengths of four or higher. **F** have a higher boiling point with shorter carbon chains. Right: The boiling point difference between **H** and **F** of same carbon chain length as a function of the relative molar carbon content shows a linear correlation.

Table S5 contains the boiling points of **H** and **F** from one to eight carbon atoms and the corresponding references.

Table S5: Boiling points (T_{vap}) of **H** and **F** from one to eight carbon atoms with the corresponding relative number of carbon atoms and the boiling point differences between **H** and **F** (ΔT_{vap}).

n(C)	n_{rel}(C)	T_{vap}(**H**) [K]	T_{vap}(**F**) [K]	ΔT_{vap}(**H-F**) [K]
1	0.200	111[113]	145[113]	-34
2	0.250	185[113]	195[113]	-10
3	0.273	231[113]	234[113]	-3
4	0.286	273[113]	271[114]	2
5	0.294	309[113]	303[115]	6
6	0.300	342[113]	330[115]	12
7	0.304	372[113]	355[113]	17
8	0.308	399[113]	379[116]	20

2.7.2 Critical Parameters of Alkanes and Perfluoroalkanes

Boiling points are only indirect measures of the strength of intermolecular interactions. Direct measures of intermolecular interactions in gases are provided by the van der Waals equation of state parameters a and b determined from critical point data.[117] The ratio of a over b is an estimate of the minimum energy of the intermolecular potential energy surface which is apparent from the derivation of the van der Waals equation of state from statistical thermodynamics.[118] Plotting the ratio a over b, determined from literature data (the references of all the individual data points are provided in Tables S6-S8), as a function of the carbon chain length for both **H** and **F**, a similar trend compared to the boiling points is observed (cf. Figure S159). **1-F** has stronger intermolecular interactions than **1-H**, but already **2-H** has stronger intermolecular interactions than **2-F** and the difference between the two classes of compounds increases with carbon chain length. Plotting the difference in the ratio a over b between **H** and **F** of same carbon chain length against the respective relative molar carbon content, a linear correlation is observed (cf. Figure S159).

Tables S6-S8 contain the critical parameters of **H** and **F** from one to eight carbon atoms and the corresponding derived van der Waals parameters and average attraction energies between particles with the respective references.

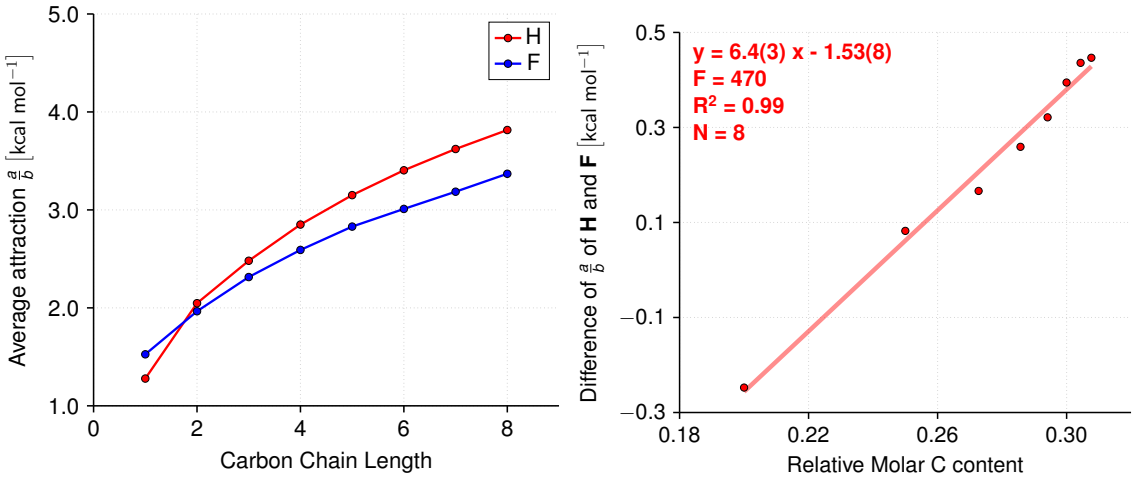

Figure S159: Left: Average attraction between molecules in the gas-phase as obtained from experimental van der Waals equation of state parameters at the critical point as a function of the carbon chain length. **1-F** has stronger intermolecular attraction than **1-H**. At longer carbon chain lengths, **H** have stronger intermolecular attraction than the corresponding **F** having the same carbon chain length. Right: The difference in intermolecular attraction between **H** and **F** of same carbon chain length as a function of the relative molar carbon content shows a linear correlation.

Table S6: Critical parameters and van der Waals equation of state parameters a and b of **H** from one to eight carbon atoms. The ratio of a and b corresponds to the average attraction between particles.

n(C)	n_{rel}(C)	T_c [K]	p_c [bar]	a [J m^3 mol^{-2}]	b [10^{-5} m^3 mol^{-1}]	$\frac{a}{b}$ [kcal mol^{-1}]
1	0.200	190.6[119]	46.10[119]	0.2298	4.297	1.278
2	0.250	305.3[119]	49.00[119]	0.5548	6.476	2.048
3	0.273	369.9[119]	42.50[119]	0.9389	9.046	2.481
4	0.286	425.0[119]	38.00[119]	1.386	11.62	2.850
5	0.294	469.8[119]	33.60[119]	1.916	14.53	3.151
6	0.300	507.6[119]	30.20[119]	2.488	17.47	3.404
7	0.304	540.0[119]	27.40[119]	3.104	20.48	3.622
8	0.308	568.9[119]	24.90[119]	3.791	23.75	3.816

Table S7: Critical parameters and van der Waals equation of state parameters a and b of **F** from one to eight carbon atoms. The ratio of a and b corresponds to the average attraction between particles.

n(C)	n_{rel}(C)	T_c [K]	p_c [bar]	a [J m^3 mol^{-2}]	b [10^{-5} m^3 mol^{-1}]	$\frac{a}{b}$ [kcal mol^{-1}]
1	0.200	227.5[119]	37.45[119]	0.4031	6.314	1.526
2	0.250	293.0[120]	30.42[120]	0.8232	10.01	1.965
3	0.273	345.1[121]	26.75[121]	1.298	13.41	2.315
4	0.286	386.4[119]	23.23[119]	1.874	17.28	2.591
5	0.294	421.9[119]	20.37[122]	2.548	21.53	2.830
6	0.300	448.8[123]	18.68[123]	3.144	24.97	3.010
7	0.304	475.0[124]	16.50[124]	3.988	29.92	3.186
8	0.308	502.3[119]	15.48[122]	4.753	33.72	3.369

Table S8: Average attraction between particles of **H** and **F** with one to eight carbon atoms and the corresponding differences between **H** and **F**.

n(C)	n_{rel}(C)	$\frac{a}{b}$(**H**) [kcal mol^{-1}]	$\frac{a}{b}$(**F**) [kcal mol^{-1}]	$\Delta\frac{a}{b}$(**H-F**) [kcal mol^{-1}]
1	0.200	1.278	1.526	-0.247
2	0.250	2.048	1.965	0.082
3	0.273	2.481	2.315	0.166
4	0.286	2.850	2.591	0.259
5	0.294	3.151	2.830	0.321
6	0.300	3.404	3.010	0.395
7	0.304	3.622	3.186	0.436
8	0.308	3.816	3.369	0.447

2.7.3 Enthalpies of Evaporation of Alkanes and Perfluoroalkanes

The enthalpies of evaporation of **H** and **F** correlate linearly with the carbon chain length (cf. Figure S160).

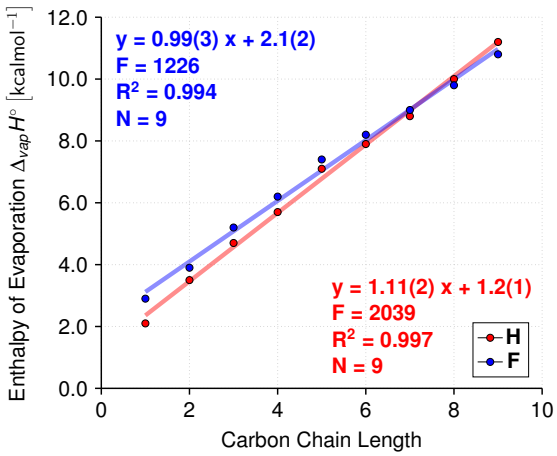

Figure S160: Enthalpies of evaporation of **H** and **F** of increasing carbon chain length.

Table S9 contains the enthalpies of evaporation of **H** and **F** with one to nine carbon atoms together with the corresponding references.

Table S9: Enthalpies of evaporation (ΔH_{vap}) of **H** and **F** with one to nine carbon atoms with the corresponding temperature ranges for which the enthalpies are valid.

n(C)	ΔH_{vap} (**H**) [kcal mol^{-1}]	T-Range [K]	ΔH_{vap} (**F**) [kcal mol^{-1}]	T-Range [K]
1	2.06 [125]	90 – 120	2.94 [125]	89 – 163
2	3.51 [126]	184	3.86 [116]	195
3	4.66 [125]	165 – 248	5.16 [125]	193 – 237
4	5.71 [127]	195 – 273	6.17 [128]	233 – 260
5	7.12 [125]	223 – 352	7.43 [125]	221 – 303
6	7.93 [125]	238 – 343	8.22 [125]	261 – 334
7	8.84 [129]	288 – 348	9.01 [125]	271 – 379
8	10.01 [130]	298 – 333	9.85 [131]	310 – 379
9	11.16 [132]	299	10.83 [133]	288 – 333

2.7.4 Bulk Moduli of Alkanes and Perfluoroalkanes

The bulk moduli of **H** and **F** show an inversion when the carbon chain length is increased (cf. Figure S161).

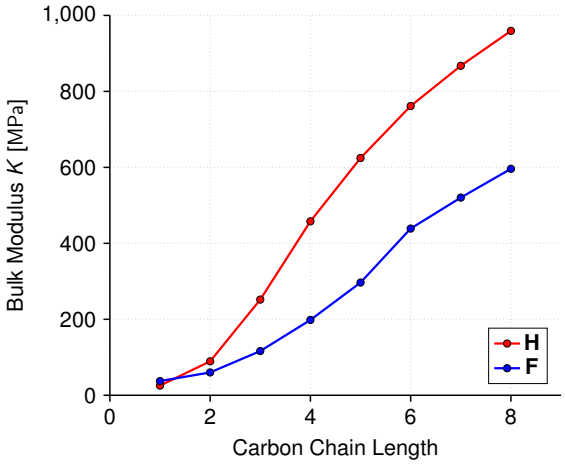

Figure S161: Bulk moduli of **H** and **F** of increasing carbon chain length.

Tables S10 and S11 contain the densities, speed of sound values and the derived bulk moduli of **H** and **F** with one to eight carbon atoms together with the corresponding references.

Table S10: Densities (ρ), speed of sound values (c) and derived bulk moduli (K) of **H** at 298 K from one to eight carbon atoms with the corresponding pressures for which the values are valid. The bulk moduli are calculated as follows: $K = \rho\, c^2$.

n(C)	n_{rel}(C)	Pressure [MPa]	ρ [kg m^{-3}]	c [m s^{-1}]	K [MPa]
1	0.200	15.0	119.7[134]	460.6[134]	25.4
2	0.250	7.5	362.0[135]	497.0[135]	89.4
3	0.273	1.3	492.3[136]	715.3[136]	251.9
4	0.286	0.6	573.3[137]	893.8[138]	458.0
5	0.294	0.1	621.0[139]	1002.9[139]	624.6
6	0.300	0.1	655.3[140]	1078.0[140]	761.5
7	0.304	0.1	679.6[141]	1129.7[141]	867.4
8	0.308	0.1	698.7[141]	1171.7[141]	959.3

Table S11: Densities (ρ), speed of sound values (c) and derived bulk moduli (K) of **F** at 298 K from one to eight carbon atoms with the corresponding pressures for which the values are valid. The bulk moduli are calculated as follows: $K = \rho\, c^2$.

n(C)	n_{rel}(C)	Pressure [MPa]	ρ [kg m^{-3}]	c [m s^{-1}]	K [MPa]
1	0.200	15.0	745.3[142]	224.3[142]	37.5
2	0.250	7.5	1100.0[142]	233.8[142]	60.1
3	0.273	1.3	1331.9[142]	295.6[142]	116.4
4	0.286	0.6	1499.5[143]	363.6[142]	198.3
5	0.294	0.1	1599.5[144]	430.7[145]	296.7
6	0.300	0.1	1682.8[146]	510.7[146]	438.9
7	0.304	0.1	1728.4[146]	548.7[146]	520.4
8	0.308	0.1	1760.6[146]	581.9[146]	596.2

2.7.5 Compressibilities of Alkanes and Perfluoroalkanes

The compressibilities of **H** and **F** show an inversion when the carbon chain length is increased (cf. Figure S162).

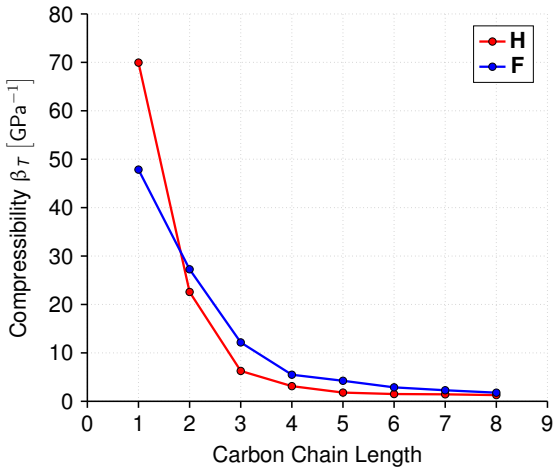

Figure S162: Isothermal compressibilities of **H** and **F** of increasing carbon chain length.

Table S12 contains the compressibilities of **H** and **F** with one to eight carbon atoms together with the corresponding references.

Table S12: Isothermal compressibilities (β_T) of **H** and **F** at 298 K with one to eight carbon atoms with the corresponding pressures for which the values are valid.

n(C)	n_{rel}(C)	Pressure [MPa]	β_T (**H**) [GPa^{-1}]	β_T (**F**) [GPa^{-1}]
1	0.200	15.0	69.95[142]	47.85[142]
2	0.250	7.5	22.58[142]	27.26[142]
3	0.273	1.3	6.27[147]	12.16[148]
4	0.286	0.6	3.13[147]	5.49[149]
5	0.294	0.1	1.80[149]	4.24[149]
6	0.300	0.1	1.50[150]	2.88[151]
7	0.304	0.1	1.44[151]	2.28[151]
8	0.308	0.1	1.28[151]	1.78[151]

2.7.6 Interal Pressures of Alkanes and Perfluoroalkanes

The internal pressures of **H** and **F** show an inversion when the carbon chain length is increased (cf. Figure S163).

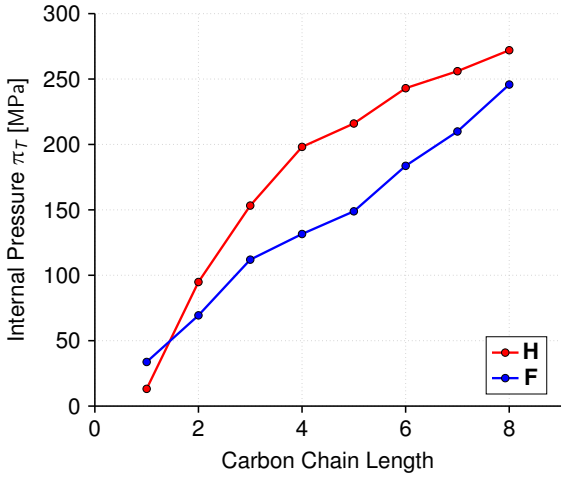

Figure S163: Internal pressures of **H** and **F** of increasing carbon chain length.

Table S13 contain the internal pressures of **H** and **F** with one to eight carbon atoms together with the corresponding references.

Table S13: Internal pressures (π_T) of **H** and **F** at 298 K with one to eight carbon atoms with the corresponding pressures for which the values are valid.

n(C)	n_{rel}(C)	Pressure [MPa]	π_T (**H**) [MPa]	π_T (**F**) [MPa]
1	0.200	15.0	13 [142]	34 [142]
2	0.250	7.5	95 [152]	69 [142]
3	0.273	1.3	153 [147]	112 [148]
4	0.286	0.6	198 [147]	132 [149]
5	0.294	0.1	216 [150]	149 [149]
6	0.300	0.1	243 [150]	184 [151]
7	0.304	0.1	256 [151]	210 [151]
8	0.308	0.1	272 [150]	246 [146,151]

2.7.7 Surface Tensions of Alkanes and Perfluoroalkanes

The surface tensions of **H** and **F** show an inversion when the carbon chain length is increased (cf. Figure S164).

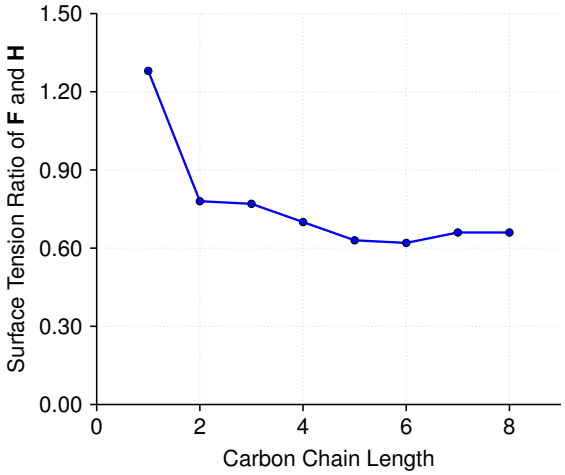

Figure S164: Ratio of surface tensions of **F** and **H** of increasing carbon chain length.

Table S14 contains the surface tensions of **H** and **F** with one to eight carbon atoms together with the corresponding references.

Table S14: Surface tensions (γ) of **H** and **F** with one to eight carbon atoms with the corresponding temperatures and pressures for which the values are valid.

n(C)	Temperature [K]	Pressure [MPa]	γ(**H**) [mN m^{-1}]	Temperature [K]	Pressure [MPa]	γ(**F**) [mN m^{-1}]
1	90.7	Triple point	17.8[153]	89.6	Triple point	22.8[154]
2	173.2	0.1	17.8[155]	173.2	Triple point	14.0[154]
3	140.0	0.1	29.3[156]	140.0	0.1	22.5[154]
4	193.2	0.1	25.3[157]	193.2	0.1	17.8[154]
5	298.0	0.1	15.0[158]	298.0	0.1	9.4[159]
6	298.0	0.1	17.8[158]	298.0	0.1	11.1[160]
7	298.0	0.1	19.5[158]	298.0	0.1	12.9[160]
8	298.0	0.1	21.3[158]	298.0	0.1	14.0[160]

2.7.8 Molar Heat Capacities of Alkanes and Perfluoroalkanes

The molar heat capacities of **H** and **F** correlate linearly with the carbon chain length (cf. Figure S165).

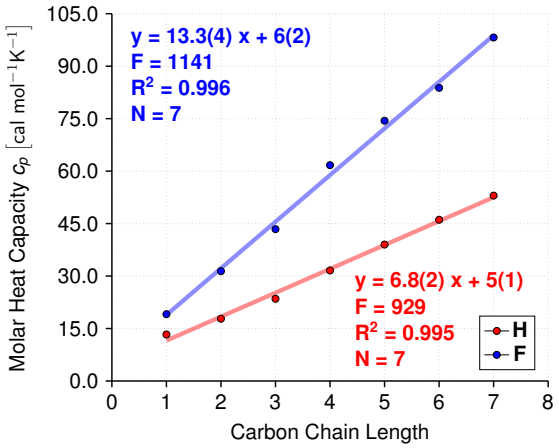

Figure S165: Molar heat capacities of **H** and **F** of increasing carbon chain length.

Table S15 contains the molar heat capacities of liquid **H** and **F** with one to seven carbon atoms together with the corresponding references.

Table S15: Molar heat capacities (c_p) of **H** and **F** with one to seven carbon atoms with the corresponding temperatures for which the values are valid.

n(C)	Temperature [K]	c_p (**H**) [cal mol^{-1} K^{-1}]	Temperature [K]	c_p (**F**) [cal mol^{-1} K^{-1}]
1	111	13.3[142]	145	19.1[161]
2	200	17.8[162]	195	31.4[163]
3	230	23.5[164]	235	43.4[165]
4	290	31.6[166]	293	61.7[142]
5	290	39.0[162]	298	74.4[145]
6	290	46.1[149]	293	83.8[145]
7	290	53.0[149]	293	98.2[167]

2.7.9 Dynamic Viscosities of Alkanes and Perfluoroalkanes

The dynamic viscosities of **H** and **F** do not show an inversion when the carbon chain length is increased (cf. Figure S166).

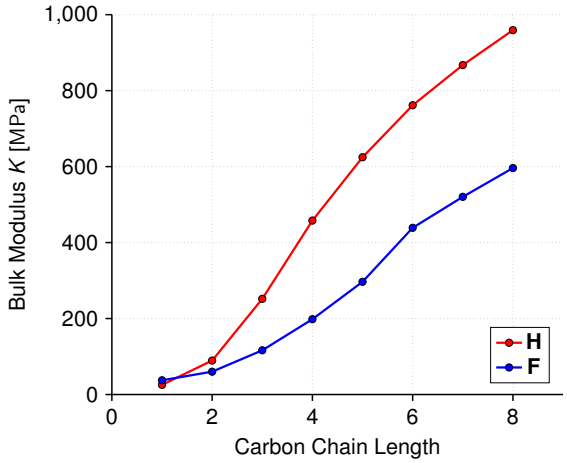

Figure S166: Dynamic viscosities of **H** and **F** of increasing carbon chain length.

Table S16 contains the dynamic viscosities of **H** and **F** with one to eight carbon atoms together with the corresponding references.

Table S16: Dynamic viscosities (μ) of **H** and **F** at 253 K with one to eight carbon atoms with the corresponding pressures for which the values are valid.

n(C)	n_{rel}(C)	Pressure [MPa]	μ(**H**) [mPa s]	μ(**F**) [mPa s]
1	0.200	15	0.019[142]	0.071[142]
2	0.250	7.5	0.084[142]	0.199[142]
3	0.273	1.3	0.157[142]	0.343[142]
4	0.286	0.1	0.250[149]	0.630[168]
5	0.294	0.1	0.340[149]	0.957[169]
6	0.300	0.1	0.450[149]	1.423[169]
7	0.304	0.1	0.690[149]	2.000[149]
8	0.308	0.1	0.980[149]	3.000[149]

2.7.10 Deviation of Computational Results from the Geometric Mean Rule

We estimated the BIEs of **HF** from the corresponding BIEs of **HH** and **FF** using the respective average BIEs of all conformers considered and taking the geometric mean of the absolute of the two BIEs. The deviation of the actual BIE and the estimated BIE was determined using equation S13. We also performed the same calculations using BAEs instead of BIEs. The corresponding results are provided in Tables S17-S19.

$$\Delta \mathrm{BIE}_{rel} = \frac{\mathrm{BIE}_{geo} - \mathrm{BIE}_{comp}}{\mathrm{BIE}_{comp}} \tag{S13}$$

Table S17: Estimation of the deviation of the BIEs of **HF** complexes from the geometric means of the corresponding **HH** and **FF** complexes using CCSD(T)-F12/VDZ, VeryTightPNO-DLPNO-CCSD(T)/CBS(34) and B97M-V/def2-QZVP interaction energies.

System	CCSD(T)-F12			VeryTight-DLPNO-CCSD(T)			B97M-V		
	BIE [kcal mol^{-1}]		$\Delta\mathrm{BIE}_{rel}$	BIE [kcal mol^{-1}]		$\Delta\mathrm{BIE}_{rel}$	BIE [kcal mol^{-1}]		$\Delta\mathrm{BIE}_{rel}$
	BIE_{comp}	BIE_{geo}		BIE_{comp}	BIE_{geo}		BIE_{comp}	BIE_{geo}	
1-HF	-0.60	-0.60	1.1 %	-0.58	-0.56	−2.8 %	-0.58	-0.56	−3.4 %
2-HF	-1.09	-1.22	11.6 %	-1.02	-1.16	13.6 %	-1.04	-1.16	12.2 %
3-HF	-1.49	-1.80	20.5 %	-1.42	-1.67	18.1 %	-1.50	-1.83	22.2 %
4-HF	-2.27	-2.40	5.7 %	-2.17	-2.22	2.3 %	-2.21	-2.34	5.6 %
5-HF	-2.86	-3.17	11.1 %	-2.73	-2.93	7.2 %	-2.92	-3.26	11.5 %
6-HF	-3.44	-3.75	8.9 %	-3.30	-3.44	4.4 %	-3.52	-3.84	9.0 %
Average			**10 %**			**7 %**			**10 %**

Table S18: Estimation of the deviation of the BIEs of **HF** complexes from the geometric means of the corresponding **HH** and **FF** complexes using the intermolecular London dispersion estimates and only the interaction distance components of the intermolecular London dispersion model (multiplied by the appropriate units to formally obtain energies).

System	Intermolecular London Dispersion BIE [kcal mol^{-1}]		ΔBIE$_{rel}$	Interaction Distances BIE [kcal mol^{-1}]		ΔBIE$_{rel}$
	BIE$_{comp}$	BIE$_{geo}$		BIE$_{comp}$ [10^{-4}]	BIE$_{geo}$ [10^{-4}]	
1-HF	-0.56	-0.58	3.2 %	-3.07	-3.16	3.0 %
2-HF	-0.98	-1.04	6.9 %	-2.10	-2.24	6.7 %
3-HF	-1.23	-1.60	29.8 %	1.39	-1.80	29.6 %
4-HF	-1.90	-1.89	−0.8 %	-1.33	-1.32	−1.0 %
5-HF	-2.34	-2.53	8.1 %	-1.09	-1.18	8.0 %
6-HF	-2.90	-3.13	8.0 %	-0.97	-1.05	7.9 %
Average			**9 %**			**9 %**

Table S19: Estimation of the deviation of the BAEs of **HF** complexes from the geometric means of the corresponding **HH** and **FF** complexes using CCSD(T)-F12/VDZ, VeryTightPNO-DLPNO-CCSD(T)/CBS(34) and B97M-V/def2-QZVP interaction energies.

System	CCSD(T)-F12 BAE [kcal mol^{-1}]		ΔBAE$_{rel}$	VeryTight-DLPNO-CCSD(T) BAE [kcal mol^{-1}]		ΔBAE$_{rel}$	B97M-V BAE [kcal mol^{-1}]		ΔBAE$_{rel}$
	BAE$_{comp}$	BAE$_{geo}$		BAE$_{comp}$	BAE$_{geo}$		BAE$_{comp}$	BAE$_{geo}$	
1-HF	-0.59	-0.60	1.1 %	-0.57	-0.56	−2.5 %	-0.57	-0.55	−2.8 %
2-HF	-1.09	-1.21	11.0 %	-1.01	-1.14	13.0 %	-1.02	-1.14	11.6 %
3-HF	-1.46	-1.77	20.8 %	-1.38	-1.65	19.4 %	-1.45	-1.81	24.2 %
4-HF	-2.20	-2.33	5.8 %	-2.08	-2.16	4.1 %	-2.13	-2.29	7.3 %
5-HF	-2.75	-3.11	13.0 %	-2.60	-2.89	10.9 %	-2.79	-3.22	15.3 %
6-HF	-3.19	-3.68	15.5 %	-3.02	-3.41	12.7 %	-3.22	-3.82	18.6 %
Average			**11 %**			**10 %**			**12 %**

Tables S17-S19 show that, on average, the BIEs of **HF** complexes are roughly 10 % weaker than estimated on the basis of the geometric mean rule. This has been observed experimentally on the basis of second interaction virial coefficients as well.[170–172] The results in Table S18 suggest that the interaction distances seem to be somewhat longer in **HF** than would be expected on the basis of the interaction distances in **HH** and **FF**. While the geometric mean rule is a commonly employed rule to estimate the strength of heteromolecular interactions on the basis of homomolecular interactions, there is no rigorous physical basis for it. The interaction of molecules interacting predominantly by dispersion can be estimated using the London dispersion formula.[106,107] In the London dispersion formula, there is a combination rule for the ionization potentials of the interacting atoms and molecules, but it is not a geometric mean rule. Additionally, the geometric mean rule is commonly used to estimate heteroatomic C_6 coefficients of interaction from homoatomic C_6 coefficients of interaction because it empirically provides good estimates but not because of the underlying physical laws. Therefore, *a priori*, there is no reason that the geometric mean rule should describe the interactions in **HF** well.

3 Mathematical Derivations

In this section mathematical derivations are presented and explained in detail. The corresponding results are applied to analyze and interpret the computational results.

3.1 Homomolecular Cuboid Model for Interaction Surfaces

The basic assumption is that the interacting molecules (linear alkanes and perfluoroalkanes) can be approximated as interacting cuboids (cf. Figure S167).

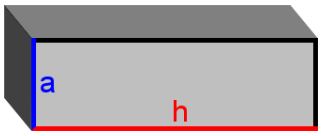

Figure S167: Cuboid model.

The total surface (S) of the cuboid can be calculated as follows:

$$S = 2a^2 + 4ah \tag{S14}$$

The interaction surface corresponds to one of the long faces of the cuboid with the area:

$$S_{int} = ah \tag{S15}$$

The length of the long face (h) in this model is approximately a linear function of the length of the carbon chain and hence of the number of carbon atoms (n) with u and v being the corresponding slope and intercept, respectively:

$$h \approx u \cdot n + v \tag{S16}$$

It follows from the combination of equations S14 and S16 that the total surface is predicted to be a linear function (with intercept q) of the number of carbon atoms for each class

of compounds (i.e. either **H** or **F**):

$$S \approx 2a^2 + 4av + 4an = 4au \cdot n + q \tag{S17}$$

Combining equations S15 and S16 it can be seen that also the interaction surface is a linear function (with intercept r) of the number of carbon atoms with the slope being a quarter of the corresponding slope of the total surface.

$$S_{int} \approx au \cdot n + av = au \cdot n + r \tag{S18}$$

Therefore, on the basis of this simple model it can be shown that comparing the slope of the total surface of the isolated molecules to the slope of the interaction surface is a means to estimate whether the interaction surface is ideal or not. Additionally, when comparing the ratio of the slopes of the total surface of **H** and **F** against the ratio of the slopes of the interaction surface area of **H** and **F** provides a means to investigate whether **H** or **F** have a closer to ideal interaction surface. The application of this model has been shown in the Supplementary Results and Discussion section.

3.2 Heteromolecular Cuboid Model for Interaction Surfaces

The model discussed in the previous section is only valid when the two interacting molecules are identical, i.e. the interacting cuboids have the same size. When they do not, the interaction surface is not equal to the long face of either of the two molecules. This is illustrated in Figure S168.

The edge of the interaction surface a_i can determined if we assume the following relationship:

$$\frac{a_1}{a_2} = \frac{d_1}{d_2} \tag{S19}$$

Using the intercept theorem of elementary geometry we can derive the following relation-

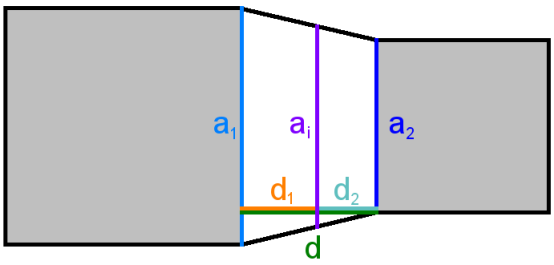

Figure S168: Cuboid model for heteromolecular interaction. View from the side on the volume of intercuboidal interaction.

ship:

$$\frac{d_1}{a_1 - a_i} = \frac{d_2}{a_i - a_2} \tag{S20}$$

Minor rearrangement leads to the following equation:

$$\frac{d_1}{d_2} = \frac{a_1 - a_i}{a_i - a_2} \tag{S21}$$

Combining equations S19 and S21 leads to:

$$\frac{a_1}{a_2} = \frac{a_1 - a_i}{a_i - a_2} \tag{S22}$$

Solving equation S22 for a_i yields:

$$a_1 a_i - a_1 a_2 = a_1 a_2 - a_2 a_i \tag{S23}$$

$$a_i(a_1 + a_2) = 2a_1 a_2 \tag{S24}$$

$$a_i = \frac{2a_1 a_2}{a_1 + a_2} \tag{S25}$$

Using equation S25, a_i can be estimated from both a_1 and a_2. Assuming that a_i corre-

sponds approximately to the slope of the interaction surface in heteromolecular complexes of **H** and **F** with respect n, it can be estimated how close to ideal the interaction geometries in the heteromolecular complexes are. The application of this model has been shown in the Supplementary Results and Discussion section.

4 Computational Raw Data

In this section, all the computational results are provided in tables and the corresponding contents are explained briefly. In addition to the abbrevations used in the main text, we used abbrevations to refer to monomers at the dimer geometry. **Hx1** refers to the **H** molecule in either **HH1** or **HF1** at the dimer geometry, **xF2** refers to the **F** molecule in either **HF2** or **FF2** at the dimer geometry. Analogous rules apply for all the additional abbreviations used. In the following tables, the corresponding dimer is always preceded by the respective monomers at the dimer geometries.

4.1 Benchmarking

The following tables provide the computational raw data for the benchmarking performed. E refers to the electronic energy, BAE refers to bond association energy, BIE refers to bond interaction energy and E-def refers to the deformation energy.

	DSD-PBEP86/def2-QZVP				B97D3/def2-QZVP			
	E [Ha]	BAE [kcal mol^{-1}]	BIE [kcal mol^{-1}]	E-def [kcal mol^{-1}]	E [Ha]	BAE [kcal mol^{-1}]	BIE [kcal mol^{-1}]	E-def [kcal mol^{-1}]
Methanes								
H	-40.45340156171				-40.45340156171			
F	-437.174440690947				-437.174440690947			
Hx1	-40.45330228048				-40.45330228048			
xH1	-40.453285931633				-40.453285931633			
HH1	-80.907464827431	-0.415	-0.55	0.135	-80.907464827431	-0.415	-0.55	0.135
Hx2	-40.453236937567				-40.453236937567			
xH2	-40.45321606935				-40.45321606935			
HH2	-80.907158820144	-0.223	-0.443	0.22	-80.907158820144	-0.223	-0.443	0.22
Hx1	-40.453289294462				-40.453289294462			
xF1	-437.174380258028				-437.174380258028			
HF1	-477.62881556709	-0.611	-0.719	0.108	-477.62881556709	-0.611	-0.719	0.108
Hx2	-40.45340085228				-40.45340085228			
xF2	-437.174418523656				-437.174418523656			
HF2	-477.628405703825	-0.354	-0.368	0.014	-477.628405703825	-0.354	-0.368	0.014
Fx1	-437.174376111767				-437.174376111767			
xF1	-437.17436253555				-437.17436253555			
FF1	-874.349672274866	-0.496	-0.586	0.09	-874.349672274866	-0.496	-0.586	0.09
Fx2	-437.174366684698				-437.174366684698			
xF2	-437.174299461049				-437.174299461049			
FF2	-874.349608232686	-0.456	-0.591	0.135	-874.349608232686	-0.456	-0.591	0.135
Ethanes								
H	-79.707934123378				-79.707934123378			
F	-674.775073674995				-674.775073674995			
Hx1	-79.70770580573				-79.70770580573			
xH1	-79.70758322253				-79.70758322253			
HH1	-159.417497446015	-1.022	-1.386	0.363	-159.417497446015	-1.022	-1.386	0.363
Hx2	-79.707788275836				-79.707788275836			
xH2	-79.70780953927				-79.70780953927			
HH2	-159.417461471667	-1	-1.169	0.17	-159.417461471667	-1	-1.169	0.17
Hx1	-79.707701164699				-79.707701164699			
xF1	-674.774994438047				-674.774994438047			
HF1	-754.484186500296	-0.74	-0.936	0.196	-754.484186500296	-0.74	-0.936	0.196
Hx2	-79.707783090038				-79.707783090038			
xF2	-674.774709820781				-674.774709820781			
HF2	-754.484272866279	-0.794	-1.117	0.323	-754.484272866279	-0.794	-1.117	0.323
Hx3	-79.707711996956				-79.707711996956			
xF3	-674.775069266901				-674.775069266901			
HF3	-754.484063454228	-0.662	-0.805	0.142	-754.484063454228	-0.662	-0.805	0.142
Hx4	-79.707931884504				-79.707931884504			
xF4	-674.77499362067				-674.77499362067			
HF4	-754.484545931517	-0.965	-1.017	0.052	-754.484545931517	-0.965	-1.017	0.052
Fx1	-674.774912767867				-674.774912767867			
xF1	-674.775027363192				-674.775027363192			
FF1	-1349.551441293	-0.812	-0.942	0.13	-1349.551441293	-0.812	-0.942	0.13
Fx2	-674.774988794396				-674.774988794396			
xF2	-674.775009188958				-674.775009188958			
FF2	-1349.55119211352	-0.656	-0.749	0.094	-1349.55119211352	-0.656	-0.749	0.094

	DSD-PBEP86/def2-QZVP				B97D3/def2-QZVP			
	E [Ha]	BAE [kcal mol^{-1}]	BIE [kcal mol^{-1}]	E-def [kcal mol^{-1}]	E [Ha]	BAE [kcal mol^{-1}]	BIE [kcal mol^{-1}]	E-def [kcal mol^{-1}]
Propanes								
H	-118.9654774391				-119.122414400952			
F	-912.375873583156				-913.046964940022			
Hx1	-118.965379676288				-119.122421422984			
xH1	-118.965377856626				-119.122421602204			
HH1	-237.934072723275	-1.956	-2.080	0.124	-238.248439969699	-2.266	-2.257	-0.009
Hx2	-118.965384882435				-119.122432551183			
xH2	-118.965388558935				-119.122421030765			
HH2	-237.932811029255	-1.165	-1.279	0.114	-238.247148535681	-1.456	-1.440	-0.016
Hx1	-118.965463991994				-119.122402248926			
xF1	-912.375583166442				-913.04688980176			
HF1	-1031.34352492383	-1.364	-1.555	0.191	-1032.17109756073	-1.078	-1.133	0.055
Hx2	-118.965640771484				-119.122412395297			
xF2	-912.375407423381				-913.04699042111			
HF2	-1031.3430212738	-1.048	-1.238	0.190	-1032.17088793157	-0.947	-0.932	-0.015
Hx3	-118.965503780129				-119.122432528751			
xF3	-912.375580479297				-913.046978971916			
HF3	-1031.34301200984	-1.042	-1.210	0.167	-1032.17111678507	-1.090	-1.070	-0.020
Hx4	-118.965583327392				-119.122405207464			
xF4	-912.375365777955				-913.046941763001			
HF4	-1031.34288682525	-0.964	-1.216	0.252	-1032.17046407035	-0.681	-0.701	0.020
Fx1	-912.375534725034				-913.046697884011			
xF1	-912.375592306062				-913.046845007231			
FF1	-1824.75336996114	-1.018	-1.407	0.389	-1826.09418060133	-0.157	-0.400	0.243
Fx2	-912.375833319941				-913.0469586885			
xF2	-912.375818181067				-913.04695662918			
FF2	-1824.75409611851	-1.474	-1.534	0.060	-1826.09402560567	-0.060	-0.069	0.009
Butanes								
H	-158.223459069769				-158.427561314396			
F	-1149.97602431515				-1150.8224663123			
Hx1	-158.223116062729				-158.42755830191			
xH1	-158.223173998622				-158.427569097518			
HH1	-316.451027070645	-2.578	-2.973	0.394	-316.860269979008	-3.230	-3.227	-0.003
Hx2	-158.223101087948				-158.427551787638			
xH2	-158.223116907561				-158.427574181297			
HH2	-316.449006884695	-1.311	-1.750	0.439	-316.858282598001	-1.983	-1.981	-0.002
Hx1	-158.223390696939				-158.427561201376			
xF1	-1149.97568757908				-1150.82248685748			
HF1	-1308.20227841443	-1.754	-2.008	0.254	-1309.25247799235	-1.538	-1.525	-0.013
Hx2	-158.223435367015				-158.42754573836			
xF2	-1149.97598112465				-1150.82252645239			
HF2	-1308.20255606827	-1.928	-1.970	0.042	-1309.25232596798	-1.442	-1.414	-0.028
Hx3	-158.223328472696				-158.427517788679			
xF3	-1149.97591924557				-1150.82258830489			
HF3	-1308.20242964852	-1.849	-1.997	0.148	-1309.25210539396	-1.304	-1.255	-0.049
Hx4	-158.22332087725				-158.427513693935			
xF4	-1149.97605430886				-1150.82252023264			
HF4	-1308.20254264709	-1.920	-1.988	0.068	-1309.2524059484	-1.492	-1.488	-0.004
Fx1	-1149.97602564114				-1150.82251030736			
xF1	-1149.97596481922				-1150.82242178566			
FF1	-2299.9547418453	-1.690	-1.727	0.037	-2301.64654471567	-1.012	-1.012	0.000
Fx2	-1149.97593439025				-1150.82260514959			
xF2	-1149.97592921202				-1150.8225410968			
FF2	-2299.95485520245	-1.761	-1.877	0.116	-2301.64627839915	-0.844	-0.710	-0.134

	DSD-PBEP86/def2-QZVP				B97D3/def2-QZVP			
	E [Ha]	BAE [kcal mol^{-1}]	BIE [kcal mol^{-1}]	E-def [kcal mol^{-1}]	E [Ha]	BAE [kcal mol^{-1}]	BIE [kcal mol^{-1}]	E-def [kcal mol^{-1}]
Pentanes								
H	-197.481196827152				-197.732670441897			
F	-1387.57653321274				-1388.59812906709			
Hx1	-197.48084504907				-197.732653420579			
xH1	-197.480842571138				-197.732653309355			
HH1	-394.967838590586	-3.417	-3.860	0.443	-395.471991778568	-4.173	-4.195	0.021
Hx2	-197.480766159988				-197.732681313157			
xH2	-197.480773210228				-197.732681237827			
HH2	-394.96525551959	-1.796	-2.332	0.536	-395.469408219742	-2.552	-2.539	-0.014
Hx1	-197.48102673258				-197.732566918995			
xF1	-1387.57639097769				-1388.59823044576			
HF1	-1585.06157430192	-2.412	-2.608	0.196	-1586.33376971721	-1.864	-1.865	0.001
Hx2	-197.481153673457				-197.732635773032			
xF2	-1387.57613843331				-1388.59797138019			
HF2	-1585.06106681064	-2.094	-2.369	0.275	-1586.33356768505	-1.737	-1.858	0.121
Hx3	-197.481031793051				-197.732648518033			
xF3	-1387.57641977966				-1388.59831798437			
HF3	-1585.06118575447	-2.168	-2.343	0.175	-1586.33360756567	-1.762	-1.657	-0.105
Hx4	-197.48109400322				-197.732632167301			
xF4	-1387.57654488909				-1388.59823416254			
HF4	-1585.06194506742	-2.645	-2.702	0.057	-1586.3339052928	-1.949	-1.907	-0.042
Fx1	-1387.57643673039				-1388.59813354821			
xF1	-1387.57640690226				-1388.59820175132			
FF1	-2775.15676607437	-2.322	-2.461	0.140	-2777.19769201507	-0.900	-0.851	-0.048
Fx2	-1387.5764108988				-1388.59810632768			
xF2	-1387.57641498716				-1388.59811001759			
FF2	-2775.15644650798	-2.121	-2.272	0.151	-2777.19778724243	-0.960	-0.986	0.026
Hexanes								
H	-236.738918710099				-237.037787409713			
F	-1625.17699658677				-1626.37391599793			
Hx1	-236.738537546223				-237.037763704464			
xH1	-236.73854118593				-237.037763465984			
HH1	-473.484100704068	-3.930	-4.406	0.476	-474.083371389092	-4.892	-4.922	0.030
Hx2	-236.738444547433				-237.037801583698			
xH2	-236.73842660549				-237.037801435229			
HH2	-473.481152583191	-2.080	-2.687	0.606	-474.080606193581	-3.157	-3.140	-0.018
Hx1	-236.738619938236				-237.037598539951			
xF1	-1625.17631682686				-1626.373687184			
HF1	-1861.91974242161	-2.402	-3.016	0.614	-1863.41438394275	-1.682	-1.944	0.262
Hx2	-236.738827977027				-237.037692122121			
xF2	-1625.17650739874				-1626.37373561144			
HF2	-1861.92002226058	-2.577	-2.941	0.364	-1863.4150261913	-2.085	-2.258	0.173
Hx3	-236.738635432864				-237.037659748394			
xF3	-1625.17659352015				-1626.37365800472			
HF3	-1861.91988138564	-2.489	-2.919	0.431	-1863.41456568502	-1.796	-2.038	0.242
Hx4	-236.73889737329				-237.037778039017			
xF4	-1625.17695873229				-1626.37392881256			
HF4	-1861.92063080005	-2.959	-2.996	0.037	-1863.41531372376	-2.266	-2.263	-0.002
Fx1	-1625.17690990042				-1626.37384278893			
xF1	-1625.17682451672				-1626.37384287734			
FF1	-3250.35887153017	-3.061	-3.224	0.162	-3252.74909255155	-0.791	-0.883	0.092
Fx2	-1625.17684427736				-1626.37360981283			
xF2	-1625.17684445309				-1626.37361437007			
FF2	-3250.35718730193	-2.004	-2.195	0.191	-3252.74774948449	0.052	-0.330	0.381

	BLYP-D3/def2-QZVP				BLYP-XDM/aug-cc-pVTZ			
	E [Ha]	BAE [kcal mol^{-1}]	BIE [kcal mol^{-1}]	E-def [kcal mol^{-1}]	E [Ha]	BAE [kcal mol^{-1}]	BIE [kcal mol^{-1}]	E-def [kcal mol^{-1}]
Methanes								
H	-40.507666231781				-40.50408117046			
F	-437.680273179664				-437.6410851716			
Hx1	-40.507663793825				-40.50407877668			
xH1	-40.507663886296				-40.50407868563			
HH1	-81.015929112992	-0.374	-0.377	0.003	-81.00886638346	-0.442	-0.445	0.003
Hx2	-40.50766597435				-40.50408190086			
xH2	-40.507665958799				-40.50408235675			
HH2	-81.015789170723	-0.287	-0.287	0.000	-81.00864152956	-0.301	-0.299	-0.001
Hx1	-40.507665604689				-40.5040816505			
xF1	-437.680354043638				-437.6411710577			
HF1	-478.188747279681	-0.507	-0.457	-0.050	-478.1463467596	-0.741	-0.687	-0.054
Hx2	-40.507664068776				-40.50407954161			
xF2	-437.680330454236				-437.6411447594			
HF2	-478.188337704603	-0.250	-0.215	-0.035	-478.1457650304	-0.376	-0.339	-0.036
Fx1	-437.680320096013				-437.641134048			
xF1	-437.680326661296				-437.641141319			
FF1	-875.361278746623	-0.460	-0.397	-0.063	-875.2832595794	-0.684	-0.618	-0.066
Fx2	-437.680335021164				-437.6411522329			
xF2	-437.680326358207				-437.6411422			
FF2	-875.361199598805	-0.410	-0.338	-0.072	-875.2832100158	-0.652	-0.575	-0.078
Ethanes								
H	-79.815156616873				-79.80889741932			
F	-675.564112602858				-675.5041374099			
Hx1	-79.815162341258				-79.80889965725			
xH1	-79.815163018095				-79.80890186263			
HH1	-159.632203093962	-1.186	-1.178	-0.008	-159.6199030076	-1.323	-1.319	-0.004
Hx2	-79.815158838352				-79.80889916564			
xH2	-79.815159006277				-79.80889969434			
HH2	-159.631993953908	-1.055	-1.052	-0.003	-159.6195886958	-1.126	-1.123	-0.003
Hx1	-79.815152287801				-79.80888922865			
xF1	-675.564262678841				-675.5042854962			
HF1	-755.380463708674	-0.750	-0.658	-0.091	-755.3146480048	-1.012	-0.924	-0.088
Hx2	-79.815154087394				-79.80889036107			
xF2	-675.564294035234				-675.5043481975			
HF2	-755.380730899065	-0.917	-0.805	-0.112	-755.3149848408	-1.224	-1.096	-0.128
Hx3	-79.815154450476				-79.80889115451			
xF3	-675.564252803315				-675.5042672149			
HF3	-755.380298349712	-0.646	-0.559	-0.087	-755.3144115428	-0.864	-0.786	-0.078
Hx4	-79.815153948316				-79.80888878577			
xF4	-675.564202388235				-675.5042288107			
HF4	-755.380531315403	-0.792	-0.737	-0.055	-755.3147866407	-1.099	-1.047	-0.052
Fx1	-675.564189783414				-675.5042101185			
xF1	-675.564154778769				-675.5041725866			
FF1	-1351.12925010851	-0.643	-0.568	-0.075	-1351.009942449	-1.046	-0.979	-0.068
Fx2	-675.564291496695				-675.504318521			
xF2	-675.564181338857				-675.5041993049			
FF2	-1351.1292612544	-0.650	-0.495	-0.155	-1351.009797189	-0.955	-0.803	-0.152

	BLYP-D3/def2-QZVP				BLYP-XDM/aug-cc-pVTZ			
	E [Ha]	BAE [kcal mol^{-1}]	BIE [kcal mol^{-1}]	E-def [kcal mol^{-1}]	E [Ha]	BAE [kcal mol^{-1}]	BIE [kcal mol^{-1}]	E-def [kcal mol^{-1}]
Propanes								
H	-119.125618426848				-119.1166834021			
F	-913.446564564769				-913.365986134			
Hx1	-119.125627103176				-119.1166912458			
xH1	-119.125627538997				-119.1166921312			
HH1	-238.254424509273	-2.000	-1.989	-0.011	-238.2368344256	-2.176	-2.166	-0.010
Hx2	-119.125645006767				-119.116707429			
xH2	-119.125622640156				-119.1166834927			
HH2	-238.253003046856	-1.108	-1.089	-0.019	-238.2351615894	-1.126	-1.111	-0.015
Hx1	-119.125602589088				-119.1166668358			
xF1	-913.446550638558				-913.3659887147			
HF1	-1032.5740183928	-1.152	-1.170	0.019	-1032.485205206	-1.591	-1.600	0.009
Hx2	-119.125616379723				-119.1166820355			
xF2	-913.446663601517				-913.3661207528			
HF2	-1032.57375782922	-0.988	-0.927	-0.061	-1032.484858136	-1.373	-1.290	-0.084
Hx3	-119.125646375114				-119.1167186599			
xF3	-913.446657677995				-913.3661003844			
HF3	-1032.57382843001	-1.033	-0.957	-0.076	-1032.484740837	-1.300	-1.206	-0.094
Hx4	-119.125607920419				-119.1166719854			
xF4	-913.446620964252				-913.3660937807			
HF4	-1032.57354083488	-0.852	-0.823	-0.029	-1032.484726896	-1.291	-1.231	-0.060
Fx1	-913.446292609158				-913.3657165162			
xF1	-913.446456657543				-913.3659003131			
FF1	-1826.89399714866	-0.545	-0.783	0.238	-1826.733914083	-1.219	-1.442	0.223
Fx2	-913.446557634289				-913.3659802527			
xF2	-913.446553569967				-913.3659759849			
FF2	-1826.89424203296	-0.698	-0.710	0.011	-1826.734432243	-1.544	-1.554	0.010
Butanes								
H	-158.436115915613				-158.4243687149			
F	-1151.32811369802				-1151.227134462			
Hx1	-158.436111588814				-158.4243689258			
xH1	-158.43612380173				-158.4243712635			
HH1	-316.87685861193	-2.903	-2.901	-0.002	-316.8537749143	-3.161	-3.159	-0.002
Hx2	-158.436103500595				-158.4243560167			
xH2	-158.436132747508				-158.4243833382			
HH2	-316.874707176155	-1.553	-1.551	-0.003	-316.8512993621	-1.608	-1.606	-0.001
Hx1	-158.43611873873				-158.4243708947			
xF1	-1151.32822958988				-1151.227208538			
HF1	-1309.767022718	-1.753	-1.678	-0.074	-1309.655076815	-2.242	-2.195	-0.048
Hx2	-158.436103097384				-158.4243552504			
xF2	-1151.32818601543				-1151.227193342			
HF2	-1309.76678996666	-1.607	-1.569	-0.037	-1309.654930862	-2.151	-2.122	-0.028
Hx3	-158.4360622433				-158.4243063835			
xF3	-1151.32824295549				-1151.227238587			
HF3	-1309.76670931223	-1.556	-1.509	-0.047	-1309.654970275	-2.176	-2.149	-0.026
Hx4	-158.436064924797				-158.4243135422			
xF4	-1151.32816625779				-1151.227171408			
HF4	-1309.7667372783	-1.574	-1.573	-0.001	-1309.654885856	-2.123	-2.134	0.011
Fx1	-1151.32812852056				-1151.227125241			
xF1	-1151.32812130777				-1151.227165941			
FF1	-2302.65820751612	-1.243	-1.228	-0.014	-2302.457352433	-1.935	-1.921	-0.014
Fx2	-1151.32828113473				-1151.227264197			
xF2	-1151.32822586146				-1151.227214535			
FF2	-2302.65831427216	-1.310	-1.134	-0.175	-2302.457714031	-2.162	-2.030	-0.132

	BLYP-D3/def2-QZVP				BLYP-XDM/aug-cc-pVTZ			
	E [Ha]	BAE [kcal mol^{-1}]	BIE [kcal mol^{-1}]	E-def [kcal mol^{-1}]	E [Ha]	BAE [kcal mol^{-1}]	BIE [kcal mol^{-1}]	E-def [kcal mol^{-1}]
Pentanes								
H	-197.445522623464				-197.57021659243			
F	-1388.22912666694				-1388.00768686124			
Hx1	-197.445500380936				-197.570199738717			
xH1	-197.445500224481				-197.570199641368			
HH1	-394.896884801564	-3.664	-3.692	0.028	-395.146708964698	-3.938	-3.959	0.021
Hx2	-197.445536493822				-197.570225693725			
xH2	-197.44553642235				-197.570225603214			
HH2	-394.894059851211	-1.892	-1.874	-0.017	-395.144494463869	-2.548	-2.537	-0.011
Hx1	-197.44542411314				-197.57010880511			
xF1	-1388.22915542896				-1388.00771916376			
HF1	-1585.68016328151	-3.460	-3.504	0.044	-1585.58191489409	-2.517	-2.565	0.047
Hx2	-197.445491204696				-197.570178336334			
xF2	-1388.22894038678				-1388.00749476257			
HF2	-1585.67945047163	-3.013	-3.149	0.137	-1585.58155331671	-2.290	-2.435	0.145
Hx3	-197.445487208859				-197.570185351125			
xF3	-1388.2292550995				-1388.00782045027			
HF3	-1585.6797459737	-3.198	-3.140	-0.058	-1585.58168345636	-2.372	-2.308	-0.064
Hx4	-197.445476716655				-197.57016950943			
xF4	-1388.22919705012				-1388.00775596823			
HF4	-1585.68047047778	-3.653	-3.637	-0.015	-1585.58219783442	-2.695	-2.681	-0.014
Fx1	-1388.22912719251				-1388.00767315185			
xF1	-1388.2291652788				-1388.00771565856			
FF1	-2776.46517364352	-4.343	-4.318	-0.025	-2776.01869143357	-2.082	-2.072	-0.009
Fx2	-1388.22905185176				-1388.00764289579			
xF2	-1388.22905941403				-1388.00764784066			
FF2	-2776.46428185928	-3.783	-3.872	0.089	-2776.01853050655	-1.981	-2.033	0.052
Hexanes								
H	-236.699295041123				-236.846336404762			
F	-1625.94218900133				-1625.68361908786			
Hx1	-236.699265179933				-236.846316725267			
xH1	-236.699264784254				-236.846316384078			
HH1	-473.405643134184	-4.426	-4.464	0.038	-473.699986719555	-4.590	-4.614	0.025
Hx2	-236.699308990341				-236.846346638323			
xH2	-236.699308885483				-236.846346514905			
HH2	-473.402553715556	-2.487	-2.470	-0.017	-473.697531634804	-3.049	-3.036	-0.013
Hx1	-236.699089660894				-236.846138988141			
xF1	-1625.94185271133				-1625.68330656475			
HF1	-1862.64774318473	-3.928	-4.268	0.340	-1862.53404066957	-2.563	-2.883	0.320
Hx2	-236.699196616116				-236.84624436968			
xF2	-1625.94194449193				-1625.68338448685			
HF2	-1862.64751687209	-3.786	-4.001	0.215	-1862.53440114756	-2.790	-2.995	0.205
Hx3	-236.699177057735				-236.846202507192			
xF3	-1625.94191343566				-1625.68335515976			
HF3	-1862.64771262641	-3.908	-4.155	0.247	-1862.53421875789	-2.675	-2.925	0.250
Hx4	-236.699286156833				-236.846318193451			
xF4	-1625.94218207656				-1625.68360831792			
HF4	-1862.64808895805	-4.145	-4.155	0.010	-1862.53480090783	-3.041	-3.059	0.018
Fx1	-1625.94210998791				-1625.68353590655			
xF1	-1625.94211897862				-1625.68355150013			
FF1	-3251.89344391726	-5.689	-5.782	0.094	-3251.37108429254	-2.413	-2.508	0.095
Fx2	-1625.94197145041				-1625.68339492751			
xF2	-1625.94197372558				-1625.68339760666			
FF2	-3251.89053102413	-3.861	-4.133	0.272	-3251.36963231621	-1.502	-1.782	0.280

	BLYP-NL/def2-QZVP				PBE-D3/def2-QZVP			
	E [Ha]	BAE [kcal mol^{-1}]	BIE [kcal mol^{-1}]	E-def [kcal mol^{-1}]	E [Ha]	BAE [kcal mol^{-1}]	BIE [kcal mol^{-1}]	E-def [kcal mol^{-1}]
Methanes								
H	-40.433704361338				-40.468623686438			
F	-437.375877997406				-437.301896329176			
Hx1	-40.43370239369				-40.468620808704			
xH1	-40.433702316336				-40.468620904186			
HH1	-80.867774570902	-0.230	-0.232	0.003	-80.938353180285	-0.694	-0.697	0.004
Hx2	-40.433703893428				-40.468623342435			
xH2	-40.433703649388				-40.468623349292			
HH2	-80.8676809263	-0.171	-0.172	0.001	-80.938198496086	-0.597	-0.597	0.000
Hx1	-40.433704613238				-40.468622899117			
xF1	-437.375949360451				-437.301950949965			
HF1	-477.810725967763	-0.718	-0.673	-0.045	-477.771926223092	-0.882	-0.849	-0.034
Hx2	-40.433702074606				-40.468621198987			
xF2	-437.375928651571				-437.301935300114			
HF2	-477.810209906563	-0.394	-0.363	-0.030	-477.771434722621	-0.574	-0.551	-0.023
Fx1	-437.375918634265				-437.301924589287			
xF1	-437.375926270295				-437.301934202071			
FF1	-874.7533666248	-1.011	-0.955	-0.056	-874.605151852988	-0.853	-0.811	-0.041
Fx2	-437.375933951719				-437.301940042731			
xF2	-437.375927525666				-437.301933667468			
FF2	-874.753349886422	-1.000	-0.934	-0.066	-874.604968104437	-0.738	-0.687	-0.051
Ethanes								
H	-79.684223508866				-79.7417710803			
F	-675.090003134662				-674.979472457831			
Hx1	-79.684231747825				-79.741779422275			
xH1	-79.684227308279				-79.741779217914			
HH1	-159.370019547555	-0.987	-0.979	-0.008	-159.485940254543	-1.505	-1.494	-0.010
Hx2	-79.684225243405				-79.741777772561			
xH2	-79.684225849981				-79.741777983379			
HH2	-159.369803890498	-0.851	-0.849	-0.003	-159.485766956578	-1.396	-1.388	-0.009
Hx1	-79.68421724922				-79.741767618115			
xF1	-675.090129486775				-674.979579223335			
HF1	-754.776058014443	-1.149	-1.074	-0.075	-754.723054213834	-1.136	-1.071	-0.065
Hx2	-79.684221309085				-79.741769849808			
xF2	-675.090177897775				-674.979609886189			
HF2	-754.776442739331	-1.391	-1.282	-0.108	-754.723344923298	-1.319	-1.233	-0.085
Hx3	-79.684219224531				-79.741770127112			
xF3	-675.090114248897				-674.979570389162			
HF3	-754.775792444717	-0.983	-0.916	-0.067	-754.722857752047	-1.013	-0.952	-0.061
Hx4	-79.684222548284				-79.741767240933			
xF4	-675.090077904307				-674.979542830408			
HF4	-754.776219880308	-1.251	-1.204	-0.046	-754.723153773823	-1.199	-1.157	-0.042
Fx1	-675.09008029082				-674.979524491432			
xF1	-675.090045036977				-674.979494959116			
FF1	-1350.18266065928	-1.666	-1.591	-0.075	-1349.96060986308	-1.045	-0.998	-0.047
Fx2	-675.090151396854				-674.979598011236			
xF2	-675.090059544163				-674.979525454922			
FF2	-1350.18221849205	-1.388	-1.260	-0.128	-1349.9605408618	-1.001	-0.889	-0.112

	BLYP-NL/def2-QZVP				PBE-D3/def2-QZVP			
	E [Ha]	BAE [kcal mol^{-1}]	BIE [kcal mol^{-1}]	E-def [kcal mol^{-1}]	E [Ha]	BAE [kcal mol^{-1}]	BIE [kcal mol^{-1}]	E-def [kcal mol^{-1}]
Propanes								
H	-118.937964398449				-119.0179306436			
F	-912.803367592912				-912.656089243053			
Hx1	-118.937973621097				-119.017937008877			
xH1	-118.937973526147				-119.017936890239			
HH1	-237.878782195759	-1.791	-1.779	-0.012	-238.039446723487	-2.250	-2.242	-0.008
Hx2	-118.93798960294				-119.017945348766			
xH2	-118.937971327401				-119.017936616299			
HH2	-237.877471248851	-0.968	-0.948	-0.020	-238.03818755883	-1.460	-1.447	-0.013
Hx1	-118.937949662138				-119.017917311258			
xF1	-912.803374073348				-912.656065869378			
HF1	-1031.74434606743	-1.891	-1.897	0.005	-1031.67655924824	-1.593	-1.617	0.023
Hx2	-118.937965036793				-119.017929374897			
xF2	-912.803492943316				-912.656157661562			
HF2	-1031.74388838031	-1.604	-1.525	-0.079	-1031.67623821865	-1.392	-1.350	-0.042
Hx3	-118.938000364735				-119.017960554628			
xF3	-912.8034622063				-912.656149631115			
HF3	-1031.74381371527	-1.557	-1.475	-0.082	-1031.67634746339	-1.461	-1.404	-0.057
Hx4	-118.937953983659				-119.017915606786			
xF4	-912.803464449168				-912.656130860455			
HF4	-1031.74386142261	-1.587	-1.533	-0.054	-1031.67606736184	-1.285	-1.268	-0.017
Fx1	-912.803125555602				-912.655866762547			
xF1	-912.803281832585				-912.656007062583			
FF1	-1825.61014285935	-2.138	-2.344	0.206	-1825.31388866106	-1.073	-1.264	0.191
Fx2	-912.80336131173				-912.656083826031			
xF2	-912.803356795842				-912.656081341146			
FF2	-1825.61098804215	-2.669	-2.679	0.011	-1825.31412272449	-1.220	-1.228	0.008
Butanes								
H	-158.191753745149				-158.294103788252			
F	-1150.5161489168				-1150.33182471274			
Hx1	-158.191749045443				-158.294102252034			
xH1	-158.191767521511				-158.294108591526			
HH1	-316.387843615443	-2.721	-2.715	-0.006	-316.593129784883	-3.089	-3.087	-0.002
Hx2	-158.191748874118				-158.294094121973			
xH2	-158.191772853829				-158.294113582637			
HH2	-316.385782429455	-1.428	-1.419	-0.009	-316.591327043135	-1.957	-1.957	0.000
Hx1	-158.19176013785				-158.294099492185			
xF1	-1150.51608945163				-1150.33180376386			
HF1	-1308.71212141691	-2.647	-2.681	0.033	-1308.62929373477	-2.112	-2.128	0.016
Hx2	-158.19173724032				-158.294082741885			
xF2	-1150.51617953716				-1150.33186209905			
HF2	-1308.71215188482	-2.666	-2.658	-0.009	-1308.6291995376	-2.053	-2.042	-0.010
Hx3	-158.191700094947				-158.29405097961			
xF3	-1150.5161873807				-1150.33188837845			
HF3	-1308.71210370547	-2.636	-2.646	0.010	-1308.62901678959	-1.938	-1.931	-0.007
Hx4	-158.191707327736				-158.294055257055			
xF4	-1150.51618299674				-1150.3318529682			
HF4	-1308.71198142107	-2.559	-2.567	0.008	-1308.62917291173	-2.036	-2.049	0.013
Fx1	-1150.51609225676				-1150.33182013943			
xF1	-1150.51615388232				-1150.33181697288			
FF1	-2301.03681570544	-2.835	-2.867	0.032	-2300.66634028935	-1.689	-1.696	0.008
Fx2	-1150.51620020772				-1150.33189325135			
xF2	-1150.51618824372				-1150.33185347854			
FF2	-2301.03752343686	-3.279	-3.222	-0.057	-2300.66637367249	-1.709	-1.648	-0.061

	BLYP-NL/def2-QZVP				PBE-D3/def2-QZVP			
	E [Ha]	BAE [kcal mol^{-1}]	BIE [kcal mol^{-1}]	E-def [kcal mol^{-1}]	E [Ha]	BAE [kcal mol^{-1}]	BIE [kcal mol^{-1}]	E-def [kcal mol^{-1}]
Pentanes								
H	-197.445522623464				-197.57021659243			
F	-1388.22912666694				-1388.00768686124			
Hx1	-197.445500380936				-197.570199738717			
xH1	-197.445500224481				-197.570199641368			
HH1	-394.896884801564	-3.664	-3.692	0.028	-395.146708964698	-3.938	-3.959	0.021
Hx2	-197.445536493822				-197.570225693725			
xH2	-197.44553642235				-197.570225603214			
HH2	-394.894059851211	-1.892	-1.874	-0.017	-395.144494463869	-2.548	-2.537	-0.011
Hx1	-197.44542411314				-197.57010880511			
xF1	-1388.22915542896				-1388.00771916376			
HF1	-1585.68016328151	-3.460	-3.504	0.044	-1585.58191489409	-2.517	-2.565	0.047
Hx2	-197.445491204696				-197.570178336334			
xF2	-1388.22894038678				-1388.00749476257			
HF2	-1585.67945047163	-3.013	-3.149	0.137	-1585.58155331671	-2.290	-2.435	0.145
Hx3	-197.445487208859				-197.570185351125			
xF3	-1388.2292550995				-1388.00782045027			
HF3	-1585.6797459737	-3.198	-3.140	-0.058	-1585.58168345636	-2.372	-2.308	-0.064
Hx4	-197.445476716655				-197.57016950943			
xF4	-1388.22919705012				-1388.00775596823			
HF4	-1585.68047047778	-3.653	-3.637	-0.015	-1585.58219783442	-2.695	-2.681	-0.014
Fx1	-1388.22912719251				-1388.00767315185			
xF1	-1388.2291652788				-1388.00771565856			
FF1	-2776.46517364352	-4.343	-4.318	-0.025	-2776.01869143357	-2.082	-2.072	-0.009
Fx2	-1388.22905185176				-1388.00764289579			
xF2	-1388.22905941403				-1388.00764784066			
FF2	-2776.46428185928	-3.783	-3.872	0.089	-2776.01853050655	-1.981	-2.033	0.052
Hexanes								
H	-236.699295041123				-236.846336404762			
F	-1625.94218900133				-1625.68361908786			
Hx1	-236.699265179933				-236.846316725267			
xH1	-236.699264784254				-236.846316384078			
HH1	-473.405643134184	-4.426	-4.464	0.038	-473.699986719555	-4.590	-4.614	0.025
Hx2	-236.699308990341				-236.846346638323			
xH2	-236.699308885483				-236.846346514905			
HH2	-473.402553715556	-2.487	-2.470	-0.017	-473.697531634804	-3.049	-3.036	-0.013
Hx1	-236.699089660894				-236.846138988141			
xF1	-1625.94185271133				-1625.68330656475			
HF1	-1862.64774318473	-3.928	-4.268	0.340	-1862.53404066957	-2.563	-2.883	0.320
Hx2	-236.699196616116				-236.84624436968			
xF2	-1625.94194449193				-1625.68338448685			
HF2	-1862.64751687209	-3.786	-4.001	0.215	-1862.53440114756	-2.790	-2.995	0.205
Hx3	-236.699177057735				-236.846202507192			
xF3	-1625.94191343566				-1625.68335515976			
HF3	-1862.64771262641	-3.908	-4.155	0.247	-1862.53421875789	-2.675	-2.925	0.250
Hx4	-236.699286156833				-236.846318193451			
xF4	-1625.94218207656				-1625.68360831792			
HF4	-1862.64808895805	-4.145	-4.155	0.010	-1862.53480090783	-3.041	-3.059	0.018
Fx1	-1625.94210998791				-1625.68353590655			
xF1	-1625.94211897862				-1625.68355150013			
FF1	-3251.89344391726	-5.689	-5.782	0.094	-3251.37108429254	-2.413	-2.508	0.095
Fx2	-1625.94197145041				-1625.68339492751			
xF2	-1625.94197372558				-1625.68339760666			
FF2	-3251.89053102413	-3.861	-4.133	0.272	-3251.36963231621	-1.502	-1.782	0.280

	PBE-dDsC/QZ4P				PBE-XDM/aug-cc-pVTZ			
	E [Ha]	BAE [kcal mol^{-1}]	BIE [kcal mol^{-1}]	E-def [kcal mol^{-1}]	E [Ha]	BAE [kcal mol^{-1}]	BIE [kcal mol^{-1}]	E-def [kcal mol^{-1}]
Methanes								
H	-0.883839257049025				-40.46393269993			
F	-0.956055451608807				-437.2587215495			
Hx1	-0.883827775253054				-40.46392923761			
xH1	-0.883830659545519				-40.46392943039			
HH1	-1.76871316340648	-0.649	-0.662	0.013	-80.92882932944	-0.605	-0.609	0.004
Hx2	-0.883832356826416				-40.46393246336			
xH2	-0.88382980334505				-40.46393271425			
HH2	-1.76857791682207	-0.564	-0.575	0.010	-80.92871381574	-0.532	-0.533	0.000
Hx1	-0.883836412011288				-40.46393176796			
xF1	-0.956129725276525				-437.258783099			
HF1	-1.84151490521401	-1.017	-0.972	-0.045	-477.7240729407	-0.890	-0.852	-0.038
Hx2	-0.883836662738119				-40.46393013783			
xF2	-0.956133370790201				-437.2587644449			
HF2	-1.84101927097868	-0.706	-0.658	-0.047	-477.7235847436	-0.584	-0.559	-0.025
Fx1	-0.956092092491527				-437.2587550137			
xF1	-0.956094119926821				-437.2587619069			
FF1	-1.91385777454594	-1.096	-1.049	-0.047	-874.5189381449	-0.938	-0.892	-0.046
Fx2	-0.95609624362216				-437.258769224			
xF2	-0.95602509416178				-437.2587615512			
FF2	-1.91376273109257	-1.037	-1.030	-0.007	-874.5186795373	-0.776	-0.721	-0.055
Ethanes								
H	-1.49005255386608				-79.73259089238			
F	-1.58681376474656				-674.9131339434			
Hx1	-1.49008654602944				-79.73259887991			
xH1	-1.49009823624231				-79.73259832731			
HH1	-2.98292756409948	-1.771	-1.721	-0.050	-159.467230186	-1.285	-1.276	-0.010
Hx2	-1.49007356230251				-79.73259725759			
xH2	-1.49007736045316				-79.73259770695			
HH2	-2.9826034868582	-1.568	-1.539	-0.029	-159.4671164218	-1.214	-1.206	-0.008
Hx1	-1.49007795529372				-79.73258682409			
xF1	-1.58687673275345				-674.9132483746			
HF1	-3.079205506044	-1.468	-1.412	-0.055	-754.6476587458	-1.214	-1.144	-0.069
Hx2	-1.49004580754786				-79.73258841946			
xF2	-1.58690666669895				-674.9132887973			
HF2	-3.07954016480729	-1.678	-1.624	-0.054	-754.6479035879	-1.367	-1.272	-0.096
Hx3	-1.49006065006389				-79.73258886887			
xF3	-1.58685863991975				-674.9132384075			
HF3	-3.07892690451456	-1.293	-1.260	-0.033	-754.6474456455	-1.080	-1.016	-0.064
Hx4	-1.4900495194976				-79.73258457144			
xF4	-1.58683697604237				-674.9132071271			
HF4	-3.0793480387753	-1.557	-1.545	-0.013	-754.6477383198	-1.263	-1.222	-0.042
Fx1	-1.58680801477139				-674.9131870047			
xF1	-1.58677107218408				-674.9131543035			
FF1	-3.17610281557898	-1.553	-1.584	0.030	-1349.828160055	-1.187	-1.141	-0.046
Fx2	-1.58692960879544				-674.9132697437			
xF2	-1.58674990194849				-674.9131862992			
FF2	-3.17584009588139	-1.388	-1.356	-0.033	-1349.828059295	-1.124	-1.006	-0.118

	PBE-dDsC/QZ4P				PBE-XDM/aug-cc-pVTZ			
	E [Ha]	BAE [kcal mol^{-1}]	BIE [kcal mol^{-1}]	E-def [kcal mol^{-1}]	E [Ha]	BAE [kcal mol^{-1}]	BIE [kcal mol^{-1}]	E-def [kcal mol^{-1}]
Propanes								
H	-2.09975507610939				-119.00413359			
F	-2.21718363507822				-912.5664076754			
Hx1	-2.09970939794028				-119.0041425869			
xH1	-2.09971467118466				-119.0041429721			
HH1	-4.20369749236946	-2.628	-2.682	0.054	-238.0114446451	-1.994	-1.982	-0.012
Hx2	-2.09972476723893				-119.0041498969			
xH2	-2.09971601644477				-119.0041393643			
HH2	-4.20219829983119	-1.687	-1.730	0.044	-238.010345195	-1.304	-1.290	-0.014
Hx1	-2.09972870659801				-119.0041188039			
xF1	-2.21713179304622				-912.5663868836			
HF1	-4.32049165871626	-2.230	-2.279	0.049	-1031.573263688	-1.708	-1.731	0.022
Hx2	-2.09972919709301				-119.0041325896			
xF2	-2.21719940278449				-912.5664868161			
HF2	-4.31993208459369	-1.878	-1.885	0.006	-1031.572985263	-1.534	-1.485	-0.049
Hx3	-2.09978812294241				-119.0041689222			
xF3	-2.21724102296353				-912.5664751765			
HF3	-4.31996925484445	-1.902	-1.845	-0.057	-1031.57313218	-1.626	-1.561	-0.065
Hx4	-2.09966068122946				-119.0041194317			
xF4	-2.21722004243295				-912.5664582747			
HF4	-4.31988888630637	-1.851	-1.888	0.036	-1031.572828909	-1.436	-1.413	-0.023
Fx1	-2.21695164738816				-912.566183157			
xF1	-2.21713917826022				-912.5663243669			
FF1	-4.43765371921319	-2.062	-2.236	0.173	-1825.134883308	-1.298	-1.491	0.193
Fx2	-2.2171596281897				-912.5664029928			
xF2	-2.21718049196758				-912.5664005967			
FF2	-4.43826148281025	-2.444	-2.461	0.017	-1825.135184858	-1.487	-1.494	0.007
Butanes								
H	-2.70961929396179				-158.275702988			
F	-2.84708193038427				-1150.218885049			
Hx1	-2.70963410406778				-158.2757069788			
xH1	-2.70959075838609				-158.27570423			
HH1	-5.42545776374939	-3.903	-3.911	0.009	-316.5558400812	-2.782	-2.779	-0.003
Hx2	-2.70955261344846				-158.2756898051			
xH2	-2.70957196991216				-158.2757117823			
HH2	-5.42298600967028	-2.352	-2.423	0.072	-316.5542335187	-1.774	-1.777	0.003
Hx1	-2.7095540019397				-158.2756978399			
xF1	-2.84698126399749				-1150.218826054			
HF1	-5.5613175934172	-2.897	-3.001	0.104	-1308.498298315	-2.328	-2.368	0.040
Hx2	-2.70958307998382				-158.2756819432			
xF2	-2.84710998549403				-1150.21890975			
HF2	-5.56140455437863	-2.951	-2.957	0.005	-1308.498186541	-2.258	-2.256	-0.002
Hx3	-2.70954178726408				-158.2756414865			
xF3	-2.8471206574374				-1150.218925325			
HF3	-5.56152197536837	-3.025	-3.049	0.024	-1308.497954154	-2.112	-2.126	0.013
Hx4	-2.70952651159695				-158.2756502936			
xF4	-2.84707225082311				-1150.218904814			
HF4	-5.5614434094447	-2.976	-3.040	0.064	-1308.498165539	-2.245	-2.266	0.021
Fx1	-2.84702286044624				-1150.218857941			
xF1	-2.84705376190627				-1150.218875907			
FF1	-5.698487416525	-2.713	-2.768	0.055	-2300.440924977	-1.980	-2.002	0.023
Fx2	-2.84709677386872				-1150.21892819			
xF2	-2.84706551099736				-1150.21889262			
FF2	-5.69912143711902	-3.111	-3.112	0.001	-2300.441021462	-2.040	-2.008	-0.032

	PBE-dDsC/QZ4P				PBE-XDM/aug-cc-pVTZ			
	E [Ha]	BAE [kcal mol^{-1}]	BIE [kcal mol^{-1}]	E-def [kcal mol^{-1}]	E [Ha]	BAE [kcal mol^{-1}]	BIE [kcal mol^{-1}]	E-def [kcal mol^{-1}]
Pentanes								
H	-3.31940480555648				-197.5472260191			
F	-3.47714194207951				-1387.871512522			
Hx1	-3.31939806439905				-197.5472150548			
xH1	-3.31939680965446				-197.5472149286			
HH1	-6.64697608220883	-5.125	-5.134	0.009	-395.1001452695	-3.573	-3.586	0.014
Hx2	-3.31936708365482				-197.5472345331			
xH2	-3.31936971469356				-197.5472344538			
HH2	-6.64393142317421	-3.214	-3.260	0.046	-395.0980889143	-2.282	-2.272	-0.011
Hx1	-3.31923178027				-197.5471273811			
xF1	-3.47718625953986				-1387.871521025			
HF1	-6.80247613150678	-3.721	-3.802	0.081	-1585.423217183	-2.810	-2.867	0.057
Hx2	-3.31936018092275				-197.5471873085			
xF2	-3.47694171588405				-1387.871267836			
HF2	-6.80181484911669	-3.306	-3.459	0.154	-1585.422773914	-2.532	-2.710	0.178
Hx3	-3.31937575387692				-197.5471946523			
xF3	-3.47723193927879				-1387.871634834			
HF3	-6.80228465793758	-3.601	-3.562	-0.038	-1585.42287852	-2.598	-2.541	-0.057
Hx4	-3.31936222636314				-197.5471763614			
xF4	-3.47715366582953				-1387.871571467			
HF4	-6.80293938538261	-4.011	-4.031	0.019	-1585.423529689	-3.006	-3.001	-0.006
Fx1	-3.47711779787034				-1387.871498195			
xF1	-3.47715613780696				-1387.871530325			
FF1	-6.96036034423541	-3.813	-3.819	0.006	-2775.747050454	-2.526	-2.524	-0.002
Fx2	-3.4771672942031				-1387.87145405			
xF2	-3.47717461137172				-1387.871459409			
FF2	-6.96013933851824	-3.674	-3.638	-0.036	-2775.74687086	-2.413	-2.483	0.070
Hexanes								
H	-3.9292195839309				-236.8187678111			
F	-4.10746799143434				-1625.524209883			
Hx1	-3.92925110925325				-236.8187493839			
xH1	-3.92925398967885				-236.818749242			
HH1	-7.86818250932209	-6.114	-6.073	-0.041	-473.6442197439	-4.194	-4.218	0.023
Hx2	-3.92917456949484				-236.8187663229			
xH2	-3.92916923776214				-236.818766197			
HH2	-7.86466338246352	-3.906	-3.966	0.060	-473.6419155928	-2.748	-2.750	0.002
Hx1	-3.92903047433647				-236.8185697565			
xF1	-4.1069535621265				-1625.523843552			
HF1	-8.0431659763061	-4.065	-4.507	0.441	-1862.347600792	-2.901	-3.255	0.354
Hx2	-3.92915437006568				-236.8186722824			
xF2	-4.10716999495156				-1625.523932796			
HF2	-8.04317603696079	-4.072	-4.299	0.228	-1862.34796281	-3.128	-3.362	0.234
Hx3	-3.92903106095917				-236.8186386995			
xF3	-4.10717084700408				-1625.523916445			
HF3	-8.04347448264836	-4.259	-4.564	0.305	-1862.347786671	-3.018	-3.283	0.265
Hx4	-3.92918353874802				-236.8187333724			
xF4	-4.10737798606225				-1625.524187215			
HF4	-8.0439177495198	-4.537	-4.616	0.079	-1862.348382683	-3.392	-3.428	0.036
Fx1	-4.10726645637324				-1625.524132314			
xF1	-4.10721697794202				-1625.52413722			
FF1	-8.22237083026386	-4.665	-4.949	0.284	-3251.053228483	-3.018	-3.112	0.094
Fx2	-4.10720896650448				-1625.524003844			
xF2	-4.10722032565206				-1625.524005858			
FF2	-8.22031744483011	-3.377	-3.695	0.318	-3251.051648578	-2.026	-2.283	0.257

	TPSS-D3/def2-QZVP				M06L/def2-QZVP			
	E [Ha]	BAE [kcal mol^{-1}]	BIE [kcal mol^{-1}]	E-def [kcal mol^{-1}]	E [Ha]	BAE [kcal mol^{-1}]	BIE [kcal mol^{-1}]	E-def [kcal mol^{-1}]
Methanes								
H	-40.545876889156				-40.531313296368			
F	-437.741373399662				-437.638884588424			
Hx1	-40.545875208204				-40.531310430462			
xH1	-40.545875210792				-40.53131106774			
HH1	-81.092700187038	-0.594	-0.596	0.002	-81.063416060228	-0.495	-0.499	0.003
Hx2	-40.545876566182				-40.531311957368			
xH2	-40.545876519163				-40.531312292159			
HH2	-81.09253878652	-0.493	-0.493	0.000	-81.06301260005	-0.242	-0.244	0.001
Hx1	-40.545876513073				-40.531311709867			
xF1	-437.741419399716				-437.638871944456			
HF1	-478.288406784797	-0.726	-0.697	-0.029	-478.171407636663	-0.759	-0.768	0.009
Hx2	-40.545875171279				-40.531312910727			
xF2	-437.741406663173				-437.638874470425			
HF2	-478.287995815984	-0.468	-0.448	-0.020	-478.17056066646	-0.228	-0.234	0.007
Fx1	-437.741394039167				-437.63886022921			
xF1	-437.741408167293				-437.638879102913			
FF1	-875.483951384018	-0.756	-0.721	-0.035	-875.279010518116	-0.779	-0.798	0.019
Fx2	-437.741412927962				-437.638877748562			
xF2	-437.741406689847				-437.638862726542			
FF2	-875.483641211926	-0.561	-0.516	-0.046	-875.278623687304	-0.536	-0.554	0.018
Ethanes								
H	-79.883012891806				-79.854027492189			
F	-675.664573839115				-675.503338370446			
Hx1	-79.883015573347				-79.854032286033			
xH1	-79.883016462659				-79.854030519234			
HH1	-159.767932292748	-1.196	-1.192	-0.004	-159.70997177197	-1.203	-1.198	-0.005
Hx2	-79.883015127177				-79.854027399091			
xH2	-79.883015124224				-79.854026017108			
HH2	-159.767884199177	-1.166	-1.163	-0.003	-159.709714805679	-1.042	-1.043	0.001
Hx1	-79.88300848243				-79.85402710114			
xF1	-675.664677033957				-675.503336062214			
HF1	-755.549074354432	-0.933	-0.872	-0.062	-755.359026159167	-1.042	-1.044	0.002
Hx2	-79.883011290343				-79.854027138122			
xF2	-675.664723690195				-675.503484037444			
HF2	-755.549319535961	-1.087	-0.994	-0.093	-755.359385947453	-1.268	-1.176	-0.091
Hx3	-79.883011523823				-79.854029980694			
xF3	-675.664657924814				-675.503355005165			
HF3	-755.548898059841	-0.823	-0.771	-0.052	-755.358531030086	-0.731	-0.719	-0.012
Hx4	-79.883010287708				-79.854027234807			
xF4	-675.664645991311				-675.503401231715			
HF4	-755.549102791869	-0.951	-0.908	-0.044	-755.359249579626	-1.182	-1.143	-0.039
Fx1	-675.664617425776				-675.503322051978			
xF1	-675.664587200765				-675.503300080168			
FF1	-1351.33046337945	-0.826	-0.790	-0.036	-1351.0084710138	-1.126	-1.160	0.034
Fx2	-675.664690876929				-675.503342738584			
xF2	-675.664621868588				-675.503351695798			
FF2	-1351.33047437217	-0.833	-0.729	-0.104	-1351.00770039685	-0.642	-0.631	-0.011

	TPSS-D3/def2-QZVP				M06L/def2-QZVP			
	E [Ha]	BAE [kcal mol^{-1}]	BIE [kcal mol^{-1}]	E-def [kcal mol^{-1}]	E [Ha]	BAE [kcal mol^{-1}]	BIE [kcal mol^{-1}]	E-def [kcal mol^{-1}]
Propanes								
H	-119.222649222907				-119.179099827686			
F	-913.586518906826				-913.367681855226			
Hx1	-119.222652996912				-119.179120817425			
xH1	-119.222653631568				-119.179120891353			
HH1	-238.448285505759	-1.874	-1.869	-0.005	-238.361394812013	-2.005	-1.979	-0.026
Hx2	-119.222663212444				-119.179106907271			
xH2	-119.222650776032				-119.179114463103			
HH2	-238.447294250109	-1.252	-1.243	-0.010	-238.360028800746	-1.148	-1.134	-0.014
Hx1	-119.222637779103				-119.179096092706			
xF1	-913.586506961758				-913.367662713436			
HF1	-1032.81130609176	-1.342	-1.356	0.015	-1032.54942797309	-1.661	-1.675	0.014
Hx2	-119.222648383933				-119.179101577484			
xF2	-913.586594959763				-913.367787273952			
HF2	-1032.81102824425	-1.167	-1.120	-0.047	-1032.54871122369	-1.211	-1.144	-0.067
Hx3	-119.222665994781				-119.179084150446			
xF3	-913.586594429269				-913.367672486197			
HF3	-1032.81121911606	-1.287	-1.229	-0.058	-1032.54867005664	-1.185	-1.201	0.016
Hx4	-119.222640517255				-119.179092651281			
xF4	-913.586586246972				-913.367819067733			
HF4	-1032.81077039232	-1.005	-0.969	-0.037	-1032.5486422136	-1.168	-1.086	-0.082
Fx1	-913.586331786741				-913.367601110676			
xF1	-913.586437691329				-913.367697999224			
FF1	-1827.17431975313	-0.804	-0.973	0.168	-1826.7380290992	-1.673	-1.713	0.041
Fx2	-913.586517451097				-913.367681747519			
xF2	-913.586514967614				-913.367676438581			
FF2	-1827.17428008465	-0.780	-0.783	0.003	-1826.73817057167	-1.761	-1.765	0.003
Butanes								
H	-158.56234695919				-158.504212619942			
F	-1151.50774503466				-1151.23169986605			
Hx1	-158.562342713572				-158.504211882524			
xH1	-158.562346989899				-158.504227177329			
HH1	-317.12888303279	-2.629	-2.631	0.003	-317.013345940843	-3.088	-3.079	-0.009
Hx2	-158.562336484009				-158.504210227948			
xH2	-158.562354961524				-158.504216918158			
HH2	-317.127468254398	-1.741	-1.742	0.002	-317.011147942597	-1.709	-1.707	-0.001
Hx1	-158.562346534096				-158.504192021048			
xF1	-1151.50763748558				-1151.23116793546			
HF1	-1310.07287900113	-1.749	-1.817	0.068	-1309.73820569109	-1.439	-1.786	0.347
Hx2	-158.562333645964				-158.504195645872			
xF2	-1151.50774102669				-1151.23166288416			
HF2	-1310.07278794136	-1.692	-1.703	0.011	-1309.73931301338	-2.134	-2.168	0.034
Hx3	-158.562304669652				-158.504175269299			
xF3	-1151.50775628473				-1151.23160089333			
HF3	-1310.07251134893	-1.518	-1.538	0.019	-1309.73906834421	-1.980	-2.066	0.086
Hx4	-158.562299787449				-158.504185404812			
xF4	-1151.50774544679				-1151.23166362074			
HF4	-1310.07280540381	-1.703	-1.732	0.029	-1309.73915565291	-2.035	-2.075	0.040
Fx1	-1151.50770754885				-1151.23162894804			
xF1	-1151.50771870599				-1151.23167791501			
FF1	-2303.01778161085	-1.438	-1.478	0.040	-2302.46635841842	-1.857	-1.915	0.058
Fx2	-1151.50774122351				-1151.23147183144			
xF2	-1151.50768784112				-1151.23150039952			
FF2	-2303.01749786521	-1.260	-1.298	0.038	-2302.46671580194	-2.081	-2.349	0.268

	TPSS-D3/def2-QZVP				M06L/def2-QZVP			
	E [Ha]	BAE [kcal mol^{-1}]	BIE [kcal mol^{-1}]	E-def [kcal mol^{-1}]	E [Ha]	BAE [kcal mol^{-1}]	BIE [kcal mol^{-1}]	E-def [kcal mol^{-1}]
Pentanes								
H	-197.902019791865				-197.829207208924			
F	-1389.42908497232				-1389.09577099359			
Hx1	-197.902004204388				-197.829246212566			
xH1	-197.902004050381				-197.829246291122			
HH1	-395.809390727747	-3.358	-3.378	0.02	-395.664740278264	-3.97	-3.921	-0.049
Hx2	-197.902017496276				-197.82923276239			
xH2	-197.902017377496				-197.829232623606			
HH2	-395.807596376246	-2.232	-2.235	0.003	-395.662425874782	-2.517	-2.485	-0.032
Hx1	-197.901916612921				-197.829090470193			
xF1	-1389.42902030315				-1389.09559494498			
HF1	-1587.33446999986	-2.112	-2.217	0.105	-1586.9295349048	-2.859	-3.043	0.184
Hx2	-197.901990335994				-197.829163666231			
xF2	-1389.4287809975				-1389.09532405391			
HF2	-1587.3341659679	-1.921	-2.13	0.209	-1586.92844471739	-2.175	-2.483	0.308
Hx3	-197.901993556334				-197.829209911164			
xF3	-1389.42917547656				-1389.09573258885			
HF3	-1587.33425127319	-1.974	-1.934	-0.04	-1586.9286525406	-2.306	-2.328	0.022
Hx4	-197.901979411593				-197.829188437833			
xF4	-1389.42913183573				-1389.0957270257			
HF4	-1587.3346836789	-2.246	-2.242	-0.004	-1586.92964572275	-2.929	-2.968	0.039
Fx1	-1389.42903955758				-1389.09572045492			
xF1	-1389.42905257742				-1389.09565299646			
FF1	-2778.86074818065	-1.618	-1.667	0.049	-2778.19610154589	-2.861	-2.967	0.106
Fx2	-1389.42901969083				-1389.09569757717			
xF2	-1389.42902355845				-1389.09569756873			
FF2	-2778.86072872366	-1.606	-1.685	0.08	-2778.19566561915	-2.588	-2.68	0.092
Hexanes								
H	-237.241693278491				-237.154200718982			
F	-1627.35045818311				-1626.95982446733			
Hx1	-237.241676867185				-237.154258624144			
xH1	-237.241676696576				-237.154258152089			
HH1	-474.489698483428	-3.961	-3.981	0.021	-474.315850648367	-4.674	-4.602	-0.072
Hx2	-237.241698189312				-237.15424527861			
xH2	-237.241698222044				-237.154245192201			
HH2	-474.4877403738	-2.732	-2.726	-0.006	-474.313284969139	-3.064	-3.009	-0.056
Hx1	-237.241509247322				-237.15402395451			
xF1	-1627.35000388271				-1626.95917484718			
HF1	-1864.59537016007	-2.02	-2.42	0.401	-1864.11852106709	-2.821	-3.34	0.519
Hx2	-237.241609105753				-237.154120938445			
xF2	-1627.35012070514				-1626.95922897748			
HF2	-1864.59588996368	-2.346	-2.611	0.265	-1864.11807012286	-2.538	-2.962	0.424
Hx3	-237.241564505658				-237.15407286172			
xF3	-1627.35014529302				-1626.95938614533			
HF3	-1864.59560733316	-2.169	-2.446	0.277	-1864.11844143075	-2.771	-3.127	0.355
Hx4	-237.24168388154				-237.154219531913			
xF4	-1627.35041899558				-1626.95973174262			
HF4	-1864.59629351458	-2.599	-2.63	0.03	-1864.11885655251	-3.032	-3.078	0.046
Fx1	-1627.35033876335				-1626.95968274096			
xF1	-1627.35036472861				-1626.95970909978			
FF1	-3254.70384325965	-1.837	-1.97	0.134	-3253.92605123883	-4.018	-4.179	0.161
Fx2	-1627.3502755816				-1626.95968417419			
xF2	-1627.35027637325				-1626.9596817135			
FF2	-3254.70260179171	-1.058	-1.286	0.229	-3253.92265301019	-1.885	-2.063	0.178

	M06L-D3/def2-QZVP				rPW86PW92-vdW-DF10/pc-3			
	E [Ha]	BAE [kcal mol^{-1}]	BIE [kcal mol^{-1}]	E-def [kcal mol^{-1}]	E [Ha]	BAE [kcal mol^{-1}]	BIE [kcal mol^{-1}]	E-def [kcal mol^{-1}]
Methanes								
H	-40.531313494154				-40.8510656396			
F	-437.63888562999				-439.6412093037			
Hx1	-40.531310628153				-40.8510693484			
xH1	-40.531311265437				-40.8510740856			
HH1	-81.063540656048	-0.573	-0.577	0.003	-81.7031539731	-0.642	-0.634	-0.008
Hx2	-40.531312155147				-40.8510589574			
xH2	-40.531312489944				-40.8510547251			
HH2	-81.06316146489	-0.335	-0.337	0.001	-81.7027364161	-0.380	-0.391	0.011
Hx1	-40.531311907622				-40.851056957			
xF1	-437.638872988599				-439.6413398624			
HF1	-478.171625635736	-0.895	-0.904	0.009	-480.4939410165	-1.045	-0.969	-0.076
Hx2	-40.531313108451				-40.8510949362			
xF2	-437.638875513836				-439.6412358168			
HF2	-478.170774711101	-0.361	-0.368	0.007	-480.4933560313	-0.678	-0.643	-0.035
Fx1	-437.63886127239				-439.6412659791			
xF1	-437.63888014626				-439.6412143835			
FF1	-875.279222636535	-0.911	-0.929	0.019	-879.2841866738	-1.109	-1.071	-0.039
Fx2	-437.638878792144				-439.641181742			
xF2	-437.63886376985				-439.6412362103			
FF2	-875.278836451879	-0.668	-0.686	0.018	-879.2840123925	-1.000	-1.001	0.000
Ethanes								
H	-79.854039272244				-80.4514493009			
F	-675.503370187583				-678.6297265259			
Hx1	-79.8540440827				-80.451449053			
xH1	-79.854042316937				-80.4514339121			
HH1	-159.710360601872	-1.432	-1.427	-0.005	-160.9052225053	-1.458	-1.468	0.010
Hx2	-79.854039175391				-80.4514491704			
xH2	-79.854037794075				-80.4514452927			
HH2	-159.710087936175	-1.261	-1.262	0.001	-160.9050497817	-1.350	-1.352	0.003
Hx1	-79.85403888336				-80.4513612733			
xF1	-675.503368020086				-678.6299899071			
HF1	-755.359543885376	-1.339	-1.341	0.002	-759.0838300134	-1.666	-1.555	-0.110
Hx2	-79.854038911322				-80.4514242626			
xF2	-675.503515992153				-678.6300688824			
HF2	-755.35991293815	-1.571	-1.480	-0.091	-759.0840111592	-1.779	-1.580	-0.199
Hx3	-79.854041757239				-80.4514557207			
xF3	-675.503387014904				-678.6299769076			
HF3	-755.35902395819	-1.013	-1.001	-0.012	-759.0835257052	-1.475	-1.313	-0.161
Hx4	-79.854039016178				-80.4513758026			
xF4	-675.503433180248				-678.6297990257			
HF4	-755.359775026334	-1.484	-1.445	-0.039	-759.0838229011	-1.661	-1.662	0.001
Fx1	-675.50335390688				-678.6297825313			
xF1	-675.503331919154				-678.6298903181			
FF1	-1351.00902692263	-1.435	-1.469	0.034	-1357.262660815	-2.013	-1.875	-0.138
Fx2	-675.503374723874				-678.6299160046			
xF2	-675.50338363883				-678.6299071005			
FF2	-1351.00820143222	-0.917	-0.906	-0.011	-1357.2623402932	-1.812	-1.580	-0.232

	M06L-D3/def2-QZVP				rPW86PW92-vdW-DF10/pc-3			
	E [Ha]	BAE [kcal mol^{-1}]	BIE [kcal mol^{-1}]	E-def [kcal mol^{-1}]	E [Ha]	BAE [kcal mol^{-1}]	BIE [kcal mol^{-1}]	E-def [kcal mol^{-1}]
Propanes								
H	-119.179174685064				-120.0545345692			
F	-913.367837461475				-917.6166781956			
Hx1	-119.179195935982				-120.0545433359			
xH1	-119.179196019286				-120.054544287			
HH1	-238.362220065339	-2.429	-2.402	-0.027	-240.1128279819	-2.359	-2.347	-0.012
Hx2	-119.179182095252				-120.0545573652			
xH2	-119.179189505402				-120.0545333223			
HH2	-238.360764436726	-1.515	-1.502	-0.014	-240.1115329459	-1.546	-1.533	-0.014
Hx1	-119.179170847752				-120.0545253421			
xF1	-913.367818203814				-917.6167229623			
HF1	-1032.55043458467	-2.148	-2.162	0.014	-1037.6749357906	-2.336	-2.314	-0.022
Hx2	-119.179176463796				-120.0545346031			
xF2	-913.36794252332				-917.6168435381			
HF2	-1032.54971371423	-1.695	-1.628	-0.067	-1037.6744857594	-2.054	-1.950	-0.104
Hx3	-119.179159110814				-120.0545501035			
xF3	-913.367828045902				-917.6168318342			
HF3	-1032.54965869595	-1.661	-1.676	0.016	-1037.674481074	-2.051	-1.945	-0.106
Hx4	-119.179167561595				-120.0545319813			
xF4	-913.36797403723				-917.616806891			
HF4	-1032.54966079082	-1.662	-1.581	-0.081	-1037.6744097202	-2.006	-1.927	-0.079
Fx1	-913.367757029184				-917.6163891716			
xF1	-913.367853075201				-917.6165921804			
FF1	-1826.73915142545	-2.182	-2.222	0.041	-1835.2367320651	-2.118	-2.354	0.235
Fx2	-913.367837394936				-917.6166736657			
xF2	-913.367832093387				-917.6166665186			
FF2	-1826.73929114994	-2.269	-2.273	0.003	-1835.2375886881	-2.656	-2.666	0.010
Butanes								
H	-158.504405429392				-159.6577013044			
F	-1151.23205085392				-1156.6027837611			
Hx1	-158.504404762333				-159.6577088502			
xH1	-158.504420022722				-159.657712478			
HH1	-317.014768736239	-3.739	-3.730	-0.009	-319.3203436152	-3.101	-3.089	-0.012
Hx2	-158.504402982743				-159.6576874725			
xH2	-158.504409827564				-159.6577182613			
HH2	-317.01242018095	-2.265	-2.264	-0.001	-319.3184440044	-1.909	-1.907	-0.002
Hx1	-158.5043848569				-159.6577115253			
xF1	-1151.23151472739				-1156.602908989			
HF1	-1309.74000445396	-2.227	-2.576	0.349	-1316.2655957806	-3.207	-3.122	-0.085
Hx2	-158.504388489769				-159.6576948043			
xF2	-1151.23201292053				-1156.6029340376			
HF2	-1309.74109149874	-2.909	-2.943	0.034	-1316.2653016023	-3.022	-2.932	-0.090
Hx3	-158.504367975808				-159.6576578688			
xF3	-1151.2319501625				-1156.602864446			
HF3	-1309.74078932977	-2.719	-2.806	0.087	-1316.2652381355	-2.983	-2.959	-0.023
Hx4	-158.504378234664				-159.6576927182			
xF4	-1151.2320140071				-1156.6028528897			
HF4	-1309.74086119089	-2.764	-2.804	0.040	-1316.2652212975	-2.972	-2.934	-0.038
Fx1	-1151.23197855604				-1156.6027323388			
xF1	-1151.23202832642				-1156.6028807005			
FF1	-2302.4681530638	-2.542	-2.602	0.060	-2313.2101861807	-2.898	-2.870	-0.029
Fx2	-1151.23182029732				-1156.6030145974			
xF2	-1151.23184890978				-1156.602804627			
FF2	-2302.46852549155	-2.776	-3.047	0.271	-2313.2109816812	-3.397	-3.239	-0.158

	M06L-D3/def2-QZVP				rPW86PW92-vdW-DF10/pc-3			
	E [Ha]	BAE [kcal mol^{-1}]	BIE [kcal mol^{-1}]	E-def [kcal mol^{-1}]	E [Ha]	BAE [kcal mol^{-1}]	BIE [kcal mol^{-1}]	E-def [kcal mol^{-1}]
Pentanes								
H	-197.829546912061				-199.2606853165			
F	-1389.09635173789				-1395.588991017			
Hx1	-197.829585908694				-199.2606771086			
xH1	-197.829585987278				-199.2606788554			
HH1	-395.666853816336	-4.869	-4.820	-0.049	-398.5283621744	-4.387	-4.396	0.009
Hx2	-197.829572457672				-199.2607009512			
xH2	-197.829572319054				-199.2607019433			
HH2	-395.664329804598	-3.286	-3.254	-0.032	-398.52585015	-2.811	-2.791	-0.020
Hx1	-197.829430387443				-199.2608299172			
xF1	-1389.09617298117				-1395.5891164208			
HF1	-1586.93208436091	-3.882	-4.067	0.185	-1594.8560653088	-4.009	-3.840	-0.169
Hx2	-197.829503425025				-199.2607321568			
xF2	-1389.09590115683				-1395.5890465671			
HF2	-1586.93083565244	-3.098	-3.408	0.310	-1594.8554131765	-3.600	-3.536	-0.064
Hx3	-197.829549637961				-199.2607080866			
xF3	-1389.09631197743				-1395.5893589664			
HF3	-1586.93105857581	-3.238	-3.261	0.023	-1594.8553784205	-3.578	-3.333	-0.245
Hx4	-197.829528116067				-199.2606733081			
xF4	-1389.09630670999				-1395.5891777798			
HF4	-1586.93219755266	-3.953	-3.993	0.040	-1594.8563005292	-4.157	-4.047	-0.110
Fx1	-1389.09630074287				-1395.5890811807			
xF1	-1389.09623211052				-1395.5891323758			
FF1	-2778.19885254001	-3.859	-3.966	0.107	-2791.1845148135	-4.099	-3.954	-0.145
Fx2	-1389.09627708287				-1395.5889126617			
xF2	-1389.09627708811				-1395.5889853576			
FF2	-2778.19826636464	-3.491	-3.584	0.094	-2791.1840640257	-3.817	-3.869	0.053
Hexanes								
H	-237.154697232514				-238.8638768436			
F	-1626.96064808145				-1634.5753070568			
Hx1	-237.154755174877				-238.8638584254			
xH1	-237.154754702224				-238.8638607577			
HH1	-474.318634788667	-5.798	-5.726	-0.072	-477.735112896	-4.618	-4.640	0.022
Hx2	-237.154741846345				-238.863865576			
xH2	-237.15474176022				-238.863878442			
HH2	-474.315825402905	-4.035	-3.980	-0.056	-477.7327391994	-3.128	-3.135	0.006
Hx1	-237.154520998888				-238.8638527077			
xF1	-1626.95999282742				-1634.5753072981			
HF1	-1864.12189613397	-4.111	-4.632	0.522	-1873.4461234753	-4.355	-4.370	0.015
Hx2	-237.154617823874				-238.8637670022			
xF2	-1626.96004847542				-1634.5751558421			
HF2	-1864.12132916802	-3.755	-4.181	0.426	-1873.445887794	-4.207	-4.371	0.164
Hx3	-237.154569569288				-238.8639312758			
xF3	-1626.96020765417				-1634.5750455547			
HF3	-1864.12174521149	-4.016	-4.372	0.356	-1873.4460397874	-4.302	-4.432	0.130
Hx4	-237.154716136238				-238.8639121156			
xF4	-1626.96055416028				-1634.5755362197			
HF4	-1864.12214472893	-4.267	-4.314	0.047	-1873.4464576914	-4.564	-4.398	-0.166
Fx1	-1626.96050589548				-1634.5750833833			
xF1	-1626.96053246581				-1634.5753596311			
FF1	-3253.92982130881	-5.350	-5.511	0.162	-3269.1590413137	-5.288	-5.396	0.107
Fx2	-1626.96051003683				-1634.5749524227			
xF2	-1626.96050748751				-1634.5749457219			
FF2	-3253.92603885371	-2.976	-3.151	0.175	-3269.1567315811	-3.839	-4.288	0.449

	M06-2X/def2-QZVP				M06-2X-D3/def2-QZVP			
	E [Ha]	BAE [kcal mol^{-1}]	BIE [kcal mol^{-1}]	E-def [kcal mol^{-1}]	E [Ha]	BAE [kcal mol^{-1}]	BIE [kcal mol^{-1}]	E-def [kcal mol^{-1}]
Methanes								
H	-40.506624277959				-40.506624419795			
F	-437.573388251481				-437.573388998429			
Hx1	-40.506533736772				-40.50653387854			
xH1	-40.506525030411				-40.506525172184			
HH1	-81.013751947257	-0.316	-0.435	0.119	-81.013857181298	-0.382	-0.501	0.119
Hx2	-40.506494112138				-40.50649425397			
xH2	-40.506481858911				-40.506482000747			
HH2	-81.013440737748	-0.121	-0.292	0.171	-81.013570468737	-0.202	-0.373	0.171
Hx1	-40.506531614822				-40.506531756636			
xF1	-437.573295171184				-437.57329591998			
HF1	-478.080871528725	-0.539	-0.656	0.117	-478.08105536543	-0.654	-0.770	0.117
Hx2	-40.506623946011				-40.506624087803			
xF2	-437.573352489113				-437.573353237384			
HF2	-478.08034858822	-0.211	-0.234	0.023	-478.08053883961	-0.330	-0.352	0.023
Fx1	-437.573285703867				-437.573286451973			
xF1	-437.573309479055				-437.57331022728			
FF1	-875.147447246175	-0.421	-0.535	0.114	-875.147624324572	-0.531	-0.645	0.114
Fx2	-437.573309538083				-437.573310286477			
xF2	-437.573257142947				-437.573257891144			
FF2	-875.147392588487	-0.387	-0.518	0.132	-875.147580909556	-0.504	-0.635	0.132
Ethanes								
H	-79.814933219858				-79.814941721041			
F	-675.401082451369				-675.40110567909			
Hx1	-79.814932721472				-79.814941234748			
xH1	-79.814824946182				-79.814833460212			
HH1	-159.631744332222	-1.178	-1.247	0.068	-159.632077942442	-1.377	-1.445	0.068
Hx2	-79.814990133969				-79.814998632432			
xH2	-79.815004418129				-79.815012917078			
HH2	-159.631483163056	-1.015	-0.934	-0.080	-159.631807916467	-1.208	-1.127	-0.080
Hx1	-79.814920621854				-79.814929124594			
xF1	-675.401064094147				-675.401087427405			
HF1	-755.217045976799	-0.647	-0.666	0.019	-755.217500515714	-0.912	-0.931	0.019
Hx2	-79.814986592888				-79.814995089083			
xF2	-675.400870979205				-675.400894310354			
HF2	-755.217122137153	-0.694	-0.794	0.099	-755.217583936528	-0.964	-1.063	0.099
Hx3	-79.814927859366				-79.814936357994			
xF3	-675.401166900331				-675.401190272276			
HF3	-755.216917432915	-0.566	-0.516	-0.050	-755.217354947991	-0.820	-0.771	-0.050
Hx4	-79.81510495871				-79.815113460836			
xF4	-675.40114701712				-675.401170343237			
HF4	-755.21738550104	-0.860	-0.711	-0.148	-755.21784826173	-1.130	-0.982	-0.148
Fx1	-675.401057099872				-675.401080355952			
xF1	-675.401160696272				-675.401183939684			
FF1	-1350.8033431572	-0.739	-0.706	-0.033	-1350.80382902467	-1.015	-0.982	-0.033
Fx2	-675.401063976818				-675.401087330707			
xF2	-675.401200970927				-675.401224292829			
FF2	-1350.80297288156	-0.507	-0.444	-0.063	-1350.80340945068	-0.752	-0.689	-0.063

	M06-2X/def2-QZVP				M06-2X-D3/def2-QZVP			
	E [Ha]	BAE [kcal mol^{-1}]	BIE [kcal mol^{-1}]	E-def [kcal mol^{-1}]	E [Ha]	BAE [kcal mol^{-1}]	BIE [kcal mol^{-1}]	E-def [kcal mol^{-1}]
Propanes								
H	-119.126434379236				-119.126492988755			
F	-913.229549836054				-913.229673716665			
Hx1	-119.12636663932				-119.126425475808			
xH1	-119.126364669245				-119.126423514884			
HH1	-238.255476484992	-1.636	-1.723	0.086	-238.25618709045	-2.009	-2.095	0.086
Hx2	-119.126372708028				-119.126431604503			
xH2	-119.12637788495				-119.126436656174			
HH2	-238.254320845063	-0.911	-0.985	0.074	-238.254963569123	-1.241	-1.315	0.074
Hx1	-119.126429880875				-119.126488401389			
xF1	-913.229337999544				-913.229461728969			
HF1	-1032.35756346057	-0.991	-1.127	0.136	-1032.35844735369	-1.431	-1.567	0.136
Hx2	-119.126570466029				-119.126629099655			
xF2	-913.229178809165				-913.229302351329			
HF2	-1032.35693072129	-0.594	-0.741	0.147	-1032.35781749967	-1.036	-1.184	0.148
Hx3	-119.126460035265				-119.126518732339			
xF3	-913.229269792262				-913.229393614863			
HF3	-1032.35687144408	-0.557	-0.716	0.160	-1032.35774283106	-0.989	-1.149	0.160
Hx4	-119.126509969017				-119.126568625486			
xF4	-913.229140940132				-913.22926423021			
HF4	-1032.35671925713	-0.461	-0.670	0.209	-1032.35761952757	-0.912	-1.121	0.209
Fx1	-913.229340746907				-913.229464861789			
xF1	-913.229376958566				-913.229500361599			
FF1	-1826.46028011037	-0.741	-0.980	0.240	-1826.46126954961	-1.206	-1.446	0.240
Fx2	-913.22954028812				-913.229664212406			
xF2	-913.22953011019				-913.22965404266			
FF2	-1826.4606776204	-0.990	-1.009	0.018	-1826.46165598907	-1.449	-1.467	0.018
Butanes								
H	-158.438067270029				-158.438227672519			
F	-1151.05752770185				-1151.05782043843			
Hx1	-158.437795653278				-158.437956121148			
xH1	-158.437862534786				-158.438022974135			
HH1	-316.879829205757	-2.318	-2.617	0.299	-316.881068992786	-2.895	-3.194	0.299
Hx2	-158.437799967936				-158.437960322424			
xH2	-158.437811227434				-158.43797172662			
HH2	-316.877879759955	-1.095	-1.424	0.328	-316.879000723385	-1.597	-1.926	0.328
Hx1	-158.438009561757				-158.438169989744			
xF1	-1151.05688945467				-1151.05717936607			
HF1	-1309.49657842429	-0.617	-1.054	0.437	-1309.49816708333	-1.330	-1.768	0.438
Hx2	-158.438051732325				-158.438212171805			
xF2	-1151.05747194133				-1151.0577640165			
HF2	-1309.49745796476	-1.169	-1.214	0.045	-1309.4990232083	-1.867	-1.912	0.045
Hx3	-158.43795787314				-158.438118181865			
xF3	-1151.0573595921				-1151.05765123724			
HF3	-1309.49737123463	-1.115	-1.289	0.174	-1309.4988937269	-1.786	-1.961	0.175
Hx4	-158.437946224707				-158.438106640633			
xF4	-1151.05752046813				-1151.0578128187			
HF4	-1309.49740087116	-1.133	-1.214	0.080	-1309.49890259192	-1.791	-1.872	0.081
Fx1	-1151.05746013013				-1151.05775193612			
xF1	-1151.05747866447				-1151.05777094118			
FF1	-2302.11664533737	-0.998	-1.071	0.073	-2302.11823777794	-1.630	-1.704	0.074
Fx2	-1151.05727793152				-1151.0575689947			
xF2	-1151.05729509385				-1151.05758610052			
FF2	-2302.11657161285	-0.951	-1.254	0.303	-2302.11816703545	-1.585	-1.890	0.305

	M06-2X/def2-QZVP				M06-2X-D3/def2-QZVP			
	E [Ha]	BAE [kcal mol^{-1}]	BIE [kcal mol^{-1}]	E-def [kcal mol^{-1}]	E [Ha]	BAE [kcal mol^{-1}]	BIE [kcal mol^{-1}]	E-def [kcal mol^{-1}]
Pentanes								
H	-197.749441168558				-197.749731142782			
F	-1388.88577417831				-1388.88626869996			
Hx1	-197.749177593733				-197.749467565986			
xH1	-197.749175663617				-197.749465635858			
HH1	-395.503705449188	-3.027	-3.359	0.332	-395.505564225936	-3.829	-4.161	0.332
Hx2	-197.749122886594				-197.749412875496			
xH2	-197.749128166813				-197.749418155953			
HH2	-395.50137342704	-1.563	-1.959	0.396	-395.503060881127	-2.258	-2.654	0.396
Hx1	-197.749278094786				-197.749568201345			
xF1	-1388.88552577365				-1388.88601837898			
HF1	-1586.63762765877	-1.514	-1.772	0.258	-1586.63989234664	-2.443	-2.702	0.259
Hx2	-197.74940852951				-197.749698556699			
xF2	-1388.88523418015				-1388.88572603339			
HF2	-1586.63692310455	-1.072	-1.431	0.359	-1586.63905065418	-1.914	-2.275	0.361
Hx3	-197.74929966772				-197.749589673233			
xF3	-1388.88561624516				-1388.88610973775			
HF3	-1586.63711300479	-1.191	-1.379	0.188	-1586.63926189702	-2.047	-2.235	0.189
Hx4	-197.749349470575				-197.749639399292			
xF4	-1388.88573977882				-1388.8862335089			
HF4	-1586.63771947515	-1.571	-1.650	0.079	-1586.63998034057	-2.498	-2.577	0.080
Fx1	-1388.88569965021				-1388.88619393033			
xF1	-1388.88554901496				-1388.88604236892			
FF1	-2777.77373030164	-1.369	-1.557	0.188	-2777.77618334649	-2.288	-2.477	0.189
Fx2	-1388.88564790934				-1388.88614150698			
xF2	-1388.88565173059				-1388.88614533993			
FF2	-2777.77351411219	-1.234	-1.390	0.156	-2777.77582504292	-2.063	-2.220	0.157
Hexanes								
H	-237.060759966413				-237.061189291471			
F	-1626.71387372348				-1626.71458324202			
Hx1	-237.060504392305				-237.060933750037			
xH1	-237.060506485745				-237.060935842857			
HH1	-474.127217935721	-3.576	-3.895	0.319	-474.129679192762	-4.581	-4.901	0.319
Hx2	-237.060452099559				-237.060881467488			
xH2	-237.060441021288				-237.060870389517			
HH2	-474.124676814695	-1.981	-2.374	0.393	-474.126942416905	-2.864	-3.257	0.393
Hx1	-237.060525268677				-237.060954958168			
xF1	-1626.71300192605				-1626.71370739825			
HF1	-1863.77666272148	-1.273	-1.968	0.694	-1863.77967947148	-2.452	-3.148	0.697
Hx2	-237.060679164864				-237.061108787726			
xF2	-1626.71323419026				-1626.71394069975			
HF2	-1863.77658346246	-1.224	-1.676	0.452	-1863.77949570621	-2.336	-2.790	0.454
Hx3	-237.060536990814				-237.06096642472			
xF3	-1626.71343238351				-1626.71414039438			
HF3	-1863.77676347337	-1.336	-1.753	0.417	-1863.77971166819	-2.472	-2.890	0.418
Hx4	-237.060774225589				-237.061203615144			
xF4	-1626.71378669138				-1626.71449534598			
HF4	-1863.77717786123	-1.596	-1.642	0.046	-1863.78010989712	-2.722	-2.768	0.046
Fx1	-1626.71382053582				-1626.71452976613			
xF1	-1626.71371185139				-1626.71442127604			
FF1	-3253.43092916116	-1.997	-2.132	0.135	-3253.43430036363	-3.222	-3.357	0.135
Fx2	-1626.71383095927				-1626.7145420632			
xF2	-1626.71382757215				-1626.71453860626			
FF2	-3253.42921985684	-0.924	-0.980	0.056	-3253.43223904757	-1.928	-1.982	0.054

	B3LYP-D3/def2-QZVP				B3LYP-dDsC/QZ4P			
	E [Ha]	BAE [kcal mol^{-1}]	BIE [kcal mol^{-1}]	E-def [kcal mol^{-1}]	E [Ha]	BAE [kcal mol^{-1}]	BIE [kcal mol^{-1}]	E-def [kcal mol^{-1}]
Methanes								
H	-40.508353810813				-0.997054523256134			
F	-437.554162389672				-1.20895404065298			
Hx1	-40.508323911401				-0.997046912167397			
xH1	-40.508319036247				-0.997046064187006			
HH1	-81.017407549216	-0.439	-0.480	0.041	-1.9948341514964	-0.455	-0.465	0.010
Hx2	-40.50830460883				-0.997022863079061			
xH2	-40.50829832882				-0.997051984170406			
HH2	-81.017206276302	-0.313	-0.379	0.066	-1.99467653524753	-0.356	-0.378	0.021
Hx1	-40.508320525556				-0.997043172266109			
xF1	-437.554164428607				-1.20899379040633			
HF1	-478.063455294679	-0.589	-0.609	0.020	-2.20704863374822	-0.653	-0.635	-0.018
Hx2	-40.508352870386				-0.997054041876732			
xF2	-437.554173188624				-1.20899682317528			
HF2	-478.063018697603	-0.315	-0.309	-0.006	-2.20666040117139	-0.409	-0.382	-0.027
Fx1	-437.554152374313				-1.20896730375955			
xF1	-437.554149622471				-1.20895840960563			
FF1	-875.109123155343	-0.501	-0.515	0.014	-2.41884083309372	-0.585	-0.574	-0.011
Fx2	-437.554153563222				-1.20896316362528			
xF2	-437.554127927127				-1.20888550538817			
FF2	-875.109097581252	-0.485	-0.512	0.027	-2.41893497945686	-0.644	-0.682	0.037
Ethanes								
H	-79.812303022174				-1.68017047467535			
F	-675.36868477534				-1.98569503969456			
Hx1	-79.812303025414				-1.68027599243754			
xH1	-79.812262434402				-1.68028143449678			
HH1	-159.626642396514	-1.278	-1.303	0.025	-3.36320553821355	-1.798	-1.662	-0.136
Hx2	-79.812325584565				-1.6802344960833			
xH2	-79.812331912901				-1.68023059195844			
HH2	-159.626482791287	-1.178	-1.145	-0.032	-3.36268782620929	-1.473	-1.395	-0.078
Hx1	-79.812292350121				-1.68020751873251			
xF1	-675.368741016648				-1.98567652827987			
HF1	-755.18232476599	-0.839	-0.810	-0.029	-3.66729405065374	-0.896	-0.885	-0.012
Hx2	-79.812326604564				-1.68021959152825			
xF2	-675.368656220824				-1.98560407575361			
HF2	-755.18254319798	-0.976	-0.979	0.003	-3.66763532723768	-1.111	-1.137	0.026
Hx3	-79.812300940751				-1.68018270017829			
xF3	-675.368766824769				-1.98564618668733			
HF3	-755.18216954899	-0.742	-0.691	-0.050	-3.66703273800714	-0.732	-0.755	0.023
Hx4	-79.812371197768				-1.68018221215156			
xF4	-675.368721459916				-1.98564763735756			
HF4	-755.182522821893	-0.963	-0.897	-0.066	-3.66748792047934	-1.018	-1.040	0.022
Fx1	-675.368688456292				-1.98564455503553			
xF1	-675.368703352579				-1.9856074618755			
FF1	-1350.73865895424	-0.809	-0.795	-0.014	-3.9725782550825	-0.746	-0.832	0.087
Fx2	-675.368746871734				-1.98570551135143			
xF2	-675.36872158297				-1.9855777713251			
FF2	-1350.7385106709	-0.716	-0.654	-0.062	-3.97226126327924	-0.547	-0.614	0.067

	B3LYP-D3/def2-QZVP				B3LYP-dDsC/QZ4P			
	E [Ha]	BAE [kcal mol^{-1}]	BIE [kcal mol^{-1}]	E-def [kcal mol^{-1}]	E [Ha]	BAE [kcal mol^{-1}]	BIE [kcal mol^{-1}]	E-def [kcal mol^{-1}]
Propanes								
H	-119.119219214312				-2.36714715632625			
F	-913.182649236586				-2.76210974389371			
Hx1	-119.11920191317				-2.36706632980892			
xH1	-119.119201781452				-2.3670493889605			
HH1	-238.241715108446	-2.056	-2.078	0.022	-4.73857531500969	-2.686	-2.798	0.112
Hx2	-119.119209050169				-2.36710943950061			
xH2	-119.11920316734				-2.36709130400842			
HH2	-238.240343040799	-1.195	-1.212	0.016	-4.736507343554	-1.389	-1.447	0.059
Hx1	-119.119209555224				-2.36714181956329			
xF1	-913.182508169149				-2.76203626172459			
HF1	-1032.30390540466	-1.278	-1.373	0.095	-5.13195340563505	-1.692	-1.742	0.049
Hx2	-119.119271328837				-2.36715869854355			
xF2	-913.18251612529				-2.76204321888593			
HF2	-1032.30350984179	-1.030	-1.081	0.051	-5.13127784362148	-1.268	-1.303	0.035
Hx3	-119.119232677646				-2.36718211964487			
xF3	-913.182556697026				-2.76212653548463			
HF3	-1032.30353365825	-1.045	-1.095	0.050	-5.1312450424375	-1.248	-1.215	-0.032
Hx4	-119.119253166967				-2.36706559788857			
xF4	-913.182479316403				-2.76209065428599			
HF4	-1032.30334789651	-0.928	-1.014	0.085	-5.13140551676806	-1.348	-1.411	0.063
Fx1	-913.182391540217				-2.76192719192125			
xF1	-913.182505601146				-2.76212374052011			
FF1	-1826.3666473172	-0.846	-1.098	0.252	-5.52633962922619	-1.330	-1.436	0.106
Fx2	-913.182641137748				-2.76209999590492			
xF2	-913.182636100043				-2.76213965001451			
FF2	-1826.36709157574	-1.125	-1.139	0.013	-5.52673757602075	-1.580	-1.567	-0.013
Butanes								
H	-158.426236778255				-3.05413458301858			
F	-1150.99577796131				-3.53814802563191			
Hx1	-158.426138319369				-3.05412734697419			
xH1	-158.426158936112				-3.0541148613696			
HH1	-316.85707412121	-2.887	-2.998	0.111	-6.11497067281755	-4.205	-4.222	0.017
Hx2	-158.426125888057				-3.0539861726772			
xH2	-158.42614701502				-3.05405243526411			
HH2	-316.854975298649	-1.570	-1.696	0.126	-6.1113762243495	-1.950	-2.094	0.145
Hx1	-158.42621214639				-3.05406171503111			
xF1	-1150.99566511654				-3.53790483499211			
HF1	-1309.42486579861	-1.789	-1.875	0.086	-6.59566950916554	-2.125	-2.324	0.198
Hx2	-158.426223340603				-3.05412213466942			
xF2	-1150.99580685855				-3.53815157758183			
HF2	-1309.42487163233	-1.793	-1.783	-0.010	-6.59590559199684	-2.273	-2.279	0.006
Hx3	-158.426174472668				-3.05407739409964			
xF3	-1150.99580787547				-3.53821539174974			
HF3	-1309.42476943426	-1.729	-1.749	0.020	-6.59609499233364	-2.392	-2.386	-0.006
Hx4	-158.426163155924				-3.05405086550945			
xF4	-1150.99581880253				-3.53815185219887			
HF4	-1309.42483058123	-1.767	-1.788	0.021	-6.59581485136437	-2.217	-2.267	0.050
Fx1	-1150.99580288325				-3.5381420883391			
xF1	-1150.9957332409				-3.53810973870566			
FF1	-2301.99390942518	-1.477	-1.489	0.012	-7.0787081224622	-1.514	-1.541	0.028
Fx2	-1150.9958170141				-3.53814654050713			
xF2	-1150.99578610147				-3.53796166792821			
FF2	-2301.99402091801	-1.547	-1.517	-0.030	-7.07899798029486	-1.695	-1.813	0.118

	B3LYP-D3/def2-QZVP				B3LYP-dDsC/QZ4P			
	E [Ha]	BAE [kcal mol^{-1}]	BIE [kcal mol^{-1}]	E-def [kcal mol^{-1}]	E [Ha]	BAE [kcal mol^{-1}]	BIE [kcal mol^{-1}]	E-def [kcal mol^{-1}]
Pentanes								
H	-197.733150514393				-3.74100920430532			
F	-1388.809137313				-4.31416645591214			
Hx1	-197.733039082328				-3.74106507503068			
xH1	-197.733038898408				-3.74106066460062			
HH1	-395.472349513822	-3.795	-3.935	0.140	-7.49125042280308	-5.793	-5.726	-0.067
Hx2	-197.733032827674				-3.74091576568679			
xH2	-197.733033165663				-3.74091237868381			
HH2	-395.469579099767	-2.057	-2.205	0.147	-7.4865145102586	-2.821	-2.941	0.119
Hx1	-197.733026822065				-3.74087673241662			
xF1	-1388.80913396051				-4.31418222324668			
HF1	-1586.54584320238	-2.231	-2.311	0.080	-8.05980476585605	-2.905	-2.978	0.073
Hx2	-197.733114611753				-3.74097135483946			
xF2	-1388.80892381137				-4.3138706767912			
HF2	-1586.54550693547	-2.020	-2.177	0.157	-8.05915003671939	-2.494	-2.703	0.209
Hx3	-197.733084956732				-3.74100361177355			
xF3	-1388.80919451388				-4.31427426559792			
HF3	-1586.54563955873	-2.103	-2.108	0.005	-8.05974693715521	-2.869	-2.804	-0.064
Hx4	-197.733098652071				-3.7409619200154			
xF4	-1388.80919109966				-4.3141525904642			
HF4	-1586.5461817346	-2.443	-2.442	-0.001	-8.06030841849651	-3.221	-3.259	0.038
Fx1	-1388.80911531471				-4.31419119145626			
xF1	-1388.80912736768				-4.31417416426328			
FF1	-2777.62145927768	-1.998	-2.018	0.020	-8.63236726693781	-2.532	-2.511	-0.020
Fx2	-1388.80908651043				-4.31429870946289			
xF2	-1388.80909045596				-4.31428571277507			
FF2	-2777.62113807622	-1.797	-1.858	0.061	-8.63187375800452	-2.222	-2.064	-0.158
Hexanes								
H	-237.040062124583				-4.42798094604148			
F	-1626.62254094344				-5.0904208285254			
Hx1	-237.039946402381				-4.42800501641623			
xH1	-237.039946748938				-4.42801128104791			
HH1	-474.087256613648	-4.476	-4.621	0.145	-8.86688887116302	-6.857	-6.823	-0.034
Hx2	-237.0399440548				-4.42784034456552			
xH2	-237.039942212862				-4.42783163507668			
HH2	-474.084273826733	-2.604	-2.753	0.149	-8.86141644369284	-3.423	-3.605	0.182
Hx1	-237.039858557189				-4.42778226592321			
xF1	-1626.62217796736				-5.08986153677259			
HF1	-1863.66631481909	-2.329	-2.685	0.356	-9.52370079737084	-3.325	-3.801	0.476
Hx2	-237.039972842364				-4.42792188817633			
xF2	-1626.6222702608				-5.09002550880112			
HF2	-1863.66655857684	-2.482	-2.708	0.226	-9.5234030053296	-3.138	-3.423	0.285
Hx3	-237.039891059779				-4.42775945462131			
xF3	-1626.62227446402				-5.09011661231521			
HF3	-1863.66643076806	-2.402	-2.676	0.275	-9.52380077722309	-3.388	-3.718	0.330
Hx4	-237.040049327837				-4.42786230693905			
xF4	-1626.62253357553				-5.09028091465909			
HF4	-1863.66702299448	-2.774	-2.786	0.013	-9.52420160022139	-3.639	-3.802	0.162
Fx1	-1626.62248565959				-5.09022452776762			
xF1	-1626.62244553499				-5.09013088581869			
FF1	-3253.24903898184	-2.483	-2.578	0.095	-10.1859513340609	-3.206	-3.511	0.305
Fx2	-1626.62233964131				-5.09022673896258			
xF2	-1626.62234210278				-5.09023467932742			
FF2	-3253.24744307792	-1.482	-1.733	0.251	-10.1844317405797	-2.253	-2.491	0.239

	B3LYP-XDM/aug-cc-pVTZ				B3LYP-NL/def2-QZVP			
	E [Ha]	BAE [kcal mol^{-1}]	BIE [kcal mol^{-1}]	E-def [kcal mol^{-1}]	E [Ha]	BAE [kcal mol^{-1}]	BIE [kcal mol^{-1}]	E-def [kcal mol^{-1}]
Methanes								
H	-40.54004623483				-40.450478955403			
F	-437.6729650577				-437.316494422571			
Hx1	-40.54004539424				-40.450449310548			
xH1	-40.54004531584				-40.450444325613			
HH1	-81.08090732403	-0.511	-0.512	0.001	-80.901395160982	-0.274	-0.315	0.040
Hx2	-40.54004647956				-40.450429536079			
xH2	-40.54004668809				-40.45042308801			
HH2	-81.08069053054	-0.375	-0.375	0.000	-80.9012505642	-0.184	-0.250	0.066
Hx1	-40.54004655243				-40.45044619739			
xF1	-437.6729909055				-437.316489488932			
HF1	-478.2142820835	-0.797	-0.781	-0.016	-477.768112140567	-0.715	-0.738	0.024
Hx2	-40.54004547394				-40.450477893705			
xF2	-437.6729821742				-437.316500472315			
HF2	-478.2136827772	-0.421	-0.411	-0.010	-477.767615192459	-0.403	-0.400	-0.003
Fx1	-437.6729765161				-437.316479767398			
xF1	-437.6729803442				-437.316477693023			
FF1	-875.3471212641	-0.747	-0.731	-0.017	-874.634451116533	-0.918	-0.937	0.020
Fx2	-437.6729853342				-437.316481129966			
xF2	-437.6729814414				-437.316456918576			
FF2	-875.3470913289	-0.729	-0.706	-0.023	-874.634482533851	-0.937	-0.969	0.032
Ethanes								
H	-79.86938267815				-79.709616974232			
F	-675.5569747212				-674.998274255037			
Hx1	-79.8693829113				-79.709618653591			
xH1	-79.86938425842				-79.709574807682			
HH1	-159.7408395862	-1.302	-1.300	-0.001	-159.420849465373	-1.014	-1.039	0.025
Hx2	-79.86938333018				-79.709639034483			
xH2	-79.86938357455				-79.709645710091			
HH2	-159.7406054811	-1.155	-1.154	-0.001	-159.420711172813	-0.927	-0.895	-0.032
Hx1	-79.86937718941				-79.709604808579			
xF1	-675.5570247102				-674.998312855404			
HF1	-755.4280621249	-1.070	-1.042	-0.028	-754.709649826696	-1.104	-1.087	-0.017
Hx2	-79.86937931324				-79.709640965284			
xF2	-675.5570424826				-674.998240837602			
HF2	-755.4283541596	-1.253	-1.213	-0.040	-754.709946837673	-1.290	-1.296	0.006
Hx3	-79.86937972961				-79.709613134606			
xF3	-675.5570249865				-674.998335271991			
HF3	-755.4278119583	-0.913	-0.883	-0.030	-754.709431502109	-0.967	-0.931	-0.036
Hx4	-79.8693781419				-79.709686859244			
xF4	-675.5570123418				-674.998299516033			
HF4	-755.4282352374	-1.178	-1.158	-0.021	-754.70991224001	-1.268	-1.208	-0.060
Fx1	-675.5569918754				-674.998277841144			
xF1	-675.5569592576				-674.998293334715			
FF1	-1351.115759828	-1.136	-1.135	-0.001	-1349.99910062199	-1.601	-1.587	-0.014
Fx2	-675.55703413				-674.998313721572			
xF2	-675.5569987096				-674.998301628671			
FF2	-1351.115487244	-0.965	-0.913	-0.052	-1349.99860191231	-1.289	-1.247	-0.042

	B3LYP-XDM/aug-cc-pVTZ				B3LYP-NL/def2-QZVP			
	E [Ha]	BAE [kcal mol^{-1}]	BIE [kcal mol^{-1}]	E-def [kcal mol^{-1}]	E [Ha]	BAE [kcal mol^{-1}]	BIE [kcal mol^{-1}]	E-def [kcal mol^{-1}]
Propanes								
H	-119.201598301				-118.971860350801			
F	-913.4402027813				-912.679965030856			
Hx1	-119.2016081296				-118.971843577662			
xH1	-119.2016090068				-118.97184304787			
HH1	-238.4065410993	-2.099	-2.086	-0.013	-237.9464806476	-1.732	-1.753	0.021
Hx2	-119.2016122714				-118.97184957987			
xH2	-119.2016043885				-118.971846332987			
HH2	-238.4050731668	-1.178	-1.165	-0.013	-237.945284491948	-0.981	-0.997	0.016
Hx1	-119.2015884645				-118.971851307233			
xF1	-913.4401371672				-912.679839542536			
HF1	-1032.644468677	-1.674	-1.721	0.047	-1031.65467464866	-1.788	-1.872	0.084
Hx2	-119.2015966378				-118.971915556045			
xF2	-913.4402177558				-912.679851308916			
HF2	-1032.64399395	-1.376	-1.368	-0.008	-1031.6541517172	-1.460	-1.497	0.037
Hx3	-119.2016043111				-118.971879792334			
xF3	-913.4402000295				-912.679873969651			
HF3	-1032.643960281	-1.355	-1.353	-0.002	-1031.65407237792	-1.410	-1.455	0.045
Hx4	-119.2015958418				-118.971894438584			
xF4	-913.4401984519				-912.679825485673			
HF4	-1032.643912768	-1.325	-1.329	0.004	-1031.65412941019	-1.446	-1.512	0.066
Fx1	-913.4399953516				-912.679728197594			
xF1	-913.4401331848				-912.679838440776			
FF1	-1826.882704387	-1.443	-1.616	0.174	-1825.36326651251	-2.094	-2.322	0.228
Fx2	-913.4401981268				-912.679957388913			
xF2	-913.440197866				-912.679952054382			
FF2	-1826.883262696	-1.793	-1.799	0.006	-1825.36416043466	-2.655	-2.668	0.013
Butanes								
H	-158.5337904438				-158.234217622374			
F	-1151.322804154				-1150.36106990829			
Hx1	-158.5337950507				-158.234118115911			
xH1	-158.5337928382				-158.234143573152			
HH1	-317.0723802489	-3.012	-3.007	-0.004	-316.472461878985	-2.527	-2.636	0.109
Hx2	-158.5337775663				-158.234111196688			
xH2	-158.5337983939				-158.234129018892			
HH2	-317.0702106113	-1.650	-1.653	0.003	-316.470561581613	-1.334	-1.457	0.122
Hx1	-158.5337893695				-158.234195051681			
xF1	-1151.322659884				-1150.36082658845			
HF1	-1309.860124587	-2.215	-2.306	0.091	-1308.59913723586	-2.416	-2.583	0.167
Hx2	-158.5337769999				-158.234201543534			
xF2	-1151.322831049				-1150.36106814525			
HF2	-1309.860178792	-2.249	-2.241	-0.008	-1308.59933611743	-2.541	-2.552	0.011
Hx3	-158.5337512364				-158.234154643924			
xF3	-1151.322828531				-1150.3610319958			
HF3	-1309.860120772	-2.213	-2.222	0.009	-1308.59925292141	-2.488	-2.552	0.063
Hx4	-158.5337451139				-158.234146167724			
xF4	-1151.322828296				-1150.36109677636			
HF4	-1309.86014538	-2.228	-2.241	0.013	-1308.59919878773	-2.454	-2.482	0.028
Fx1	-1151.322800231				-1150.36104091546			
xF1	-1151.32276843				-1150.36102432983			
FF1	-2302.648844431	-2.031	-2.056	0.025	-2300.72650548168	-2.739	-2.786	0.047
Fx2	-1151.322812817				-1150.36102132587			
xF2	-1151.322790862				-1150.36102394809			
FF2	-2302.649147154	-2.221	-2.224	0.003	-2300.72706800781	-3.092	-3.152	0.059

	B3LYP-XDM/aug-cc-pVTZ				B3LYP-NL/def2-QZVP			
	E [Ha]	BAE [kcal mol^{-1}]	BIE [kcal mol^{-1}]	E-def [kcal mol^{-1}]	E [Ha]	BAE [kcal mol^{-1}]	BIE [kcal mol^{-1}]	E-def [kcal mol^{-1}]
Pentanes								
H	-197.8659489804				-197.496482909712			
F	-1389.205622122				-1388.04244626475			
Hx1	-197.8659433981				-197.496370920763			
xH1	-197.8659433077				-197.496370742356			
HH1	-395.7381838128	-3.944	-3.951	0.007	-394.998388860074	-3.403	-3.544	0.141
Hx2	-197.8659519449				-197.496364500639			
xH2	-197.8659518889				-197.496364815149			
HH2	-395.7354185071	-2.209	-2.205	-0.004	-394.99579381963	-1.775	-1.923	0.148
Hx1	-197.865852492				-197.496360722111			
xF1	-1389.205596126				-1388.04235714598			
HF1	-1587.076100221	-2.842	-2.919	0.077	-1585.54404865606	-3.213	-3.345	0.133
Hx2	-197.8659135457				-197.496446410431			
xF2	-1389.205393922				-1388.04216195353			
HF2	-1587.075597068	-2.526	-2.692	0.165	-1585.54341962774	-2.818	-3.019	0.201
Hx3	-197.86593217				-197.496409475625			
xF3	-1389.205692479				-1388.0424375512			
HF3	-1587.0757676	-2.633	-2.600	-0.034	-1585.54363859131	-2.955	-3.007	0.052
Hx4	-197.8659151811				-197.496427024841			
xF4	-1389.205658447				-1388.04246456623			
HF4	-1587.076465052	-3.071	-3.069	-0.002	-1585.544449251	-3.464	-3.487	0.024
Fx1	-1389.205612339				-1388.04241412298			
xF1	-1389.205615196				-1388.04238298251			
FF1	-2778.415868008	-2.901	-2.912	0.010	-2776.09146253957	-4.123	-4.183	0.060
Fx2	-1389.205593735				-1388.04236809276			
xF2	-1389.205596532				-1388.04237257564			
FF2	-2778.415479694	-2.658	-2.692	0.034	-2776.09075739337	-3.680	-3.776	0.095
Hexanes								
H	-237.1981241153				-236.758745814544			
F	-1627.088508879				-1625.72382769832			
Hx1	-237.1981125141				-236.758631934014			
xH1	-237.1981125193				-236.758632128411			
HH1	-474.403658019	-4.650	-4.664	0.015	-473.524009146021	-4.090	-4.233	0.143
Hx2	-237.1981249154				-236.758629631867			
xH2	-237.1981247898				-236.758627791465			
HH2	-474.4005742217	-2.715	-2.714	-0.001	-473.521196078234	-2.325	-2.472	0.147
Hx1	-237.1979436564				-236.758535587396			
xF1	-1627.088138214				-1625.72334756807			
HF1	-1864.291567151	-3.096	-3.442	0.346	-1862.48833751328	-3.617	-4.050	0.433
Hx2	-237.198031358				-236.758656104133			
xF2	-1627.088215248				-1625.7234691238			
HF2	-1864.291600104	-3.117	-3.359	0.242	-1862.48821653987	-3.541	-3.822	0.281
Hx3	-237.1980042966				-236.758580029361			
xF3	-1627.088247962				-1625.72353392107			
HF3	-1864.291688815	-3.173	-3.411	0.239	-1862.48839934114	-3.656	-3.944	0.288
Hx4	-237.198104247				-236.758733091263			
xF4	-1627.088486132				-1625.72379892127			
HF4	-1864.292106221	-3.435	-3.461	0.027	-1862.48883097724	-3.927	-3.953	0.026
Fx1	-1627.088442847				-1625.72377353118			
xF1	-1627.088441655				-1625.7237226291			
FF1	-3254.182882935	-3.680	-3.764	0.084	-3251.4564103505	-5.494	-5.594	0.100
Fx2	-1627.088332941				-1625.72369557978			
xF2	-1627.088334003				-1625.72369592969			
FF2	-3254.180988466	-2.492	-2.712	0.220	-3251.45379994909	-3.856	-4.021	0.166

	ωB97X-D3/def2-QZVP				B2PLYP-D3/def2-QZVP			
	E [Ha]	BAE [kcal mol^{-1}]	BIE [kcal mol^{-1}]	E-def [kcal mol^{-1}]	E [Ha]	BAE [kcal mol^{-1}]	BIE [kcal mol^{-1}]	E-def [kcal mol^{-1}]
Methanes								
H	-40.523989637157				-40.501525442575			
F	-437.604661912271				-437.541182245921			
Hx1	-40.523958818407				-40.501446942421			
xH1	-40.523952957948				-40.501434196638			
HH1	-81.048851651381	-0.547	-0.590	0.042	-81.003553381963	-0.315	-0.422	0.107
Hx2	-40.523938643624				-40.501394733956			
xH2	-40.523934636742				-40.501378294744			
HH2	-81.048619995006	-0.402	-0.469	0.067	-81.003311524393	-0.164	-0.338	0.174
Hx1	-40.523954720257				-40.501436128894			
xF1	-437.604640614853				-437.541140557009			
HF1	-478.129715242635	-0.667	-0.703	0.035	-478.043568259918	-0.540	-0.622	0.082
Hx2	-40.52398868047				-40.501525205944			
xF2	-437.604655117936				-437.541172358575			
HF2	-478.129197680029	-0.343	-0.348	0.005	-478.043195963977	-0.306	-0.313	0.006
Fx1	-437.604636895287				-437.541133784091			
xF1	-437.604633921286				-437.541122660487			
FF1	-875.210027471615	-0.442	-0.475	0.033	-875.083127853354	-0.479	-0.547	0.068
Fx2	-437.604636547421				-437.541126333705			
xF2	-437.60461399148				-437.541069463641			
FF2	-875.209681141116	-0.224	-0.270	0.046	-875.083115092591	-0.471	-0.577	0.106
Ethanes								
H	-79.841952885754				-79.80171482493			
F	-675.448326150121				-675.348142403687			
Hx1	-79.841965343636				-79.801710238646			
xH1	-79.841926996393				-79.801607002674			
HH1	-159.686114201806	-1.386	-1.394	0.008	-159.605183749063	-1.101	-1.171	0.071
Hx2	-79.841983721594				-79.801774040706			
xH2	-79.841987498528				-79.80179036455			
HH2	-159.685931987125	-1.271	-1.230	-0.041	-159.605162209406	-1.087	-1.003	-0.085
Hx1	-79.84195629888				-79.801699202244			
xF1	-675.448348741906				-675.34817193922			
HF1	-755.291684980701	-0.882	-0.866	-0.016	-755.15124127724	-0.869	-0.860	-0.009
Hx2	-79.841987844431				-79.801772945268			
xF2	-675.448272357927				-675.347943484417			
HF2	-755.291863624704	-0.994	-1.006	0.012	-755.15135631432	-0.941	-1.029	0.088
Hx3	-79.841960791932				-79.801713402284			
xF3	-675.448381829863				-675.348231835444			
HF3	-755.29145741176	-0.739	-0.700	-0.040	-755.151128114893	-0.797	-0.742	-0.055
Hx4	-79.842024474054				-79.801889026458			
xF4	-675.448346068047				-675.348160777516			
HF4	-755.291839284107	-0.979	-0.922	-0.057	-755.151543381146	-1.058	-0.937	-0.121
Fx1	-675.448303824525				-675.348099109757			
xF1	-675.448320250528				-675.348185542113			
FF1	-1350.89738287022	-0.458	-0.476	0.018	-1350.69779134423	-0.945	-0.945	0.000
Fx2	-675.448352028375				-675.348170135301			
xF2	-675.448355279647				-675.34817248712			
FF2	-1350.89732933296	-0.425	-0.390	-0.035	-1350.6975505268	-0.794	-0.758	-0.036

	ωB97X-D3/def2-QZVP				B2PLYP-D3/def2-QZVP			
	E [Ha]	BAE [kcal mol^{-1}]	BIE [kcal mol^{-1}]	E-def [kcal mol^{-1}]	E [Ha]	BAE [kcal mol^{-1}]	BIE [kcal mol^{-1}]	E-def [kcal mol^{-1}]
Propanes								
H	-119.162726065561				-119.105210215662			
F	-913.291719045601				-913.155050293842			
Hx1	-119.162695070299				-119.10514416426			
xH1	-119.162692889302				-119.105143096442			
HH1	-238.328850095919	-2.132	-2.173	0.040	-238.213251959607	-1.777	-1.860	0.084
Hx2	-119.162706441179				-119.105147026118			
xH2	-119.162703605184				-119.105149844914			
HH2	-238.327705821858	-1.414	-1.441	0.026	-238.212028075626	-1.009	-1.086	0.078
Hx1	-119.162716984175				-119.105202967554			
xF1	-913.29155321797				-913.15480750992			
HF1	-1032.45660270664	-1.354	-1.464	0.110	-1032.26234259515	-1.307	-1.463	0.157
Hx2	-119.162772681517				-119.105343906942			
xF2	-913.291550162414				-913.154685909976			
HF2	-1032.45604535644	-1.004	-1.081	0.077	-1032.26190882555	-1.034	-1.179	0.145
Hx3	-119.162738260944				-119.10522666714			
xF3	-913.291567156462				-913.154825449426			
HF3	-1032.45609706258	-1.037	-1.124	0.088	-1032.26190458293	-1.032	-1.162	0.131
Hx4	-119.162768485575				-119.10530053403			
xF4	-913.291522226192				-913.15464452575			
HF4	-1032.45581721102	-0.861	-0.958	0.097	-1032.26176526591	-0.944	-1.142	0.198
Fx1	-913.291493984464				-913.154750679567			
xF1	-913.291582517194				-913.154832708672			
FF1	-1826.58395235351	-0.323	-0.550	0.227	-1826.31180125185	-1.067	-1.392	0.325
Fx2	-913.291712160794				-913.155041347573			
xF2	-913.291705256765				-913.155029570048			
FF2	-1826.58408810623	-0.408	-0.421	0.013	-1826.31242949808	-1.461	-1.480	0.019
Butanes								
H	-158.483603881961				-158.408887655819			
F	-1151.13425298519				-1150.96116059696			
Hx1	-158.48349004351				-158.408626897532			
xH1	-158.483511459698				-158.40866740057			
HH1	-316.972065459881	-3.048	-3.178	0.129	-316.821645845627	-2.429	-2.731	0.302
Hx2	-158.483466320688				-158.408610158148			
xH2	-158.483486572891				-158.408627419287			
HH2	-316.970241636398	-1.904	-2.064	0.160	-316.819664647858	-1.186	-1.523	0.337
Hx1	-158.48354732995				-158.408830755428			
xF1	-1151.1339725387				-1150.96092036433			
HF1	-1309.62039470818	-1.593	-1.804	0.211	-1309.37294829445	-1.820	-2.006	0.186
Hx2	-158.483588010416				-158.408873263134			
xF2	-1151.13424019064				-1150.96114954222			
HF2	-1309.62065279537	-1.754	-1.772	0.018	-1309.37308930181	-1.908	-1.924	0.016
Hx3	-158.483515962317				-158.4087814023			
xF3	-1151.13422976682				-1150.96111582064			
HF3	-1309.62054294867	-1.686	-1.755	0.070	-1309.37297091449	-1.834	-1.929	0.095
Hx4	-158.483518180739				-158.408773871218			
xF4	-1151.13427030414				-1150.96120481247			
HF4	-1309.62077132318	-1.829	-1.872	0.043	-1309.3730294492	-1.871	-1.914	0.044
Fx1	-1151.13425764979				-1150.96118010287			
xF1	-1151.13416854247				-1150.96111256877			
FF1	-2302.27002381851	-0.952	-1.003	0.050	-2301.92513364923	-1.765	-1.783	0.018
Fx2	-1151.13420064653				-1150.96113065191			
xF2	-1151.13416285207				-1150.9611182198			
FF2	-2302.26990137633	-0.876	-0.965	0.089	-2301.92525259683	-1.839	-1.885	0.045

	ωB97X-D3/def2-QZVP				B2PLYP-D3/def2-QZVP			
	E [Ha]	BAE [kcal mol^{-1}]	BIE [kcal mol^{-1}]	E-def [kcal mol^{-1}]	E [Ha]	BAE [kcal mol^{-1}]	BIE [kcal mol^{-1}]	E-def [kcal mol^{-1}]
Pentanes								
H	-197.804347904371				-197.712361038809			
F	-1388.97697980544				-1388.76760173007			
Hx1	-197.804223766805				-197.712087919601			
xH1	-197.804222482112				-197.712086405016			
HH1	-395.615046486167	-3.985	-4.142	0.157	-395.429871069013	-3.231	-3.575	0.344
Hx2	-197.804224068999				-197.712028914123			
xH2	-197.804225500517				-197.71203319141			
HH2	-395.612918324993	-2.650	-2.804	0.155	-395.427117971479	-1.503	-1.918	0.414
Hx1	-197.804224254005				-197.712204066394			
xF1	-1388.97691771509				-1388.76752380962			
HF1	-1586.78499878521	-2.304	-2.420	0.117	-1586.48375666583	-2.381	-2.528	0.147
Hx2	-197.804311161946				-197.712324581324			
xF2	-1388.97670903974				-1388.76728895971			
HF2	-1586.78448732797	-1.983	-2.176	0.193	-1586.48334090172	-2.120	-2.339	0.219
Hx3	-197.804293796985				-197.71222655078			
xF3	-1388.97700660947				-1388.76755484894			
HF3	-1586.78463209596	-2.074	-2.091	0.017	-1586.48345527394	-2.192	-2.305	0.114
Hx4	-197.804301042282				-197.712283326489			
xF4	-1388.97700293732				-1388.76763965797			
HF4	-1586.78532871107	-2.511	-2.526	0.015	-1586.48412805957	-2.614	-2.639	0.025
Fx1	-1388.97695969876				-1388.7675389959			
xF1	-1388.97691785676				-1388.76753067382			
FF1	-2777.95575603242	-1.127	-1.179	0.051	-2777.53912677457	-2.462	-2.546	0.084
Fx2	-1388.9769331607				-1388.76751015058			
xF2	-1388.97693387251				-1388.76751466087			
FF2	-2777.95577326012	-1.138	-1.196	0.058	-2777.53869663949	-2.192	-2.304	0.112
Hexanes								
H	-237.125118325372				-237.015822517878			
F	-1626.81975475692				-1626.57403644275			
Hx1	-237.124964081574				-237.015536615949			
xH1	-237.12496706719				-237.015538978194			
HH1	-474.257659667059	-4.658	-4.850	0.192	-474.037695992657	-3.797	-4.154	0.357
Hx2	-237.12496511198				-237.015471000698			
xH2	-237.124959201718				-237.015460028627			
HH2	-474.255328318038	-3.195	-3.391	0.196	-474.034799057409	-1.979	-2.427	0.448
Hx1	-237.124901996346				-237.015565777105			
xF1	-1626.81925712925				-1626.57347489366			
HF1	-1863.94854834778	-2.306	-2.754	0.448	-1863.59376760533	-2.453	-2.966	0.513
Hx2	-237.125029189562				-237.015735172815			
xF2	-1626.8193767355				-1626.57363065423			
HF2	-1863.94866330396	-2.378	-2.672	0.293	-1863.59402880792	-2.617	-2.926	0.309
Hx3	-237.124922336206				-237.015576673154			
xF3	-1626.8194470484				-1626.57369241852			
HF3	-1863.9487005088	-2.402	-2.718	0.316	-1863.59387350454	-2.519	-2.889	0.370
Hx4	-237.125094592074				-237.015803753604			
xF4	-1626.819717558				-1626.57401459891			
HF4	-1863.94934295751	-2.805	-2.843	0.038	-1863.59457044326	-2.956	-2.982	0.025
Fx1	-1626.81969422358				-1626.57396307011			
xF1	-1626.8196370696				-1626.57389438932			
FF1	-3253.64174854085	-1.405	-1.517	0.112	-3253.15315918619	-3.192	-3.327	0.135
Fx2	-1626.81958770749				-1626.57386470851			
xF2	-1626.81958872181				-1626.57386612718			
FF2	-3253.6402260916	-0.450	-0.659	0.209	-3253.15137948001	-2.075	-2.290	0.215

	B97M-V/def2-QZVP				ωB97M-V/def2-QZVP			
	E [Ha]	BAE [kcal mol^{-1}]	BIE [kcal mol^{-1}]	E-def [kcal mol^{-1}]	E [Ha]	BAE [kcal mol^{-1}]	BIE [kcal mol^{-1}]	E-def [kcal mol^{-1}]
Methanes								
H	-40.5346275635259				-40.4957485046463			
F	-437.567748985576				-437.613280285495			
Hx1	-40.5346279941849				-40.4957476962338			
xH1	-40.5346247297872				-40.4957471970221			
HH1	-81.0699247132812	-0.420	-0.422	0.002	-80.9922062646482	-0.445	-0.446	0.001
Hx2	-40.5346145302907				-40.4957483738133			
xH2	-40.5346145512595				-40.4957478718937			
HH2	-81.069772953125	-0.325	-0.341	0.016	-80.9920540519836	-0.350	-0.350	0.000
Hx1	-40.5346178172627				-40.4957471698063			
xF1	-437.567736175916				-437.613286002039			
HF1	-478.103530368362	-0.724	-0.738	0.014	-478.110294093698	-0.794	-0.791	-0.003
Hx2	-40.5346206892954				-40.4957467708123			
xF2	-437.567733592544				-437.613278250184			
HF2	-478.10302721959	-0.408	-0.422	0.014	-478.109724388104	-0.436	-0.439	0.002
Fx1	-437.567739928678				-437.613283661763			
xF1	-437.56774125294				-437.613285923743			
FF1	-875.136811462286	-0.824	-0.835	0.011	-875.228020669945	-0.916	-0.911	-0.006
Fx2	-437.567737482119				-437.613282413706			
xF2	-437.567741311718				-437.613284222453			
FF2	-875.13677297774	-0.800	-0.812	0.012	-875.227932974225	-0.861	-0.857	-0.004
Ethanes								
H	-79.8634676185315				-79.799771959001			
F	-675.401483616651				-675.463447286677			
Hx1	-79.8634844120543				-79.7997728170933			
xH1	-79.863460913367				-79.79977221734			
HH1	-159.728890124617	-1.227	-1.220	-0.006	-159.601538230249	-1.251	-1.251	-0.001
Hx2	-79.8634675051755				-79.7997721413314			
xH2	-79.8634685947661				-79.7997722602839			
HH2	-159.728711983365	-1.115	-1.114	-0.001	-159.601272359127	-1.085	-1.084	0.000
Hx1	-79.8634630201355				-79.7997690954954			
xF1	-675.401451126738				-675.463452268948			
HF1	-755.266529348869	-0.990	-1.014	0.023	-755.264975628052	-1.102	-1.101	-0.001
Hx2	-79.8634810660224				-79.7997721460025			
xF2	-675.401447878314				-675.463462280309			
HF2	-755.266806810393	-1.164	-1.178	0.014	-755.265257510737	-1.279	-1.270	-0.010
Hx3	-79.8634860682731				-79.7997723075836			
xF3	-675.40145709312				-675.463453606389			
HF3	-755.266293482318	-0.842	-0.847	0.005	-755.264707655317	-0.934	-0.930	-0.004
Hx4	-79.8634696687753				-79.799770814186			
xF4	-675.40146509215				-675.463456299702			
HF4	-755.266701156412	-1.098	-1.108	0.010	-755.265131492954	-1.200	-1.195	-0.005
Fx1	-675.401462834626				-675.463444391719			
xF1	-675.401425395704				-675.4634096174			
FF1	-1350.80494647974	-1.242	-1.292	0.050	-1350.92912982858	-1.403	-1.428	0.025
Fx2	-675.401443320877				-675.46345649593			
xF2	-675.401457663878				-675.463443424911			
FF2	-1350.80453933562	-0.987	-1.028	0.042	-1350.92869936838	-1.133	-1.129	-0.003

	B97M-V/def2-QZVP				ωB97M-V/def2-QZVP			
	E [Ha]	BAE [kcal mol^{-1}]	BIE [kcal mol^{-1}]	E-def [kcal mol^{-1}]	E [Ha]	BAE [kcal mol^{-1}]	BIE [kcal mol^{-1}]	E-def [kcal mol^{-1}]
Propanes								
H	-119.195746349543				-119.107038420108			
F	-913.235611080036				-913.313990815918			
Hx1	-119.195751040919				-119.107040019672			
xH1	-119.195751235565				-119.107040513007			
HH1	-238.39464926539	-1.981	-1.975	-0.006	-238.217140494273	-1.922	-1.920	-0.002
Hx2	-119.195739574173				-119.107038139443			
xH2	-119.195751301128				-119.10703954224			
HH2	-238.393564206149	-1.300	-1.301	0.001	-238.215968431749	-1.187	-1.186	-0.001
Hx1	-119.195747158019				-119.107034110003			
xF1	-913.235520036749				-913.313926445028			
HF1	-1032.43412446875	-1.736	-1.793	0.057	-1032.42389439752	-1.798	-1.841	0.043
Hx2	-119.195743229829				-119.107036115086			
xF2	-913.235560448272				-913.313977042428			
HF2	-1032.43353788276	-1.368	-1.402	0.034	-1032.42330712558	-1.429	-1.439	0.010
Hx3	-119.195723331443				-119.107032036408			
xF3	-913.235563818858				-913.313967916387			
HF3	-1032.43346160282	-1.320	-1.364	0.044	-1032.42327916938	-1.412	-1.430	0.018
Hx4	-119.195749362503				-119.107037004719			
xF4	-913.23555428915				-913.313966963938			
HF4	-1032.43357510583	-1.392	-1.425	0.034	-1032.42329048709	-1.419	-1.435	0.016
Fx1	-913.235469341764				-913.31383468207			
xF1	-913.235578542832				-913.313949338467			
FF1	-1826.47408473935	-1.796	-1.906	0.109	-1826.63103234849	-1.914	-2.038	0.124
Fx2	-913.235612323517				-913.313987791468			
xF2	-913.235615386666				-913.313989209126			
FF2	-1826.47469791244	-2.181	-2.178	-0.003	-1826.63157041598	-2.252	-2.255	0.003
Butanes								
H	-158.528256438714				-158.414400341613			
F	-1151.06934645219				-1151.1640864102			
Hx1	-158.528262190079				-158.414400900464			
xH1	-158.52825623994				-158.414398581128			
HH1	-317.061134263997	-2.900	-2.896	-0.003	-316.833382584199	-2.875	-2.876	0.001
Hx2	-158.528249584874				-158.414392074961			
xH2	-158.528251642459				-158.414399841277			
HH2	-317.059063280091	-1.600	-1.608	0.007	-316.831466359715	-1.673	-1.678	0.006
Hx1	-158.52825034829				-158.414397671149			
xF1	-1151.06898226145				-1151.16366761481			
HF1	-1309.60073427327	-1.965	-2.197	0.232	-1309.58192322833	-2.156	-2.421	0.264
Hx2	-158.52823774443				-158.414385410504			
xF2	-1151.06933204032				-1151.16407399966			
HF2	-1309.60105583654	-2.167	-2.188	0.021	-1309.5823188575	-2.405	-2.422	0.017
Hx3	-158.528239204002				-158.414375365031			
xF3	-1151.06927688162				-1151.16401449552			
HF3	-1309.60112646316	-2.211	-2.266	0.054	-1309.58221193721	-2.338	-2.398	0.061
Hx4	-158.52821183069				-158.414357925721			
xF4	-1151.06935916862				-1151.16409150155			
HF4	-1309.60108941313	-2.188	-2.208	0.020	-1309.58217743759	-2.316	-2.339	0.023
Fx1	-1151.06930291287				-1151.16402939764			
xF1	-1151.06928533926				-1151.1640367469			
FF1	-2302.14220640668	-2.205	-2.270	0.066	-2302.33203272416	-2.422	-2.489	0.067
Fx2	-1151.06921196654				-1151.16394851121			
xF2	-1151.06926765903				-1151.16398611436			
FF2	-2302.14260320689	-2.454	-2.588	0.134	-2302.33234525607	-2.618	-2.768	0.149

	B97M-V/def2-QZVP				ωB97M-V/def2-QZVP			
	E [Ha]	BAE [kcal mol^{-1}]	BIE [kcal mol^{-1}]	E-def [kcal mol^{-1}]	E [Ha]	BAE [kcal mol^{-1}]	BIE [kcal mol^{-1}]	E-def [kcal mol^{-1}]
Pentanes								
H	-197.860420190153				-197.721684828828			
F	-1388.90335480808				-1389.01437615101			
Hx1	-197.860427954992				-197.72168355061			
xH1	-197.860428009057				-197.721683538158			
HH1	-395.72725042996	-4.022	-4.013	-0.010	-395.449466982842	-3.826	-3.828	0.002
Hx2	-197.860419374304				-197.72168020287			
xH2	-197.860419308318				-197.721680192709			
HH2	-395.724782048332	-2.473	-2.474	0.001	-395.447055883623	-2.313	-2.319	0.006
Hx1	-197.860362802645				-197.721592909566			
xF1	-1388.90313394693				-1389.01419305294			
HF1	-1586.76833452294	-2.861	-3.036	0.175	-1586.74095269262	-3.070	-3.242	0.173
Hx2	-197.860386963496				-197.721651403275			
xF2	-1388.90297341392				-1389.01398801318			
HF2	-1586.76769650998	-2.461	-2.721	0.260	-1586.74026116524	-2.636	-2.900	0.265
Hx3	-197.860419965385				-197.721673539593			
xF3	-1388.90327547579				-1389.01433273858			
HF3	-1586.76811046652	-2.721	-2.770	0.050	-1586.7405471167	-2.815	-2.849	0.034
Hx4	-197.860403595305				-197.721654258961			
xF4	-1388.90330580609				-1389.01434436298			
HF4	-1586.76874488396	-3.119	-3.160	0.041	-1586.74126733087	-3.267	-3.306	0.039
Fx1	-1388.90332861873				-1389.01434732485			
xF1	-1388.90322727535				-1389.01426868359			
FF1	-2777.81202574803	-3.336	-3.432	0.096	-2778.03455550893	-3.642	-3.727	0.086
Fx2	-1388.90329675328				-1389.01430694186			
xF2	-1388.90329883243				-1389.01430989324			
FF2	-2777.81154904871	-3.037	-3.108	0.072	-2778.03400258757	-3.295	-3.380	0.085
Hexanes								
H	-237.192833856703				-237.029020009266			
F	-1626.73729652087				-1626.86466363313			
Hx1	-237.19284438643				-237.029016679569			
xH1	-237.192844278365				-237.029016563773			
HH1	-474.393219481582	-4.739	-4.726	-0.013	-474.065308054862	-4.561	-4.565	0.004
Hx2	-237.19283615573				-237.029017404975			
xH2	-237.19283597222				-237.029017250157			
HH2	-474.390341587435	-2.933	-2.930	-0.003	-474.062647937146	-2.892	-2.895	0.003
Hx1	-237.192672123572				-237.028850242377			
xF1	-1626.73663012081				-1626.86406776417			
HF1	-1863.93516865747	-3.162	-3.681	0.520	-1863.8991389047	-3.423	-3.904	0.480
Hx2	-237.19277205658				-237.028936080516			
xF2	-1626.73677829964				-1626.86419522586			
HF2	-1863.93487160703	-2.975	-3.339	0.364	-1863.89888879657	-3.266	-3.613	0.347
Hx3	-237.192733450481				-237.028904043426			
xF3	-1626.73699148147				-1626.86434932274			
HF3	-1863.93532506853	-3.260	-3.514	0.254	-1863.89920268402	-3.463	-3.733	0.270
Hx4	-237.192820554453				-237.028999680929			
xF4	-1626.73721092159				-1626.86459071103			
HF4	-1863.93568561775	-3.486	-3.548	0.062	-1863.89952682884	-3.667	-3.725	0.059
Fx1	-1626.73724201235				-1626.86461397394			
xF1	-1626.73721598677				-1626.86458414399			
FF1	-3253.48167011514	-4.441	-4.526	0.085	-3253.73707536975	-4.862	-4.943	0.081
Fx2	-1626.73729341561				-1626.86462285499			
xF2	-1626.7372905027				-1626.8646201186			
FF2	-3253.4796346857	-3.164	-3.169	0.006	-3253.73473241604	-3.392	-3.445	0.053

	GFN1-xTB				GFN2-xTB			
	E [Ha]	BAE [kcal mol^{-1}]	BIE [kcal mol^{-1}]	E-def [kcal mol^{-1}]	E [Ha]	BAE [kcal mol^{-1}]	BIE [kcal mol^{-1}]	E-def [kcal mol^{-1}]
Methanes								
H	-4.2742696				-4.1751772			
F	-22.6940918				-21.0784782			
Hx1	-4.2742692				-4.1751781			
xH1	-4.2742691				-4.1751779			
HH1	-8.5491539	-0.386	-0.386	0.001	-8.3509684	-0.385	-0.384	-0.001
Hx2	-4.2742694				-4.175177			
xH2	-4.2742694				-4.175177			
HH2	-8.5490736	-0.335	-0.336	0.000	-8.3509953	-0.402	-0.402	0.000
Hx1	-4.2742695				-4.1751775			
xF1	-22.6940844				-21.078461			
HF1	-26.9692182	-0.538	-0.542	0.005	-25.2552051	-0.972	-0.983	0.011
Hx2	-4.274269				-4.1751774			
xF2	-22.6940862				-21.0784656			
HF2	-26.9689881	-0.393	-0.397	0.004	-25.2543451	-0.433	-0.441	0.008
Fx1	-22.6940837				-21.0784644			
xF1	-22.6940859				-21.0784657			
FF1	-45.3888706	-0.431	-0.440	0.009	-42.157921	-0.605	-0.622	0.017
Fx2	-22.6940858				-21.0784645			
xF2	-22.6940851				-21.0784651			
FF2	-45.389012	-0.520	-0.528	0.008	-42.1587683	-1.137	-1.154	0.017
Ethanes								
H	-7.4698011				-7.3362538			
F	-35.0833459				-32.6629925			
Hx1	-7.4697937				-7.3362454			
xH1	-7.4697931				-7.3362451			
HH1	-14.9405102	-0.570	-0.579	0.010	-14.6737975	-0.809	-0.820	0.011
Hx2	-7.469805				-7.3362563			
xH2	-7.4698048				-7.336256			
HH2	-14.9407083	-0.694	-0.689	-0.005	-14.6738098	-0.817	-0.814	-0.003
Hx1	-7.4697961				-7.3362487			
xF1	-35.0833841				-32.6630363			
HF1	-42.5546094	-0.918	-0.897	-0.021	-40.000975	-1.085	-1.060	-0.024
Hx2	-7.4698035				-7.3362565			
xF2	-35.0833714				-32.6630238			
HF2	-42.5547999	-1.037	-1.020	-0.018	-40.0014073	-1.356	-1.335	-0.021
Hx3	-7.4698018				-7.3362549			
xF3	-35.0834075				-32.6630687			
HF3	-42.5544514	-0.819	-0.779	-0.039	-40.0007921	-0.970	-0.921	-0.049
Hx4	-7.4697963				-7.3362503			
xF4	-35.0833905				-32.663046			
HF4	-42.5547811	-1.025	-1.000	-0.025	-40.00123	-1.245	-1.213	-0.031
Fx1	-35.0833412				-32.6629955			
xF1	-35.0833382				-32.6629733			
FF1	-70.1680971	-0.882	-0.890	0.008	-65.3283223	-1.467	-1.477	0.010
Fx2	-35.0833867				-32.6630406			
xF2	-35.0833903				-32.6630414			
FF2	-70.1678576	-0.732	-0.678	-0.053	-65.327514	-0.959	-0.899	-0.061

	GFN1-xTB				GFN2-xTB			
	E [Ha]	BAE [kcal mol^{-1}]	BIE [kcal mol^{-1}]	E-def [kcal mol^{-1}]	E [Ha]	BAE [kcal mol^{-1}]	BIE [kcal mol^{-1}]	E-def [kcal mol^{-1}]
Propanes								
H	-10.6678644				-10.5006884			
F	-47.478235				-44.2593142			
Hx1	-10.667849				-10.5006704			
xH1	-10.6678495				-10.5006713			
HH1	-21.3377442	-1.265	-1.284	0.019	-21.0034143	-1.279	-1.301	0.022
Hx2	-10.6678618				-10.5006749			
xH2	-10.6678592				-10.5006797			
HH2	-21.3375013	-1.112	-1.117	0.005	-21.0030408	-1.044	-1.058	0.014
Hx1	-10.667857				-10.5006844			
xF1	-47.4781965				-44.2592979			
HF1	-58.1484026	-1.445	-1.474	0.029	-54.7631668	-1.986	-1.998	0.013
Hx2	-10.6678692				-10.5006904			
xF2	-47.4782409				-44.259336			
HF2	-58.1480296	-1.211	-1.205	-0.007	-54.762107	-1.321	-1.306	-0.015
Hx3	-10.6678763				-10.5006824			
xF3	-47.478166				-44.2592531			
HF3	-58.1478846	-1.120	-1.156	0.036	-54.7624164	-1.515	-1.557	0.042
Hx4	-10.6678609				-10.5006869			
xF4	-47.4782496				-44.2593396			
HF4	-58.1481061	-1.259	-1.252	-0.007	-54.7620801	-1.304	-1.289	-0.015
Fx1	-47.4781669				-44.2592672			
xF1	-47.4781744				-44.2592326			
FF1	-94.958487	-1.266	-1.346	0.081	-88.5215965	-1.863	-1.943	0.081
Fx2	-47.4782286				-44.2592935			
xF2	-47.4782255				-44.2592879			
FF2	-94.9584804	-1.262	-1.272	0.010	-88.5210537	-1.522	-1.551	0.029
Butanes								
H	-13.8657005				-13.6649277			
F	-59.8743382				-55.8564535			
Hx1	-13.8656727				-13.6649028			
xH1	-13.8656729				-13.6649012			
HH1	-27.7342996	-1.819	-1.854	0.035	-27.3327093	-1.791	-1.823	0.032
Hx2	-13.8656857				-13.6649116			
xH2	-13.8656895				-13.6649131			
HH2	-27.734063	-1.670	-1.687	0.016	-27.332256	-1.506	-1.526	0.019
Hx1	-13.8656974				-13.6649209			
xF1	-59.8742641				-55.855973			
HF1	-73.7432699	-2.028	-2.076	0.048	-69.5252193	-2.408	-2.714	0.306
Hx2	-13.8656844				-13.6649098			
xF2	-59.8743571				-55.8564096			
HF2	-73.7432047	-1.987	-1.985	-0.002	-69.5250389	-2.295	-2.334	0.039
Hx3	-13.8656755				-13.6649073			
xF3	-59.8742799				-55.8562086			
HF3	-73.7431685	-1.964	-2.016	0.052	-69.5248617	-2.184	-2.351	0.166
Hx4	-13.8656489				-13.6648761			
xF4	-59.8743031				-55.8563515			
HF4	-73.74315	-1.952	-2.007	0.054	-69.5252092	-2.402	-2.498	0.096
Fx1	-59.8743214				-55.8563084			
xF1	-59.8742851				-55.8564035			
FF1	-119.7511698	-1.565	-1.608	0.044	-111.7159843	-1.931	-2.053	0.122
Fx2	-59.8743327				-55.8562082			
xF2	-59.8743167				-55.8562336			
FF2	-119.7513298	-1.665	-1.682	0.017	-111.7159599	-1.916	-2.208	0.292

	GFN1-xTB				GFN2-xTB			
	E [Ha]	BAE [kcal mol^{-1}]	BIE [kcal mol^{-1}]	E-def [kcal mol^{-1}]	E [Ha]	BAE [kcal mol^{-1}]	BIE [kcal mol^{-1}]	E-def [kcal mol^{-1}]
Pentanes								
H	-17.0636017				-16.8291968			
F	-72.2702448				-67.4531152			
Hx1	-17.0635767				-16.8291766			
xH1	-17.0635767				-16.8291767			
HH1	-34.1311917	-2.503	-2.534	0.031	-33.6621913	-2.383	-2.408	0.025
Hx2	-17.0635417				-16.8291432			
xH2	-17.0635416				-16.8291431			
HH2	-34.1308895	-2.313	-2.388	0.075	-33.6615485	-1.980	-2.047	0.067
Hx1	-17.0635349				-16.8291103			
xF1	-72.2702331				-67.4529268			
HF1	-89.3378093	-2.487	-2.536	0.049	-84.2866131	-2.699	-2.871	0.173
Hx2	-17.063592				-16.829182			
xF2	-72.2701361				-67.4528301			
HF2	-89.3373658	-2.208	-2.283	0.074	-84.28638	-2.553	-2.741	0.188
Hx3	-17.0635774				-16.8291771			
xF3	-72.2702059				-67.4529919			
HF3	-89.3375131	-2.301	-2.340	0.040	-84.286467	-2.607	-2.697	0.090
Hx4	-17.0635703				-16.8291588			
xF4	-72.2702151				-67.45299			
HF4	-89.3382124	-2.740	-2.778	0.038	-84.2877218	-3.395	-3.497	0.102
Fx1	-72.2702465				-67.4531375			
xF1	-72.2701741				-67.4530318			
FF1	-144.544152	-2.298	-2.341	0.043	-134.9106641	-2.782	-2.821	0.038
Fx2	-72.2701706				-67.4529609			
xF2	-72.2701712				-67.4529641			
FF2	-144.5436885	-2.007	-2.100	0.093	-134.9105592	-2.716	-2.908	0.192
Hexanes								
H	-20.2615114				-19.993518			
F	-84.6661981				-79.0497328			
Hx1	-20.2614814				-19.9934906			
xH1	-20.2614812				-19.9934906			
HH1	-40.5277942	-2.994	-3.032	0.038	-39.9913636	-2.716	-2.750	0.034
Hx2	-20.2614866				-19.9934879			
xH2	-20.2614866				-19.993488			
HH2	-40.5275329	-2.830	-2.861	0.031	-39.9908767	-2.410	-2.448	0.038
Hx1	-20.261371				-19.9933547			
xF1	-84.6661926				-79.0494161			
HF1	-104.9325144	-3.015	-3.107	0.092	-99.0476992	-2.791	-3.093	0.301
Hx2	-20.2614556				-19.9934451			
xF2	-84.6661703				-79.0494934			
HF2	-104.9322243	-2.833	-2.886	0.052	-99.0484417	-3.257	-3.453	0.196
Hx3	-20.2614009				-19.9933942			
xF3	-84.6661321				-79.0495118			
HF3	-104.9324373	-2.967	-3.077	0.111	-99.0483868	-3.223	-3.439	0.216
Hx4	-20.26149				-19.9934927			
xF4	-84.6662103				-79.0496579			
HF4	-104.9327494	-3.163	-3.168	0.006	-99.0492782	-3.782	-3.845	0.063
Fx1	-84.6662603				-79.0498048			
xF1	-84.6661137				-79.0496731			
FF1	-169.3374135	-3.148	-3.162	0.014	-158.1054502	-3.755	-3.748	-0.008
Fx2	-84.6660886				-79.0497135			
xF2	-84.6660887				-79.0497093			
FF2	-169.3358244	-2.151	-2.289	0.137	-158.1043577	-3.070	-3.097	0.027

	CCSD(T)/CBS(34)				CCSD(T)-F12/cc-pVTZ-F12			
	E [Ha]	BAE [kcal mol^{-1}]	BIE [kcal mol^{-1}]	E-def [kcal mol^{-1}]	E [Ha]	BAE [kcal mol^{-1}]	BIE [kcal mol^{-1}]	E-def [kcal mol^{-1}]
Methanes								
H	-40.458835527101				-40.45435366861			
F	-437.223954430823				-437.196105711662			
Hx1	-40.458834706746				-40.454352711424			
xH1	-40.458834717192				-40.454352729683			
HH1	-80.918492058307	-0.515	-0.516	0.001	-80.909526118263	-0.514	-0.515	0.001
Hx2	-40.458835276684				-40.454353408584			
xH2	-40.458835303851				-40.454353444011			
HH2	-80.918319964781	-0.407	-0.407	0.000	-80.909349843905	-0.403	-0.403	0.000
Hx1	-40.458835268385				-40.454353365614			
xF1	-437.223941360422				-437.196096332932			
HF1	-477.684050987955	-0.791	-0.800	0.008	-477.651705876698	-0.782	-0.788	0.006
Hx2	-40.458834628794				-40.454352680522			
xF2	-437.223944619657				-437.196098546992			
HF2	-477.683463240106	-0.422	-0.429	0.007	-477.65115094201	-0.434	-0.439	0.005
Fx1	-437.223941775041				-437.196095349424			
xF1	-437.223944397226				-437.196098227114			
FF1	-874.449194822515	-0.807	-0.821	0.014	-874.39350561	-0.812	-0.823	0.011
Fx2	-437.22394399808				-437.196098160978			
xF2	-437.22394355781				-437.196097317972			
FF2	-874.449076217401	-0.733	-0.746	0.013	-874.39354404	-0.836	-0.846	0.010
Ethanes								
H	-79.7138450153				-79.70583503191			
F	-674.847888197				-674.80435257993			
Hx1	-79.7138452637				-79.705835449029			
xH1	-79.7138454003				-79.705835579999			
HH1	-159.429906212	-1.391	-1.390	0.000	-159.413841250544	-1.362	-1.362	-0.001
Hx2	-79.7138461745				-79.705836312437			
xH2	-79.7138461967				-79.705836348597			
HH2	-159.429649819	-1.230	-1.228	-0.001	-159.413578137522	-1.197	-1.196	-0.002
Hx1	-79.7138414857				-79.705831263297			
xF1	-674.847870399				-674.804342241885			
HF1	-754.563396384	-1.044	-1.057	0.013	-754.511897859996	-1.073	-1.082	0.009
Hx2	-79.7138447957				-79.705834711312			
xF2	-674.847863242				-674.804337089012			
HF2	-754.56365468	-1.206	-1.222	0.016	-754.51217783368	-1.249	-1.259	0.010
Hx3	-79.7138447729				-79.705834703832			
xF3	-674.847874756				-674.804346513413			
HF3	-754.563187335	-0.912	-0.921	0.009	-754.511681101996	-0.937	-0.941	0.004
Hx4	-79.7138426297				-79.705832418504			
xF4	-674.847881523				-674.804350855375			
HF4	-754.5635855	-1.162	-1.168	0.006	-754.512089033869	-1.193	-1.196	0.003
Fx1	-674.847870779				-674.804338967135			
xF1	-674.847842902				-674.804311243574			
FF1	-1349.69774921	-1.238	-1.277	0.039	-1349.61078209367	-1.303	-1.338	0.034
Fx2	-674.847862818				-674.804336120495			
xF2	-674.847878159				-674.804346634521			
FF2	-1349.69740997	-1.025	-1.047	0.022	-1349.6103776125	-1.049	-1.064	0.014

	CCSD(T)/CBS(LPNO-CEPA/1)				CCSD(T)/CBS(MP2)			
	E [Ha]	BAE [kcal mol^{-1}]	BIE [kcal mol^{-1}]	E-def [kcal mol^{-1}]	E [Ha]	BAE [kcal mol^{-1}]	BIE [kcal mol^{-1}]	E-def [kcal mol^{-1}]
Methanes								
H	-40.4564853618				-40.4632579788			
F	-437.207904623				-437.225925685			
Hx1	-40.4564845778				-40.4632569638			
xH1	-40.4564845839				-40.4632569849			
HH1	-80.913723895	-0.473	-0.474	0.001	-80.927347218	-0.522	-0.523	0.001
Hx2	-40.4564851119				-40.4632577139			
xH2	-40.4564851404				-40.4632577534			
HH2	-80.9135240798	-0.347	-0.348	0.000	-80.9271742318	-0.413	-0.413	0.000
Hx1	-40.4564851171				-40.4632576571			
xF1	-437.207886651				-437.225917531			
HF1	-477.665767595	-0.864	-0.876	0.011	-477.690700627	-0.952	-0.957	0.005
Hx2	-40.4564844873				-40.4632569533			
xF2	-437.207892259				-437.225919405			
HF2	-477.665121095	-0.459	-0.467	0.008	-477.690079237	-0.562	-0.567	0.005
Fx1	-437.207888553				-437.2259161			
xF1	-437.207891506				-437.225919049			
FF1	-874.41713011	-0.829	-0.847	0.018	-874.453433305	-0.993	-1.003	0.010
Fx2	-437.207890753				-437.225919088			
xF2	-437.207888541				-437.225918125			
FF2	-874.417154865	-0.844	-0.863	0.019	-874.453417584	-0.983	-0.992	0.009
Ethanes								
H	-79.7091919342				-79.7212675812			
F	-674.822345166				-674.852088075			
Hx1	-79.7091881043				-79.7212678453			
xH1	-79.7091902863				-79.7212680513			
HH1	-159.420507656	-1.333	-1.336	0.003	-159.444715599	-1.368	-1.368	0.000
Hx2	-79.7091843925				-79.7212685565			
xH2	-79.7091840582				-79.7212685932			
HH2	-159.420317214	-1.213	-1.223	0.010	-159.444450167	-1.202	-1.200	-0.001
Hx1	-79.7091861193				-79.7212637383			
xF1	-674.82231885				-674.852079549			
HF1	-754.533408886	-1.175	-1.195	0.020	-754.575383674	-1.273	-1.280	0.008
Hx2	-79.7091893595				-79.7212670805			
xF2	-674.822316344				-674.85207526			
HF2	-754.533737159	-1.381	-1.400	0.020	-754.575703261	-1.473	-1.481	0.008
Hx3	-79.7091916675				-79.7212670955			
xF3	-674.822327984				-674.852082795			
HF3	-754.533186584	-1.035	-1.046	0.011	-754.575109569	-1.101	-1.104	0.004
Hx4	-79.7091914325				-79.7212649525			
xF4	-674.822329425				-674.852086932			
HF4	-754.533616941	-1.305	-1.315	0.010	-754.575592487	-1.404	-1.406	0.002
Fx1	-674.822316889				-674.852075278			
xF1	-674.822509246				-674.852049182			
FF1	-1349.64711979	-1.525	-1.439	-0.085	-1349.70662753	-1.538	-1.571	0.032
Fx2	-674.822308924				-674.852073779			
xF2	-674.822327979				-674.852082752			
FF2	-1349.64646961	-1.117	-1.150	0.034	-1349.70611771	-1.218	-1.231	0.012

	CCSD(T)/CBS(LPNO-CEPA/1)				CCSD(T)/CBS(MP2)			
	E [Ha]	BAE [kcal mol^{-1}]	BIE [kcal mol^{-1}]	E-def [kcal mol^{-1}]	E [Ha]	BAE [kcal mol^{-1}]	BIE [kcal mol^{-1}]	E-def [kcal mol^{-1}]
Propanes								
H	-118.965353755				-118.982669996			
F	-912.437655968				-912.478703185			
Hx1	-118.965348083				-118.982665214			
xH1	-118.965349908				-118.982665615			
HH1	-237.933847853	-1.971	-1.977	0.006	-237.968529133	-2.001	-2.007	0.006
Hx2	-118.965348909				-118.982666863			
xH2	-118.965349885				-118.982665607			
HH2	-237.93270847	-1.256	-1.261	0.005	-237.967300652	-1.230	-1.235	0.005
Hx1	-118.965348859				-118.982664774			
xF1	-912.437461087				-912.478628787			
HF1	-1031.40590608	-1.817	-1.943	0.125	-1031.46454325	-1.989	-2.039	0.050
Hx2	-118.9653506				-118.982667866			
xF2	-912.437577231				-912.478667995			
HF2	-1031.40538374	-1.490	-1.541	0.051	-1031.46396683	-1.628	-1.651	0.023
Hx3	-118.965351507				-118.982672817			
xF3	-912.437516045				-912.478658971			
HF3	-1031.40527507	-1.422	-1.511	0.089	-1031.46392093	-1.599	-1.625	0.026
Hx4	-118.965347544				-118.982664418			
xF4	-912.437622762				-912.478657386			
HF4	-1031.40545173	-1.532	-1.557	0.025	-1031.46400574	-1.652	-1.684	0.032
Fx1	-912.43739287				-912.478550971			
xF1	-912.437577494				-912.478663612			
FF1	-1824.87823528	-1.834	-2.049	0.214	-1824.96079523	-2.127	-2.247	0.120
Fx2	-912.437637249				-912.478699771			
xF2	-912.43763246				-912.478702192			
FF2	-1824.8789201	-2.264	-2.291	0.026	-1824.96135146	-2.476	-2.478	0.003
Butanes								
H	-158.221640465				-158.24418516			
F	-1150.05230427				-1150.1049852			
Hx1	-158.221639528				-158.244180372			
xH1	-158.22163919				-158.244179874			
HH1	-316.447849443	-2.867	-2.868	0.001	-316.492931507	-2.862	-2.869	0.006
Hx2	-158.22163578				-158.244177995			
xH2	-158.221639435				-158.244184027			
HH2	-316.446048691	-1.737	-1.740	0.004	-316.491078586	-1.699	-1.705	0.005
Hx1	-158.221639274				-158.244182832			
xF1	-1150.05190277				-1150.10461504			
HF1	-1308.27754688	-2.260	-2.513	0.253	-1308.35302406	-2.418	-2.652	0.234
Hx2	-158.221627277				-158.244169385			
xF2	-1150.05225178				-1150.10496833			
HF2	-1308.27786347	-2.459	-2.500	0.041	-1308.35336097	-2.630	-2.650	0.020
Hx3	-158.22161186				-158.244154117			
xF3	-1150.05235518				-1150.10490613			
HF3	-1308.27792249	-2.496	-2.482	-0.014	-1308.35327611	-2.576	-2.645	0.069
Hx4	-158.221594367				-158.24413582			
xF4	-1150.05227058				-1150.10498577			
HF4	-1308.27772791	-2.374	-2.424	0.050	-1308.35323683	-2.552	-2.582	0.031
Fx1								
xF1								
FF1								
Fx2								
xF2								
FF2								

	CCSD(T)-F12/cc-pVDZ-F12				ExtremePNO-DLPNO-CCSD(T)/CBS(34)			
	E [Ha]	BAE [kcal mol^{-1}]	BIE [kcal mol^{-1}]	E-def [kcal mol^{-1}]	E [Ha]	BAE [kcal mol^{-1}]	BIE [kcal mol^{-1}]	E-def [kcal mol^{-1}]
Methanes								
H	-40.447999976925				-40.45883236544			
F	-437.122744137689				-437.222431231796			
Hx1	-40.447999035723				-40.458831557834			
xH1	-40.447999052373				-40.458831565443			
HH1	-80.896787083326	-0.494	-0.495	0.001	-80.918472574501	-0.507	-0.508	0.001
Hx2	-40.447999717363				-40.458832115762			
xH2	-40.447999751484				-40.458832142124			
HH2	-80.8966197003	-0.389	-0.389	0.000	-80.91829878399	-0.398	-0.398	0.000
Hx1	-40.447999679402				-40.458832110835			
xF1	-437.122738504592				-437.22241605469			
HF1	-477.571962046076	-0.764	-0.768	0.004	-477.682488234706	-0.768	-0.778	0.010
Hx2	-40.447998998258				-40.458831475222			
xF2	-437.122739653581				-437.222420508373			
HF2	-477.571417478363	-0.423	-0.426	0.003	-477.681915605826	-0.409	-0.416	0.007
Fx1	-437.122736072511				-437.222420849004			
xF1	-437.12273923139				-437.222420265875			
FF1	-874.246755931905	-0.795	-0.804	0.008	-874.446072896779	-0.760	-0.773	0.013
Fx2	-437.122739514482				-437.222420272937			
xF2	-437.122738258817				-437.222419671603			
FF2	-874.246821616374	-0.837	-0.843	0.007	-874.445976788717	-0.699	-0.713	0.014
Ethanes								
H	-79.693734466298				-79.713724795789			
F	-674.691619616535				-674.845120739521			
Hx1	-79.693734710715				-79.713725039495			
xH1	-79.693734890698				-79.713725166933			
HH1	-159.389578828691	-1.324	-1.324	0.000	-159.429612933537	-1.358	-1.357	0.000
Hx2	-79.693735549941				-79.713725933073			
xH2	-79.693735582632				-79.71372595889			
HH2	-159.389340370727	-1.174	-1.173	-0.001	-159.429369053514	-1.204	-1.203	-0.001
Hx1	-79.693730594262				-79.713721272974			
xF1	-674.691616880024				-674.845096137316			
HF1	-754.387028471939	-1.051	-1.055	0.004	-754.560453063559	-1.009	-1.026	0.018
Hx2	-79.693734076935				-79.713724566739			
xF2	-674.691613869448				-674.845091893913			
HF2	-754.387305120539	-1.224	-1.228	0.004	-754.560690601218	-1.158	-1.176	0.018
Hx3	-79.693734078752				-79.713724557059			
xF3	-674.691620113649				-674.845102202878			
HF3	-754.38682317727	-0.922	-0.922	0.000	-754.56023653073	-0.873	-0.885	0.012
Hx4	-79.693731851176				-79.713722423374			
xF4	-674.691622374721				-674.845111211258			
HF4	-754.387213663146	-1.167	-1.167	0.000	-754.560622627775	-1.115	-1.123	0.007
Fx1	-674.691609506162				-674.84509839362			
xF1	-674.691584467383				-674.845070795438			
FF1	-1349.38531064049	-1.300	-1.328	0.028	-1349.69207685299	-1.152	-1.197	0.045
Fx2	-674.691612139525				-674.845090367952			
xF2	-674.691617643655				-674.845107306051			
FF2	-1349.38490896877	-1.048	-1.054	0.006	-1349.69178287617	-0.967	-0.995	0.027

	CCSD(T)-F12/cc-pVDZ-F12				ExtremePNO-DLPNO-CCSD(T)/CBS(34)			
	E [Ha]	BAE [kcal mol^{-1}]	BIE [kcal mol^{-1}]	E-def [kcal mol^{-1}]	E [Ha]	BAE [kcal mol^{-1}]	BIE [kcal mol^{-1}]	E-def [kcal mol^{-1}]
Propanes								
H	-118.942844355675				-118.972067786382			
F	-912.260942870335				-912.468011042762			
Hx1	-118.942839980005				-118.972064160139			
xH1	-118.942840442653				-118.972064477887			
HH1	-237.888877693659	-2.001	-2.006	0.005	-237.947319736954	-1.998	-2.002	0.004
Hx2	-118.942841158761				-118.972063930754			
xH2	-118.942840842427				-118.972065101736			
HH2	-237.887635306472	-1.222	-1.226	0.004	-237.946073662057	-1.216	-1.220	0.004
Hx1	-118.942839183879				-118.972063607711			
xF1	-912.260867578635				-912.467944538586			
HF1	-1031.20646186905	-1.678	-1.729	0.050	-1031.44266454604	-1.623	-1.667	0.044
Hx2	-118.94284228285				-118.972065686724			
xF2	-912.260913751534				-912.467957771246			
HF2	-1031.20602157557	-1.402	-1.422	0.020	-1031.44216043208	-1.306	-1.341	0.035
Hx3	-118.942846184931				-118.972067499376			
xF3	-912.260901002422				-912.467959335761			
HF3	-1031.20597874094	-1.375	-1.400	0.025	-1031.44222455346	-1.346	-1.379	0.033
Hx4	-118.942839145392				-118.972063186267			
xF4	-912.260903629426				-912.467944476894			
HF4	-1031.2060135717	-1.397	-1.425	0.028	-1031.44222367377	-1.346	-1.391	0.045
Fx1	-912.260782171931				-912.467890738825			
xF1	-912.260901047332				-912.46797888394			
FF1	-1824.52474494826	-1.794	-1.921	0.127	-1824.93856280435	-1.594	-1.690	0.096
Fx2	-912.260939151683				-912.468006315844			
xF2	-912.260941184676				-912.468010463395			
FF2	-1824.5252075978	-2.084	-2.088	0.003	-1824.93906806307	-1.911	-1.915	0.003
Butanes								
H	-158.192066667656				-158.230530166731			
F	-1149.82992018262				-1150.09061289021			
Hx1	-158.192061823679				-158.2305277631			
xH1	-158.192061035021				-158.230525723237			
HH1	-316.388735463913	-2.888	-2.894	0.007	-316.465617221183	-2.859	-2.864	0.004
Hx2	-158.192059116789				-158.230524542646			
xH2	-158.192064851329				-158.230527376907			
HH2	-316.386870245669	-1.717	-1.723	0.006	-316.463744573946	-1.684	-1.690	0.005
Hx1	-158.192063771568				-158.230526351675			
xF1	-1149.82961839877				-1150.09016731751			
HF1	-1308.0253277113	-2.096	-2.288	0.191	-1308.32425492421	-1.953	-2.235	0.282
Hx2	-158.192050371468				-158.230515759292			
xF2	-1149.82991506622				-1150.090587977			
HF2	-1308.02561181709	-2.275	-2.288	0.013	-1308.32465110068	-2.201	-2.226	0.025
Hx3	-158.192036332102				-158.230503871159			
xF3	-1149.82986329354				-1150.09052306273			
HF3	-1308.02552777129	-2.222	-2.277	0.055	-1308.3245961659	-2.167	-2.240	0.073
Hx4	-158.192017187497				-158.230485613852			
xF4	-1149.82992664017				-1150.09061091914			
HF4	-1308.02550927225	-2.210	-2.237	0.027	-1308.32465110068	-2.201	-2.231	0.029
Fx1					-1150.09055716374			
xF1					-1150.0905491159			
FF1					-2300.1845317021	-2.074	-2.149	0.075
Fx2					-1150.09045281713			
xF2					-1150.09047895973			
FF2					-2300.18475070843	-2.212	-2.396	0.184

	NormalPNO-DLPNO-CCSD(T)/CBS(34)				TightPNO-DLPNO-CCSD(T)/CBS(34)			
	E [Ha]	BAE [kcal mol^{-1}]	BIE [kcal mol^{-1}]	E-def [kcal mol^{-1}]	E [Ha]	BAE [kcal mol^{-1}]	BIE [kcal mol^{-1}]	E-def [kcal mol^{-1}]
Methanes								
H	-40.458979789634				-40.458900385254			
F	-437.220645058674				-437.221777818776			
Hx1	-40.458979070777				-40.458899578178			
xH1	-40.458979077608				-40.458899585582			
HH1	-80.91873445578	-0.486	-0.487	0.001	-80.918578889665	-0.488	-0.489	0.001
Hx2	-40.458979540573				-40.458900135613			
xH2	-40.458979566395				-40.458900161934			
HH2	-80.918553742962	-0.373	-0.373	0.000	-80.91842154816	-0.390	-0.390	0.000
Hx1	-40.45897956448				-40.458900130834			
xF1	-437.2206309157				-437.221765937366			
HF1	-477.680560993753	-0.587	-0.596	0.009	-477.681817954508	-0.715	-0.723	0.008
Hx2	-40.45897895856				-40.458899495379			
xF2	-437.220634165649				-437.221769183984			
HF2	-477.680109428997	-0.304	-0.311	0.007	-477.681280973822	-0.378	-0.384	0.006
Fx1	-437.220632521522				-437.221765711528			
xF1	-437.220632066669				-437.22176977829			
FF1	-874.44219105764	-0.565	-0.581	0.016	-874.444720881471	-0.731	-0.744	0.013
Fx2	-437.220630217326				-437.22176920529			
xF2	-437.22063446222				-437.221768841067			
FF2	-874.442052003138	-0.478	-0.494	0.016	-874.44457747893	-0.641	-0.652	0.011
Ethanes								
H	-79.713874124651				-79.713808937866			
F	-674.84225036989				-674.843921099744			
Hx1	-79.713872984657				-79.713809212295			
xH1	-79.713874471439				-79.713809324241			
HH1	-159.429854718811	-1.322	-1.322	0.000	-159.429733420158	-1.328	-1.327	0.000
Hx2	-79.713875126026				-79.713810055344			
xH2	-79.713875151483				-79.713810081251			
HH2	-159.429616023382	-1.172	-1.171	-0.001	-159.429493298095	-1.177	-1.175	-0.001
Hx1	-79.713872503343				-79.713807074755			
xF1	-674.842225642529				-674.84390260749			
HF1	-754.557504425239	-0.866	-0.882	0.017	-754.559243623915	-0.950	-0.963	0.013
Hx2	-79.713874433134				-79.713808702769			
xF2	-674.842226803085				-674.843906279609			
HF2	-754.557705400251	-0.992	-1.007	0.015	-754.559482525291	-1.100	-1.109	0.009
Hx3	-79.71387385788				-79.713808693182			
xF3	-674.842228598466				-674.843907832661			
HF3	-754.557239608612	-0.700	-0.714	0.014	-754.559079021046	-0.846	-0.855	0.008
Hx4	-79.713871135672				-79.713806646741			
xF4	-674.842239667514				-674.843917052641			
HF4	-754.557610235492	-0.932	-0.941	0.009	-754.559449746863	-1.079	-1.083	0.004
Fx1	-674.842230574223				-674.843904021205			
xF1	-674.842247809953				-674.843869802666			
FF1	-1349.68593238178	-0.898	-0.912	0.014	-1349.6895815669	-1.091	-1.134	0.043
Fx2	-674.842227722824				-674.843886664823			
xF2	-674.842244913549				-674.843910702744			
FF2	-1349.68564419369	-0.718	-0.735	0.018	-1349.68923248412	-0.872	-0.901	0.028

	NormalPNO-DLPNO-CCSD(T)/CBS(34)				TightPNO-DLPNO-CCSD(T)/CBS(34)			
	E [Ha]	BAE [kcal mol^{-1}]	BIE [kcal mol^{-1}]	E-def [kcal mol^{-1}]	E [Ha]	BAE [kcal mol^{-1}]	BIE [kcal mol^{-1}]	E-def [kcal mol^{-1}]
Propanes								
H	-118.972132968789				-118.972167148961			
F	-912.463755063015				-912.466215512477			
Hx1	-118.972126403027				-118.972158957498			
xH1	-118.972126506231				-118.972159476421			
HH1	-237.947370069894	-1.948	-1.956	0.008	-237.947426946602	-1.941	-1.951	0.010
Hx2	-118.972126637966				-118.972158904248			
xH2	-118.972127230858				-118.972160491154			
HH2	-237.946010605398	-1.095	-1.102	0.008	-237.94626001514	-1.208	-1.218	0.009
Hx1	-118.972124584908				-118.972160730635			
xF1	-912.463837010732				-912.466129682442			
HF1	-1031.4382638712	-1.491	-1.445	-0.046	-1031.44086140384	-1.555	-1.613	0.058
Hx2	-118.972126160584				-118.972162530038			
xF2	-912.463729571619				-912.46615666121			
HF2	-1031.4378065979	-1.204	-1.224	0.020	-1031.44041814971	-1.277	-1.317	0.040
Hx3	-118.972128306644				-118.972164158349			
xF3	-912.463800210181				-912.466163376212			
HF3	-1031.43775808144	-1.173	-1.148	-0.025	-1031.44044683014	-1.295	-1.330	0.035
Hx4	-118.972126524598				-118.972160357895			
xF4	-912.463707942626				-912.46613786162			
HF4	-1031.43776318789	-1.177	-1.210	0.034	-1031.4404378602	-1.290	-1.343	0.053
Fx1	-912.463828656995				-912.46608508582			
xF1	-912.463758260495				-912.466172958188			
FF1	-1824.92959361174	-1.307	-1.259	-0.048	-1824.93471712658	-1.435	-1.543	0.109
Fx2	-912.463776044488				-912.466209322132			
xF2	-912.463767854572				-912.466212076848			
FF2	-1824.92968283165	-1.363	-1.342	-0.021	-1824.93507707936	-1.660	-1.666	0.006
Butanes								
H	-158.230488269785				-158.230620228219			
F	-1150.08536238358				-1150.08821681391			
Hx1	-158.230455597828				-158.230615017062			
xH1	-158.230468825232				-158.230613642962			
HH1	-316.465418788441	-2.788	-2.820	0.033	-316.465679348846	-2.785	-2.793	0.007
Hx2	-158.230453964235				-158.230611156389			
xH2	-158.23046035736				-158.230617580791			
HH2	-316.463373653961	-1.504	-1.543	0.039	-316.463908297992	-1.674	-1.681	0.007
Hx1	-158.23046944099				-158.230615513641			
xF1	-1150.0846351836				-1150.08771116569			
HF1	-1308.3181972081	-1.472	-1.941	0.468	-1308.32189804079	-1.921	-2.241	0.320
Hx2	-158.23047175533				-158.230603385692			
xF2	-1150.08531658225				-1150.08817328028			
HF2	-1308.31891191766	-1.921	-1.960	0.039	-1308.32227519998	-2.157	-2.195	0.038
Hx3	-158.230450789595				-158.230589327012			
xF3	-1150.08517794591				-1150.08810668018			
HF3	-1308.31868840588	-1.781	-1.920	0.139	-1308.32217862525	-2.097	-2.185	0.089
Hx4	-158.230425195218				-158.230569980284			
xF4	-1150.08531267617				-1150.08820129335			
HF4	-1308.31867097241	-1.770	-1.841	0.071	-1308.32220383099	-2.113	-2.154	0.041
Fx1	-1150.08522612095				-1150.08815864686			
xF1	-1150.08520973919				-1150.08814110261			
FF1	-2300.17306169007	-1.466	-1.648	0.181	-2300.17949081754	-1.918	-2.002	0.084
Fx2	-1150.08504471506				-1150.08802522914			
xF2	-1150.08518408051				-1150.08806632909			
FF2	-2300.17306236078	-1.467	-1.778	0.311	-2300.17960669457	-1.991	-2.206	0.215

	NormalPNO-DLPNO-CCSD(T)/CBS(34)				TightPNO-DLPNO-CCSD(T)/CBS(34)			
	E [Ha]	BAE [kcal mol^{-1}]	BIE [kcal mol^{-1}]	E-def [kcal mol^{-1}]	E [Ha]	BAE [kcal mol^{-1}]	BIE [kcal mol^{-1}]	E-def [kcal mol^{-1}]
Pentanes								
H	-197.488752226916				-197.489046101804			
F	-1387.70699376063				-1387.71050735664			
Hx1	-197.488720324413				-197.489041714705			
xH1	-197.488720312273				-197.489041706961			
HH1	-394.983304864186	-3.640	-3.680	0.040	-394.983878502499	-3.631	-3.636	0.006
Hx2	-197.488718314884				-197.489036751423			
xH2	-197.488718287335				-197.489036726222			
HH2	-394.980697750479	-2.004	-2.046	0.043	-394.981591213658	-2.196	-2.207	0.012
Hx1	-197.48863896484				-197.488945867352			
xF1	-1387.70684319738				-1387.71034583079			
HF1	-1585.19947836648	-2.342	-2.508	0.166	-1585.20381128164	-2.672	-2.836	0.164
Hx2	-197.48871662501				-197.489013289816			
xF2	-1387.70658610746				-1387.71013796355			
HF2	-1585.19898809687	-2.034	-2.313	0.278	-1585.20325589262	-2.323	-2.576	0.252
Hx3	-197.488736432724				-197.48903155831			
xF3	-1387.7069336869				-1387.71048612585			
HF3	-1585.19944778121	-2.323	-2.371	0.048	-1585.20359800258	-2.538	-2.560	0.022
Hx4	-197.488703868569				-197.489007214974			
xF4	-1387.70689166249				-1387.71049681111			
HF4	-1585.1997595802	-2.519	-2.613	0.094	-1585.20419633452	-2.913	-2.944	0.031
Fx1	-1387.70688247019				-1387.71049027577			
xF1	-1387.70692240684				-1387.71041886084			
FF1	-2775.41768992575	-2.323	-2.438	0.115	-2775.4253988967	-2.751	-2.817	0.066
Fx2	-1387.706958301				-1387.7104822998			
xF2	-1387.70684032426				-1387.71049053408			
FF2	-2775.41738019717	-2.129	-2.247	0.119	-2775.42522895213	-2.644	-2.671	0.026
Hexanes								
H	-236.747058132828				-236.747501883392			
F	-1625.32854816406				-1625.33277572995			
Hx1	-236.747001322901				-236.74749361514			
xH1	-236.747001155531				-236.747493470246			
HH1	-473.500874618682	-4.241	-4.312	0.071	-473.501816683307	-4.275	-4.286	0.010
Hx2	-236.747007677672				-236.747494086152			
xH2	-236.747007622285				-236.747494034557			
HH2	-473.497979196046	-2.424	-2.487	0.063	-473.499304559628	-2.699	-2.709	0.010
Hx1	-236.74688716963				-236.747315564704			
xF1	-1625.3279818125				-1625.33219611172			
HF1	-1862.07988175585	-2.683	-3.146	0.463	-1862.0849724539	-2.946	-3.427	0.481
Hx2	-236.746973440593				-236.747408823833			
xF2	-1625.32814618926				-1625.33230949939			
HF2	-1862.07974344451	-2.596	-2.901	0.305	-1862.08486937564	-2.881	-3.232	0.351
Hx3	-236.746932240669				-236.747374558127			
xF3	-1625.32818213363				-1625.33247236672			
HF3	-1862.07975632521	-2.604	-2.913	0.309	-1862.08516480069	-3.067	-3.337	0.270
Hx4	-236.747013583376				-236.747476792503			
xF4	-1625.32856153143				-1625.33270972626			
HF4	-1862.0802881985	-2.938	-2.958	0.020	-1862.0855392657	-3.302	-3.359	0.057
Fx1	-1625.32848543712				-1625.33272867229			
xF1	-1625.32847640981				-1625.33270905255			
FF1	-3250.6621173447	-3.151	-3.235	0.084	-3250.67149979911	-3.733	-3.804	0.071
Fx2	-1625.32839954454				-1625.33270649309			
xF2	-1625.32838038054				-1625.33270736838			
FF2	-3250.66024838001	-1.978	-2.176	0.199	-3250.66966163483	-2.579	-2.666	0.086

	VeryTightPNO-DLPNO-CCSD(T)/CBS(34)				MP2/CBS(34)			
	E [Ha]	BAE [kcal mol^{-1}]	BIE [kcal mol^{-1}]	E-def [kcal mol^{-1}]	E [Ha]	BAE [kcal mol^{-1}]	BIE [kcal mol^{-1}]	E-def [kcal mol^{-1}]
Methanes								
H	-40.458829605571				-40.473039630273			
F	-437.222292901903				-437.404761018784			
Hx1	-40.458828797064				-40.473040873783			
xH1	-40.458828804595				-40.473040735131			
HH1	-80.918462536915	-0.504	-0.505	0.001	-80.946816065582	-0.462	-0.461	-0.001
Hx2	-40.458829355838				-40.473039514805			
xH2	-40.458829382253				-40.473039419455			
HH2	-80.918296349692	-0.400	-0.400	0.000	-80.946682691332	-0.379	-0.379	0.000
Hx1	-40.458829350677				-40.473040033543			
xF1	-437.222278372874				-437.40474154585			
HF1	-477.68231594593	-0.749	-0.758	0.009	-477.878852364044	-0.660	-0.672	0.012
Hx2	-40.458828714761				-40.473040071465			
xF2	-437.222282187068				-437.404746621481			
HF2	-477.68174550036	-0.391	-0.398	0.007	-477.8783357398	-0.336	-0.345	0.009
Fx1	-437.222279356036				-437.40474438795			
xF1	-437.222281940974				-437.404746562853			
FF1	-874.445721163073	-0.712	-0.728	0.015	-874.810534395821	-0.635	-0.655	0.020
Fx2	-437.222281580913				-437.404745587253			
xF2	-437.222281240395				-437.404745861874			
FF2	-874.445626004777	-0.653	-0.667	0.014	-874.810424401864	-0.566	-0.585	0.019
Ethanes								
H	-79.713696715595				-79.749427666505			
F	-674.844748222117				-675.131824576874			
Hx1	-79.713696909679				-79.749425053668			
xH1	-79.713697027752				-79.749425373311			
HH1	-159.429547825058	-1.352	-1.352	0.000	-159.50112155962	-1.422	-1.425	0.003
Hx2	-79.713697858593				-79.749427274354			
xH2	-79.71369788307				-79.749427151209			
HH2	-159.429296305	-1.194	-1.193	-0.001	-159.500802427155	-1.222	-1.222	0.001
Hx1	-79.713693127083				-79.749425362763			
xF1	-674.844727527179				-675.131791138192			
HF1	-754.559997736102	-0.974	-0.990	0.015	-754.882709901028	-0.915	-0.937	0.022
Hx2	-79.713696479885				-79.749428775361			
xF2	-674.844725764402				-675.131778944523			
HF2	-754.560240266736	-1.127	-1.141	0.014	-754.882930636669	-1.053	-1.081	0.028
Hx3	-79.713696488727				-79.749428544236			
xF3	-674.844735472761				-675.131797431439			
HF3	-754.559803688484	-0.853	-0.861	0.008	-754.882520217856	-0.796	-0.812	0.016
Hx4	-79.71369435948				-79.749427595914			
xF4	-674.844741687269				-675.131808410933			
HF4	-754.560181534136	-1.090	-1.095	0.006	-754.882899595339	-1.034	-1.044	0.010
Fx1	-674.844730329606				-675.131800185421			
xF1	-674.844694142796				-675.131771704903			
FF1	-1349.69128091431	-1.120	-1.165	0.045	-1350.26528087191	-1.024	-1.072	0.048
Fx2	-674.844722848258				-675.131780367396			
xF2	-674.84473794725				-675.131806232494			
FF2	-1349.69097989253	-0.931	-0.953	0.022	-1350.26498223949	-0.837	-0.876	0.039

	VeryTightPNO-DLPNO-CCSD(T)/CBS(34)				MP2/CBS(34)			
	E [Ha]	BAE [kcal mol^{-1}]	BIE [kcal mol^{-1}]	E-def [kcal mol^{-1}]	E [Ha]	BAE [kcal mol^{-1}]	BIE [kcal mol^{-1}]	E-def [kcal mol^{-1}]
Propanes								
H	-118.972022669517				-119.029774534044			
F	-912.467399702174				-912.858925862397			
Hx1	-118.97201944583				-119.029771061025			
xH1	-118.972019819919				-119.029771147672			
HH1	-237.947221518947	-1.993	-1.997	0.004	-238.062918904442	-2.115	-2.119	0.004
Hx2	-118.972019145367				-119.029759395825			
xH2	-118.972020582871				-119.029774551531			
HH2	-237.945963119191	-1.203	-1.207	0.004	-238.061466882786	-1.203	-1.213	0.009
Hx1	-118.972018348951				-119.029776667231			
xF1	-912.467328616063				-912.858844561952			
HF1	-1031.44196843866	-1.598	-1.645	0.047	-1031.89118353796	-1.558	-1.608	0.050
Hx2	-118.972020762989				-119.029771569985			
xF2	-912.467355375762				-912.858856805422			
HF2	-1031.44148288504	-1.293	-1.322	0.029	-1031.89068976309	-1.248	-1.294	0.045
Hx3	-118.97202241253				-119.029748713332			
xF3	-912.467353911319				-912.858864466224			
HF3	-1031.44153026236	-1.323	-1.352	0.029	-1031.8907011493	-1.255	-1.310	0.055
Hx4	-118.972018370909				-119.029777076259			
xF4	-912.46734077082				-912.858844347636			
HF4	-1031.44151527512	-1.313	-1.353	0.040	-1031.89072660804	-1.271	-1.321	0.050
Fx1	-912.467271830224				-912.858811311382			
xF1	-912.467366321716				-912.858891153689			
FF1	-1824.937286182	-1.560	-1.662	0.101	-1825.72022386377	-1.489	-1.582	0.094
Fx2	-912.467407755647				-912.858925679747			
xF2	-912.467405993299				-912.85892957805			
FF2	-1824.93774235481	-1.847	-1.838	-0.009	-1825.72050550751	-1.665	-1.663	-0.002
Butanes								
H	-158.230471666199				-158.310243431337			
F	-1150.08978210425				-1150.5857899199			
Hx1	-158.230467683388				-158.310242735017			
xH1	-158.230466661263				-158.310238832543			
HH1	-316.465455021217	-2.831	-2.837	0.006	-316.625417394412	-3.094	-3.097	0.003
Hx2	-158.230464211975				-158.310238001219			
xH2	-158.23046848121				-158.310234651012			
HH2	-316.463577552471	-1.653	-1.660	0.007	-316.623153129918	-1.673	-1.682	0.009
Hx1	-158.23046833367				-158.310237829722			
xF1	-1150.08935614244				-1150.58528336107			
HF1	-1308.32330003111	-1.912	-2.181	0.269	-1308.89911851347	-1.936	-2.257	0.321
Hx2	-158.230456313239				-158.310226978252			
xF2	-1150.0897675522				-1150.5857556517			
HF2	-1308.32366338457	-2.140	-2.158	0.019	-1308.89953734719	-2.199	-2.231	0.032
Hx3	-158.230443028036				-158.310236274444			
xF3	-1150.08970423561				-1150.5856774136			
HF3	-1308.32364876576	-2.130	-2.197	0.067	-1308.89938822685	-2.105	-2.180	0.075
Hx4	-158.230424358444				-158.310205841967			
xF4	-1150.08978603459				-1150.58579187308			
HF4	-1308.3236474947	-2.130	-2.157	0.027	-1308.89936664775	-2.092	-2.114	0.022
Fx1	-1150.08973688692				-1150.58572786092			
xF1	-1150.08971569626				-1150.58571096713			
FF1	-2300.18280329497	-2.033	-2.103	0.070	-2301.17478923392	-2.014	-2.102	0.088
Fx2	-1150.08964160566				-1150.58558761295			
xF2	-1150.08967256438				-1150.58564200617			
FF2	-2300.18297058111	-2.138	-2.294	0.157	-2301.17474134423	-1.984	-2.204	0.220

	VeryTightPNO-DLPNO-CCSD(T)/CBS(34)				MP2/CBS(34)			
	E [Ha]	BAE [kcal mol^{-1}]	BIE [kcal mol^{-1}]	E-def [kcal mol^{-1}]	E [Ha]	BAE [kcal mol^{-1}]	BIE [kcal mol^{-1}]	E-def [kcal mol^{-1}]
Pentanes								
H	-197.488869247624				-197.590632808594			
F	-1387.71242766832				-1388.31295287017			
Hx1	-197.488864109103				-197.59063744064			
xH1	-197.488864093842				-197.590637515538			
HH1	-394.983595378707	-3.675	-3.682	0.006	-395.187736422226	-4.060	-4.055	-0.006
Hx2	-197.488860150701				-197.590618761916			
xH2	-197.488860121898				-197.590618731269			
HH2	-394.981206562891	-2.176	-2.188	0.011	-395.184803119208	-2.220	-2.237	0.018
Hx1	-197.48876966214				-197.590538222972			
xF1	-1387.71224464374				-1388.31274431025			
HF1	-1585.20546998969	-2.619	-2.796	0.177	-1585.90794462138	-2.735	-2.926	0.190
Hx2	-197.488836289482				-197.590595633557			
xF2	-1387.71204256854				-1388.31254553895			
HF2	-1585.20497316136	-2.307	-2.569	0.262	-1585.90736306987	-2.370	-2.649	0.279
Hx3	-197.488853939243				-197.590628115447			
xF3	-1387.71237286413				-1388.3128896462			
HF3	-1585.20534848053	-2.542	-2.586	0.044	-1585.90764798382	-2.549	-2.592	0.043
Hx4	-197.488831405326				-197.590606824727			
xF4	-1387.71240260176				-1388.3129124386			
HF4	-1585.20598263007	-2.940	-2.980	0.039	-1585.90826976091	-2.939	-2.981	0.042
Fx1	-1387.71239215427				-1388.31291871597			
xF1	-1387.71230238936				-1388.31282284606			
FF1	-2775.42952881838	-2.933	-3.034	0.101	-2776.63059909978	-2.945	-3.048	0.103
Fx2	-1387.71237991222				-1388.31291228651			
xF2	-1387.71238372849				-1388.31291311482			
FF2	-2775.42925194185	-2.759	-2.816	0.058	-2776.63016866222	-2.675	-2.725	0.050
Hexanes								
H	-236.747299412113				-236.871048982949			
F	-1625.33502778657				-1626.04005403153			
Hx1	-236.747290444749				-236.871054554354			
xH1	-236.747290295613				-236.871054435193			
HH1	-473.501448018185	-4.298	-4.309	0.011	-473.749753465073	-4.804	-4.797	-0.007
Hx2	-236.747291722787				-236.871043108598			
xH2	-236.747291664414				-236.871043000593			
HH2	-473.498806834847	-2.641	-2.650	0.010	-473.746396898488	-2.698	-2.705	0.007
Hx1	-236.747113053312				-236.870890601574			
xF1	-1625.33448744958				-1626.03946006817			
HF1	-1862.08692414107	-2.885	-3.341	0.456	-1862.91599873187	-3.072	-3.544	0.472
Hx2	-236.747209098801				-236.870968561554			
xF2	-1625.33458032738				-1626.03956825392			
HF2	-1862.08688708679	-2.861	-3.199	0.337	-1862.91585254711	-2.980	-3.336	0.355
Hx3	-236.747171848673				-236.870935192859			
xF3	-1625.33475026021				-1626.03976029794			
HF3	-1862.08717179529	-3.040	-3.294	0.254	-1862.91607419783	-3.119	-3.375	0.256
Hx4	-236.747275187722				-236.871030273572			
xF4	-1625.33496500237				-1626.03998106786			
HF4	-1862.08759012109	-3.303	-3.357	0.055	-1862.91638935568	-3.317	-3.375	0.058
Fx1	-1625.33499435808				-1626.04002176516			
xF1	-1625.33497001083				-1626.03998505914			
FF1	-3250.67627600161	-3.903	-3.961	0.057	-3252.0865009415	-4.012	-4.075	0.064
Fx2	-1625.33497440454				-1626.04004998724			
xF2	-1625.33497575486				-1626.04004725869			
FF2	-3250.67450174373	-2.790	-2.856	0.066	-3252.084493053	-2.752	-2.758	0.007

	RI-MP2/CBS(34)				RI-SCS-MP2/CBS(34)			
	E [Ha]	BAE [kcal mol^{-1}]	BIE [kcal mol^{-1}]	E-def [kcal mol^{-1}]	E [Ha]	BAE [kcal mol^{-1}]	BIE [kcal mol^{-1}]	E-def [kcal mol^{-1}]
Methanes								
H	-40.435492481401				-40.445986267425			
F	-437.189772434115				-437.165045632345			
Hx1	-40.435492969586				-40.445986282521			
xH1	-40.435492884472				-40.445986229959			
HH1	-80.871766282232	-0.490	-0.490	-0.001	-80.892444412396	-0.296	-0.296	0.000
Hx2	-40.435492314922				-40.445986067793			
xH2	-40.435492264406				-40.445986044929			
HH2	-80.871582920018	-0.375	-0.375	0.000	-80.892330101407	-0.224	-0.225	0.000
Hx1	-40.43549264231				-40.445986277061			
xF1	-437.18976163049				-437.165037591519			
HF1	-477.626398860948	-0.712	-0.718	0.007	-477.611773322418	-0.465	-0.470	0.005
Hx2	-40.435492429291				-40.445985904851			
xF2	-437.189764248269				-437.165039420644			
HF2	-477.625823413853	-0.350	-0.356	0.005	-477.611329772827	-0.187	-0.191	0.004
Fx1	-437.189761186263				-437.165036066588			
xF1	-437.189763962477				-437.165039059105			
FF1	-874.380673358703	-0.708	-0.721	0.012	-874.330813181171	-0.453	-0.463	0.010
Fx2	-437.189763775124				-437.165039133253			
xF2	-437.18976311495				-437.165038158121			
FF2	-874.38046847986	-0.580	-0.591	0.011	-874.330631616688	-0.339	-0.348	0.009
Ethanes								
H	-79.674742123241				-79.68836916151			
F	-674.79145751654				-674.752574362835			
Hx1	-79.674740048867				-79.688367073939			
xH1	-79.674740350804				-79.688367533178			
HH1	-159.351741835024	-1.417	-1.419	0.002	-159.378102816602	-0.856	-0.859	0.002
Hx2	-79.674742198032				-79.688368699852			
xH2	-79.674742113684				-79.688368637248			
HH2	-159.351429924236	-1.221	-1.221	0.000	-159.37796412311	-0.769	-0.770	0.001
Hx1	-79.674739018593				-79.688365478233			
xF1	-674.79143655709				-674.752564517323			
HF1	-754.467725395654	-0.957	-0.973	0.015	-754.44186013616	-0.575	-0.584	0.008
Hx2	-79.674742818406				-79.688369215021			
xF2	-674.791431613982				-674.752561013076			
HF2	-754.467953106209	-1.100	-1.116	0.016	-754.441995471855	-0.660	-0.668	0.008
Hx3	-79.674742604006				-79.688369108877			
xF3	-674.791438050698				-674.752567696445			
HF3	-754.467520102061	-0.829	-0.841	0.012	-754.441746150483	-0.504	-0.508	0.004
Hx4	-79.674741121841				-79.688367667324			
xF4	-674.791446559011				-674.752572213556			
HF4	-754.467893735162	-1.063	-1.071	0.008	-754.441938747135	-0.625	-0.627	0.002
Fx1	-674.791441432108				-674.75256196063			
xF1	-674.791411187472				-674.752530607489			
FF1	-1349.58460524901	-1.061	-1.100	0.039	-1349.50617392248	-0.643	-0.679	0.035
Fx2	-674.791428576729				-674.752558707676			
xF2	-674.791442232505				-674.752567166265			
FF2	-1349.58430540736	-0.872	-0.900	0.028	-1349.50603764072	-0.558	-0.572	0.014

	RI-MP2/CBS(34)				RI-SCS-MP2/CBS(34)			
	E [Ha]	BAE [kcal mol^{-1}]	BIE [kcal mol^{-1}]	E-def [kcal mol^{-1}]	E [Ha]	BAE [kcal mol^{-1}]	BIE [kcal mol^{-1}]	E-def [kcal mol^{-1}]
Propanes								
H	-118.917917059007				-118.933987930226			
F	-912.393212253362				-912.339665036802			
Hx1	-118.917911407732				-118.933985828876			
xH1	-118.91791163553				-118.933986370387			
HH1	-237.839242613518	-2.139	-2.146	0.007	-237.870011144179	-1.277	-1.279	0.002
Hx2	-118.917903734797				-118.933984163937			
xH2	-118.9179143726				-118.93398666009			
HH2	-237.83778980864	-1.227	-1.237	0.010	-237.869137080427	-0.729	-0.732	0.003
Hx1	-118.917917177098				-118.933984506492			
xF1	-912.393131515729				-912.33957670393			
HF1	-1031.31370320277	-1.615	-1.666	0.051	-1031.27521852806	-0.982	-1.040	0.058
Hx2	-118.917914208475				-118.933985961423			
xF2	-912.393163254693				-912.339616805787			
HF2	-1031.31324610535	-1.328	-1.361	0.033	-1031.27497139944	-0.827	-0.859	0.032
Hx3	-118.917899530606				-118.933978140383			
xF3	-912.393167716094				-912.339618284443			
HF3	-1031.31325363174	-1.333	-1.372	0.039	-1031.27506561233	-0.886	-0.922	0.035
Hx4	-118.917916648783				-118.933987568864			
xF4	-912.393151940683				-912.339600185458			
HF4	-1031.31330092862	-1.363	-1.401	0.038	-1031.27491074012	-0.789	-0.830	0.041
Fx1	-912.393063604665				-912.339501548281			
xF1	-912.393179392134				-912.339613845924			
FF1	-1824.78881466499	-1.500	-1.614	0.114	-1824.68070106287	-0.860	-0.995	0.135
Fx2	-912.393212148871				-912.339664416705			
xF2	-912.393215641175				-912.33966745534			
FF2	-1824.7892023759	-1.743	-1.741	-0.002	-1824.6808973028	-0.983	-0.982	-0.001
Butanes								
H	-158.161214371129				-158.179685179575			
F	-1149.99467502283				-1149.92634565488			
Hx1	-158.161211184182				-158.179681801609			
xH1	-158.161208403364				-158.179680065527			
HH1	-316.327427388356	-3.137	-3.142	0.006	-316.362406870214	-1.905	-1.911	0.005
Hx2	-158.161208558704				-158.179676459869			
xH2	-158.16120696587				-158.179682829791			
HH2	-316.325175210878	-1.723	-1.732	0.008	-316.361049469501	-1.054	-1.061	0.007
Hx1	-158.16120951982				-158.179682840458			
xF1	-1149.99428134088				-1149.92600093304			
HF1	-1308.15918358405	-2.067	-2.317	0.250	-1308.10806379463	-1.276	-1.493	0.218
Hx2	-158.161197784108				-158.179671037446			
xF2	-1149.99465477503				-1149.92633479001			
HF2	-1308.15952831722	-2.283	-2.307	0.023	-1308.10831726004	-1.435	-1.450	0.016
Hx3	-158.16119976441				-158.179662776496			
xF3	-1149.99460473627				-1149.92630267501			
HF3	-1308.1594674361	-2.245	-2.299	0.053	-1308.10819478085	-1.358	-1.399	0.041
Hx4	-158.161170552327				-158.179639514864			
xF4	-1149.99468844172				-1149.92636242434			
HF4	-1308.1593934866	-2.199	-2.218	0.019	-1308.10824966733	-1.392	-1.410	0.018
Fx1	-1149.99462978799				-1149.926316129			
xF1	-1149.9946152374				-1149.92627851558			
FF1	-2299.99261428004	-2.048	-2.114	0.066	-2299.85491059159	-1.393	-1.453	0.061
Fx2	-1149.99452833668				-1149.92623692003			
xF2	-1149.99457012064				-1149.92625282515			
FF2	-2299.99278332072	-2.154	-2.312	0.158	-2299.85489779506	-1.385	-1.511	0.126

	RI-MP2/CBS(34)				RI-SCS-MP2/CBS(34)			
	E [Ha]	BAE [kcal mol^{-1}]	BIE [kcal mol^{-1}]	E-def [kcal mol^{-1}]	E [Ha]	BAE [kcal mol^{-1}]	BIE [kcal mol^{-1}]	E-def [kcal mol^{-1}]
Pentanes								
H	-197.404462162306				-197.425337724747			
F	-1387.59646061689				-1387.51332788493			
Hx1	-197.404463077491				-197.425334214906			
xH1	-197.404463123273				-197.425334213012			
HH1	-394.815475718482	-4.111	-4.110	-0.001	-394.854663930587	-2.503	-2.507	0.004
Hx2	-197.404448993591				-197.425325317936			
xH2	-197.40444897344				-197.425325292134			
HH2	-394.812540564044	-2.269	-2.286	0.017	-394.852813553745	-1.342	-1.357	0.016
Hx1	-197.404361090133				-197.42523983588			
xF1	-1387.59628966361				-1387.51318734358			
HF1	-1585.0054873144	-2.864	-3.035	0.171	-1584.94152957574	-1.797	-1.947	0.150
Hx2	-197.404427449449				-197.425306347887			
xF2	-1387.5961038781				-1387.51298761459			
HF2	-1585.00490723059	-2.500	-2.746	0.246	-1584.9411915187	-1.585	-1.818	0.233
Hx3	-197.404453656203				-197.42532658121			
xF3	-1387.59642608015				-1387.51332367002			
HF3	-1585.00522889461	-2.702	-2.729	0.027	-1584.94144681702	-1.745	-1.755	0.010
Hx4	-197.404429825236				-197.425304769556			
xF4	-1387.59643678052				-1387.51332164591			
HF4	-1585.00584065694	-3.086	-3.121	0.035	-1584.94177947046	-1.954	-1.979	0.025
Fx1	-1387.59642976193				-1387.51330085803			
xF1	-1387.5963601874				-1387.51324484781			
FF1	-2775.19770855459	-3.004	-3.086	0.082	-2775.02976879154	-1.953	-2.023	0.069
Fx2	-1387.5964296109				-1387.51330161886			
xF2	-1387.59643112323				-1387.5133027558			
FF2	-2775.19736543233	-2.789	-2.827	0.038	-2775.0296231026	-1.862	-1.894	0.032
Hexanes								
H	-236.647743952463				-236.671014658316			
F	-1625.1982147814				-1625.10029601806			
Hx1	-236.64774368556				-236.671007251215			
xH1	-236.647743546025				-236.671007184506			
HH1	-473.303240272074	-4.865	-4.865	0.000	-473.346749513861	-2.962	-2.971	0.009
Hx2	-236.647735652197				-236.671007256512			
xH2	-236.647735579256				-236.671007195554			
HH2	-473.299965399022	-2.810	-2.820	0.010	-473.344733159233	-1.697	-1.706	0.009
Hx1	-236.647567121088				-236.670836191603			
xF1	-1625.19765538289				-1625.09977559826			
HF1	-1861.85109980175	-3.226	-3.688	0.462	-1861.7742809699	-1.864	-2.302	0.439
Hx2	-236.647657407232				-236.670924343473			
xF2	-1625.19776112768				-1625.09987433242			
HF2	-1861.8509344224	-3.122	-3.461	0.339	-1861.77442790802	-1.956	-2.277	0.321
Hx3	-236.647619640759				-236.670890983152			
xF3	-1625.19793075979				-1625.10001291096			
HF3	-1861.85120433896	-3.292	-3.548	0.256	-1861.77446496225	-1.979	-2.235	0.255
Hx4	-236.647720860827				-236.670993950899			
xF4	-1625.19815109942				-1625.10024212975			
HF4	-1861.8515083028	-3.482	-3.537	0.054	-1861.77489373176	-2.248	-2.295	0.047
Fx1	-1625.19816042238				-1625.10023607984			
xF1	-1625.19814840912				-1625.10022541542			
FF1	-3250.40287990912	-4.048	-4.123	0.076	-3250.20471563305	-2.588	-2.670	0.082
Fx2	-1625.19818263553				-1625.10022309199			
xF2	-1625.19818061266				-1625.1002218105			
FF2	-3250.40096728658	-2.847	-2.889	0.042	-3250.20328463178	-1.690	-1.782	0.092

	RI-MP3/CBS(34)			
	E [Ha]	BAE [kcal mol^{-1}]	BIE [kcal mol^{-1}]	E-def [kcal mol^{-1}]
Methanes				
H	-40.450132125006			
F	-437.17451400149			
Hx1	-40.450132335882			
xH1	-40.450132270113			
HH1	-80.901004636956	-0.465	-0.464	0.000
Hx2	-40.45013194056			
xH2	-40.450131906272			
HH2	-80.900854151209	-0.370	-0.370	0.000
Hx1	-40.45013219751			
xF1	-437.174471626474			
HF1	-477.625662076919	-0.638	-0.664	0.027
Hx2	-40.450131893386			
xF2	-437.174483188876			
HF2	-477.625143108106	-0.312	-0.331	0.019
Fx1	-437.174483057299			
xF1	-437.174483723941			
FF1	-874.349921058965	-0.560	-0.599	0.038
Fx2	-437.174480664149			
xF2	-437.174483324126			
FF2	-874.349860161874	-0.522	-0.562	0.040

4.2 Rigid Geometry Scans

The following tables provide the results of the rigid geometry scans using RI-MP2 and DLPNO-CCSD(T). $R_{C\text{-}C}$ refers to the distance of the carbon chains of the interacting molecules, E refers to the electronic energy of the whole system and BIE refers to the bond interaction energy at the respective distance.

RI-MP2/CBS(34)								
$R_{C\text{-}C}$ [Å]	E [Ha]	BIE [kcal mol^{-1}]	$R_{C\text{-}C}$ [Å]	E [Ha]	BIE [kcal mol^{-1}]	$R_{C\text{-}C}$ [Å]	E [Ha]	BIE [kcal mol^{-1}]
1-HH1			1-HH2			1-HF1		
3.30371146716	-80.871314375168	-0.206096699090305	3.5804338401	-80.871164919099	-0.113164914840978	3.40464005758	-477.625676691007	-0.265071426879289
3.41383518274	-80.871597872807	-0.383994153421553	3.69978163477	-80.871426494135	-0.277305728087989	3.5181280595	-477.626115103494	-0.540179415973888
3.52395889831	-80.871729151672	-0.466372884943958	3.81912942944	-80.871547069978	-0.35296821191429	3.63161606142	-477.626324103687	-0.671329017164381
3.63408261388	-80.87176721384	-0.490257255966371	3.93847722411	-80.871583062571	-0.375553905014655	3.74510406334	-477.626395230664	-0.715961869083122
3.74420632945	-80.871750641883	-0.479858195943085	4.05782501878	-80.87157063085	-0.367752882306686	3.85859206526	-477.626385375171	-0.7097774538695
3.85433004502	-80.871703827028	-0.450481430908516	4.17717281345	-80.871532862273	-0.344052742418505	3.97208006718	-477.62632960142	-0.674778896716017
3.9644537606	-80.871642239594	-0.411834732591534	4.29652060812	-80.871483605481	-0.31314363878198	4.0855680691	-477.626249854687	-0.62473706621551
4.07457747617	-80.871575555299	-0.369989705716685	4.41586840279	-80.871430861487	-0.280046282847654	4.19905607102	-477.626159826906	-0.568243780733287
4.18470119174	-80.871509508202	-0.328544526614265	4.53521619746	-80.871379053245	-0.247536120157735	4.31254407294	-477.626068293851	-0.510805921528554
4.29482490731	-80.871447308882	-0.289513864038841	4.65456399213	-80.871330503495	-0.217070692078107	4.42603207486	-477.625980579791	-0.455764517883792
4.40494862289	-80.871390531901	-0.253885770557731	4.7739117868	-80.871286325796	-0.189348767418662	4.53952007678	-477.625899782159	-0.405063238330317
4.51507233846	-80.871339632057	-0.22194563622367	4.89325958147	-80.871246927011	-0.16462565656329	4.6530080787	-477.625827083041	-0.359443853002518
4.62519605403	-80.87129472787	-0.193767833454524	5.01260737614	-80.871212291518	-0.142891556572556	4.76649608062	-477.625762480478	-0.318905132683972
4.7353197696	-80.871255339209	-0.169051075512503	5.13195517081	-80.871182151959	-0.12397869775697	4.87998408254	-477.625705211272	-0.282968163370774
4.84544348517	-80.871220937473	-0.147463660249133	5.25130296548	-80.871156105264	-0.107634149879229	4.99347208446	-477.625654186379	-0.250949559587473
4.95556720075	-80.871190963884	-0.128654949185662	5.37065076015	-80.871133691272	-0.093569157549499	5.10696008638	-477.625608333626	-0.222176522686138
1-HF2			1-FF1			1-FF2		
3.82497722955	-477.62504796232	0.130970790454453	3.67080659217	-874.379996195724	-0.295586445116713	3.88048063632	-874.378909067058	0.38768979579546
3.95247647054	-477.625494231289	-0.149067215527506	3.79316681191	-874.380426057967	-0.565329075173816	4.00982999086	-874.37977942358	-0.158467167517413
4.07997571152	-477.625718009162	-0.289489950890891	3.91552703165	-874.380618388711	-0.686018439157131	4.13917934541	-874.38023142074	-0.442099667628959
4.20747495251	-477.625810847935	-0.347747160511797	4.03788725139	-874.380673966356	-0.720893937910469	4.26852869995	-874.380435608704	-0.57022954956144
4.33497419349	-477.625830372334	-0.359998905872243	4.16024747113	-874.380653092282	-0.707795258761323	4.39787805449	-874.380499010687	-0.610014894545747
4.46247343448	-477.62581113238	-0.347925652466979	4.28260769087	-874.38059112512	-0.668910277477654	4.52722740904	-874.380486609748	-0.602233187837231
4.58997267546	-477.62577295038	-0.323966085714584	4.40496791061	-874.38050848369	-0.617051997262556	4.65657676358	-874.380436292132	-0.570658407087547
4.71747191645	-477.625726952577	-0.295102028549269	4.52732813035	-874.38041696968	-0.55962608896922	4.78592611813	-874.380368917421	-0.528380137648465
4.84497115743	-477.625679340599	-0.265225061275488	4.64968835009	-874.380323552297	-0.501005796083257	4.91527547267	-874.380295094996	-0.482055866526288
4.97247039842	-477.625633475402	-0.236444215652078	4.77204856983	-874.380232455284	-0.443841557400714	5.04462482721	-874.380219736624	-0.434767774159215
5.0999696394	-477.625591165247	-0.209894192519202	4.89440878957	-874.380146230332	-0.389734583098939	5.17397418176	-874.38014501555	-0.387879592361225
5.22746888039	-477.625553027746	-0.185962549322063	5.01676900931	-874.380066334319	-0.339599078038824	5.3033235363	-874.380072123443	-0.342139104621549
5.35496812137	-477.62551904461	-0.164637809521719	5.13912922904	-874.379993496201	-0.293892468889151	5.43267289085	-874.380002129658	-0.298217341401261
5.48246736236	-477.625488818465	-0.145670617180479	5.26148944878	-874.379927978382	-0.252779416789085	5.56202224539	-874.379936225471	-0.256861839711385
5.60996660334	-477.625461807651	-0.128721075498562	5.38384966852	-874.379869761769	-0.216247940543583	5.69137159993	-874.379875615966	-0.218828801038807
5.73746584433	-477.625437491047	-0.113462176132189	5.50620988826	-874.379818653798	-0.184177204550751	5.82072095448	-874.379821292258	-0.184740159668724

RI-MP2/CBS(34)											
$R_{C\text{-}C}$ [Å]	E [Ha]	BIE [kcal mol^{-1}]	$R_{C\text{-}C}$ [Å]	E [Ha]	BIE [kcal mol^{-1}]	$R_{C\text{-}C}$ [Å]	E [Ha]	BIE [kcal mol^{-1}]	$R_{C\text{-}C}$ [Å]	E [Ha]	BIE [kcal mol^{-1}]
2-HH1			2-HH2			2-HF1			2-HF2		
3.34273389134	-159.350949729516	-0.922018398173698	3.58048380658	-159.350668726325	-0.743231388291426	3.90237412775	-754.466415720511	-0.150693154709938	3.77935622887	-754.466513107231	-0.212521672565869
3.45415835439	-159.351483696921	-1.25708800362146	3.6998332668	-159.351214217536	-1.08553229117745	4.03245326534	-754.46722702637	-0.659795267527997	3.90533476983	-754.467382928067	-0.75834248783057
3.56558281743	-159.351716524255	-1.40318936151428	3.81918272702	-159.351431486543	-1.22187065146477	4.16253240293	-754.467602413971	-0.895354543593359	4.03131331079	-754.467799578388	-1.01979451116568
3.67700728048	-159.3517571959	-1.42871120407237	3.93853218724	-159.351451338471	-1.23432792437205	4.29261154053	-754.467721543581	-0.970109502483782	4.15729185176	-754.467943916397	-1.11036797970522
3.78843174352	-159.351680946545	-1.38086401142086	4.05788164746	-159.351359553442	-1.17673194909463	4.42269067812	-754.467698133337	-0.955419352577752	4.28327039272	-754.467932549948	-1.1032354253245
3.89985620657	-159.351538617298	-1.29155106049343	4.17723110768	-159.351210676546	-1.08331028640017	4.55276981571	-754.467602149935	-0.895188858517378	4.40924893368	-754.467838024083	-1.04391954946647
4.01128066961	-159.351363735611	-1.18181114507059	4.29658056789	-159.351038299307	-0.975141935818958	4.6828489533	-754.467475245236	-0.815554957554053	4.53522747464	-754.467704079445	-0.959868020106714
4.12270513266	-159.351177757921	-1.06510838264619	4.41593002811	-159.3508623665	-0.864742432641196	4.81292809089	-754.467341108038	-0.731382595017946	4.66120601561	-754.467556383622	-0.86718749191109
4.2341295957	-159.350993889131	-0.949728974946194	4.53527948833	-159.350694154815	-0.759188006661367	4.94300722849	-754.467212226479	-0.650508195708087	4.78718455657	-754.467409568235	-0.775059445649848
4.34555405875	-159.350819791931	-0.840481332556879	4.65462894855	-159.350539508614	-0.66214605041769	5.07308636608	-754.467094288005	-0.576500685938342	4.91316309753	-754.46727156323	-0.688459997589334
4.45697852179	-159.35065970828	-0.740027324924059	4.77397840877	-159.350400932039	-0.575187936741347	5.20316550367	-754.466989026833	-0.510448303231085	5.03914163849	-754.467146174173	-0.609777176338748
4.56840298483	-159.3505146464	-0.648999620904695	4.89332786899	-159.350278886194	-0.498603012730381	5.33324464126	-754.466896061924	-0.452111942110083	5.16512017945	-754.467034615334	-0.539772947978748
4.67982744788	-159.350385523694	-0.567973899581551	5.01267732921	-159.350172657412	-0.431943445621594	5.46332377885	-754.466814045371	-0.400645778116915	5.29109872042	-754.466936475194	-0.478189080324272
4.79125191092	-159.350271514084	-0.496431789178482	5.13202678943	-159.350080889958	-0.374358498834959	5.59340291644	-754.466741355745	-0.355032349072305	5.41707726138	-754.466850389759	-0.424169654296725
4.90267637397	-159.350171547197	-0.433701620495597	5.25137624965	-159.350001949135	-0.324822384506947	5.72348205404	-754.466676479586	-0.314321944697857	5.54305580234	-754.466774551942	-0.37658070563698
5.01410083701	-159.350084338888	-0.378977580388251	5.37072570987	-159.349934154841	-0.28228082274943	5.85356119163	-754.466618192283	-0.277746109865832	5.6690343433	-754.466707115693	-0.334263820517917
2-HF3			2-HF4			2-FF1			2-FF2		
4.1164580051	-754.465943261392	0.148966552401164	3.78617705941	-754.466356019137	-0.105633868741545	4.18662183349	-1349.58217947699	0.422403352588597	4.58731127773	-1349.5813414665	0.959677054642131
4.25367327193	-754.466936785684	-0.474479353459763	3.91238296139	-754.467275370218	-0.682535381962415	4.3261758946	-1349.5835459017	-0.435041098515189	4.74022165365	-1349.58313615688	-0.166508161808554
4.39088853877	-754.467377534664	-0.751053514099607	4.03858886337	-754.467722182154	-0.962914104935162	4.46572995572	-1349.5842539442	-0.879344475282897	4.89313202958	-1349.58396180227	-0.684608466212446
4.52810380561	-754.46751435537	-0.836909803329708	4.16479476535	-754.467881858744	-1.0631126779284	4.60528401684	-1349.58456095936	-1.07199939680257	5.0460424055	-1349.5842695924	-0.877749688734245
4.66531907244	-754.467494946883	-0.824730793866361	4.29100066733	-754.467876041844	-1.05946251803348	4.74483807795	-1349.58463511239	-1.1185311256706	5.19895278143	-1349.58431622788	-0.907013894243422
4.80253433928	-754.467402560086	-0.76675720350744	4.41720656931	-754.467782122607	-1.00052730704131	4.88439213907	-1349.58458250581	-1.08551999827309	5.35186315735	-1349.58424199907	-0.860434612702404
4.93974960612	-754.467282170608	-0.691211665448513	4.54341247129	-754.4676477723	-0.91622121655931	5.02394620018	-1349.58446694233	-1.01300281972825	5.50477353327	-1349.58412001749	-0.783890015647134
5.07696487295	-754.467157190089	-0.612785205716842	4.66961837327	-754.467501219054	-0.824257666286135	5.1635002613	-1349.5843245924	-0.923676890028927	5.6576839092	-1349.58398553846	-0.699503150226163
5.21418013979	-754.467039177046	-0.538730903183184	4.79582427525	-754.467358163094	-0.734488696041244	5.30305432242	-1349.58417461646	-0.829565566759294	5.81059428512	-1349.58385309267	-0.616392162298197
5.35139540663	-754.466933228916	-0.472247447856241	4.92203017723	-754.467226396483	-0.651803899323041	5.44260838353	-1349.58402639816	-0.736557179317194	5.96350466105	-1349.58372709484	-0.537327330218131
5.48861067346	-754.466840851946	-0.414280024018215	5.04823607921	-754.467108882831	-0.578062969323857	5.58216244465	-1349.58388418813	-0.647319038235104	6.11641503697	-1349.58360844471	-0.462873249592967
5.6258259403	-754.466761441066	-0.364448944440687	5.17444198119	-754.467005803652	-0.513379807938976	5.72171650576	-1349.58374993791	-0.563075753253711	6.2693254129	-1349.58349791419	-0.393514301106348
5.76304120714	-754.46669317709	-0.321612652765051	5.30064788317	-754.466915846803	-0.456931032925216	5.86127056688	-1349.58362490683	-0.484617566034023	6.42223578882	-1349.58339702867	-0.330207681553587
5.90025647397	-754.466633760049	-0.284327896673321	5.42685378515	-754.466837029369	-0.407472346390664	6.000824628	-1349.5835103514	-0.412732948445053	6.57514616474	-1349.58330754626	-0.274056621394634
6.03747174081	-754.466581039945	-0.251245531937668	5.55305968713	-754.466767228252	-0.363671484190652	6.14037868911	-1349.58340756083	-0.348230891898363	6.72805654067	-1349.58323065162	-0.225804506319726
6.17468700765	-754.466533425286	-0.22136688229853	5.67926558911	-754.466704176365	-0.324105827764389	6.27993275023	-1349.58331754881	-0.291747496648453	6.88096691659	-1349.58316650397	-0.185551248249558

RI-MP2/CBS(34)											
$R_{C\text{-}C}$ [Å]	E [Ha]	BIE [kcal mol^{-1}]	$R_{C\text{-}C}$ [Å]	E [Ha]	BIE [kcal mol^{-1}]	$R_{C\text{-}C}$ [Å]	E [Ha]	BIE [kcal mol^{-1}]	$R_{C\text{-}C}$ [Å]	E [Ha]	BIE [kcal mol^{-1}]
3-HH1			3-HH2			3-HF1			3-HF2		
3.43594668895	-237.837861377554	-1.27907407939742	4.03806907476	-237.836522602713	-0.442077485178922	4.05575650873	-1031.3113995789	-0.220184335009038	4.26586656335	-1031.31130221495	-0.141033872547684
3.55047824525	-237.83874095408	-1.83101668258137	4.17267137725	-237.837307613826	-0.934679395787768	4.19094839235	-1031.31285655846	-1.13445281238934	4.40806211546	-1031.31258788714	-0.947805352137851
3.66500980155	-237.839150172	-2.0878048042995	4.30727367975	-237.837678630023	-1.16749557440859	4.32614027597	-1031.3135109562	-1.54509359396339	4.55025766757	-1031.31312693244	-1.28606138480416
3.77954135785	-237.839254745088	-2.15342540775082	4.44187598224	-237.837790617196	-1.23776858643242	4.4613321596	-1031.31370274065	-1.66544015327481	4.69245321968	-1031.31325615605	-1.36715042447023
3.89407291414	-237.839169394898	-2.09986735491477	4.57647828473	-237.837749307621	-1.21184643676427	4.59652404322	-1031.31364340516	-1.62820657126654	4.83464877179	-1031.31317832977	-1.31831369633365
4.00860447044	-237.838973324662	-1.97683142425481	4.71108058722	-237.837624452991	-1.13349897356532	4.73171592685	-1031.31345993928	-1.51307999333098	4.97684432391	-1031.31300847649	-1.21172915401553
4.12313602674	-237.838719333703	-1.81744969118365	4.84568288971	-237.837460299879	-1.03049134060137	4.86690781047	-1031.31322601078	-1.3662876433813	5.11903987602	-1031.3128076432	-1.08570436176005
4.23766758304	-237.838442099831	-1.64348280999129	4.98028519221	-237.837283714427	-0.919682296494421	5.00209969409	-1031.31298287917	-1.21372025469163	5.26123542813	-1031.31260627994	-0.959347008409867
4.35219913934	-237.83816395024	-1.46894130643353	5.1148874947	-237.837110149298	-0.810768533697704	5.13729157772	-1031.31275244341	-1.06911963218628	5.40343098024	-1031.31241863296	-0.841596750793424
4.46673069564	-237.837898055062	-1.30208956315436	5.24948979719	-237.836947820504	-0.708905677556631	5.27248346134	-1031.3125449229	-0.938898546110254	5.54562653235	-1031.31225064694	-0.736183931626196
4.58126225193	-237.837651986313	-1.14767909190598	5.38409209968	-237.836800543288	-0.616487829211417	5.40767534497	-1031.31236339598	-0.824988683906854	5.68782208446	-1031.312103845	-0.644064323480366
4.69579380823	-237.837429162035	-1.00785474641623	5.51869440218	-237.836669547111	-0.534286487082257	5.54286722859	-1031.3122066766	-0.726645788258997	5.83001763658	-1031.31197713831	-0.564554675212889
4.81032536453	-237.837230414556	-0.883138820407496	5.65329670467	-237.836554616218	-0.462166262866155	5.67805911222	-1031.31207134739	-0.641725426859504	5.97221318869	-1031.31186788429	-0.495996742516836
4.92485692083	-237.83705498468	-0.773054911207008	5.78789900716	-237.836454635955	-0.399427700619418	5.81325099584	-1031.31195328892	-0.567642618461369	6.1144087408	-1031.31177282207	-0.43634429884862
5.03938847713	-237.836901102104	-0.676492136882983	5.92250130965	-237.836368497742	-0.345375155893108	5.94844287946	-1031.31184871055	-0.502018700555898	6.25660429291	-1031.31168888208	-0.383671159899212
5.15392003343	-237.836766974394	-0.592325728133181	6.05710361214	-237.836294568794	-0.298984040612549	6.08363476309	-1031.31175472753	-0.443043464998624	6.39879984502	-1031.31161371676	-0.336504209394797
3-HF3			3-HF4			3-FF1			3-FF2		
4.37726127205	-1031.31209771694	-0.646629838228183	4.22420781328	-1031.31058766216	0.30178644078492	4.44732592776	-1824.78445056558	1.1247675713992	4.42086165258	-1824.78052595176	3.70345943850342
4.52316998112	-1031.31297410286	-1.19657030593169	4.36501474039	-1031.31220980401	-0.716122938275052	4.59557012535	-1824.78702710472	-0.492035149025557	4.56822370767	-1824.78559165462	0.524682901343512
4.66907869019	-1031.31328584863	-1.39219373007186	4.5058216675	-1031.3129888652	-1.20499121573787	4.74381432294	-1824.7882612566	-1.26647714607955	4.71558576275	-1824.78802608247	-1.00294363826856
4.81498739925	-1031.31329098054	-1.39541405223501	4.6466285946	-1031.31327446575	-1.38420826671427	4.89205852053	-1824.78875098608	-1.57378703449108	4.86294781784	-1824.7890464368	-1.6432256471596
4.96089610832	-1031.3131452053	-1.30393870815846	4.78743552171	-1031.31328710823	-1.39214154268117	5.04030271812	-1824.78884791919	-1.63461347932528	5.01030987293	-1824.78934412849	-1.83003000302429
5.10680481739	-1031.31293825837	-1.17407754889265	4.92824244882	-1031.31316088249	-1.31293369488555	5.18854691572	-1824.78875142358	-1.57406156983622	5.15767192801	-1824.78929792993	-1.80103996888578
5.25271352646	-1031.3127180476	-1.03589320439887	5.06904937593	-1031.31297302434	-1.19505092601954	5.33679111331	-1824.78856912456	-1.45966720766942	5.3050339831	-1824.78910640865	-1.68085855125686
5.39862223553	-1031.31250807999	-0.904136539977102	5.20985630304	-1031.31276593365	-1.06509955615817	5.4850353109	-1824.78835469745	-1.32511216466507	5.45239603818	-1824.78886681809	-1.53051320490476
5.5445309446	-1031.31231861639	-0.78524633599342	5.35066323015	-1031.31256212623	-0.937208469160786	5.63327950849	-1824.78813210007	-1.18543019989738	5.59975809327	-1824.78862081133	-1.37614163241176
5.69043965366	-1031.31215278152	-0.681183383866519	5.49147015726	-1031.31237305927	-0.818567160510878	5.78152370608	-1824.78791128926	-1.04686932459436	5.74712014836	-1824.78838193633	-1.22624530685852
5.83634836273	-1031.31200985422	-0.591495149038477	5.63227708437	-1031.31220392045	-0.71243094856727	5.92976790367	-1824.78769733805	-0.912612913443614	5.89448220344	-1824.7881525155	-1.08228156249431
5.9822570718	-1031.31188725786	-0.514564771713646	5.77308401148	-1031.3120562612	-0.619773370310587	6.07801210127	-1824.78749441437	-0.785276381722467	6.04184425853	-1824.78793286868	-0.944451101921318
6.12816578087	-1031.31178179961	-0.44838872065294	5.91389093859	-1031.31192944759	-0.540196628606443	6.22625629886	-1824.78730661091	-0.667427931326234	6.18920631361	-1824.78772482796	-0.813903579109802
6.27407448994	-1031.31169039359	-0.391030577172944	6.0546978657	-1031.31182148696	-0.472450310477856	6.37450049645	-1824.78713747843	-0.56129569770496	6.3365683687	-1824.78753178467	-0.692767085753593
6.419983199	-1031.31161042869	-0.340851844900511	6.19550479281	-1031.31172959288	-0.414785904664084	6.52274469404	-1824.78698940015	-0.468375174214675	6.48393042379	-1824.78735736284	-0.583315735083428
6.56589190807	-1031.31153990507	-0.296597605194244	6.33631171992	-1031.31165070082	-0.365280389624495	6.67098889163	-1824.78686323827	-0.389207399138361	6.63129247887	-1824.78720417806	-0.48719083425142

RI-MP2/CBS(34)											
$R_{C\text{-}C}$ [Å]	E [Ha]	BIE [kcal mol^{-1}]	$R_{C\text{-}C}$ [Å]	E [Ha]	BIE [kcal mol^{-1}]	$R_{C\text{-}C}$ [Å]	E [Ha]	BIE [kcal mol^{-1}]	$R_{C\text{-}C}$ [Å]	E [Ha]	BIE [kcal mol^{-1}]
4-HH1			4-HH2			4-HF1			4-HF2		
3.45206253651	-316.32564440408	-2.0236029269884	4.10663636738	-316.323655396208	-0.778031196860239	4.0391979304	-1308.15613439667	-0.403824918087795	4.07104188193	-1308.15630426445	-0.283449362666392
3.56713128772	-316.326814175797	-2.75764576182457	4.24352424629	-316.324630880772	-1.3901570025344	4.17383786142	-1308.15806771584	-1.6170010134617	4.206743278	-1308.15829111768	-1.53021858789934
3.68220003894	-316.327342334374	-3.08907027268291	4.38041212521	-316.325073551191	-1.66793688430191	4.30847779243	-1308.15894102419	-2.16501027683348	4.34244467406	-1308.15922061181	-2.11348496056763
3.79726879016	-316.327453943624	-3.15910613443404	4.51730000412	-316.325185961149	-1.73847519790526	4.44311772345	-1308.15918831531	-2.32018779753475	4.47814607013	-1308.15951830946	-2.30029305633781
3.91233754137	-316.327306557984	-3.06662024900802	4.65418788303	-316.325104942558	-1.68763526451575	4.57775765446	-1308.15909063928	-2.25889516332134	4.61384746619	-1308.15946100554	-2.26433430355895
4.02740629259	-316.327008835124	-2.87979633372436	4.79107576194	-316.324919958382	-1.57155594151658	4.71239758547	-1308.15882413314	-2.09166003548013	4.74954886225	-1308.15922245654	-2.11464254607102
4.14247504381	-316.326633873091	-2.64450410563114	4.92796364086	-316.324687461667	-1.42566205018004	4.84703751649	-1308.15849258775	-1.88361216230285	4.88525025832	-1308.15890683864	-1.91658932364805
4.25754379502	-316.32622991513	-2.39101665800716	5.06485151977	-316.324441569378	-1.27136230924812	4.9816774475	-1308.15815260346	-1.6702687992403	5.02095165438	-1308.15857311715	-1.70717592696354
4.37261254624	-316.325827446367	-2.13846369622711	5.20173939868	-316.324201776109	-1.12088976116512	5.11631737851	-1308.1578323836	-1.4693278033358	5.15665305045	-1308.15825227922	-1.50584708636506
4.48768129746	-316.32544457813	-1.89821025020886	5.33862727759	-316.32397834577	-0.980685106651279	5.25095730953	-1308.15754406009	-1.28840206926593	5.29235444651	-1308.1579588236	-1.32170090457441
4.60275004867	-316.325090964031	-1.67631405296552	5.47551515651	-316.323775969878	-0.85369231711096	5.38559724054	-1308.15729098345	-1.12959407995991	5.42805584258	-1308.15769792257	-1.15798303643523
4.71781879989	-316.324770885697	-1.47546186594108	5.61240303542	-316.323596084211	-0.74081235681695	5.52023717155	-1308.15707192951	-0.992135657372862	5.56375723864	-1308.15746967203	-1.01475366015454
4.83288755111	-316.324485020144	-1.29607852314568	5.74929091433	-316.323438289386	-0.641794609190055	5.65487710257	-1308.1568834251	-0.873847354168304	5.69945863471	-1308.15727156061	-0.890436867274115
4.94795630232	-316.324232086675	-1.13736037507459	5.88617879324	-316.323301187214	-0.555761697351135	5.78951703358	-1308.1567210049	-0.77192713989117	5.83516003077	-1308.15709986937	-0.782698987581169
5.06302505354	-316.324009740335	-0.997835940200208	6.02306667216	-316.323182885079	-0.481525986857464	5.92415696459	-1308.15657993674	-0.683405532999417	5.97086142683	-1308.1569505106	-0.68897494428149
5.17809380476	-316.323815166165	-0.875738805132298	6.15995455107	-316.323081295161	-0.417777350838629	6.05879689561	-1308.15645578943	-0.605501919889615	6.1065628229	-1308.15681959356	-0.606823261375745
4-HF3			4-HF4			4-FF1			4-FF2		
4.08162960506	-1308.15519200744	0.384345310824318	4.17634016747	-1308.15638707146	-0.331373579686099	4.75115085185	-2299.98867221467	0.359444153805805	4.63747496367	-2299.98657913224	1.58090035586702
4.21768392523	-1308.15772169597	-1.20305820794187	4.31555150639	-1308.15828290484	-1.521026986684	4.90952254691	-2299.991298698	-1.28869901907521	4.79205746246	-2299.99031882083	-0.765789664186952
4.3537382454	-1308.15895653107	-1.97792893211324	4.4547628453	-1308.15914304788	-2.06077489326169	5.06789424198	-2299.99236170672	-1.95574706206679	4.94663996125	-2299.99206476011	-1.86138310355788
4.48979256557	-1308.159421429	-2.26965678762324	4.59397418422	-1308.15939429479	-2.21843470960689	5.22626593704	-2299.9926239729	-2.12032157473662	5.10122246004	-2299.99271294703	-2.26812653677373
4.62584688574	-1308.15945200837	-2.28884563193011	4.73318552313	-1308.15931096664	-2.1661455062285	5.3846376321	-2299.99251293278	-2.05064284720833	5.25580495883	-2299.99278955683	-2.31619991184578
4.76190120591	-1308.15925682531	-2.1663664126243	4.87239686205	-1308.15906392204	-2.01112267910198	5.54300932716	-2299.99225113552	-1.88636258628532	5.41038745762	-2299.99259634766	-2.19495932721164
4.89795552608	-1308.15895978383	-1.9799700697201	5.01160820097	-1308.15875343387	-1.81628841097728	5.70138102222	-2299.99194493412	-1.69421830697097	5.56496995641	-2299.9922949113	-2.00580515570587
5.03400984625	-1308.1586307797	-1.77351686117214	5.15081953988	-1308.15843400863	-1.61584604640579	5.85975271728	-2299.99163773285	-1.50144659958264	5.7195524552	-2299.99196533771	-1.79899460555096
5.17006416641	-1308.15830727499	-1.57051459078367	5.2900308788	-1308.15813261128	-1.42671635407394	6.01812441235	-2299.99134245093	-1.31615439728859	5.87413495398	-2299.99164178973	-1.59596518260961
5.30611848658	-1308.15800791066	-1.38266063754606	5.42924221771	-1308.15786050491	-1.25596702885299	6.17649610741	-2299.99106125625	-1.13970207145246	6.02871745277	-2299.99133512726	-1.4035315774029
5.44217280675	-1308.15774038252	-1.21478419509867	5.56845355663	-1308.15762030431	-1.10523887680595	6.33486780247	-2299.99079739006	-0.974123537405948	6.18329995156	-2299.99104708878	-1.22278470233029
5.57822712692	-1308.157506039	-1.06773141620461	5.70766489555	-1308.15741020914	-0.973402167106314	6.49323949753	-2299.99055208258	-0.820190769743027	6.33788245035	-2299.9907779907	-1.05392310767921
5.71428144709	-1308.15730269285	-0.940129780514541	5.84687623446	-1308.15722656343	-0.858162744242505	6.65161119259	-2299.99033241357	-0.682346384685167	6.49246494914	-2299.99052950073	-0.897993297538926
5.85033576726	-1308.15712639721	-0.829502596250264	5.98608757338	-1308.15706527243	-0.756951113646242	6.80998288765	-2299.99014268995	-0.563293015838413	6.64704744793	-2299.99030444649	-0.75676962963825
5.98639008743	-1308.15697257382	-0.732976961661903	6.12529891229	-1308.1569225265	-0.667376690112234	6.96835458272	-2299.98998434538	-0.463930297955702	6.80162994672	-2299.99010552769	-0.63194619812905
6.1224444076	-1308.1568368484	-0.647807974734881	6.26451025121	-1308.15679513315	-0.58743615613474	7.12672627778	-2299.98985577784	-0.383252948662157	6.95621244551	-2299.98993418862	-0.524429308299203

RI-MP2/CBS(34)											
$R_{C\text{-}C}$ [Å]	E [Ha]	BIE [kcal mol^{-1}]	$R_{C\text{-}C}$ [Å]	E [Ha]	BIE [kcal mol^{-1}]	$R_{C\text{-}C}$ [Å]	E [Ha]	BIE [kcal mol^{-1}]	$R_{C\text{-}C}$ [Å]	E [Ha]	BIE [kcal mol^{-1}]
5-HH1			5-HH2			5-HF1			5-HF2		
3.45905710032	-394.813085628483	-2.61008030011037	4.15692279807	-394.809603043717	-0.442442300372499	4.10335551576	-1585.00185437984	-0.755286779080415	4.32605659689	-1585.00169258799	-0.728701928505616
3.57435900366	-394.814633576371	-3.58143226509733	4.29548689134	-394.811368359287	-1.5501945451278	4.24013403296	-1585.00419094514	-2.22150364135994	4.47025848346	-1585.00388581532	-2.10497285674995
3.68966090701	-394.815342800908	-4.02647738125208	4.43405098461	-394.81222066863	-2.08502673265863	4.37691255015	-1585.0052218196	-2.86838713148758	4.61446037002	-1585.00477682229	-2.66408817185668
3.80496281035	-394.815505454051	-4.12854376944743	4.57261507788	-394.812520570453	-2.27321796785117	4.51369106734	-1585.00549862548	-3.04208544367686	4.75866225658	-1585.00494629473	-2.77043373347148
3.9202647137	-394.815326837432	-4.01646014881367	4.71117917115	-394.812499360426	-2.25990847496456	4.65046958453	-1585.00536571698	-2.95868410071194	4.90286414315	-1585.00474170385	-2.64205101797572
4.03556661704	-394.814948731591	-3.779195151424	4.84974326442	-394.812302974418	-2.13667439439266	4.78724810173	-1585.00503125628	-2.74880684288633	5.04706602971	-1585.00436807736	-2.4075968557349
4.15086852038	-394.814467116977	-3.4769774183292	4.98830735769	-394.812019659631	-1.95889168142722	4.92402661892	-1585.00461599273	-2.48822503094976	5.19126791627	-1585.00394105381	-2.13963553252256
4.26617042373	-394.81394529263	-3.14952769682034	5.12687145096	-394.811704559238	-1.76116319957018	5.06080513611	-1585.00418645284	-2.21868468059866	5.33546980283	-1585.0035210091	-1.8760534975401
4.38147232707	-394.813423420483	-2.82204798034053	5.26543554423	-394.811388393271	-1.56276605989907	5.1975836533	-1585.00377719983	-1.96187453953059	5.4796716894	-1585.00313626399	-1.63462229589709
4.49677423042	-394.812925537337	-2.50962158927386	5.4039996375	-394.811088331554	-1.37447448970653	5.33436217049	-1585.00340473237	-1.72814767961713	5.62387357596	-1585.00279734042	-1.42194454484144
4.61207613376	-394.812464642187	-2.22040551615564	5.54256373077	-394.810813008687	-1.201706782239	5.47114068769	-1585.00307510737	-1.52130486928165	5.76807546252	-1585.00250483238	-1.23839297849057
4.7273780371	-394.812046486195	-1.95800866956047	5.68112782403	-394.810565947916	-1.04667380780804	5.60791920488	-1585.0027879402	-1.3411047495023	5.91227734909	-1585.00225413988	-1.08108105967767
4.84267994045	-394.811672266429	-1.72318222103633	5.8196919173	-394.810347649498	-0.909689482341613	5.74469772207	-1585.00253894343	-1.18485691727122	6.05647923565	-1585.00203864698	-0.945857223349749
4.95798184379	-394.811340517787	-1.51500680519635	5.95825601057	-394.810156893262	-0.789988137021487	5.88147623926	-1585.00232198658	-1.04871443847593	6.20068112221	-1585.0018517505	-0.828577911464193
5.07328374714	-394.811048347524	-1.33166719711931	6.09682010384	-394.809991531633	-0.686222148187047	6.01825475645	-1585.00213082188	-0.928756778114617	6.34488300878	-1585.00168790661	-0.725764318200819
5.18858565048	-394.810792216973	-1.17094284981632	6.23538419711	-394.809848980926	-0.596770229030101	6.15503327365	-1585.00196021505	-0.821699376025003	6.48908489534	-1585.00154295276	-0.634804404070654
5-HF3			5-HF4			5-FF1			5-FF2		
4.28282642262	-1585.00117601367	-0.185916823298706	4.08325326395	-1585.00156467174	-0.438043018372701	4.5471930552	-2775.19101248781	1.11537394351929	4.89471861206	-2775.19067480704	1.37168995849074
4.42558730337	-1585.0037138363	-1.77842456700206	4.21936170608	-1585.00417563905	-2.07644974165176	4.69876615704	-2775.19509961334	-1.44933604803141	5.05787589912	-2775.19483264114	-1.23739033040057
4.56834818412	-1585.0048705519	-2.50427456473713	4.35547014821	-1585.00541528991	-2.85434240078111	4.85033925888	-2775.19698422899	-2.63195022321876	5.22103318619	-2775.19670237998	-2.41066916641524
4.71110906488	-1585.00522277345	-2.72529692429295	4.49157859034	-1585.00582358259	-3.11054992567687	5.00191236072	-2775.1976487433	-3.04893924825614	5.38419047326	-2775.19732169336	-2.79929417999859
4.85386994563	-1585.00513440654	-2.6698458511116	4.62768703247	-1585.00575716769	-3.06887394674497	5.15348546256	-2775.19767813052	-3.06738000745009	5.54734776033	-2775.19730548382	-2.78912253991441
4.99663082639	-1585.00482861738	-2.47796025620382	4.7637954746	-1585.00544556325	-2.87333920853112	5.3050585644	-2775.19740897956	-2.89848522991247	5.7105050474	-2775.1970010412	-2.5980819116781
5.13939170714	-1585.00443591668	-2.2315368464422	4.89990391674	-1585.00502916063	-2.61204261949776	5.45663166624	-2775.19701638743	-2.65212994886732	5.87366233447	-2775.19659212646	-2.34148403821221
5.28215258789	-1585.00402819551	-1.97568794954848	5.03601235887	-1585.00458814091	-2.33529856695896	5.60820476808	-2775.19659197969	-2.38581007120587	6.03681962154	-2775.19616659829	-2.07446108000413
5.42491346865	-1585.00364241596	-1.73360762703843	5.172120801	-1585.0041645749	-2.06950688274864	5.75977786992	-2775.1961737625	-2.12337482248571	6.1999769086	-2775.19575963046	-1.81908491118905
5.5676743494	-1585.00329539503	-1.51584870571103	5.30822924313	-1585.00377776481	-1.82677988660407	5.91135097176	-2775.19577430191	-1.87270951779577	6.36313419567	-2775.19538092313	-1.58144247366034
5.71043523016	-1585.00299214504	-1.32555646406865	5.44433768526	-1585.00343396224	-1.61104051681445	6.0629240736	-2775.19539654296	-1.63566219779472	6.52629148274	-2775.1950309865	-1.36185392313259
5.85319611091	-1585.00273080417	-1.16156259213067	5.58044612739	-1585.00313235281	-1.42177774208845	6.21449717544	-2775.19504220271	-1.41331033365139	6.68944876981	-2775.19470948101	-1.16010618201415
5.99595699166	-1585.00250599392	-1.02049203049938	5.71655456953	-1585.00286878135	-1.25638415373111	6.36607027728	-2775.19471468778	-1.20779161237415	6.85260605688	-2775.19441796739	-0.977178623861053
6.13871787242	-1585.00231114745	-0.898224024539625	5.85266301166	-1585.00263794612	-1.11153286010746	6.51764337912	-2775.19441860577	-1.02199734588709	7.01576334395	-2775.19415932317	-0.814876925328425
6.28147875317	-1585.00214007931	-0.790877146031166	5.98877145379	-1585.00243455607	-0.983903676785985	6.66921648096	-2775.19415799273	-0.858460194427516	7.17892063102	-2775.19393594099	-0.674702490968874
6.42423963392	-1585.00198783895	-0.695344877827	6.12487989592	-1585.00225389129	-0.870534815626312	6.8207895828	-2775.19393263197	-0.717044182211092	7.34207791808	-2775.19374824127	-0.55691913849892

RI-MP2/CBS(34)											
$R_{C\text{-}C}$ [Å]	E [Ha]	BIE [kcal mol^{-1}]	$R_{C\text{-}C}$ [Å]	E [Ha]	BIE [kcal mol^{-1}]	$R_{C\text{-}C}$ [Å]	E [Ha]	BIE [kcal mol^{-1}]	$R_{C\text{-}C}$ [Å]	E [Ha]	BIE [kcal mol^{-1}]
6-HH1			6-HH2			6-HF1			6-HF2		
3.66066245322	-473.299921047196	-2.78226130187702	4.10083752819	-473.297115542932	-1.0318210312603	4.07836427965	-1861.84505717283	0.103746861768915	4.2821480345	-1861.84646193192	-0.65474150770167
3.78268453499	-473.302064635571	-4.12738331555836	4.23753211246	-473.298853708634	-2.12253647666118	4.21430975564	-1861.84874646628	-2.21131973058476	4.42488630232	-1861.84942330538	-2.51303140992823
3.90470661677	-473.303035173339	-4.73640495986073	4.37422669673	-473.299690756044	-2.64779165663346	4.35025523163	-1861.85047104451	-3.29350890848152	4.56762457013	-1861.85067242442	-3.2968654417069
4.02672869854	-473.303270922303	-4.88433966823978	4.51092128101	-473.299959550278	-2.8164625850181	4.48620070762	-1861.85106037463	-3.66331914207303	4.71036283795	-1861.85096468256	-3.48026019341498
4.14875078031	-473.303063236651	-4.75401495398663	4.64761586528	-473.299888314835	-2.77176166965859	4.6221461836	-1861.85102680542	-3.64225414475207	4.85310110577	-1861.85075559058	-3.34905299504737
4.27077286209	-473.30260498797	-4.46645956523825	4.78431044955	-473.299627253157	-2.6079429933954	4.75809165959	-1861.85067875421	-3.42348471315776	4.99583937358	-1861.85031350551	-3.07164042526913
4.39279494386	-473.302022180777	-4.10074253008972	4.92100503383	-473.299273217238	-2.38578210010279	4.89403713558	-1861.85019453786	-3.11999836602954	5.1385776414	-1861.84979073654	-2.74359794382697
4.51481702564	-473.301393483241	-3.70622886996847	5.0576996181	-473.298886621118	-2.14318937219434	5.02998261157	-1861.84967264042	-2.79250277799404	5.28131590922	-1861.84926804331	-2.41560299008894
4.63683910741	-473.300768293732	-3.31391653003787	5.19439420237	-473.298501022173	-1.90122238104138	5.16592808756	-1861.84916507911	-2.47400324727853	5.42405417703	-1861.84878396714	-2.11184060721597
4.75886118918	-473.300174800302	-2.94149377994536	5.33108878664	-473.298137364226	-1.673023574009	5.30187356355	-1861.84869748588	-2.1805840654492	5.56679244485	-1861.84835355296	-1.84175163147618
4.88088327096	-473.299627601647	-2.59812143977331	5.46778337092	-473.297804606073	-1.46421468042836	5.43781903953	-1861.84828016435	-1.91871085167361	5.70953071267	-1861.84797925419	-1.60687560726726
5.00290535273	-473.2991326992	-2.28756546559147	5.60447795519	-473.297506390366	-1.27708149898708	5.57376451552	-1861.84791439698	-1.68918836179048	5.85226898048	-1861.84765688837	-1.40458800111637
5.1249274345	-473.298690881967	-2.01032096609199	5.74117253946	-473.297242974478	-1.11178553369175	5.70970999151	-1861.84759639775	-1.48964083224581	5.9950072483	-1861.84737926743	-1.23037823102515
5.24694951628	-473.29829948655	-1.76471663383702	5.87786712374	-473.297012694476	-0.967282650745907	5.8456554675	-1861.84732001195	-1.31620612418237	6.13774551612	-1861.84713854397	-1.07932197931729
5.36897159805	-473.297955938149	-1.54913675745529	6.01456170801	-473.296812874207	-0.841893538840237	5.98160094349	-1861.84707847812	-1.1646413576151	6.28048378393	-1861.84692769202	-0.947010383089046
5.49099367983	-473.297655337072	-1.36050673373376	6.15125629228	-473.296640384628	-0.733654693868979	6.11754641948	-1861.84686555392	-1.03102940486261	6.42322205175	-1861.84674121046	-0.829991437511718
6-HF3			6-HF4			6-FF1			6-FF2		
4.20626486631	-1861.84465613971	0.561157148702416	4.20917353341	-1861.84733034042	-0.915147375290368	4.33323976416	-3250.39431899719	1.24863988110531	5.1937903833	-3250.38387467508	7.83669794339467
4.34647369519	-1861.84866024618	-1.95145759605987	4.34947931786	-1861.84996300203	-2.56716747729046	4.47768108963	-3250.39932794826	-1.89452437016434	5.36691672941	-3250.39420638939	1.35344933103976
4.48668252407	-1861.85052048804	-3.1187769871152	4.48978510231	-1861.85116960267	-3.32432081036078	4.62212241511	-3250.40178886551	-3.43877325905846	5.54004307552	-3250.39891420176	-1.60074753283396
4.62689135294	-1861.85115845884	-3.51910970837523	4.63009088675	-1861.85151536121	-3.54128756985137	4.76656374058	-3250.4027632384	-4.05020147883085	5.71316942163	-3250.40072495566	-2.73701276011462
4.76710018182	-1861.85113663334	-3.50541400036872	4.7703966712	-1861.85137478002	-3.45307154128961	4.91100506605	-3250.40290814767	-4.141133418719	5.88629576774	-3250.40113422805	-2.99383506243881
4.9073090107	-1861.85078769241	-3.28645026089423	4.91070245565	-1861.85098851568	-3.21068700831444	5.05544639152	-3250.402624422	-3.96309287264205	6.05942211385	-3250.40092932957	-2.86525932490142
5.04751783957	-1861.85030102682	-2.98106299252424	5.0510082401	-1861.85050239709	-2.9056429877064	5.19988771699	-3250.40214608261	-3.66293037381702	6.23254845996	-3250.400500485	-2.59615529448057
5.18772666845	-1861.84977945004	-2.65376862159188	5.19131402454	-1861.84999858695	-2.58949735182845	5.34432904247	-3250.40160164861	-3.32129288059625	6.40567480607	-3250.40002518241	-2.29789841619149
5.32793549733	-1861.84927606355	-2.33788883004489	5.33161980899	-1861.84951968893	-2.28898430720369	5.48877036794	-3250.40105489086	-2.9781972126034	6.57880115218	-3250.39957050652	-2.01258498757397
5.46814432621	-1861.84881659355	-2.04956705209131	5.47192559344	-1861.84908487884	-2.01613685624049	5.63321169341	-3250.40053189351	-2.65001142067059	6.75192749829	-3250.39915099629	-1.74933834372686
5.60835315508	-1861.8484112345	-1.79520040778716	5.61223137788	-1861.84869976552	-1.7744745992921	5.77765301888	-3250.40003943985	-2.34099208340666	6.9250538444	-3250.39876343966	-1.50614288675123
5.74856198396	-1861.84806062379	-1.57518886555791	5.75253716233	-1861.84836267356	-1.56294620086836	5.92209434435	-3250.39957737158	-2.05103986645607	7.09818019051	-3250.39840501753	-1.28122960453476
5.88877081284	-1861.84775943391	-1.38618936223002	5.89284294678	-1861.84806863088	-1.37843163353495	6.06653566983	-3250.39914571985	-1.78017431628966	7.27130653662	-3250.39807815327	-1.07611918471522
6.02897964171	-1861.84749938082	-1.22300358467988	6.03314873123	-1861.84781163376	-1.21716350579867	6.2109769953	-3250.39874724346	-1.53012660651303	7.44443288273	-3250.39778802378	-0.894060180948259
6.16918847059	-1861.84727176679	-1.08017362451372	6.17345451567	-1861.84758574059	-1.07541340154042	6.35541832077	-3250.39838667548	-1.30386678310688	7.61755922884	-3250.39753544248	-0.735563022419248
6.30939729947	-1861.84706929155	-0.953118493001637	6.31376030012	-1861.84738558549	-0.949814179911805	6.49985964624	-3250.39806851767	-1.10421974285525	7.79068557495	-3250.39732750376	-0.605079505610587

TightPNO-DLPNO-CCSD(T)/cc-pVQZ

$R_{C\text{-}C}$ [Å]	BIE [kcal mol^{-1}]	$R_{C\text{-}C}$ [Å]	BIE [kcal mol^{-1}]	$R_{C\text{-}C}$ [Å]	BIE [kcal mol^{-1}]	$R_{C\text{-}C}$ [Å]	BIE [kcal mol^{-1}]	$R_{C\text{-}C}$ [Å]	BIE [kcal mol^{-1}]	$R_{C\text{-}C}$ [Å]	BIE [kcal mol^{-1}]	$R_{C\text{-}C}$ [Å]	BIE [kcal mol^{-1}]	$R_{C\text{-}C}$ [Å]	BIE [kcal mol^{-1}]
1-HH1		1-HH2		1-HF1		1-HF2								1-FF1		1-FF2	
3.30371146716	-0.112609	3.5804338401	-0.0419088	3.40464005758	-0.0721955	3.82497722955	0.2242							3.67080659217	-0.0907777	3.88048063632	0.482832
3.41383518274	-0.300277	3.69978163477	-0.214587	3.5181280595	-0.347836	3.95247647054	-0.0596355							3.79316681191	-0.366859	4.00982999086	-0.0434683
3.52395889831	-0.389495	3.81912942944	-0.295629	3.63161606142	-0.479656	4.07997571152	-0.196788							3.91552703165	-0.487365	4.13917934541	-0.306829
3.63408261388	-0.419488	3.93847722411	-0.326033	3.74510406334	-0.517481	4.20747495251	-0.252219							4.03788725139	-0.477106	4.26852869995	-0.422088
3.74420632945	-0.414464	4.05782501878	-0.325639	3.85859206526	-0.505145	4.33497419349	-0.264318							4.16024747113	-0.434117	4.39787805449	-0.447067
3.85433004502	-0.388837	4.17717281345	-0.305492	3.97208006718	-0.462119	4.46247343448	-0.248703							4.28260769087	-0.390042	4.52722740904	-0.415557
3.9644537606	-0.354816	4.29652060812	-0.279457	4.0855680691	-0.40885	4.58997267546	-0.215904							4.40496791061	-0.295796	4.65657676358	-0.355531
4.07457747617	-0.315621	4.41586840279	-0.253394	4.19905607102	-0.343115	4.71747191645	-0.179351							4.52732813035	-0.217168	4.78592611813	-0.284486
4.18470119174	-0.273674	4.53521619746	-0.22228	4.31254407294	-0.278651	4.84497115743	-0.139164							4.64968835009	-0.146014	4.91527547267	-0.216121
4.29482490731	-0.234539	4.65456399213	-0.191847	4.42603207486	-0.217661	4.97247039842	-0.101815							4.77204856983	-0.0759355	5.04462482721	-0.15038
4.40494862289	-0.202115	4.7739117868	-0.164035	4.53952007678	-0.165643	5.0999696394	-0.0687836							4.89440878957	-0.0134125	5.17397418176	-0.0907891
4.51507233846	-0.172812	4.89325958147	-0.140377	4.6530080787	-0.111975	5.22746888039	-0.0391888							5.01676900931	0.0394407	5.3033235363	-0.0368613
4.62519605403	-0.145541	5.01260737614	-0.119173	4.76649608062	-0.0640438	5.35496812137	-0.0120497							5.13912922904	0.0840676	5.43267289085	0.00691842
4.7353197696	-0.12392	5.13195517081	-0.10222	4.87998408254	-0.0216397	5.48246736236	0.0115913							5.26148944878	0.123147	5.56202224539	0.0470864
4.84544348517	-0.103927	5.25130296548	-0.0862979	4.99347208446	0.0175056	5.60996660334	0.0329467							5.38384966852	0.158872	5.69137159993	0.0838928
4.95556720075	-0.0899487	5.37065076015	-0.0726374	5.10696008638	0.0514087	5.73746584433	0.0514417							5.50620988826	0.18999	5.82072095448	0.114971
2-HH1		2-HH2		2-HF1		2-HF2		2-HF3		2-HF4		2-FF1				2-FF2	
3.34273389134	-0.507082	3.58048380658	-0.414245	3.90237412775	0.0969077	3.77935622887	0.0675529	4.1164580051	0.35832	3.78617705941	0.18243	4.18662183349	0.713446	4.58731127773	1.21386		
3.45415835439	-0.897779	3.6998332668	-0.811118	4.03245326534	-0.4305	3.90533476983	-0.50209	4.25367327193	-0.282909	3.91238296139	-0.417481	4.3261758946	-0.123781	4.74022165365	0.104539		
3.56558281743	-1.09092	3.81918272702	-0.982045	4.16253240293	-0.672959	4.03131331079	-0.774183	4.39088853877	-0.56882	4.03858886337	-0.724556	4.46572995572	-0.558518	4.89313202958	-0.399381		
3.67700728048	-1.15075	3.93853218724	-1.02402	4.29261154053	-0.749613	4.15729185176	-0.869884	4.52810380561	-0.653699	4.16479476535	-0.827095	4.60528401684	-0.737665	5.0460424055	-0.564898		
3.78843174352	-1.13225	4.05788164746	-0.990036	4.42269067812	-0.734984	4.28327039272	-0.867846	4.66531907244	-0.638451	4.29100066733	-0.82778	4.74483807795	-0.758373	5.19895278143	-0.573188		
3.89985620657	-1.06784	4.17723110768	-0.914908	4.55276981571	-0.678422	4.40924893368	-0.810097	4.80253433928	-0.577486	4.41720656931	-0.773283	4.88439213907	-0.692446	5.35186315735	-0.506162		
4.01128066961	-0.974643	4.29658056789	-0.828953	4.6828489533	-0.586352	4.53522747464	-0.719285	4.93974960612	-0.492962	4.54341247129	-0.679954	5.02394620018	-0.594191	5.50477353327	-0.407677		
4.12270513266	-0.874077	4.41593002811	-0.738431	4.81292809089	-0.496506	4.66120601561	-0.616672	5.07696487295	-0.405076	4.66961837327	-0.578967	5.1635002613	-0.469877	5.6576839092	-0.299621		
4.2341295957	-0.792078	4.53527948833	-0.639432	4.94300722849	-0.404911	4.78718455657	-0.507038	5.21418013979	-0.316983	4.79582427525	-0.475324	5.30305432242	-0.354923	5.81059428512	-0.201467		
4.34555405875	-0.692637	4.65462894855	-0.547928	5.07308636608	-0.322186	4.91316309753	-0.402337	5.35139540663	-0.235586	4.92203017723	-0.38176	5.44260838353	-0.243377	5.96350466105	-0.114678		
4.45697852179	-0.611091	4.77397840877	-0.471391	5.20316550367	-0.236508	5.03914163849	-0.306846	5.48861067346	-0.167641	5.04823607921	-0.29298	5.58216244465	-0.137027	6.11641503697	-0.0368178		
4.56840298483	-0.528576	4.89332786899	-0.39677	5.33324464126	-0.165429	5.16512017945	-0.222755	5.6258259403	-0.107273	5.17444198119	-0.211981	5.72171650576	-0.0491073	6.2693254129	0.0371114		
4.67982744788	-0.457589	5.01267732921	-0.340982	5.46332377885	-0.100063	5.29109872042	-0.15255	5.76304120714	-0.0552279	5.30064788317	-0.141477	5.86127056688	0.0264806	6.42223578882	0.0932827		
4.79125191092	-0.387747	5.13202678943	-0.286831	5.59340291644	-0.0459152	5.41707726138	-0.0840435	5.90025647397	-0.00395252	5.42685378515	-0.078384	6.000824628	0.0923936	6.57514616474	0.149055		
4.90267637397	-0.328123	5.25137624965	-0.239485	5.72348205404	0.0053974	5.54305580234	-0.0255223	6.03747174081	0.0362027	5.55305968713	-0.0211873	6.14037868911	0.153425	6.72805654067	0.186285		
5.01410083701	-0.276534	5.37072570987	-0.204714	5.85356119163	0.0511367	5.6690343433	0.026357	6.17468700765	0.0729573	5.67926558911	0.0289137	6.27993275023	0.201559	6.88096691659	0.218014		
3-HH1		3-HH2		3-HF1		3-HF2		3-HF3		3-HF4		3-FF1				3-FF2	
3.43594668895	-0.597062	4.03806907476	-0.114213	4.05575650873	0.228009	4.26586656335	0.226684	4.37726127205	-0.293392	4.22420781328	0.798957	4.44732592776	1.64127	4.42086165258	4.42426		
3.55047824525	-1.25341	4.17267137725	-0.658265	4.19094839235	-0.721951	4.40806211546	-0.619477	4.52316998112	-0.866789	4.36501474039	-0.270346	4.59557012535	0.0122426	4.56822370767	1.21394		
3.66500980155	-1.6037	4.30727367975	-0.941821	4.32614027597	-1.15691	4.55025766757	-0.981608	4.66907869019	-1.08102	4.5058216675	-0.789156	4.74381432294	-0.742174	4.71558576275	-0.353331		
3.77954135785	-1.72195	4.44187598224	-1.06276	4.4613321596	-1.28733	4.69245321968	-1.06881	4.81498739925	-1.09102	4.6466285946	-0.990677	4.89205852053	-1.05222	4.86294781784	-0.990336		
3.89407291414	-1.70594	4.57647828473	-1.05557	4.59652404322	-1.27007	4.83464877179	-1.02173	4.96089610832	-1.00969	4.78743552171	-1.01854	5.04030271812	-1.10688	5.01030987293	-1.20215		
4.00860447044	-1.61299	4.71108058722	-0.988879	4.73171592685	-1.16315	4.97684432391	-0.913895	5.10680481739	-0.889177	4.92824244882	-0.950691	5.18854691572	-1.03835	5.15767192801	-1.18195		
4.12313602674	-1.48567	4.84568288971	-0.895304	4.86690781047	-1.01086	5.11903987602	-0.781867	5.25271352646	-0.744296	5.06904937593	-0.837481	5.33679111331	-0.893223	5.3050339831	-1.03852		
4.23766758304	-1.38261	4.98028519221	-0.80586	5.00209969409	-0.844059	5.26123542813	-0.646347	5.39862223553	-0.603626	5.20985630304	-0.70491	5.4850353109	-0.716528	5.45239603818	-0.829339		
4.35219913934	-1.23418	5.1148874947	-0.703956	5.13729157772	-0.679288	5.40343098024	-0.518883	5.5445309446	-0.475589	5.35066323015	-0.576705	5.63327950849	-0.546162	5.59975809327	-0.623749		
4.46673069564	-1.10031	5.24948979719	-0.604706	5.27248346134	-0.533556	5.54562653235	-0.392423	5.69043965366	-0.360389	5.49147015726	-0.445555	5.78152370608	-0.383508	5.74712014836	-0.440116		
4.58126225193	-0.967273	5.38409209968	-0.510882	5.40767534497	-0.399039	5.68782208446	-0.280126	5.83634836273	-0.261203	5.63227708437	-0.328321	5.92976790367	-0.232854	5.89448220344	-0.264919		
4.69579380823	-0.829829	5.51869440218	-0.436706	5.54286722859	-0.293142	5.83001763658	-0.183479	5.9822570718	-0.175272	5.77308401148	-0.224751	6.07801210127	-0.116461	6.04184425853	-0.106823		
4.81032536453	-0.713197	5.65329670467	-0.364543	5.67805911222	-0.186403	5.97221318869	-0.10242	6.12816578087	-0.10574	5.91389093859	-0.144229	6.22625629886	-0.00584207	6.18920631361	0.0204041		
4.92485692083	-0.60631	5.78789000716	-0.301609	5.81325099584	-0.0950333	6.1144087408	-0.0350295	6.27407448994	-0.0411108	6.0546978657	-0.0736421	6.37450049645	0.0940649	6.3365683687	0.136018		
5.03938847713	-0.509879	5.92250130965	-0.250749	5.94844287946	-0.0172386	6.25660429291	0.0269559	6.419983199	0.0144938	6.19550479281	-0.0102317	6.52274469404	0.173002	6.48393042379	0.233225		
5.15392003343	-0.443403	6.05710361214	-0.204221	6.08363476309	0.052602	6.39879984502	0.0790619	6.56589190807	0.0619782	6.33631171992	0.0481404	6.67098889163	0.235852	6.63129247887	0.313131		

4.3 Energy Decomposition Analysis

The following tables provide the computational raw data for the SAPT and LED computations. In SAPT, El refers to electrostatics, Ex refers to exchange, In refers to induction, Disp refers to dispersion, BIE refers to the bond interaction energy. In LED, BIE refers to the bond interaction energy, HF_{int} refers to the HF component of the interaction energy, HF_{prep} refers to the HF component of the electronic preparation energy, Cor_{int} refers to the correlation energy component of the interaction energy, Cor_{prep} refers to the correlation energy component of the interaction energy, El refers to electrostatics, Ex refers to exchange, Disp refers to dispersion, CT refers to charge-transfer and (T) refers to the perturbative triples correction component of the interaction energy.

	sSAPT0/jun-cc-pVDZ				
	El [kcal mol^{-1}]	Ex [kcal mol^{-1}]	In [kcal mol^{-1}]	Disp [kcal mol^{-1}]	BIE [kcal mol^{-1}]
Methanes					
HH1	-0.1655	0.6412	-0.0454	-0.5785	-0.1481
HH2	-0.1462	0.5257	-0.0347	-0.4368	-0.0918
HF1	-0.3017	0.7804	-0.0274	-0.6775	-0.2258
HF2	-0.1219	0.5724	-0.0204	-0.4542	-0.0237
FF1	0.2219	0.3977	-0.0081	-0.5809	0.0306
FF2	-0.3626	0.7541	-0.0157	-0.5896	-0.2134
Ethanes					
HH1	-0.5483	1.8674	-0.1497	-1.7955	-0.6241
HH2	-0.4353	1.4234	-0.1084	-1.4379	-0.5576
HF1	-0.2777	1.1779	-0.0506	-1.1746	-0.3242
HF2	-0.4147	1.4056	-0.0604	-1.3314	-0.4001
HF3	-0.2454	1.0090	-0.0469	-1.0072	-0.2900
HF4	-0.3753	1.4296	-0.0620	-1.3305	-0.3371
FF1	-0.4096	1.1732	-0.0311	-1.1293	-0.3963
FF2	-0.1611	0.8058	-0.0168	-0.8516	-0.2234
Propanes					
HH1	-0.8415	2.9705	-0.2724	-2.9617	-1.1029
HH2	-0.5316	1.8318	-0.1310	-1.8072	-0.6356
HF1	-0.5894	1.8992	-0.0864	-1.9644	-0.7395
HF2	-0.4091	1.4736	-0.0774	-1.5875	-0.5995
HF3	-0.3821	1.1785	-0.0666	-1.4111	-0.6805
HF4	-0.5801	1.9893	-0.1124	-1.8131	-0.5141
FF1	-0.5519	1.6868	-0.0511	-1.7687	-0.6843
FF2	-0.6313	2.4109	-0.0701	-2.1253	-0.4148
Butanes					
HH1	-1.2350	4.1487	-0.3776	-4.2930	-1.7530
HH2	-0.6707	2.3040	-0.1641	-2.4901	-1.0174
HF1	-0.8010	2.4715	-0.1385	-2.6728	-1.1391
HF2	-0.8034	2.6421	-0.1427	-2.7558	-1.0578
HF3	-0.9149	3.0342	-0.1571	-2.8962	-0.9310
HF4	-0.7539	2.4869	-0.1227	-2.6009	-0.9885
FF1	-0.4532	1.3455	-0.0419	-1.9254	-1.0746
FF2	-0.6180	2.0733	-0.0511	-2.3286	-0.9236
Pentanes					
HH1	-1.6127	5.3858	-0.4846	-5.6800	-2.3877
HH2	-0.9523	3.3861	-0.2346	-3.5262	-1.3221
HF1	-0.8901	3.1166	-0.1770	-3.5828	-1.5310
HF2	-0.7447	2.4912	-0.1432	-3.0342	-1.4293
HF3	-0.9255	2.9806	-0.1629	-3.1994	-1.3049
HF4	-1.1477	3.6389	-0.1916	-3.7320	-1.4286
FF1	-0.8443	2.6409	-0.0869	-3.1834	-1.4728
FF2	-0.7482	2.2696	-0.0656	-2.7247	-1.2681
Hexanes					
HH1	-1.9335	6.3845	-0.5775	-6.7867	-2.9085
HH2	-1.1511	3.9393	-0.2797	-4.2908	-1.7757
HF1	-1.2676	4.3638	-0.2421	-4.6080	-1.7497
HF2	-1.0073	3.2889	-0.1952	-3.9062	-1.8178
HF3	-1.2177	4.1424	-0.2232	-4.3421	-1.6370
HF4	-1.1879	3.7916	-0.1979	-4.1249	-1.7157
FF1	-1.2223	3.7755	-0.1188	-4.4151	-1.9792
FF2	-0.9438	3.2711	-0.0952	-3.2594	-1.0259

	SAPT2+/aug-cc-pVDZ				
	El [kcal mol^{-1}]	Ex [kcal mol^{-1}]	In [kcal mol^{-1}]	Disp [kcal mol^{-1}]	BIE [kcal mol^{-1}]
Methanes					
HH1	-0.2178	0.7190	-0.0332	-0.9490	-0.4810
HH2	-0.1889	0.5757	-0.0265	-0.7285	-0.3681
HF1	-0.3655	0.9508	-0.0389	-1.2066	-0.6601
HF2	-0.1820	0.6794	-0.0238	-0.8256	-0.3520
FF1	-0.0219	0.5850	-0.0164	-1.1912	-0.6445
FF2	-0.3762	1.0425	-0.0251	-1.2385	-0.5973
Ethanes					
HH1	-0.6603	2.0879	-0.1456	-2.5149	-1.2329
HH2	-0.5398	1.5928	-0.0983	-2.0682	-1.1136
HF1	-0.4080	1.4149	-0.0517	-1.9006	-0.9453
HF2	-0.5421	1.6830	-0.0615	-2.1682	-1.0888
HF3	-0.3560	1.2121	-0.0474	-1.6361	-0.8273
HF4	-0.5234	1.7117	-0.0629	-2.1633	-1.0378
FF1	-0.5011	1.5888	-0.0380	-2.1004	-1.0507
FF2	-0.3240	1.1032	-0.0255	-1.6084	-0.8547
Propanes					
HH1	-1.0134	3.3548	-0.2747	-3.9636	-1.8969
HH2	-0.6837	2.1044	-0.1294	-2.5143	-1.2229
HF1	-0.7669	2.2922	-0.0860	-3.0472	-1.6079
HF2	-0.5547	1.7538	-0.0795	-2.4207	-1.3011
HF3	-0.4724	1.4037	-0.0660	-2.1720	-1.3067
HF4	-0.7464	2.3460	-0.1137	-2.7717	-1.2859
FF1	-0.6796	2.2708	-0.0590	-3.0945	-1.5623
FF2	-1.0800	3.2783	-0.0939	-3.8724	-1.7680
Butanes					
HH1	-1.5017	4.7227	-0.3845	-5.6107	-2.7743
HH2	-0.8830	2.6888	-0.1624	-3.3967	-1.7533
HF1	-0.9912	2.9380	-0.1369	-3.9650	-2.1551
HF2	-1.0355	3.1456	-0.1395	-4.1051	-2.1345
HF3	-1.2138	3.6455	-0.1601	-4.3913	-2.1197
HF4	-0.9982	2.9997	-0.1266	-3.9696	-2.0947
FF1	-0.5589	1.8385	-0.0456	-3.2464	-2.0124
FF2	-0.9603	2.8616	-0.0641	-4.0849	-2.2477
Pentanes					
HH1	-1.9734	6.1493	-0.4936	-7.3317	-3.6494
HH2	-1.2628	3.9647	-0.2305	-4.8190	-2.3475
HF1	-1.1901	3.7200	-0.1764	-5.1941	-2.8406
HF2	-0.9764	2.9917	-0.1396	-4.4419	-2.5663
HF3	-1.2059	3.5841	-0.1649	-4.7320	-2.5187
HF4	-1.4824	4.3690	-0.1937	-5.5860	-2.8931
FF1	-1.1151	3.5558	-0.0953	-5.2701	-2.9247
FF2	-1.0010	3.1049	-0.0762	-4.6981	-2.6704
Hexanes					
HH1	-2.3649	7.3092	-0.5928	-8.6740	-4.3225
HH2	-1.5342	4.6407	-0.2760	-5.7280	-2.8975
HF1	-1.6978	5.1984	-0.2405	-6.6419	-3.3819
HF2	-1.2957	3.9296	-0.1860	-5.6633	-3.2155
HF3	-1.6355	4.9790	-0.2202	-6.4036	-3.2803
HF4	-1.5591	4.5665	-0.2048	-6.0923	-3.2896
FF1					
FF2					

	SAPT2+(3)δMP2/aug-cc-pVTZ				
	El [kcal mol^{-1}]	Ex [kcal mol^{-1}]	In [kcal mol^{-1}]	Disp [kcal mol^{-1}]	BIE [kcal mol^{-1}]
Methanes					
HH1	-0.1791	0.6892	0.0131	-1.0104	-0.4871
HH2	-0.1677	0.5564	0.0050	-0.7739	-0.3802
HF1	-0.3451	0.9132	0.0155	-1.3281	-0.7445
HF2	-0.1545	0.6526	0.0047	-0.9071	-0.4043
FF1	0.0308	0.5667	0.0128	-1.3359	-0.7256
FF2	-0.3345	0.9961	0.0226	-1.4161	-0.7319
Ethanes					
HH1	-0.5997	2.0146	-0.0873	-2.6366	-1.3090
HH2	-0.4776	1.5343	-0.0449	-2.1652	-1.1534
HF1	-0.3472	1.3605	-0.0087	-2.0483	-1.0437
HF2	-0.4817	1.6153	-0.0134	-2.3402	-1.2201
HF3	-0.3046	1.1665	-0.0126	-1.7588	-0.9095
HF4	-0.4533	1.6452	-0.0168	-2.3288	-1.1538
FF1	-0.4285	1.5217	0.0113	-2.3362	-1.2317
FF2	-0.2579	1.0556	0.0164	-1.7875	-0.9735

	SAPT2+(CCD)δMP2/aug-cc-pVTZ				
	El [kcal mol^{-1}]	Ex [kcal mol^{-1}]	In [kcal mol^{-1}]	Disp [kcal mol^{-1}]	BIE [kcal mol^{-1}]
Methanes					
HH1	-0.1913	0.6892	0.0131	-1.0340	-0.5230
HH2	-0.1781	0.5564	0.0050	-0.7922	-0.4088
HF1	-0.3709	0.9132	0.0155	-1.3356	-0.7777
HF2	-0.1751	0.6526	0.0047	-0.9128	-0.4305
FF1	-0.0209	0.5667	0.0128	-1.3205	-0.7619
FF2	-0.3675	0.9961	0.0226	-1.4031	-0.7520
Ethanes					
HH1	-0.6321	2.0146	-0.0873	-2.7030	-1.4079
HH2	-0.5082	1.5343	-0.0449	-2.2152	-1.2340
HF1	-0.3890	1.3605	-0.0087	-2.0472	-1.0844
HF2	-0.5270	1.6153	-0.0134	-2.3406	-1.2658
HF3	-0.3396	1.1665	-0.0126	-1.7581	-0.9438
HF4	-0.5014	1.6452	-0.0168	-2.3296	-1.2026
FF1	-0.4839	1.5217	0.0113	-2.2962	-1.2472
FF2	-0.3110	1.0556	0.0165	-1.7604	-0.9993

	LED-TightPNO-DLPNO-CCSD(T)/cc-pVQZ									
	BIE [kcal mol^{-1}]	HF_{int} [kcal mol^{-1}]	HF_{prep} [kcal mol^{-1}]	Cor_{int} [kcal mol^{-1}]	Cor_{prep} [kcal mol^{-1}]	El [kcal mol^{-1}]	Ex [kcal mol^{-1}]	Disp [kcal mol^{-1}]	CT [kcal mol^{-1}]	(T) [kcal mol^{-1}]
Methanes										
HH1	-0.4228	-1.2560	1.6863	-1.1074	0.2543	-0.8259	-0.4302	-0.8187	-0.1601	-0.1286
HH2	-0.3297	-1.0838	1.4214	-0.8440	0.1767	-0.7351	-0.3487	-0.6170	-0.1283	-0.0987
HF1	-0.5185	-2.4290	2.8692	-1.2994	0.3406	-1.8757	-0.5532	-1.0008	-0.3593	-0.1555
HF2	-0.2619	-1.6811	2.0975	-0.8740	0.1957	-1.2863	-0.3949	-0.6878	-0.1370	-0.0982
FF1	-0.4643	-1.3964	1.9097	-1.1205	0.1430	-1.0429	-0.3535	-1.0144	-0.0288	-0.0774
FF2	-0.4332	-2.6955	3.0986	-1.2149	0.3786	-2.1537	-0.5418	-1.0339	-0.0694	-0.1117
Ethanes										
HH1	-1.1517	-3.6255	4.7819	-2.9893	0.6811	-2.3506	-1.2749	-2.1308	-1.0814	-0.3656
HH2	-1.0192	-2.9478	3.8134	-2.4352	0.5504	-1.9577	-0.9901	-1.7526	-0.4609	-0.2980
HF1	-0.7522	-3.4510	4.2879	-2.0180	0.4288	-2.6373	-0.8136	-1.5815	-0.6836	-0.2209
HF2	-0.8819	-4.2212	5.1375	-2.3180	0.5198	-3.2486	-0.9726	-1.7994	-0.3167	-0.2623
HF3	-0.6621	-3.0106	3.7186	-1.7161	0.3459	-2.3083	-0.7022	-1.3516	-0.8224	-0.1755
HF4	-0.8379	-4.2216	5.1991	-2.3141	0.4986	-3.2384	-0.9831	-1.7782	-0.9072	-0.2598
FF1	-0.7582	-4.0169	4.7685	-2.0074	0.4976	-3.2117	-0.8052	-1.7281	-0.1235	-0.1558
FF2	-0.5745	-2.7525	3.3443	-1.4919	0.3256	-2.1830	-0.5695	-1.3087	-0.0785	-0.1047
Propanes										
HH1	-1.7283	-5.9781	7.8295	-4.6709	1.0912	-3.9172	-2.0610	-3.2331	-1.0388	-0.5887
HH2	-1.0701	-3.5448	4.7036	-2.8678	0.6389	-2.3730	-1.1717	-2.1021	-0.9529	-0.3469
HF1	-1.2931	-5.6153	6.8290	-3.2221	0.7152	-4.3250	-1.2902	-2.4638	-1.3955	-0.3501
HF2	-1.0645	-4.3570	5.3336	-2.5406	0.4995	-3.3559	-1.0011	-2.0141	-0.8686	-0.2619
HF3	-1.0688	-3.6071	4.3367	-2.2434	0.4450	-2.7964	-0.8107	-1.7972	-0.3503	-0.2249
HF4	-1.0177	-5.6779	6.9699	-2.9264	0.6167	-4.4056	-1.2723	-2.2746	-1.3889	-0.3081
FF1	-1.0959	-5.8027	6.9031	-2.9673	0.7711	-4.6354	-1.1673	-2.5310	-0.1811	-0.2552
FF2	-1.0919	-7.9548	9.5825	-3.7118	0.9923	-6.3266	-1.6282	-3.1194	-0.2646	-0.3279
Butanes										
HH1	-2.5133	-8.2529	10.7756	-6.5687	1.5327	-5.4007	-2.8522	-4.5348	-1.5720	-0.8308
HH2	-1.5119	-4.5493	6.0109	-3.8277	0.8542	-3.0525	-1.4969	-2.8106	-0.8198	-0.4618
HF1	-1.8065	-7.2869	8.8276	-4.1659	0.8188	-5.6628	-1.6241	-3.2559	-1.0812	-0.4189
HF2	-1.7537	-7.5827	9.2840	-4.3375	0.8825	-5.8714	-1.7113	-3.3495	-1.3807	-0.4503
HF3	-1.6842	-8.5403	10.4982	-4.6658	1.0237	-6.5875	-1.9528	-3.5165	-2.2677	-0.5072
HF4	-1.7015	-7.2192	8.8152	-4.1794	0.8819	-5.5690	-1.6502	-3.2311	-0.7695	-0.4494
FF1	-1.4874	-4.8906	5.7644	-3.0415	0.6803	-3.8994	-0.9911	-2.6752	-0.1417	-0.2245
FF2	-1.5431	-7.0455	8.4265	-3.8582	0.9340	-5.6061	-1.4394	-3.3005	-0.4170	-0.3120
Pentanes										
HH1	-3.2890	-10.7154	13.9828	-8.5458	1.9895	-7.0186	-3.6968	-5.9167	-1.6238	-1.0800
HH2	-1.9799	-6.6387	8.8281	-5.4121	1.2428	-4.4628	-2.1759	-3.9376	-1.1283	-0.6561
HF1	-2.3580	-8.8550	10.9050	-5.4759	1.0680	-6.8193	-2.0357	-4.2590	-2.5971	-0.5548
HF2	-2.1264	-7.3394	8.9512	-4.6544	0.9162	-5.6642	-1.6752	-3.6163	-1.9033	-0.4716
HF3	-2.0523	-8.5165	10.4056	-4.9817	1.0403	-6.5740	-1.9426	-3.7850	-1.6877	-0.5215
HF4	-2.3477	-10.4022	12.6961	-5.8867	1.2451	-8.0478	-2.3544	-4.5378	-1.5210	-0.6332
FF1	-2.0535	-9.0827	10.8071	-5.0100	1.2320	-7.2488	-1.8338	-4.2965	-0.3063	-0.4072
FF2	-1.9018	-7.8007	9.2848	-4.4262	1.0402	-6.2235	-1.5772	-3.8356	-0.2504	-0.3401
Hexanes										
HH1	-3.8853	-12.6854	16.5336	-10.0815	2.3480	-8.3072	-4.3783	-6.9774	-1.9601	-1.2727
HH2	-2.4579	-7.7052	10.2079	-6.4026	1.4419	-5.1818	-2.5234	-4.6784	-1.4741	-0.7692
HF1	-2.7893	-12.0610	14.9135	-7.0105	1.3687	-9.3009	-2.7601	-5.4285	-3.2386	-0.7015
HF2	-2.6772	-9.5310	11.6349	-5.9277	1.1466	-7.3766	-2.1543	-4.6434	-2.1057	-0.5937
HF3	-2.6872	-11.4912	14.1912	-6.7359	1.3488	-8.8474	-2.6439	-5.1350	-2.7370	-0.6878
HF4	-2.6969	-10.9335	13.3236	-6.3840	1.2970	-8.4645	-2.4690	-4.9660	-1.0364	-0.6677
FF1	-2.7133	-12.7262	15.1942	-6.8939	1.7126	-10.1625	-2.5636	-5.8944	-0.4389	-0.5606
FF2	-1.7413	-10.4968	12.7335	-5.2852	1.3072	-8.3808	-2.1161	-4.4953	-0.3793	-0.4107

	LED-TightPNO-DLPNO-CCSD(T)/cc-pVQZ								
	C1-C2 [kcal mol^{-1}]	C1-X2 [kcal mol^{-1}]	X1-C2 [kcal mol^{-1}]	X1-X2 [kcal mol^{-1}]	C1-CX2 [kcal mol^{-1}]	CX1-C2 [kcal mol^{-1}]	X1-CX2 [kcal mol^{-1}]	CX1-X2 [kcal mol^{-1}]	CX1-CX2 [kcal mol^{-1}]
Methanes									
HH1	-0.2706	0.0000	0.0000	0.0000	-0.1704	-0.1668	0.0000	0.0000	-0.2109
HH2	-0.1264	0.0000	0.0000	0.0000	-0.1643	-0.1585	0.0000	0.0000	-0.1677
HF1	0.0000	-0.3181	0.0000	0.0000	-0.1573	0.0000	0.0000	-0.2113	-0.3141
HF2	0.0000	-0.2481	0.0000	0.0000	-0.0612	0.0000	0.0000	-0.2390	-0.1395
FF1	0.0000	0.0000	0.0000	-0.8033	0.0000	0.0000	-0.0833	-0.0804	-0.0474
FF2	0.0000	0.0000	0.0000	-0.7698	0.0000	0.0000	-0.0983	-0.0995	-0.0663
Ethanes									
HH1	-0.5235	0.0000	0.0000	0.0000	-0.5514	-0.5281	0.0000	0.0000	-0.5278
HH2	-0.4541	0.0000	0.0000	0.0000	-0.4152	-0.4155	0.0000	0.0000	-0.4679
HF1	-0.0325	-0.6689	0.0000	0.0000	-0.1131	-0.0468	0.0000	-0.3996	-0.3206
HF2	-0.0410	-0.6807	0.0000	0.0000	-0.1997	-0.0501	0.0000	-0.4986	-0.3294
HF3	-0.0328	-0.5701	0.0000	0.0000	-0.1065	-0.0324	0.0000	-0.3206	-0.2892
HF4	-0.0350	-0.7182	0.0000	0.0000	-0.1814	-0.0553	0.0000	-0.4276	-0.3606
FF1	-0.0041	-0.0647	-0.0774	-1.1472	-0.0120	0.0000	-0.1757	-0.1877	-0.0593
FF2	-0.0029	-0.0540	-0.0517	-0.8749	-0.0027	-0.0030	-0.1227	-0.1349	-0.0618
Propanes									
HH1	-0.8321	0.0000	0.0000	0.0000	-0.8191	-0.8014	0.0000	0.0000	-0.7806
HH2	-0.6254	0.0000	0.0000	0.0000	-0.5182	-0.4588	0.0000	0.0000	-0.4997
HF1	-0.0882	-0.9498	0.0000	0.0000	-0.2729	-0.0954	0.0000	-0.4897	-0.5679
HF2	-0.0704	-0.7875	0.0000	0.0000	-0.2031	-0.0823	0.0000	-0.4863	-0.3845
HF3	-0.0565	-0.8134	0.0000	0.0000	-0.1432	-0.0517	0.0000	-0.4645	-0.2679
HF4	-0.0630	-0.9620	0.0000	0.0000	-0.1641	-0.0658	0.0000	-0.6632	-0.3565
FF1	-0.0121	-0.1233	-0.1474	-1.4830	-0.0160	-0.0201	-0.3913	-0.2191	-0.1186
FF2	-0.0109	-0.1486	-0.1484	-1.7565	-0.0108	-0.0107	-0.4198	-0.4199	-0.1936
Butanes									
HH1	-1.2381	0.0000	0.0000	0.0000	-1.1032	-1.1108	0.0000	0.0000	-1.0827
HH2	-0.9501	0.0000	0.0000	0.0000	-0.5990	-0.6018	0.0000	0.0000	-0.6597
HF1	-0.1387	-1.3930	0.0000	0.0000	-0.3278	-0.1489	0.0000	-0.6875	-0.5601
HF2	-0.1437	-1.5151	0.0000	0.0000	-0.3282	-0.1331	0.0000	-0.6633	-0.5662
HF3	-0.1548	-1.4167	0.0000	0.0000	-0.3691	-0.1443	0.0000	-0.7451	-0.6865
HF4	-0.1472	-1.2261	0.0000	0.0000	-0.3592	-0.1228	0.0000	-0.6787	-0.6970
FF1	-0.0197	-0.2013	-0.1742	-1.5540	-0.0050	-0.0116	-0.2745	-0.2947	-0.1402
FF2	-0.0234	-0.2229	-0.2279	-1.7060	-0.0092	-0.0091	-0.4586	-0.4372	-0.2063
Pentanes									
HH1	-1.6107	0.0000	0.0000	0.0000	-1.4902	-1.4898	0.0000	0.0000	-1.3260
HH2	-1.4310	0.0000	0.0000	0.0000	-0.8713	-0.8699	0.0000	0.0000	-0.7653
HF1	-0.2157	-1.8426	0.0000	0.0000	-0.4046	-0.1918	0.0000	-0.8317	-0.7726
HF2	-0.1911	-1.5619	0.0000	0.0000	-0.4135	-0.1505	0.0000	-0.6544	-0.6449
HF3	-0.2032	-1.5620	0.0000	0.0000	-0.4087	-0.1682	0.0000	-0.7561	-0.6868
HF4	-0.2250	-1.7000	0.0000	0.0000	-0.5546	-0.1659	0.0000	-0.9732	-0.9191
FF1	-0.0400	-0.3166	-0.3293	-2.2452	-0.0265	-0.0285	-0.5381	-0.5037	-0.2686
FF2	-0.0270	-0.2582	-0.2582	-2.1589	-0.0077	-0.0078	-0.4711	-0.4674	-0.1792
Hexanes									
HH1	-2.0050	0.0000	0.0000	0.0000	-1.6503	-1.6288	0.0000	0.0000	-1.6934
HH2	-1.7640	0.0000	0.0000	0.0000	-0.9824	-0.9822	0.0000	0.0000	-0.9498
HF1	-0.3184	-2.4036	0.0000	0.0000	-0.4817	-0.2211	0.0000	-1.0655	-0.9382
HF2	-0.2587	-2.0403	0.0000	0.0000	-0.4899	-0.1794	0.0000	-0.8557	-0.8194
HF3	-0.2867	-2.1555	0.0000	0.0000	-0.5224	-0.2095	0.0000	-1.0138	-0.9471
HF4	-0.2808	-1.9099	0.0000	0.0000	-0.5101	-0.1942	0.0000	-1.1094	-0.9616
FF1	-0.0604	-0.4425	-0.4499	-3.0478	-0.0536	-0.0465	-0.6475	-0.6226	-0.5236
FF2	-0.0362	-0.3166	-0.3152	-2.4311	-0.0163	-0.0170	-0.5533	-0.5451	-0.2646

4.4 Simple Interaction Models

The first table contains the computational raw data for determination of the adiabatic ionization potential, as well as, the molecular polarizabilities, the molecular volumes and the molecular surfaces. E(X) refers to the electronic energy of the ground-state, E(X^+) refers to the electronic energy of the ionized state, IP refers to the ionization potential, α_{iso} refers to the isotropic polarizability. The following tables contain all the data of the London dispersion interaction models. I_{eff} refers to the pre-factor in the London dispersion formula derived from the ionization potentials of the two molecules, r(C-C) refers to the intermolecular distance of the respective carbon chains, r(Disp) refers to the r^{-6}-weighted average distance of the atom types interacting most strongly by dispersion, $\alpha_1\alpha_2$ refers to the product of the polarizabilities of the interacting molecules, E_{disp}(C-C) refers to energy derived from the intermolecular London dispersion model using the carbon chain distance, E_{disp}(Disp) refers to the energy derived from the intermolecular London dispersion model using the r^{-6}-weighted average distance between the molecules. C-C, C-H, H-H, C-F, F-F and H-F refer to the percentage of the contribution of the interaction between these types of atoms to the overall atom-pairwise intermolecular dispersion, E_{disp}.

	IP: RI-MP2/CBS(34). α_{iso}: MP2/def2-TZVPPD. V/A: COSMO						
	E(X) [Ha]	E(X^+) [Ha]	IP [eV]	α_{iso} [amu]	α_{iso} [Å^3]	Molecular volume [Å^3]	Molecular surface [Å^2]
Methanes							
H	-40.435492481401	-39.903689641836	14.471	16.404	2.428	37.71	55.61
F	-437.189772434115	-436.58679506406	16.408	19.075	2.824	69.11	87.97
Ethanes							
H	-79.674742123241	-79.205808283572	12.76	28.111	4.161	59.30	78.43
F	-674.79145751654	-674.255658948474	14.58	32.023	4.741	106.05	119.63
Propanes							
H	-118.917917059007	-118.46471168706	12.332	40.027	5.925	80.62	98.91
F	-912.393212253362	-911.886017735483	13.801	44.803	6.632	141.47	146.50
Butanes							
H	-158.161214371129	-157.722388749223	11.941	52.079	7.71	101.87	118.95
F	-1149.99467502283	-1149.50545348592	13.312	57.668	8.537	176.18	172.42
Pentanes							
H	-197.404462162306	-196.962312056686	12.032	64.209	9.505	122.95	138.91
F	-1387.59646061689	-1387.12010519885	12.962	70.643	10.458	210.99	198.59
Hexanes							
H	-236.647743952463	-236.214008280866	11.803	76.469	11.32	144.00	158.44
F	-1625.1982147814	-1624.73095229536	12.715	83.772	12.401	245.73	224.77

	Intermolecular London Dispersion Model					
	r(C-C) [Å]	r(Disp) [Å]	I_{eff} [eV]	$\alpha_1\alpha_2$ [Å^6]	E_{disp} (C-C) [kcal mol^{-1}]	E_{disp} (Disp) [kcal mol^{-1}]
Methanes						
HH1	3.671	3.671	7.236	5.897	-0.603	-0.603
HH2	3.978	3.978	7.236	5.897	-0.372	-0.372
HF1	3.783	3.717	7.689	6.857	-0.622	-0.692
HF2	4.250	4.026	7.689	6.857	-0.310	-0.428
FF1	4.079	3.874	8.204	7.974	-0.492	-0.670
FF2	4.312	3.845	8.204	7.974	-0.352	-0.700
Ethanes						
HH1	3.714	3.857	6.380	17.318	-1.456	-1.160
HH2	3.978	3.994	6.380	17.318	-0.964	-0.941
HF1	4.336	4.118	6.805	19.727	-0.699	-0.953
HF2	4.199	4.038	6.805	19.727	-0.847	-1.071
HF3	4.574	4.225	6.805	19.727	-0.507	-0.816
HF4	4.207	4.040	6.805	19.727	-0.838	-1.067
FF1	4.652	4.112	7.290	22.473	-0.559	-1.172
FF2	5.097	4.293	7.290	22.473	-0.323	-0.905
Propanes						
HH1	3.818	4.064	6.166	35.111	-2.419	-1.661
HH2	4.487	4.459	6.166	35.111	-0.918	-0.953
HF1	4.506	4.280	6.513	39.301	-1.057	-1.441
HF2	4.740	4.451	6.513	39.301	-0.781	-1.138
HF3	4.864	4.522	6.513	39.301	-0.669	-1.035
HF4	4.694	4.350	6.513	39.301	-0.828	-1.307
FF1	4.941	4.270	6.901	43.990	-0.721	-1.733
FF2	4.912	4.113	6.901	43.990	-0.748	-2.168
Butanes						
HH1	3.836	4.187	5.971	59.437	-3.855	-2.278
HH2	4.563	4.642	5.971	59.437	-1.360	-1.227
HF1	4.488	4.471	6.295	65.815	-1.754	-1.794
HF2	4.523	4.406	6.295	65.815	-1.673	-1.958
HF3	4.535	4.368	6.295	65.815	-1.647	-2.062
HF4	4.640	4.468	6.295	65.815	-1.435	-1.800
FF1	5.279	4.581	6.656	72.878	-0.775	-1.815
FF2	5.153	4.420	6.656	72.878	-0.896	-2.251
Pentanes						
HH1	3.843	4.305	6.016	90.350	-5.833	-2.952
HH2	4.619	4.737	6.016	90.350	-1.936	-1.663
HF1	4.559	4.527	6.240	99.403	-2.389	-2.494
HF2	4.807	4.652	6.240	99.403	-1.740	-2.118
HF3	4.759	4.617	6.240	99.403	-1.848	-2.215
HF4	4.537	4.510	6.240	99.403	-2.460	-2.550
FF1	5.052	4.514	6.481	109.363	-1.474	-2.899
FF2	5.439	4.577	6.481	109.363	-0.947	-2.667
Hexanes						
HH1	4.067	4.439	5.901	128.146	-5.777	-3.421
HH2	4.556	4.844	5.901	128.146	-2.923	-2.025
HF1	4.532	4.590	6.121	140.383	-3.433	-3.178
HF2	4.758	4.722	6.121	140.383	-2.562	-2.682
HF3	4.674	4.636	6.121	140.383	-2.852	-2.995
HF4	4.677	4.709	6.121	140.383	-2.840	-2.728
FF1	4.815	4.516	6.357	153.790	-2.715	-3.988
FF2	5.771	4.686	6.357	153.790	-0.916	-3.194

	Atom-pairwise London Dispersion Model 1: Atom-type dependent ionization potentials						
	C-C [%]	C-H [%]	H-H [%]	C-F [%]	F-F [%]	H-F [%]	E_{disp} [kcal mol^{-1}]
1-HH1	20.89	46.01	33.1	0	0	0	0.461
1-HH2	17.36	45.41	37.23	0	0	0	0.343
2-HH1	22.98	46.66	30.36	0	0	0	1.302
2-HH2	23.27	45.96	30.77	0	0	0	1.043
3-HH1	25.22	45.22	29.57	0	0	0	2.054
3-HH2	24.3	46.3	29.4	0	0	0	1.226
4-HH1	27.37	45.38	27.25	0	0	0	2.967
4-HH2	26.4	46.25	27.35	0	0	0	1.661
5-HH1	28.43	45.28	26.29	0	0	0	3.885
5-HH2	26.61	46.11	27.28	0	0	0	2.308
6-HH1	29.46	45.12	25.41	0	0	0	4.662
6-HH2	28.67	45.97	25.37	0	0	0	2.84
1-HF1	4.06	4.45	0	42.43	0	49.06	0.648
1-HF2	3	4.12	0	39.1	0	53.78	0.435
2-HF1	6.29	6.31	0	43.44	0	43.96	1.054
2-HF2	4.52	8.16	0	29.04	0	58.28	1.332
2-HF3	5.9	5.9	0	43.57	0	44.64	0.901
2-HF4	6.42	6.32	0	43.03	0	44.23	1.193
3-HF1	8.65	7.27	0	43.41	0	40.67	1.693
3-HF2	7.88	7.09	0	43.35	0	41.69	1.341
3-HF3	7.3	6.2	0	43.9	0	42.6	1.188
3-HF4	6.48	5.9	0	43.86	0	43.75	1.499
4-HF1	9.99	7.53	0	43.21	0	39.27	2.19
4-HF2	9.36	7.1	0	44.9	0	38.64	2.296
4-HF3	9.77	7.43	0	44.35	0	38.46	2.45
4-HF4	9.95	7.75	0	43.14	0	39.16	2.2
5-HF1	10.74	7.73	0	45.1	0	36.43	2.923
5-HF2	10.75	7.73	0	44.89	0	36.63	2.506
5-HF3	10.23	7.31	0	45.05	0	37.41	2.623
5-HF4	7.78	9.14	0	34	0	49.08	3.466
6-HF1	10.98	7.79	0	45.67	0	35.55	3.759
6-HF2	10.87	7.43	0	45.48	0	36.22	3.277
6-HF3	11.22	7.83	0	44.9	0	36.05	3.636
6-HF4	11.67	8.09	0	43.51	0	36.73	3.385
1-FF1	0.7	0	0	14.67	84.64	0	0.786
1-FF2	0.49	0	0	12.92	86.6	0	0.803
2-FF1	1.64	0	0	21.61	76.75	0	1.369
2-FF2	1.7	0	0	21.27	77.03	0	1.054
3-FF1	2.33	0	0	24.74	72.93	0	1.97
3-FF2	2.21	0	0	23.67	74.12	0	2.387
4-FF1	3.27	0	0	28.06	68.67	0	2.067
4-FF2	3.34	0	0	28.13	68.54	0	2.61
5-FF1	3.96	0	0	30.03	66.01	0	3.297
5-FF2	3.45	0	0	28.22	68.32	0	2.944
6-FF1	4.26	0	0	30.75	65	0	4.513
6-FF2	3.58	0	0	28.32	68.1	0	3.55

	Atom-pairwise London Dispersion Model 2: Atom-type dependent pre-factors A						
	C-C [%]	C-H [%]	H-H [%]	C-F [%]	F-F [%]	H-F [%]	E_{disp} [kcal mol^{-1}]
1-HH1	21.59	48.93	29.48	0	0	0	0.45
1-HH2	18.04	48.59	33.36	0	0	0	0.333
2-HH1	23.64	49.42	26.93	0	0	0	1.277
2-HH2	23.96	48.72	27.32	0	0	0	1.022
3-HH1	25.93	47.86	26.21	0	0	0	2.014
3-HH2	24.97	48.98	26.05	0	0	0	1.203
4-HH1	28.05	47.88	24.07	0	0	0	2.92
4-HH2	27.05	48.78	24.16	0	0	0	1.635
5-HH1	29.09	47.71	23.2	0	0	0	3.829
5-HH2	27.26	48.64	24.1	0	0	0	2.272
6-HH1	30.12	47.49	22.4	0	0	0	4.6
6-HH2	29.29	48.36	22.35	0	0	0	2.802
1-HF1	3.99	4.51	0	41.03	0	50.47	0.665
1-HF2	2.95	4.16	0	37.71	0	55.18	0.448
2-HF1	6.2	6.41	0	42.08	0	45.32	1.078
2-HF2	4.42	8.2	0	27.88	0	59.51	1.376
2-HF3	5.81	5.98	0	42.21	0	46	0.922
2-HF4	6.32	6.41	0	41.69	0	45.58	1.221
3-HF1	8.54	7.39	0	42.11	0	41.97	1.73
3-HF2	7.77	7.2	0	42.03	0	43	1.371
3-HF3	7.2	6.3	0	42.56	0	43.95	1.215
3-HF4	6.39	5.99	0	42.51	0	45.11	1.534
4-HF1	9.86	7.65	0	41.94	0	40.55	2.237
4-HF2	9.25	7.22	0	43.61	0	39.92	2.344
4-HF3	9.65	7.55	0	43.07	0	39.73	2.501
4-HF4	9.82	7.88	0	41.87	0	40.43	2.247
5-HF1	10.62	7.87	0	43.83	0	37.68	2.982
5-HF2	10.63	7.87	0	43.63	0	37.88	2.557
5-HF3	10.11	7.44	0	43.78	0	38.67	2.676
5-HF4	7.63	9.23	0	32.79	0	50.35	3.563
6-HF1	10.87	7.94	0	44.42	0	36.78	3.832
6-HF2	10.75	7.56	0	44.22	0	37.46	3.342
6-HF3	11.1	7.97	0	43.65	0	37.28	3.708
6-HF4	11.54	8.23	0	42.27	0	37.96	3.454
1-FF1	0.72	0	0	14.95	84.32	0	0.764
1-FF2	0.51	0	0	13.18	86.32	0	0.78
2-FF1	1.7	0	0	21.99	76.31	0	1.334
2-FF2	1.76	0	0	21.64	76.6	0	1.027
3-FF1	2.41	0	0	25.15	72.45	0	1.921
3-FF2	2.28	0	0	24.07	73.65	0	2.328
4-FF1	3.38	0	0	28.49	68.13	0	2.018
4-FF2	3.44	0	0	28.56	68	0	2.548
5-FF1	4.08	0	0	30.47	65.45	0	3.222
5-FF2	3.56	0	0	28.65	67.78	0	2.875
6-FF1	4.39	0	0	31.18	64.42	0	4.412
6-FF2	3.7	0	0	28.75	67.55	0	3.467

4.5 Interaction Descriptors

In the following table, $Q_{atom}(C)$ refers to the largest Q_{atom} of carbon in the respective molecule on its van der Waals surface, $Q_{atom}(C)$ refers to the corresponding Q_{atom} of either hydrogen or fluorine (depending on the molecule), the same is analogously valid for the P_{atom} values. $Q_{tot}(ave)$ refers to the average Q_{tot} value of the molecule on its van der Waals surface, $Q_{tot}(max)$ refers to the corresponding maximum on the van der Waals surface, the same is analogously valid for the P_{tot} values.

Molecule	$Q_{atom}(C)$	$Q_{atom}(X)$	$P_{atom}(C)$ [kcal$^{0.5}$ mol$^{-0.5}$]	$P_{atom}(X)$ [kcal$^{0.5}$ mol$^{-0.5}$]	$Q_{tot}(ave)$	$Q_{tot}(max)$	$P_{tot}(ave)$ [kcal$^{0.5}$ mol$^{-0.5}$]	$P_{tot}(max)$ [kcal$^{0.5}$ mol$^{-0.5}$]
1-H	0.0307	0.0369	0.545	0.384	0.282	0.324	3.59	4.32
2-H	0.0310	0.0360	0.552	0.374	0.337	0.450	4.43	6.21
3-H	0.0310	0.0356	0.551	0.369	0.373	0.561	4.98	7.88
4-H	0.0314	0.0351	0.559	0.365	0.400	0.600	5.41	8.53
5-H	0.0312	0.0347	0.554	0.361	0.420	0.636	5.73	9.14
6-H	0.0312	0.0345	0.555	0.358	0.437	0.658	6.00	9.50
1-F	0.0101	0.0383	0.180	0.721	0.238	0.330	4.46	6.16
2-F	0.0163	0.0383	0.290	0.720	0.282	0.406	5.26	7.54
3-F	0.0171	0.0377	0.305	0.709	0.310	0.513	5.77	9.51
4-F	0.0179	0.0372	0.317	0.699	0.331	0.524	6.16	9.69
5-F	0.0179	0.0368	0.317	0.692	0.347	0.551	6.45	10.18
6-F	0.0176	0.0370	0.313	0.696	0.363	0.579	6.73	10.69

4.6 Interaction Geometries

The following table contains volumes, surfaces and the $n_{contacts}$ measure of the intermolecular complexes. V_{COSMO} refers to the molecular COSMO volume, ΔV_{COSMO} refers to the volume change upon interaction, S_{COSMO} refers to the molecular COSMO surface, ΔS_{COSMO} refers to the surface change upon interaction, $n_{contacts}$ refers to the newly introduced $n_{contacts}$ measure.

	V_{COSMO} [Å^3]	ΔV_{COSMO} [Å^3]	S_{COSMO} [Å^2]	ΔS_{COSMO} [Å^2]	$n_{contacts}$
Methanes					
HH1	77.77	2.357	100.72	-10.50	4.973
HH2	77.39	1.979	102.01	-9.22	3.723
HF1	109.92	3.103	126.83	-16.75	6.047
HF2	109.00	2.183	131.60	-11.98	3.969
FF1	141.29	3.074	153.64	-22.30	5.571
FF2	139.94	1.723	156.76	-19.17	5.361
Ethanes					
HH1	119.93	1.339	136.08	-20.79	13.564
HH2	120.65	2.055	137.73	-19.14	10.852
HF1	167.27	1.926	174.25	-23.82	9.027
HF2	167.30	1.953	173.50	-24.56	10.304
HF3	167.98	2.635	179.06	-19.00	7.631
HF4	166.94	1.595	173.84	-24.23	10.235
FF1	214.21	2.106	209.44	-29.82	8.749
FF2	214.17	2.071	213.09	-26.18	6.722
Propanes					
HH1	163.64	2.389	169.04	-28.77	20.921
HH2	164.61	3.361	175.40	-22.42	12.507
HF1	223.24	1.147	213.32	-32.09	14.288
HF2	224.50	2.405	220.54	-24.87	11.174
HF3	225.97	3.879	218.70	-26.71	10.059
HF4	223.74	1.650	217.79	-27.62	12.591
FF1	281.81	-1.132	257.26	-35.75	12.486
FF2	280.93	-2.008	250.52	-42.49	15.662
Butanes					
HH1	205.46	1.717	199.06	-38.84	29.619
HH2	207.27	3.527	209.17	-28.73	16.632
HF1	281.10	3.051	252.00	-39.37	18.309
HF2	278.49	0.434	248.90	-42.46	19.075
HF3	279.30	1.246	251.43	-39.94	20.303
HF4	280.42	2.371	250.39	-40.98	18.450
FF1	352.49	0.129	304.55	-40.29	13.325
FF2	351.13	-1.226	296.80	-48.04	16.643
Pentanes					
HH1	248.41	2.516	230.61	-47.21	38.483
HH2	249.76	3.873	238.07	-39.75	23.268
HF1	334.17	0.233	286.31	-51.19	24.154
HF2	335.10	1.159	291.69	-45.81	20.691
HF3	334.55	0.614	294.84	-42.66	21.835
HF4	335.24	1.298	284.72	-52.78	25.827
FF1	420.03	-1.958	341.67	-55.51	21.323
FF2	421.83	-0.157	340.53	-56.65	19.185
Hexanes					
HH1	289.01	1.004	262.38	-54.50	45.440
HH2	292.90	4.895	274.70	-42.17	27.772
HF1	392.17	2.434	325.93	-57.28	30.733
HF2	392.10	2.361	327.56	-55.65	26.282
HF3	390.82	1.081	325.35	-57.86	29.614
HF4	392.61	2.874	326.57	-56.64	28.076
FF1	486.80	-4.663	377.79	-71.76	29.102
FF2	489.62	-1.846	390.76	-58.78	22.435

4.7 Predicted Microscopic and Macroscopic Mixing Behavior

The following table contains the macroscopic bond association energies obtained on the basis of Flory-Huggins solution theory. N_{coord} refers to the average coordination number of one molecule, BAE_{macro} refers to the macroscopic bond association energies, the corresponding method used for the respective microscopic bond association energy is provided in parenthesis. For each method, the first column gives the value of the respective complex, the second column gives the average over all complexes of a specific type (i.e. all **1-HH** complexes considered).

	N_{coord}	BAE_{macro}(VeryTightPNO) [kcal mol^{-1}]		BAE_{macro}(B97M-V) [kcal mol^{-1}]		BAE_{macro}(CCSD(T)-F12) [kcal mol^{-1}]	
Methanes							
HH1	5.296	-5.340	-5.082	-4.451	-4.186	-5.232	-4.962
HH2	6.033	-4.824		-3.921		-4.693	
HF1	4.287	-6.421	-5.553	-6.208	-5.550	-6.553	-5.808
HF2	5.991	-4.684		-4.892		-5.063	
FF1	3.945	-5.622	-5.806	-6.504	-6.923	-6.277	-6.978
FF2	4.589	-5.991		-7.343		-7.679	
Ethanes							
HH1	3.773	-10.202	-9.995	-9.257	-9.198	-9.991	-9.809
HH2	4.099	-9.788		-9.140		-9.627	
HF1	4.158	-8.103	-8.746	-8.235	-8.845	-8.737	-9.439
HF2	4.032	-9.084		-9.389		-9.872	
HF3	5.211	-8.886		-8.778		-9.608	
HF4	4.088	-8.910		-8.978		-9.541	
FF1	4.011	-8.984	-8.746	-9.964	-9.490	-10.428	-10.002
FF2	4.569	-8.507		-9.016		-9.576	
Propanes							
HH1	3.438	-13.703	-12.162	-13.619	-12.545	-13.759	-12.269
HH2	4.412	-10.620		-11.471		-10.779	
HF1	3.824	-12.220	-12.200	-13.280	-12.819	-12.837	-12.930
HF2	4.934	-12.760		-13.503		-13.837	
HF3	4.594	-12.153		-12.132		-12.635	
HF4	4.442	-11.667		-12.363		-12.411	
FF1	4.098	-12.790	-12.763	-14.723	-14.882	-14.706	-14.540
FF2	3.448	-12.735		-15.041		-14.375	
Butanes							
HH1	3.063	-17.341	-15.515	-17.762	-15.508	-17.688	-15.955
HH2	4.141	-13.689		-13.253		-14.222	
HF1	3.701	-14.148	-14.877	-14.543	-15.274	-15.516	-15.762
HF2	3.431	-14.681		-14.867		-15.608	
HF3	3.647	-15.540		-16.129		-16.208	
HF4	3.555	-15.141		-15.555		-15.715	
FF1	4.279	-17.397	-16.370	-18.870	-18.241	-19.653	-18.482
FF2	3.589	-15.342		-17.612		-17.311	
Pentanes							
HH1	2.942	-21.628	-18.419	-23.670	-20.479	-22.206	-19.049
HH2	3.495	-15.210		-17.287		-15.893	
HF1	3.297	-17.265	-18.295	-18.864	-19.615	-18.237	-19.326
HF2	3.684	-16.997		-18.131		-17.969	
HF3	3.956	-20.114		-21.524		-21.250	
HF4	3.197	-18.802		-19.942		-19.846	
FF1	3.577	-20.983	-20.162	-23.868	-22.579	-23.524	-22.616
FF2	3.505	-19.342		-21.290		-21.708	
Hexanes							
HH1	2.907	-24.989	-22.415	-27.553	-24.795	-25.857	-23.460
HH2	3.757	-19.841		-22.038		-21.064	
HF1	3.345	-19.299	-20.370	-21.152	-21.703	-20.373	-21.498
HF2	3.443	-19.704		-20.487		-20.801	
HF3	3.311	-20.134		-21.588		-21.248	
HF4	3.383	-22.342		-23.583		-23.569	
FF1	3.132	-24.452	-22.894	-27.820	-26.007	-27.296	-25.619
FF2	3.824	-21.336		-24.194		-23.942	

References

(1) Neese, F. The ORCA program system. *WIREs Comput. Mol. Sci.* **2012**, *2*, 73–78.

(2) Neese, F. Software update: The ORCA program system, version 4.0. *Wiley Interdiscip. Rev. Comput. Mol. Sci.* **2017**, 1–6.

(3) Turney, J. M.; Simmonett, A. C.; Parrish, R. M.; Hohenstein, E. G.; Evangelista, F. A.; Fermann, J. T.; Mintz, B. J.; Burns, L. A.; Wilke, J. J.; Abrams, M. L.; Russ, N. J.; Leininger, M. L.; Janssen, C. L.; Seidl, E. T.; Allen, W. D.; Schaefer, H. F.; King, R. A.; Valeev, E. F.; Sherrill, C. D.; Crawford, T. D. Psi4: an open-source ab initio electronic structure program. *WIREs Comput. Mol. Sci.* **2012**, *2*, 556–565.

(4) Parrish, R. M.; Burns, L. A.; Smith, D. G.; Simmonett, A. C.; DePrince, A. E.; Hohenstein, E. G.; Bozkaya, U.; Sokolov, A. Y.; Di Remigio, R.; Richard, R. M.; Gonthier, J. F.; James, A. M.; McAlexander, H. R.; Kumar, A.; Saitow, M.; Wang, X.; Pritchard, B. P.; Verma, P.; Schaefer, H. F.; Patkowski, K.; King, R. A.; Valeev, E. F.; Evangelista, F. A.; Turney, J. M.; Crawford, T. D.; Sherrill, C. D. Psi4 1.1: An Open-Source Electronic Structure Program Emphasizing Automation, Advanced Libraries, and Interoperability. *J. Chem. Theory Comput.* **2017**, *13*, 3185–3197.

(5) Werner, H. J.; Knowles, P. J.; Knizia, G.; Manby, F. R.; Schütz, M. Molpro: A general-purpose quantum chemistry program package. *Wiley Interdiscip. Rev. Comput. Mol. Sci.* **2012**, *2*, 242–253.

(6) Frisch, M. J.; Trucks, G. W.; Schlegel, H. B.; Scuseria, G. E.; Robb, M. A.; Cheeseman, J. R.; Scalmani, G.; Barone, V.; Mennucci, B.; Petersson, G. A.; Nakatsuji, H.; Caricato, M.; Li, X.; Hratchian, H. P.; Izmaylov, A. F.; Bloino, J.; Zheng, G.; Sonnenberg, J. L.; Hada, M.; Ehara, M.; Toyota, K.; Fukuda, R.; Hasegawa, J.; Ishida, M.; Nakajima, T.; Honda, Y.; Kitao, O.; Nakai, H.; Vreven, T.; Montgomery, J. A., Jr.; Peralta, J. E.; Ogliaro, F.; Bearpark, M.; Heyd, J. J.; Brothers, E.; Kudin, K. N.;

Staroverov, V. N.; Kobayashi, R.; Normand, J.; Raghavachari, K.; Rendell, A.; Burant, J. C.; Iyengar, S. S.; Tomasi, J.; Cossi, M.; Rega, N.; Millam, J. M.; Klene, M.; Knox, J. E.; Cross, J. B.; Bakken, V.; Adamo, C.; Jaramillo, J.; Gomperts, R.; Stratmann, R. E.; Yazyev, O.; Austin, A. J.; Cammi, R.; Pomelli, C.; Ochterski, J. W.; Martin, R. L.; Morokuma, K.; Zakrzewski, V. G.; Voth, G. A.; Salvador, P.; Dannenberg, J. J.; Dapprich, S.; Daniels, A. D.; Farkas, .; Foresman, J. B.; Ortiz, J. V.; Cioslowski, J.; Fox, D. J. Gaussian 09 Revision D.01. Gaussian Inc. Wallingford CT 2009.

(7) Baerends, E. J.; Ziegler, T.; Autschbach, J.; Bashford, D.; Berces, A.; Bickelhaupt, F. M.; Bo, C.; Boerrigter, P. M.; Cavallo, L.; Chong, D. P.; Deng, L.; Dickson, R. M.; Ellis, D. E.; van Faassen, M.; Fan, L.; Fischer, T. H.; Fonseca Guerra, C.; Franchini, M.; Ghysels, A.; Giammona, A. ADF2016.

(8) Shao, Y.; Gan, Z.; Epifanovsky, E.; Gilbert, A. T.; Wormit, M.; Kussmann, J.; Lange, A. W.; Behn, A.; Deng, J.; Feng, X.; Ghosh, D.; Goldey, M.; Horn, P. R.; Jacobson, L. D.; Kaliman, I.; Khaliullin, R. Z.; Kus, T.; Landau, A.; Liu, J.; Proynov, E. I.; Rhee, Y. M.; Richard, R. M.; Rohrdanz, M. A.; Steele, R. P.; Sundstrom, E. J.; Woodcock, H. L.; Zimmerman, P. M.; Zuev, D.; Albrecht, B.; Alguire, E.; Austin, B.; Beran, G. J.; Bernard, Y. A.; Berquist, E.; Brandhorst, K.; Bravaya, K. B.; Brown, S. T.; Casanova, D.; Chang, C. M.; Chen, Y.; Chien, S. H.; Closser, K. D.; Crittenden, D. L.; Diedenhofen, M.; Distasio, R. A.; Do, H.; Dutoi, A. D.; Edgar, R. G.; Fatehi, S.; Fusti-Molnar, L.; Ghysels, A.; Golubeva-Zadorozhnaya, A.; Gomes, J.; Hanson-Heine, M. W.; Harbach, P. H.; Hauser, A. W.; Hohenstein, E. G.; Holden, Z. C.; Jagau, T. C.; Ji, H.; Kaduk, B.; Khistyaev, K.; Kim, J.; Kim, J.; King, R. A.; Klunzinger, P.; Kosenkov, D.; Kowalczyk, T.; Krauter, C. M.; Lao, K. U.; Laurent, A. D.; Lawler, K. V.; Levchenko, S. V.; Lin, C. Y.; Liu, F.; Livshits, E.; Lochan, R. C.; Luenser, A.; Manohar, P.; Manzer, S. F.; Mao, S. P.; Mardirossian, N.; Marenich, A. V.;

Maurer, S. A.; Mayhall, N. J.; Neuscamman, E.; Oana, C. M.; Olivares-Amaya, R.; Oneill, D. P.; Parkhill, J. A.; Perrine, T. M.; Peverati, R.; Prociuk, A.; Rehn, D. R.; Rosta, E.; Russ, N. J.; Sharada, S. M.; Sharma, S.; Small, D. W.; Sodt, A.; Stein, T.; Stück, D.; Su, Y. C.; Thom, A. J.; Tsuchimochi, T.; Vanovschi, V.; Vogt, L.; Vydrov, O.; Wang, T.; Watson, M. A.; Wenzel, J.; White, A.; Williams, C. F.; Yang, J.; Yeganeh, S.; Yost, S. R.; You, Z. Q.; Zhang, I. Y.; Zhang, X.; Zhao, Y.; Brooks, B. R.; Chan, G. K.; Chipman, D. M.; Cramer, C. J.; Goddard, W. A.; Gordon, M. S.; Hehre, W. J.; Klamt, A.; Schaefer, H. F.; Schmidt, M. W.; Sherrill, C. D.; Truhlar, D. G.; Warshel, A.; Xu, X.; Aspuru-Guzik, A.; Baer, R.; Bell, A. T.; Besley, N. A.; Chai, J. D.; Dreuw, A.; Dunietz, B. D.; Furlani, T. R.; Gwaltney, S. R.; Hsu, C. P.; Jung, Y.; Kong, J.; Lambrecht, D. S.; Liang, W.; Ochsenfeld, C.; Rassolov, V. A.; Slipchenko, L. V.; Subotnik, J. E.; Van Voorhis, T.; Herbert, J. M.; Krylov, A. I.; Gill, P. M.; Head-Gordon, M. Advances in molecular quantum chemistry contained in the Q-Chem 4 program package. *Mol. Phys.* **2015**, *113*, 184–215.

(9) Kannemann, F. O.; Becke, A. D. van der Waals Interactions in Density-Functional Theory: Intermolecular Complexes. *J. Chem. Theory Comput.* **2010**, *6*, 1081–1088.

(10) Otero-de-la Roza, A.; Johnson, E. R. Non-covalent interactions and thermochemistry using XDM-corrected hybrid and range-separated hybrid density functionals Non-covalent interactions and thermochemistry using XDM-corrected hybrid and range-separated hybrid density functionals. *J. Chem. Phys.* **2013**, *138*, 204109.

(11) Grimme, S.; Antony, J.; Ehrlich, S.; Krieg, H. A consistent and accurate ab initio parametrization of density functional dispersion correction (DFT-D) for the 94 elements H-Pu. *J. Chem. Phys.* **2010**, *132*, 154104.

(12) Weymuth, T.; Proppe, J.; Reiher, M. Statistical Analysis of Semiclassical Dispersion Corrections. **2018**, 1–34.

(13) Grimme, S.; Bannwarth, C.; Shushkov, P. A Robust and Accurate Tight-Binding Quantum Chemical Method for Structures, Vibrational Frequencies, and Noncovalent Interactions of Large Molecular Systems Parametrized for All spd-Block Elements (Z = 1-86). *J. Chem. Theory Comput.* **2017**, *13*, 1989–2009.

(14) Ahrens, J.; Geveci, B.; Law, C. In *ParaView: An End-User Tool for Large Data Visualization*; Handbook, V., Ed.; Elsevier, 2005.

(15) Ayachit, U. *The ParaView Guide: A Parallel Visualization Application*; Kitware, 2015.

(16) Krawczuk, A.; Pérez, D.; MacChi, P. PolaBer: A program to calculate and visualize distributed atomic polarizabilities based on electron density partitioning. *J. Appl. Crystallogr.* **2014**, *47*, 1452–1458.

(17) Keith, T. A. *AIMAll (Version 17.11.14)*; TK Gristmill Software, 2017 (aim.tkgristmill.com).

(18) Lu, T.; Chen, F. Multiwfn: A multifunctional wavefunction analyzer. *J. Comput. Chem.* **2012**, *33*, 580–592.

(19) Johnson, E. R.; Keinan, S.; Mori-Sánchez, P.; Contreras-Garcia, J.; Cohen, A. J.; Yang, W. Revealing Noncovalent Interactions. *J. Am. Chem. Soc.* **2010**, *132*, 6498–6506.

(20) Contreras-Garcia, J.; Johnson, E. R.; Keinan, S.; Chaudret, R.; Piquemal, J. P.; Beratan, D. N.; Yang, W. NCIPLOT: A program for plotting noncovalent interaction regions. *J. Chem. Theory Comput.* **2011**, *7*, 625–632.

(21) Schrödinger, LLC, The PyMOL Molecular Graphics System, Version 1.8, Schrödinger, LLC. *The PyMOL Molecular Graphics System, Version 1.8;* 2015.

(22) *Chemcraft - graphical software for visualization of quantum chemistry computations.*; https://www.chemcraftprog.com.

(23) Foundation, P. S. *Python Language Reference, version 3.6*; Available at http://www.python.org.

(24) Kozuch, S.; Martin, J. M. L. Spin-component-scaled double hybrids: An extensive search for the best fifth-rung functionals blending DFT and perturbation theory. *J. Comput. Chem.* **2013**, *34*, 2327–2344.

(25) Weigend, F.; Ahlrichs, R. Balanced basis sets of split valence, triple zeta valence and quadruple zeta valence quality for H to Rn: Design and assessment of accuracy. *Phys. Chem. Chem. Phys.* **2005**, *7*, 3297–305.

(26) Johnson, E. R.; Otero-de-la Roza, A.; Dale, S. G.; DiLabio, G. A. Efficient basis sets for non-covalent interactions in XDM-corrected density-functional theory. *J. Chem. Phys.* **2013**, *139*, 214109.

(27) Neese, F.; Wennmohs, F.; Hansen, A.; Becker, U. Efficient, approximate and parallel Hartree-Fock and hybrid DFT calculations. A 'chain-of-spheres' algorithm for the Hartree-Fock exchange. *Chem. Phys.* **2009**, *356*, 98–109.

(28) Kossmann, S.; Neese, F. Efficient structure optimization with second-order many-body perturbation theory: The RIJCOSX-MP2 method. *J. Chem. Theory Comput.* **2010**, *6*, 2325–2338.

(29) Weigend, F. Accurate Coulomb-fitting basis sets for H to Rn. *Phys. Chem. Chem. Phys.* **2006**, *8*, 1057–1065.

(30) Hellweg, A.; Hättig, C.; Höfener, S.; Klopper, W. Optimized accurate auxiliary basis sets for RI-MP2 and RI-CC2 calculations for the atoms Rb to Rn. *Theor. Chem. Acc.* **2007**, *117*, 587–597.

(31) Dunning, T. H. Gaussian basis sets for use in correlated molecular calculations. I. The atoms boron through neon and hydrogen. *J. Chem. Phys.* **1989**, *90*, 1007–1023.

(32) Kendall, R. A.; Dunning, T. H.; Harrison, R. J. Electron affinities of the first-row atoms revisited. Systematic basis sets and wave functions. *J. Chem. Phys.* **1992**, *96*, 6796–6806.

(33) Liakos, D. G.; Neese, F. Is It Possible To Obtain Coupled Cluster Quality Energies at near Density Functional Theory Cost? Domain-Based Local Pair Natural Orbital Coupled Cluster vs Modern Density Functional Theory. *J. Chem. Theory Comput.* **2015**, *11*, 4054–4063.

(34) Pavošević, F.; Peng, C.; Pinski, P.; Riplinger, C.; Neese, F.; Valeev, E. F. SparseMaps - A systematic infrastructure for reduced scaling electronic structure methods. V. Linear scaling explicitly correlated coupled-cluster method with pair natural orbitals. *J. Chem. Phys.* **2017**, *146*, 174108.

(35) Bannwarth, C.; Ehlert, S.; Grimme, S. GFN2-xTB - an Accurate and Broadly Parametrized Self-Consistent Tight-Binding Quantum Chemical Method with Multipole Electrostatics and Density-Dependent Dispersion Contributions. **2018**, 10.26434/chemrxiv.7246238.v2.

(36) Adler, T. B.; Knizia, G.; Werner, H. J. A simple and efficient CCSD(T)-F12 approximation. *J. Chem. Phys.* **2007**, *127*, 221106.

(37) Knizia, G.; Adler, T. B.; Werner, H. J. Simplified CCSD(T)-F12 methods: Theory and benchmarks. *J. Chem. Phys.* **2009**, *130*, 054104.

(38) Peterson, K. A.; Adler, T. B.; Werner, H. J. Systematically convergent basis sets for explicitly correlated wavefunctions: The atoms H, He, B-Ne, and Al-Ar. *J. Chem. Phys.* **2008**, *128*, 084102.

(39) Sinanoglu, O. Many-electron theory of atoms and molecules. I. Shells, electron pairs vs many-electron correlations. *J. Chem. Phys.* **1962**, *36*, 706–717.

(40) Cizek, J. On the Correlation Problem in Atomic and Molecular Systems. Calculation of Wavefunction Components in Ursell-Type Expansion Using Quantum-Field Theoretical Methods. *J. Chem. Phys.* **1966**, *45*, 4256.

(41) Vahtras, O.; Almlöf, J.; Feyereisen, M. W. Integral approximations for LCAO-SCF calculations. *Chem. Phys. Lett.* **1993**, *213*, 514–518.

(42) Feyereisen, M.; Fitzgerald, G.; Komornicki, A. Use of approximate integrals in ab initio theory. An application in MP2 energy calculations. *Chem. Phys. Lett.* **1993**, *208*, 359–363.

(43) Neese, F.; Wennmohs, F.; Hansen, A. Efficient and accurate local approximations to coupled-electron pair approaches: An attempt to revive the pair natural orbital method. *J. Chem. Phys.* **2009**, *130*, 114108.

(44) Riplinger, C.; Neese, F. An efficient and near linear scaling pair natural orbital based local coupled cluster method. *J. Chem. Phys.* **2013**, *138*, 034106.

(45) Riplinger, C.; Sandhoefer, B.; Hansen, A.; Neese, F. Natural triple excitations in local coupled cluster calculations with pair natural orbitals. *J. Chem. Phys.* **2013**, *139*, 134101.

(46) Weigend, F. A fully direct RI-HF algorithm: Implementation, optimised auxiliary basis sets, demonstration of accuracy and efficiency. *Phys. Chem. Chem. Phys.* **2002**, *4*, 4285–4291.

(47) Moller, C.; Plesset, M. S. Note on an Approximation Treatment for Many-Electron Systems. *Phys. Rev.* **1934**, *46*, 618–622.

(48) Grimme, S. Improved second-order Møller-Plesset perturbation theory by separate scaling of parallel- and antiparallel-spin pair correlation energies. *J. Chem. Phys.* **2003**, *118*, 9095–9102.

(49) Pople, J. A.; Binkley, J. S.; Seeger, R. Theoretical models incorporating electron correlation. *Int. J. Quantum Chem.* **1976**, *10*, 1–19.

(50) Pople, J. A.; Seeger, R.; Krishnan, R. Variational configuration interaction methods and comparison with perturbation theory. *Int. J. Quantum Chem.* **1977**, *11*, 149–163.

(51) Mardirossian, N.; Head-Gordon, M. Mapping the genome of meta-generalized gradient approximation density functionals: The search for B97M-V. *J. Chem. Phys.* **2015**, *142*, 074111.

(52) Newton, M. D.; Ostlund, N. S.; Pople, J. A. Projection of Diatomic Differential Overlap: Least-Squares Projection of Two-Center Distributions onto One-Center Functions. *J. Chem. Phys.* **1968**, *49*, 5192–5194.

(53) Baerends, E.; Ellis, D.; Ros, P. Self-consistent molecular Hartree—Fock—Slater calculations I. The computational procedure. *Chem. Phys.* **1973**, *2*, 41 – 51.

(54) Skylaris, C.-K.; Gagliardi, L.; Handy, N.; Ioannou, A.; Spencer, S.; Willetts, A. On the resolution of identity Coulomb energy approximation in density functional theory. *THEOCHEM* **2000**, *501–502*, 229 – 239.

(55) Weigend, F. Hartree-fock exchange fitting basis sets for H to Rn. *J. Comput. Chem.* **2008**, *29*, 167–175.

(56) Mardirossian, N.; Head-Gordon, M. ω B97M-V: A combinatorially optimized, range-separated hybrid, meta-GGA density functional with VV10 nonlocal correlation. *J. Chem. Phys.* **2016**, *144*, 214110.

(57) Becke, A. D. Density-functional exchange-energy approximation with correct asymptotic behavior. *Phys. Rev. A* **1988**, *38*, 3098–3100.

(58) Lee, C.; Yang, W.; Parr, R. G. Development of the Colle-Salvetti correlation-energy formula into a functional of the electron density. *Phys. Rev. B* **1988**, *37*, 785–789.

(59) Becke, A. D. Density-functional thermochemistry. III. The role of exact exchange. *J. Chem. Phys.* **1993**, *98*, 5648–5652.

(60) Becke, A. D.; Johnson, E. R. Exchange-hole dipole moment and the dispersion interaction. *J. Chem. Phys.* **2005**, *122*, 154104.

(61) Becke, A. D.; Johnson, E. R. A density-functional model of the dispersion interaction. *J. Chem. Phys.* **2005**, *123*, 154101.

(62) Johnson, E. R.; Becke, A. D. A post-Hartree-Fock model of intermolecular interactions. *J. Chem. Phys.* **2005**, *123*, 024101.

(63) Johnson, E. R.; Becke, A. D. A post-Hartree-Fock model of intermolecular interactions: Inclusion of higher-order corrections. *J. Chem. Phys.* **2006**, *124*, 174104.

(64) Becke, A. D.; Johnson, E. R. Exchange-hole dipole moment and the dispersion interaction revisited. *J. Chem. Phys.* **2007**, *127*, 154104.

(65) Perdew, J. P.; Burke, K.; Ernzerhof, M. Generalized gradient approximation made simple. *Phys. Rev. Lett.* **1996**, *77*, 3865–3868.

(66) Zhao, Y.; Truhlar, D. G. A new local density functional for main-group thermochemistry, transition metal bonding, thermochemical kinetics, and noncovalent interactions. *J. Chem. Phys.* **2006**, *125*, 194101.

(67) Vydrov, O. A.; Van Voorhis, T. Nonlocal van der Waals density functional: The simpler the better. *J. Chem. Phys.* **2010**, *133*, 244103.

(68) Hujo, W.; Grimme, S. Performance of the van der waals density functional VV10 and (hybrid)GGA variants for thermochemistry and noncovalent interactions. *J. Chem. Theory Comput.* **2011**, *7*, 3866–3871.

(69) Grimme, S.; Ehrlich, S.; Goerigk, L. Effect of the damping function in dispersion corrected density functional theory. *J. Comput. Chem.* **2011**, *32*, 1456–1465.

(70) Zhao, Y.; Truhlar, D. G. The M06 suite of density functionals for main group thermochemistry, thermochemical kinetics, noncovalent interactions, excited states, and transition elements: Two new functionals and systematic testing of four M06-class functionals and 12 other function. *Theor. Chem. Acc.* **2008**, *120*, 215–241.

(71) Steinmann, S. N.; Corminboeuf, C. A system-dependent density-based dispersion correction. *J. Chem. Theory Comput.* **2010**, *6*, 1990–2001.

(72) Steinmann, S. N.; Corminboeuf, C. Comprehensive benchmarking of a density-dependent dispersion correction. *J. Chem. Theory Comput.* **2011**, *7*, 3567–3577.

(73) Steinmann, S. N.; Corminboeuf, C. A generalized-gradient approximation exchange hole model for dispersion coefficients. *J. Chem. Phys.* **2011**, *134*, 044117.

(74) Van Lenthe, E.; Baerends, E. J. Optimized Slater-type basis sets for the elements 1-118. *J. Comput. Chem.* **2003**, *24*, 1142–1156.

(75) Franchini, M.; Philipsen, P. H. T.; Van Lenthe, E.; Visscher, L. Accurate Coulomb potentials for periodic and molecular systems through density fitting. *J. Chem. Theory Comput.* **2014**, *10*, 1994–2004.

(76) Grimme, S. Semiempirical hybrid density functional with perturbative second-order correlation. *J. Chem. Phys.* **2006**, *124*, 034108.

(77) Tao, J.; Perdew, J. P.; Staroverov, V. N.; Scuseria, G. E. Climbing the density functional ladder: Nonempirical meta–generalized gradient approximation designed for molecules and solids. *Phys. Rev. Lett.* **2003**, *91*, 3–6.

(78) Lin, Y. S.; Li, G. D.; Mao, S. P.; Chai, J. D. Long-range corrected hybrid density functionals with improved dispersion corrections. *J. Chem. Theory Comput.* **2013**, *9*, 263–272.

(79) Lee, K.; Murray, É. D.; Kong, L.; Lundqvist, B. I.; Langreth, D. C. Higher-accuracy van der Waals density functional. *Phys. Rev. B - Condens. Matter Mater. Phys.* **2010**, *82*, 3–6.

(80) Jensen, F. Polarization consistent basis sets: Principles. *J. Chem. Phys.* **2001**, *115*, 9113–9125.

(81) Jensen, F. Polarization consistent basis sets. II. Estimating the Kohn–Sham basis set limit. *J. Chem. Phys.* **2002**, *116*, 7372–7379.

(82) Jensen, F. Polarization consistent basis sets. III. The importance of diffuse functions. *J. Chem. Phys.* **2002**, *117*, 9234–9240.

(83) Grimme, S. Semiempirical GGA-type density functional constructed with a long-range dispersion correction. *J. Comput. Chem.* **2006**, *27*, 1787–1799.

(84) Parker, T. M.; Burns, L. A.; Parrish, R. M.; Ryno, A. G.; Sherrill, C. D. Levels of symmetry adapted perturbation theory (SAPT). I. Efficiency and performance for interaction energies. *J. Chem. Phys.* **2014**, *140*, 094106.

(85) Papajak, E.; Zheng, J.; Xu, X.; Leverentz, H. R.; Truhlar, D. G. Perspectives on Basis Sets Beautiful: Seasonal Plantings of Diffuse Basis Functions. *J. Chem. Theory Comput.* **2011**, *7*, 3027–3034.

(86) Papajak, E.; Truhlar, D. G. Convergent Partially Augmented Basis Sets for Post-Hartree - Fock Calculations of Molecular Properties and Reaction Barrier Heights. *J. Chem. Theory Comput.* **2011**, 10–18.

(87) Gonthier, J. F.; Sherrill, C. D. Density-fitted open-shell symmetry-adapted perturbation theory and application to π-stacking in benzene dimer cation and ionized DNA base pair steps. *J. Chem. Phys.* **2016**, *145*, 134106.

(88) Schneider, W. B.; Bistoni, G.; Sparta, M.; Saitow, M.; Riplinger, C.; Auer, A. A.; Neese, F. Decomposition of Intermolecular Interaction Energies within the Local Pair Natural Orbital Coupled Cluster Framework. *J. Chem. Theory Comput.* **2016**, *12*, 4778–4792.

(89) Wuttke, A.; Mata, R. A. Visualizing dispersion interactions through the use of local orbital spaces. *J. Comput. Chem.* **2017**, *38*, 15–23.

(90) Werner, H. J.; Manby, F. R.; Knowles, P. J. Fast linear scaling second-order Møller-Plesset perturbation theory (MP2) using local and density fitting approximations. *J. Chem. Phys.* **2003**, *118*, 8149–8160.

(91) Head-Gordon, M.; Pople, J. A.; Frisch, M. J. MP2 energy evaluation by direct methods. *Chem. Phys. Lett.* **1988**, *153*, 503–506.

(92) Rappoport, D.; Furche, F. Property-optimized Gaussian basis sets for molecular response calculations. *J. Chem. Phys.* **2010**, *133*, 134105.

(93) Klamt, A. Conductor-like Screening Model for Real Solvents: A New Approach to the Quantitative Calculation of Solvation Phenomena. *J. Phys. Chem.* **1995**, *99*, 2224–2235.

(94) Pye, C. C.; Ziegler, T.; van Lenthe, E. L.; Louwen, J. N. An implementation of the conductor-like screening model of solvation within the Amsterdam density functional package — Part II. COSMO for real solvents. *Can. J. Chem.* **2009**, *87*, 790–797.

(95) Rezáč, J.; Riley, K. E.; Hobza, P. Benchmark Calculations of Noncovalent Interactions of Halogenated Molecules. *J. Chem. Theory Comput.* **2012**, *8*, 4285–4292.

(96) Burns, L. A.; Marshall, M. S.; Sherrill, C. D. Appointing silver and bronze standards for noncovalent interactions: A comparison of spin-component-scaled (SCS), explicitly

correlated (F12), and specialized wavefunction approaches. *J. Chem. Phys.* **2014**, *141*, 234111.

(97) Friedrich, J. Efficient Calculation of Accurate Reaction Energies - Assessment of Different Models in Electronic Structure Theory. *J. Chem. Theory Comput.* **2015**, *11*, 3596–3609.

(98) Sirianni, D. A.; Burns, L. A.; Sherrill, C. D. Comparison of explicitly correlated methods for computing high-accuracy benchmark energies for noncovalent interactions. *J. Chem. Theory Comput.* **2017**, *13*, 86–99.

(99) Liakos, D. G.; Sparta, M.; Kesharwani, M. K.; Martin, J. M. L.; Neese, F. Exploring the accuracy limits of local pair natural orbital coupled-cluster theory. *J. Chem. Theory Comput.* **2015**, *11*, 1525–1539.

(100) Minenkov, Y.; Wang, H.; Wang, Z.; Sarathy, S. M.; Cavallo, L. Heats of Formation of Medium-Sized Organic Compounds from Contemporary Electronic Structure Methods. *J. Chem. Theory Comput.* **2017**, *13*, 3537–3560.

(101) Minenkov, Y.; Sliznev, V. V.; Cavallo, L. Accurate Gas Phase Formation Enthalpies of Alloys and Refractories Decomposition Products. *Inorg. Chem.* **2017**, *56*, 1386–1401.

(102) Jurecka, P.; Sponer, J.; Cerný, J.; Hobza, P. Benchmark database of accurate (MP2 and CCSD(T) complete basis set limit) interaction energies of small model complexes, DNA base pairs, and amino acid pairs. *Phys. Chem. Chem. Phys.* **2006**, *8*, 1985–1993.

(103) Liakos, D. G.; Neese, F. Improved correlation energy extrapolation schemes based on local pair natural orbital methods. *J. Phys. Chem. A* **2012**, *116*, 4801–4816.

(104) Chattoraj, J.; Risthaus, T.; Rubner, O.; Heuer, A.; Grimme, S. A multi-scale approach to characterize pure CH4, CF4, and CH4/CF4 mixtures. *J. Chem. Phys.* **2015**, *142*, 164508.

(105) Caldeweyher, E.; Bannwarth, C.; Grimme, S. Extension of the D3 dispersion coefficient model. *J. Chem. Phys.* **2017**, *147*, 034112.

(106) London, F. Zur Theorie und Systematik der Molekularkräfte. *Zeitschrift für Phys.* **1930**, *63*, 245–279.

(107) Eisenschitz, R.; London, F. Über das Verhältnis der van der Waalsschen Kräfte zu den homöopolaren Bindungskräften. *Zeitschrift für Phys.* **1930**, *60*, 491–527.

(108) Alvarez, S. A cartography of the van der Waals territories. *Dalt. Trans.* **2013**, *42*, 8617.

(109) Huggins, M. L. Thermodynamic Properties of Solutions of Long-chain Compounds. *Ann. N.Y. Acad. Sci.* **1942**, *43*, 1–32.

(110) Flory, P. J. Thermodynamics of High Polymer Solutions. **1942**, *10*, 51–61.

(111) Grosse, A. V.; Cady, G. H. Properties of Fluorocarbons. *Ind. Eng. Chem.* **1947**, *39*, 367–374.

(112) Smart, B. E. Fluorine substituent effects (on bioactivity). *J. Fluorine Chem.* **2001**, *109*, 3–11.

(113) Acree, W. E., Jr.; Chickos, J. S. In *NIST Chemistry WebBook, NIST Standard Reference Database Number 69*; Linstrom, P. J., Mallard, W. G., Eds.; National Institute of Standards and Technology: Gaithersburg MD, 20899, (retrieved September 17, 2018); Chapter Boiling Point Data.

(114) Gilmour, J. B.; Zwicker, J. O.; Katz, J.; Scott, R. L. Fluorocarbon solutions at low temperatures. V. The liquid mixtures C2H6 + C2F6, C3H8 + C2F6, CH4 + C3F8, C2H6 + C3F8, C3H8 + C3F8, C4C10 + C3F8, iso-C4H10 + C3F8, C3H8 + C4F10, n-C6H14 + C4F10, n-C7H16 + C4F10, n-C,H20 + n-C4F10, and n-C10H22 + n-C4F10. *J. Phys. Chem.* **1967**, *71*, 3259–3270.

(115) Weast, R. C., Grasselli, J. G., Eds. *CRC Handbook of Data on Organic Compounds*; CRC Press, Inc.: Boca Raton, FL, 1989.

(116) Majer, V.; Svoboda, V. *Enthalpies of Vaporization of Organic Compounds: A Critical Review and Data Compilation*; Blackwell Scientific Publications: Oxford, UK, 1985.

(117) van der Waals, J. D. *Nobel Lectures, Physics 1901-1921*; Elsevier Publishing Company: Amsterdam, 1967; pp 254–265.

(118) Hill, T. L. *An Introduction to Statistical Thermodynamics*; Dover Publications: New York, 1986; pp 286–289.

(119) Acree, W. E., Jr.; Chickos, J. S. In *NIST Chemistry WebBook, NIST Standard Reference Database Number 69*; Linstrom, P. J., Mallard, W. G., Eds.; National Institute of Standards and Technology: Gaithersburg MD, 20899, (retrieved September 17, 2018); Chapter Phase Transition Enthalpy Measurements of Organic and Organometallic Compounds.

(120) Saikawa, K.; Kijima, J.; Uematsu, M.; Watanabe, K. Determination of the critical temperature and density of hexafluoroethane. *J. Chem. Eng. Data* **1979**, *24*, 165–167.

(121) Leu, A. D.; Robinson, D. B. High-pressure vapor-liquid equilibrium phase properties of the octafluoropropane (K-218)-chlorodifluoromethane (Freon-22) binary system. *J. Chem. Eng. Data* **1992**, *37*, 7–10.

(122) Vandana, V.; Rosenthal, D. J.; Teja, A. S. The critical properties of perfluoro n-alkanes. *Fluid Phase Equilib.* **1994**, *99*, 209–218.

(123) Mousa, A. H. N. Study of vapor pressure and critical properties of perfluoro-n-hexane. *J. Chem. Eng. Data* **1978**, *23*, 133–134.

(124) Steele, W. V.; Chirico, R. D.; Knipmeyer, S. E.; Nguyen, A. Vapor Pressure, Heat Capacity, and Density along the Saturation Line, Measurements for Cyclohexanol, 2-Cyclohexen-1-one, 1,2-Dichloropropane, 1,4-Di-tert-butylbenzene, (±)-2-Ethylhexanoic Acid, 2-(Methylamino)ethanol, Perfluoro-n-heptane, and Sulfolane. *J. Chem. Eng. Data* **1997**, *42*, 1021–1036.

(125) Stephenson, R. M.; Malanowski, S. *Handbook of the Thermodynamics of Organic Compounds*; Elsevier: New York, Amsterdam, London, 1987.

(126) Witt, R. K.; Kemp, J. D. The Heat Capacity of Ethane from 15°K. To the Boiling Point. The Heat of Fusion and the Heat of Vaporization. *J. Am. Chem. Soc.* **1937**, *59*, 273–276.

(127) Aston, J. G.; Sagenkahn, M. L.; Szasz, G. J.; Moessen, G. W.; Zuhr, H. F. The Heat Capacity and Entropy, Heats of Fusion and Vaporization and the Vapor Pressure of Trimethylamine. The Entropy from Spectroscopic and Molecular Data. *J. Am. Chem. Soc.* **1944**, *66*, 1171–1177.

(128) Simons, J. H.; Mausteller, J. W. The properties of n-butforane and its mixtures with n-butane. *J. Chem. Phys.* **1952**, *20*, 1516–1519.

(129) Van Ness, H. C.; Soczek, C. A.; Peloquin, G. L.; Machado, R. L. Thermodynamic Excess Properties Of Three Alcohol-Hydrocarbon Systems. *J. Chem. Eng. Data* **1967**, *12*, 217–224.

(130) Michou-Saucet, M. A.; Jose, J.; Michou-Saucet, C.; Merlin, J. C. Pressions de vapeur et enthalpies libres d'exces de systemes binaires: Hexamethylphosphorotriamide (HMPT) + n-hexane; n-heptane; n-octane: A 298,15 K; 303,15 K; 313,15 K; 323,15 K; 333,15 K. *Thermochim. Acta* **1984**, *75*, 85–106.

(131) Varushchenko, R.; Bulgakova, L. L.; Minzabekyants, P. S.; Makarov, K. *Russ. J. Phys. Chem.* **1981**, *55*, 1480.

(132) Viton, C.; Chavret, M.; Jose, J. Enthalpies of vaporization of normal alkanes from nonane to pentadecane at temperatures from 298 to 359 K. *ELDATA: Int. Electron. J. Phys. Chem. Data* **1996**, *2*, 103.

(133) Lo Nostro, P.; Scalise, L.; Baglioni, P. Phase separation in binary mixtures containing linear perfluoroalkanes. *J. Chem. Eng. Data* **2005**, *50*, 1148–1152.

(134) Straty, G. C. Velocity of sound in dense fluid methane. *Cryogenics* **1974**, *14*, 367–370.

(135) Tsumura, R.; Straty, G. C. Speed of sound in saturated and compressed fluid ethane. *Cryogenics* **1977**, *17*, 195–200.

(136) Younglove, B. A. Velocity of Sound in Liquid Propane. *J. Res. Natl. Bur. Stand.* **1980**, *86*, 165–170.

(137) Hwang, C.-a.; Holste, J. C.; Hall, K. R.; Gammon, B. E.; Marsh, K. N.; Parrish, W. R. PVT Properties and Bubble Point Pressures for Compositionally Characterized Commercial Grade Butane, 2-Methylpropane, and Natural Gasoline. *J. Chem. Eng. Data* **1996**, *41*, 1517–1521.

(138) Hawary, A. E.; Meier, K. Measurements of the Speed of Sound in Liquid n-Butane. *J. Chem. Eng. Data* **2016**, *61*, 3858–3867.

(139) Chávez, M.; Palaclos, J. M.; Tsumura, R.; Palaclos, J. M.; Tsumura, R. Speed of Sound in Saturated Liquid n-Pentane. *J. Chem. Eng. Data* **1982**, *27*, 350–351.

(140) Mascato, E.; Mosteiro, L.; Piñeiro, M. M.; García, J.; Iglesias, T. P.; Legido, J. L. Density, speed of sound and refractive index of (n-hexane + cyclohexane + 1-hexanol) at T = 298.15 K. *J. Chem. Thermodyn.* **2001**, *33*, 1081–1096.

(141) Devi, R.; Gahlyan, S.; Rani, M.; Maken, S. Thermodynamic and acoustic properties of binary mixtures of diisopropyl ether, benzene and alkanes at 298.15, 308.15 and

318.15 K: Prigogine-Flory-Patterson theory and graph theory. *J. Mol. Liq.* **2019**, *275*, 364–377.

(142) Acree, W. E., Jr.; Chickos, J. S. In *NIST Chemistry WebBook, NIST Standard Reference Database Number 69*; Linstrom, P. J., Mallard, W. G., Eds.; National Institute of Standards and Technology: Gaithersburg MD, 20899, (retrieved December 15, 2018); Chapter REFPROP version 7.

(143) Brown, J. A.; Mears, W. H. Physical properties of n-perfluorobutane. *J. Phys. Chem.* **1958**, *62*, 960–962.

(144) Burger, L. L.; Cady, G. H. Physical Properties of Perfluoropentanes. *J. Am. Chem. Soc.* **1951**, *73*, 4243–4246.

(145) Cochran, A.; North, M.; Chemistry, A. Ultrasonic Studies of Perfluoro-n-alkanes. *J. Chem. Soc., Faraday Trans. 2* **1974**, *70*, 1274–1279.

(146) Hallewell, G.; Vacek, V.; Vinš, V. Properties of saturated fluorocarbons: Experimental data and modeling using perturbed-chain-SAFT. *Fluid Phase Equilib.* **2010**, *292*, 64–70.

(147) Kayukawa, Y.; Hasumoto, M.; Kano, Y.; Watanabe, K. Liquid-phase thermodynamic properties for propane (1), n-butane (2), and isobutane (3). *J. Chem. Eng. Data* **2005**, *50*, 556–564.

(148) Defibaugh, D. R.; Moldover, M. R. Compressed and Saturated Liquid Densities for 18 Halogenated Organic Compounds [†]. *J. Chem. Eng. Data* **1997**, *42*, 160–168.

(149) Campos-Vallette, M.; Campos-Vallette, M.; Diaz-Fleming, G. Some physical and thermodynamic properties of n-CnF2n+2 compounds with n = 4-8. *Semina* **1983**, *4*, 405–409.

(150) Marcus, Y. Internal pressure of liquids and solutions. *Chem. Rev.* **2013**, *113*, 6536–6551.

(151) Serratrice, G.; Delpuech, J.-J.; Diguet, R. Compressibilites Isothermes des Fluorocarbures. Relation avec la Solubilite des Gaz. *Nouv. J. Chim.* **1982**, *6*, 489–493.

(152) Straty, G. C.; Tsumura, R. PVT and vapor pressure measurements on ethane. *J. Res. Natl. Bur. Stand.* **1976**, *80A*, 35–39.

(153) Prausnitz, J. M.; Sprow, F. B. Surface tensions of simple liquid mixtures. *Trans. Faraday Soc.* **1966**, *62*, 1105–1111.

(154) Cachadiña, I.; Tian, J.; Mulero, A. New corresponding-states correlation model for the surface tension of refrigerants. *J. Chem. Thermodyn.* **2017**, *110*, 201–210.

(155) Leadbetter, A. J.; Taylor, D. J.; Vincent, B. THE DENSITIES AND SURFACE TENSIONS OF LIQUID ETHANE AND NITROUS OXIDE. *Can. J. Chem.* **1964**, *42*, 2930–2932.

(156) Baidakov, V.; Khotienkova, M. Capillary constant and surface tension of propane (R-290) with helium dissolved in it. *Int. J. Refrig.* **2018**,

(157) Tian, J.; Zheng, M.; Yi, H.; Zhang, L.; Liu, S. Corresponding state-based correlations for the surface tension of saturated fluids. *Mod. Phys. Lett. B* **2017**, *31*, 1750110.

(158) Grigoryev, B. A.; Nemzer, B. V.; Kurumov, D. S.; Sengers, J. V. Surface tension of normal pentane, hexane, heptane, and octane. *Int. J. Thermophys.* **1992**, *13*, 453–464.

(159) Rohrback, G. H.; Cady, G. H. Surface Tensions and Refractive Indices of the Perfluoropentanes. *J. Am. Chem. Soc.* **1949**, *71*, 1938–1940.

(160) Kennan, R. P.; Pollack, G. L. Solubility of xenon in perfluoroalkanes: Temperature dependence and thermodynamics. *J. Chem. Phys.* **1988**, *89*, 517–521.

(161) Smith, J. H.; Pace, E. L. The Thermodynamic Properties of Carbon Tetrafluoride from 12 K to Its Boiling Point. The Significance of the Parameter nu. *J. Phys. Chem.* **1969**, *73*, 4232–4236.

(162) Parks, G. S.; Huffman, H. M. Thermal data on organic compounds. IX. A study of the effect of unsaturation on the heat capacities, entropies and free energies of some hydrocarbons and other compounds. *J. Am. Chem. Soc.* **1930**, *52*, 4381–4391.

(163) Pace, E. L.; Aston, J. G.; Pace, E. L. The Thermodynamics of Hexafluoroethane from Calorimetric and Spectroscopic Data. *J. Am. Chem. Soc.* **1948**, *70*, 566–570.

(164) Kemp, J. D.; Egan, C. J. Hindered Rotation of the Methyl Groups in Propane. The Heat Capacity, Vapor Pressure, Heats of Fusion and Vaporization of Propane. Entropy and Density of the Gas. *J. Am. Chem. Soc.* **1938**, *60*, 1521–1525.

(165) Pace, E. L.; Plaush, A. C. Thermodynamic Properties of Octafluoropropane from 14°K to Its Normal Boiling Point. An Estimate of the Barrier to Internal Rotation from the Entropy and Heat Capacity of the Gas. *J. Chem. Phys.* **1967**, *47*, 38–43.

(166) Aston, J. G.; Kennedy, R. M.; Schumann, S. C. The Heat Capacity and Entropy, Heats of Fusion and Vaporization and the Vapor Pressure of Isobutane. *J. Am. Chem. Soc.* **1940**, *62*, 2059–2063.

(167) Yarrington, R. M.; Kay, W. B. The Liquid Specific Heats of Some Fluorocarbon Compounds. *J. Phys. Chem.* **1957**, *61*, 1259–1260.

(168) McCabe, C.; Bedrov, D.; Borodin, O.; Smith, G. D.; Cummings, P. T. Transport Properties of Perfluoroalkanes Using Molecular Dynamics Simulation: Comparison of United- and Explicit-Atom Models. *Ind. Eng. Chem. Res.* **2003**, *42*, 6956–6961.

(169) Morgado, P.; Laginhas, C. M.; Lewis, J. B.; McCabe, C.; Martins, L. F.; Filipe, E. J.

Viscosity of liquid perfluoroalkanes and perfluoroalkylalkane surfactants. *J. Phys. Chem. B* **2011**, *115*, 9130–9139.

(170) Dantzler, E. M.; Knobler, C. M.; Windsor, M. L. Interaction Virial Coefficients in Hydrocarbon Mixtures. *J. Phys. Chem.* **1968**, *72*, 684.

(171) Dantzler, E. M.; Knobler, C. M. Interaction Virial Coefficients in Fluorocarbon Mixtures. *J. Phys. Chem.* **1969**, *73*, 1335–1341.

(172) Dantzler Siebert, E. M.; Knobler, C. M. Interaction virial coefficients in hydrocarbon-fluorocarbon mixtures. *J. Phys. Chem.* **1971**, *75*, 3863–3870.